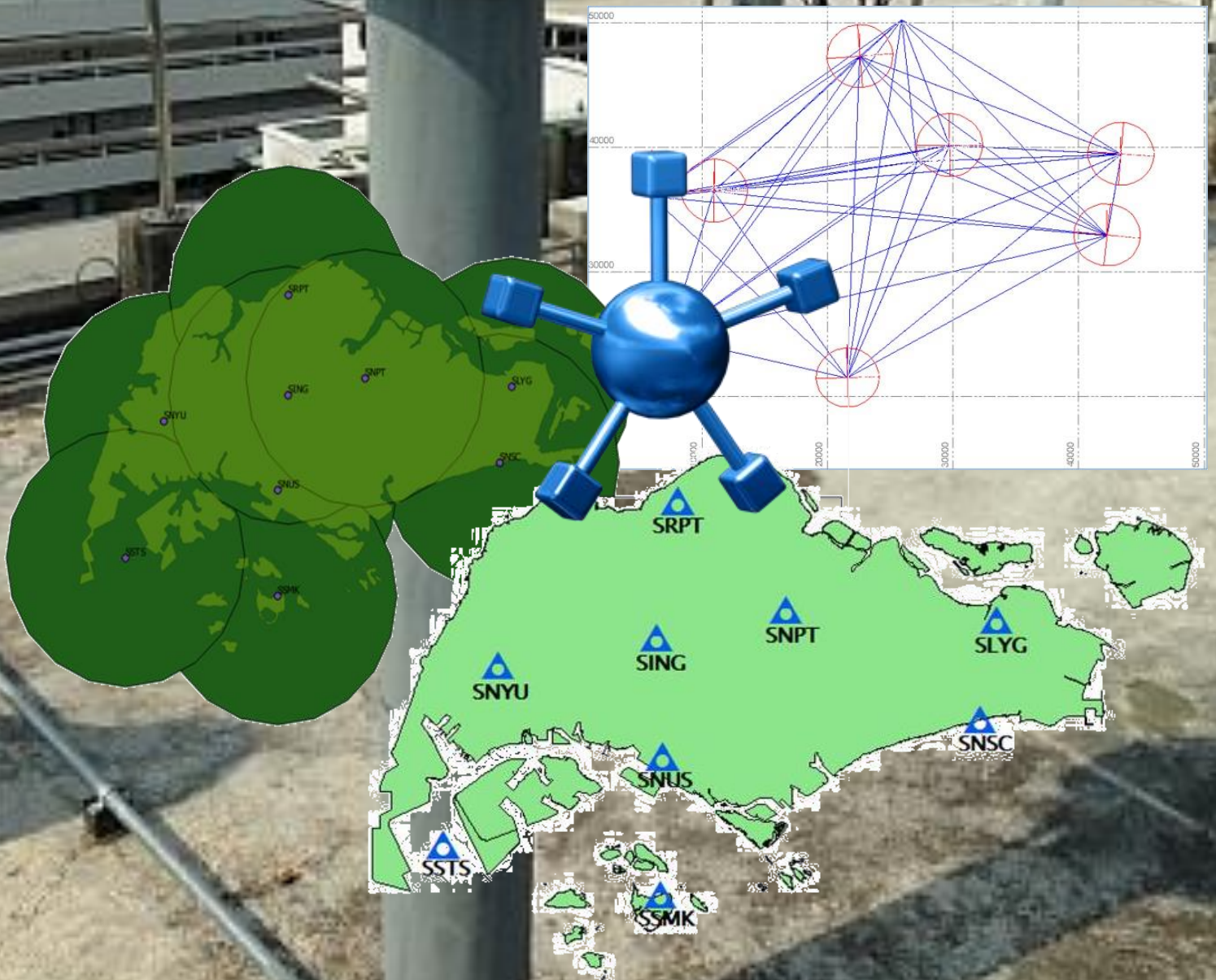E. Mulder

Integrity Monitoring for the Singapore Satellite Positioning Reference Network infrastructure

Integrity Monitoring (IM) for the Singapore Satellite Positioning Reference Network (SiReNT) infrastructure

By

E. Mulder

in partial fulfilment of the requirements for the degree of

Master of Civil Engineering
in Geoscience and Remote Sensing

at the Delft University of Technology,
to be defended on May 28, 2019 at 9:00 AM.

Student number:	4036530	
Project duration:	February 2017 – May 2019	
Thesis committee:	Prof. Dr. Ir. P. Teunissen,	TU Delft
	Dr. Ir. S. Verhagen,	TU Delft
	Dr. Ir. C. Slobbe	TU Delft

TU Delft

Abstract

The topic of this thesis is Integrity Monitoring (IM), with special focus on the Singapore Satellite Positioning Reference Network (SiReNT) infrastructure. This network infrastructure supports and improves Global Navigation Satellite System (GNSS) applications, related to positioning, navigation, tracking and (deformation) monitoring.
This project focuses on what IM is with regards to the SiReNT infrastructure, and how the current methodology can be improved so that its output is easier to interpret/understand for its users.

This research consists of two parts, a theory study, and a data study. The theory study is aimed at developing a fundamental understanding of GNSS and integrity, and the need for an IM component, as well as what comprises IM around the globe. The data study, which includes IM data processing, is performed to develop an understanding of the stability and performance of the SiReNT infrastructure itself, and its sensitivity to several degrading factors. For this the IM displacement data of a period of up to 5 months is analysed, in combination with the atmospheric information, and the number and geometry of tracked satellites. The Trimble method, with its default thresholds, has been applied to this IM displacement data, in order to determine what percentage was supposedly reliable, and inside these thresholds. It was also investigated whether these thresholds are performing adequately, if applied, and whether they have any impact on simultaneous recorded Rover data. The latter was assumed; the IM displacement data is thought to be usable to control the Rover data.

When it comes to positioning solutions, the quality parameters include, integrity, accuracy, precision, availability, reliability, continuity, capacity and redundancy. These quality parameters are affected by several degrading factors.

At the moment the Trimble Pivot Platform (TPP) is used to perform the network processing, as well as the integrity monitoring of the Continuous Operating Reference Stations (CORS) of the SiReNT infrastructure (and with that the impact of several of these degrading factors). This method is an example of the so-called external monitoring method. 'External' as the monitoring does not take place within the receiver itself, such as in the other method available; Receiver Autonomous Integrity Monitoring (RAIM). The external monitoring method and RAIM can either be used individually and/or independently, or in some sort of combination, complementing each other.
In several other countries, namely the Netherlands, Australia (Victoria), Hong Kong, and Malaysia, variants of the external monitoring method are applied in performing IM of their GNSS infrastructures. Usually this includes baseline and coordinate processing/comparison, both in real-time and through post-processing (often using the Bernese GNSS software). All of them have backup systems in place.
When it comes to IM visualization, even though there are similarities, the approaches differ per country. Some only visualise as much as the status of their reference stations, others visualise the real-time positioning solution of their IM stations, or have a complete dashboard visualising a number of parameters.

From this research can be concluded that the integrity (in terms of CORS' stability and positioning solution quality) of the SiReNT infrastructure is actually quite good. Of the IM displacement data which was supposedly reliable (following from the applied method), over 99% was within the set thresholds, for all CORS. The default thresholds (therefore) are

considered to be quite a good trade-off; they filter out most of the main disturbances (especially the ones which are assumed to be related to sudden severe fluctuations in the Ionospheric activity), while minimizing the amount of data loss.

There is room for improvements however; as a start, the (overall) redundancy should be increased, making the SiReNT infrastructure more robust and increase its reliability. The method in which the IM is currently performed could be improved in several ways as well. This could for example be done by tracking more constellations/signals, constructing additional CORS and backup systems, and using multiple different hardware brands for the equipment that is used in the SiReNT infrastructure. Also, the SiReNT infrastructure should be monitored with respect to surrounding IGS stations, rather than using a CORS that is part of the SiReNT infrastructure itself as a reference. An important addition to the IM component could be the feedback from the Rover data and performance (the initialization time, and positioning solution quality).
Currently made assumptions related to that do turn out to be erroneous, however. Any threshold applied to the IM displacement data cannot be used to control the Rover data.

The way in which the output resulting from this IM is visualised, should be more intuitive/easy to interpret. For this a dashboard is to be developed (in design following the example of the dashboard of the Dutch Cadastre), which homepage should be visualizing several parameters, all in real-time. This would enable the (end-)user to see what is the current status with regards to all these parameters, in one view. One would however also be able to access further information related to these parameters, by selecting the one of interest. These parameters are to be the number of tracked satellites, the number of connected users, an indication of the Ionospheric delay, the predicted geometric error, and the Rover performance.
The content of the information presented to the public should be kept to a minimum (only the necessary), where the content presented to the system administrators can be more elaborate.

The conclusions of this research point towards the need for further research into how the applied methods/algorithms and thresholds (as well as the other available options) can be utilized in order to improve the IM procedure in Singapore. On top of that, the impact of interference should be identified and monitored. Being able to do this, will improve the (integrity of the) infrastructure and the information provided by it.

Acknowledgment

Contents

- Data Study -

List of figures

Chapter 9

Appendix 1

Appendix 13

List of tables

       An overview of how often certain events were recorded, individually or together.
       The number of days on which sudden severe fluctuations in the Tropospheric activity and/or GRIM value, or in the Ionospheric activity, or a combination of both of these, or none of these, were recorded, is presented in the column with the different shades of blue. This is presented as a percentage of the total number of days in September, October, and those months combined (whole period I).
       The number of days on which there was a record of at least one supposedly unreliable displacement (u), or at least one supposedly reliable displacement (r) exceeding the thresholds, is represented in the column with the different shades of red. This is presented as a percentage of the total number of days on which there was either a sudden severe fluctuation in the Tropospheric activity and/or GRIM value, or in the Ionospheric activity, or a combination of both of these, or none of these. This is again presented for September, October, and those months combined (whole period I).

Besides that, the total number of days where sudden severe fluctuations in the Tropospheric activity and/or GRIM value, or in the Ionospheric activity, or a combination of both of these, or none of these, were recorded, coincided with a record of at least one supposedly unreliable displacement, or at least one reliable displacement exceeding the thresholds. In this case, it is presented as the percentage of the total number of days in this two-month period.
The darkness of the shades increased with increasing percentages.

Chapter 8

Appendix 1

Abbreviations

AFN	Australian Fiducial Network
AGRS.NL	GNSS Reference System (in the Netherlands)
AL	Alarm Limit
ANKASA	Malaysia national space agency
APREF	Asia-Pacific Reference Frame
ATMO	Trimble Atmosphere
CMR	Compact Measurement Record
CORS	Continuously Operating Reference Stations
CRS	Coordinate Reference System
DCC	Data Control Centre
DIA	Detection, Identification, Adaptation
DGPS / DGNSS	Differential GPS / GNSS
DOP	Dilution Of Precision
EPN	EUREF Permanent GNSS Network
EUREF	Regional Reference Frame Sub-Commission for Europe
EUV	Extreme Ultra Violet
FDE	Failure Detection and Exclusion
FDI	Failure Detection and Isolation
FKP	Flächen Korrektur Parameter
GDOP	Geometric Dilution Of Precision
GNSS	Global Navigation Satellite System
GPRS	General Packet Radio Service
GPS	Global Positioning System
GPSL	GPSLands
GRIM	Geometric Residual Integrity Monitoring (index)
H_0	Null Hypothesis (default model)
H_a	Alternative Hypothesis (alternative model)
HDOP	Horizontal Dilution Of Precision
IGS	International GNSS Service
IM	Integrity monitoring
IPWV	Integrated Precipitable Water Vapor
IRIM	Ionospheric Residual Integrity Monitoring (index)
ITRF	International Terrestrial Reference Frame
KNMI	Royal Netherlands meteorological institute
MAC	Master Auxiliary Concept
MTTD	Minimum Time To Detect
NETPOS	Netherlands Positioning Service
NMEA	National Marine Electronics Association
NTRIP	Networked Transport of RTCM via Internet Protocol
PDOP	Position Dilution Of Precision
PIVOT	Progressive Infrastructure via Overlaid Technology
POP	Period of Operation
PP	Post Processing
PWV	Precipitable Water Vapour
PUB	Public Utilities Board
QZSS	Quasi-Zenith Satellite System
RAIM	Receiver Autonomous Integrity Monitoring
RF	Radio Frequency
RFI	Radio Frequency Interference

RMS	Root-Mean-Square
RT	Reaction Time
RTK	Real-Time Kinematic
RTO	Real-Time Output
RTCM	Radio Technical Commission for Maritime Services
SatRef	Hong Kong Satellite Positioning Reference Station Network
SiReNT	Singapore Satellite Positioning Reference Network
SLA	Singapore Land Authority
STD	Slant Total Delay
SNR	Signal-to-noise ratio
TAC	Trimble Accounting
TDC	Trimble Dynamic Control
TDOP	Time Dilution Of Precision
TDS	Trimble Data Shop
TEC	Total Electron Content
TED	Trimble Ephemeris Download
TEQC	Translation, Editing and Quality Checking
TIC	Trimble Instrument Configurator
TIM	Trimble Integrity Manager
TNC	Trimble NTRIP Caster
TPP	Trimble Pivot Platform
TRI	Trimble Rover Integrity
TSM	Trimble Streaming Manager
TTA	Time To Alert
TTG	Trimble Transformation Generator
TU Delft	Delft Technological University
UERE	User Equivalent Range Error
UPS	Uninterrupted Power Supply
UTM	University Technology Malaysia
VHF	Very High Frequency
VDOP	Vertical Dilution Of Precision
VRS	Virtual Reference Station
ZTD	Zenith Troposphere Delay

1.

Introduction

The topic of this thesis is Integrity Monitoring (IM), with special focus on the Singapore Satellite Positioning Reference Network (SiReNT) infrastructure. This network infrastructure is aimed at supporting and improving real-time positioning, navigation, tracking and (deformation) monitoring in Singapore. Similar network infrastructures, containing multiple continuously operating reference stations (CORS), are being operational (and/or developed) in many countries worldwide [7]. These network infrastructures are normally operated by state authorities and private companies, providing the users with correction data with regard to their Global Navigation Satellite System (GNSS) observations (estimated positions), on demand or continuously. The obtained correction data is used by the Rover to correct its own observations and determine a positioning solution (more about the general GNSS concept and network infrastructures in section 1.1.). Note that in this report, when spoken of positioning and observations, this refers to both positioning and navigation, and observations and measurements, respectively.

The advantage of this network approach is that the specific coverage region is extended with a fairly homogeneous positioning quality throughout this region, as well as an improved integrity [7][14]. The latter is the case as the quality of the corrections provided by one of the CORS can be checked against those provided by another. Besides that, if one of the CORS is offline or providing faulty corrections, the other CORS in the network infrastructure can take over without any or with only (very) little accuracy loss. These CORS can simultaneously be used as base stations in the Single Base differential/relative positioning techniques.

As mentioned at the start of this introduction, the topic of this thesis is IM. But what is integrity and how can/why should integrity be monitored? According to several dictionaries, the general definition of the term integrity is:

 'quality expressed in terms of several key words including uprightness, honesty, sincerity, veracity and trustworthiness' [25].

Hence the integrity of a system refers to a quality measure of the system, in terms of these key parameters. The integrity of a GNSS based infrastructure consists out of several parts; the system's stability and positioning solution quality, and thus integrity, the (correction and raw) data integrity, the connectivity integrity and the integrity of the system equipment and the power supply. These are all very important when determining precise and accurate positioning solutions. In case the provided information exceeds set limits or when the system goes unmonitored, the information is not necessarily fulfilling the promised and preset quality constraints. In that case, the user(s) need(s) to be notified, and the provided information

improved, as soon as possible. Some applications are more stringent than others; this is closely related to the type of application in which the infrastructure is adopted.

This thesis is mainly aimed at the system's stability and positioning solution quality. For this, recorded displacement data (from both the SiReNT infrastructure and a Rover) could be analysed (more on this later). The term 'IM displacement data' is referring to the differences of the estimated positions from the reference value(s), as observed by SiReNT, and its CORS. The term 'Rover displacement data' is referring to the differences of the estimated positions of the Rover, from the reference value.
The main methods that are currently used to monitor the system's integrity are reviewed later on.

In this Introduction chapter, after first having introduced the general concept of IM (further developed in Chapter 2), the background of this research is presented, together with its reasons and objectives. First, GNSS is reviewed in general, followed by the SiReNT infrastructure and some examples of applications. Finally, the problems, and following from that the research question(s) is/are presented together with the objectives of this research.

1.1 The GNSS context

Before we go into IM specifically, first a general review with regards to GNSS. Knowing (exact) positions of persons or objects becomes increasingly important. GNSS, consisting of radionavigation based satellite systems, plays an important role in this and is involved in a lot of (critical) applications [23]. These systems are ranging systems that exploit the propagation (time) of (line-of-sight) radio signals transmitted by the satellites [14][15].
Using this, one can determine the ranges between the satellites and the receivers (more about this in section 1.1.2). By applying trilateration to these ranges the position on or relative to (the surface of) the earth can be determined [23]. Note that these signals (and thus ranges) are not only biased by the satellite and receiver clock, but also affected and degraded by all sorts of errors caused by for example the Ionosphere and Troposphere (these errors are reviewed in section 2.2).

The basic formulation of position determination involves 4 unknowns that need to be solved at every epoch; the user position components (x, y, z,) and the receiver clock error. Therefore, in this case at least 4 simultaneously measured GNSS signals are required. In reality, often there are more unknowns to be solved however. Hence more simultaneously measured GNSS signals are required. The geometry of the GNSS satellites relative to the receiver(s) plays an important role as well (e.g. dilution of precision, see section 2.2.2).

1.1.1 The system architecture

The large number of constellations and thus incoming GNSS signals can increase the observation redundancy and thereby strongly improve the availability and integrity of the GNSS service [17]. All these individual systems comprise a space segment, a control segment, and a user segment [14][15][23][32]. The space segment consists of all the satellites in space. The control segment consists of the tracking stations and the computing centers located around the world. This segment tracks the satellites that are within line-of-sight, and monitors them and their transmissions. The computing centers in place determine

and analyze the satellite ephemerides and clock solutions and calculate the respective predictions. These predictions are then uploaded into the appropriate satellite, in order for the correct information to be broadcasted to the user segment. This segment is also responsible for maintaining the health of the system.

The user segment consists of the user(s) of the provided GNSS signals (see 1.2.2. for example applications in Singapore).

IGS

The International GNSS Service (IGS) serves as a control infrastructure for the GNSS system as a whole (and acts as an overall information services provider) [15]. It is a continuously operating infrastructure consisting of reference (tracking) stations all around the world. The IGS infrastructure collects, archives and distributes GNSS observation data in order to provide the following key products [14][15][16][23]:

- Coordinates and velocities of the IGS reference stations around the world,
- High-accuracy GNSS satellite ephemerides,
- The GNSS satellite and IGS reference (tracking) station clock information,
- Atmospheric (Ionospheric and Tropospheric) information,
- Earth rotation parameters.

These products are used for user positioning, for the maintenance and improvement of the International Terrestrial Reference Frame (ITRF), and for scientific analyses such as monitoring the Earth's deformations and Ionospheric monitoring.

1.1.2 Signals and range determination

The transmitted navigation signals used to determine the ranges are electromagnetic waves with frequencies from 1.151 MHz – 1.610 MHz [15][32]. These navigation signals consist of carrier signals (in the L-band, and possibly in the future in the C-band), which are modulated in order to contain information for the user segment. Several types of observation types can be extracted from them; the pseudorange (code) observations, the carrier phase observations, Doppler observations, and the information data [21][23][32]. The pseudorange observations and the carrier phase observations are used in the positioning solution determination, where the Doppler observations (Doppler shift) are mainly used to determine the speed of the satellites relative to the receiver. The information data includes the satellite clock information and corrections, and information on orbit and Ionospheric parameters, as well as system status messages [23][32].

When the pseudorange observations are used, decimeter level accuracy can be provided, whereas when the carrier phase observations are used accuracy at the millimeter level (centimeter level in relative positioning) can be provided [23]. This is related to the difference in the period length of the signal between the pseudorange and carrier phase observations. The smaller the period of the used signal is, the more accurate the ranges can be determined. The pseudorange, ρ and the carrier phase, ϕ can be expressed as [23]:

$$(1.1.1) \quad \rho = r + I_\rho + T_\rho + c[\delta t_{rec} - \delta t^{sat}] + \varepsilon_\rho$$

and

$$(1.1.2) \quad \phi = r + I_\phi + T_\phi + c[\delta t_{rec} - \delta t^{sat}] + \lambda A + \varepsilon_\phi$$

respectively, with r, I_ρ (and I_ϕ), T_ρ (and T_ϕ), c, δt_{rec}, δt^{sat}, λ and ε_ρ (and ε_ϕ) representing the geometric range between the satellite and the receiver, the Ionospheric delay, the Tropospheric delay, the speed of light, the receiver clock offset, the satellite clock offset, the wavelength and the noise and errors, respectively [23]. The initial phases, the clock biases at t_0, and the integer ambiguity N (constant) are contained in phase ambiguity A. Note that all parameters, except for A, are functions of time. However, for notational convenience, this is omitted from this expression.

Figure 2.1: Visualization of the received code (top), the receiver-generated replica (bottom) and the time delay (= transit time) between them [21].

Algorithms in place enable the GNSS receivers to directly synchronize (by the means of signal correlation) the received navigation signals with the receiver-generated replica signal, as accurate as possible, in order to determine the (biased) geometric range between the receiver and the satellite. For more information on correlation in general, see Appendix 9.

From the time shift (sometimes called 'code delay') needed to get the maximum correlation between the code and its receiver-generated replica, the propagation/transit time of the signal can be calculated (see Figure 1.1). By multiplying this propagation time with the propagation speed of radio (electromagnetic) waves (the speed of light) the (biased) geometric range between the satellite and the receiver antenna phase centers can be determined.

When the carrier phase observations are used, the fractional phase cycle is measured continuously [14][18][23]. This carrier phase measurement determines the difference in phase between the received and receiver-generated replica signal by finding the maximum correlation (similar to the code correlation).

When using relative positioning, the (biased) geometric range difference between the adopted reference station and the receiver antenna phase centers can be expressed in an integer number of full carrier phase cycles between the two (the integer ambiguity N, which in fact are now the integer double-difference ambiguity parameters (see 1.1.3 and [7][21][23]) plus the carrier phase measurement (see Figure 1.2). This integer ambiguity N needs to be resolved (unresolved = Float solution, resolved = Fixed solution) in order to be able to deliver positioning solutions with a precision at centimeter level when using relative positioning. The time it takes the receiver to get a fixed solution (the integer ambiguities are resolved) after activation, is called the time-to-fix or the initialization period, and is an important measure of a receiver's performance. Further information is not required for this thesis, for more detailed information on the different GNSS constellations and their signals please refer to [15][32].
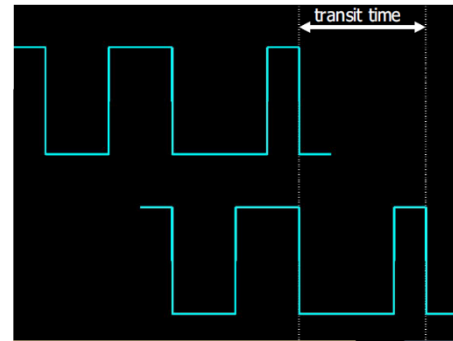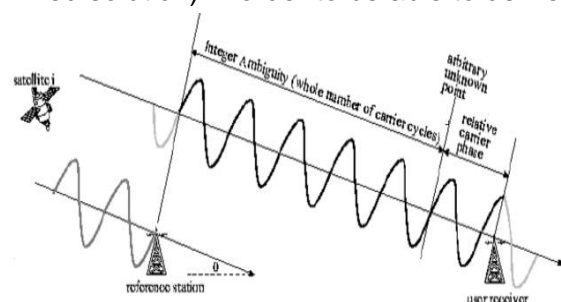
Figure 1.1: Visualization of relative positioning; the (biased) geometric range difference (the integer ambiguity and the carrier phase measurement) between the reference station and the receiver antenna [21].

GNSS systems have many capabilities, for example positioning and tracking. For this several different techniques (static and kinematic) are available, such as precise point positioning and differential positioning/relative positioning. The latter are of interest with regard to this thesis and therefore reviewed further in the next section.

1.1.3 Differential/relative GNSS and GNSS networks

Differential and relative positioning are sometimes explained to be based on pseudorange observations and carrier phase observations respectively [7]. However, most systems use a combination of the two, hence these definitions have become nearly interchangeable.

Both techniques are realized by simultaneously measuring the position of two (or more) receivers, locking onto and tracking the same satellites continuously [7][8][14][15]. Usually, one of these receivers, the base station (sometimes a CORS), is a (reference) point or is set up over a (reference) point with accurately known coordinates and remains stationary throughout the measurements. The other receiver(s) (Rover(s)) is/are moved from one (unknown) point to the next, recording observations continuously or for a brief period of time at each point of interest.

When only pseudorange observations are used, the base station continuously compares its known coordinates with the measured coordinates, resulting in range differences (range error correction factors) [7]. These range error correction factors are transmitted to the Rover(s) in real-time. At the Rover, these are combined with the observations simultaneously made by the Rover.

When carrier phase observations are used as well, the between-satellite single differences of the between-receiver single differences, also known as double differences of the observations are computed in order for the Rover(s) to fix the phase ambiguities [7][21][23]. Double differences can be formed when two receivers observe two satellites (near) simultaneously. This way, when using small baselines (the distance between the base station and the Rover), the effects of correlated measurement errors related to atmospheric effects and satellite orbit errors (distance dependent errors) and satellite clock errors are almost perfectly eliminated. For more information on this refer to [7][21][23].

By using any correction stream the Rover(s) compute(s) its position referenced to the by the base station adopted coordinate system.

Permanently operating network infrastructures are based on the same concept [8][9][14][21]. These usually provide both Single Base corrections (as described before) and network corrections (Network approach). For the latter approach, the GNSS observations from each of the CORS are transmitted to the central Data Control Centre (DCC) center. There they are stored and processed; a continuous computation of the atmospheric effects, satellite orbit errors and carrier phase ambiguities takes place. Besides that, the location dependent errors (multipath, antenna, clock) of the network are modelled and the network integrity is monitored. In order to do this, a permanent network of equally spaced CORS is required. At the DCC the data from all (or a specific subset of the) CORS is combined to determine a network solution (all the integer ambiguities must be fixed for each CORS in real-time), dependent on the Rover antenna's location.

There are several different methods including the Virtual Reference Station (VRS), Master Auxiliary Concept (MAC), and Flächen Korrektur Parameter (FKP) [12][29]. When using the

VRS method, the Rover(s) correct(s) its/their own observations with the correction(s) that is/are determined for the virtual observations (of the VRS). For this the Rover needs to provide the DCC with its approximate position [7][21], such that a VRS (and its required correction) can be generated on this position (and thus very close to the Rover(s) position(s), resulting in (a) very small baseline(s)). When using the MAC method, the Rover receives the observations of one Master station as well as the observation differences between the Master station and Auxiliary stations. The Master station is selected based on proximity to the Rover (minimizing the bassline). The Rover then has to interpolate and model itself using this data. When using the FKP method, the Rover receives detailed information on the different error sources from the DCC, after which it determines the individual corrections for the specific Rover position itself.

As mentioned before, by using the network approach, a homogeneous accuracy and availability is ensured, the baseline limitation is extended within the bounds of the network infrastructure and the reliability and integrity are improved [7][14].

1.2. SiReNT and applications

1.2.1 SiReNT

SiReNT is the national reference network infrastructure in Singapore [2][30]. It is developed as an initiative by the Singapore Land Authority (SLA) to support real-time high-quality positioning, navigation, tracking and monitoring. It consists of 9 CORS nationwide (see Figure 1.3) and supports GNSS; four global systems (GPS, Glonass, Beidou, Galileo), and one regional system (QZSS) when using Single Base and GPS, Glonass and Beidou when using
the Network approach. In case of the latter the VRS method is applied [30].
Of the 9 CORS, 8 are usable for general purposes. Extra channels are available to track additional signals in the future [2][30].
The SiReNT CORS set-up consists of weather-proof steel cabinets housing, containing

Annotation	Full name / location
SNYU	Nanyang Technological University
SRPT	Republic Polytechnic
SNPT	Nanyang Polytechnic
SLYG	Loyang
SNSC	National Sailing Centre
SNUS	National University of Singapore
SSMK	Semakau Landfill
SSTS	Sultan Shoal
SING	- / Earth Observatory of Singapore (EOS)

Figure 1.3: Overview of the SiReNT GNSS Reference Infrastructure and the relative locations of its CORS. Source: screenshot from SiReNT TTP Web App.

Trimble NetR8/Trimble NetR9 GNSS receivers with dual-frequency capability and modem/routers (see Figure 1.4). There are also sensors installed to monitor atmospheric parameters, and for back-up, each CORS is provided with power and communications redundancy.

The GNSS observations are transmitted from each of the CORS to the SiReNT DCC, where they are processed and stored. Using this (or a subset of this) data, the appropriate corrections (regarding for example the Ionospheric errors, Tropospheric errors and ephemeris errors) are determined, based on the VRS location. This correction data for relative positioning (in the RTCM (Radio Technical Commission for Maritime Services) or the Trimble CMR (Compact Measurement Record) format) is transmitted to the user in real-time via a GPRS (General Packet Radio Service)/3G/4G datalink. When using the SiReNT infrastructure, Rover(s) can determine positions down to centimeter level or sub-meter accuracy, depending on the service used. SiReNT provides several services:

- Differential GNSS (DGNSS, also known as DGPS) services, providing sub-meter accuracy, in real-time.
- RTK, providing centimeter accuracy (3-5 centimeter), in real-time.
- Post Processing (PP) On-Demand, providing millimeter accuracy (3-5 millimeter). This data is accessible through the SiReNT Web App.

Note however, that these accuracies are dependent on the user's equipment specifications as well as processing software used. For both DGPS and RTK, there is a Single Base and a Network approach available.

Figure 1.4: An example of the SiReNT CORS set-up; a weather-proof steel cabinet housing, containing Trimble NetR8/Trimble NetR9 GNSS receivers, modem/routers and back-up batteries in case of a power outage (left) and the antenna (right). Source: SLA.

By using this infrastructure, the observations are referenced to SVY 21 plane coordinate system and datum. This is a local coordinate system defined through information from SLA, in order to satisfy national mapping requirements. The system is based on the Transverse Mercator projection from geographical coordinates referenced to the WGS84 ellipsoid.

1.2.2 Applications

Some examples of the applications using the information provided by the SiReNT infrastructure include a semi-automated piling system, a semi-automated tower crane system, autonomous vehicles/shuttles, and 3D and utility mapping [44].

The semi-automated piling system (see Figure 1.5) is used on construction sites for setting out foundation piles at specific positions as well as on-site checking of pile positions that are suspected to have shifted. This system is developed after consulting SLA and is currently operational across Singapore.

The semi-automated tower crane system is used for heavy lifting at construction sites (see Figure 1.5). Successful trials have taken place at an actual construction site and as a result this system will be deployed in upcoming construction projects across Singapore.

As for the autonomous vehicles/shuttles, numerous autonomous vehicle developers across Singapore, both trialing and in operational, are using the SiReNT infrastructure for positioning purposes (currently operationally used in Gardens by the Bay, see Figure 1.5).

Figure 1.5: Applications using SiReNT; the semi-automated piling system (top), the semi-automated tower crane system (bottom left), and autonomous vehicles at Gardens by the Bay (bottom right). Source: SLA

SLA's project to map Singapore in 3D consists of the collection of aerial and terrestrial imagery and point clouds for 3D modeling. All the data is combined and (geo)referenced to the local reference frame (SVY21) via the use of SiReNT.

Other applications include (Cadastral) surveying, (height) monitoring (for example of structures near the airport), and tracking (for example of containers in the port).

All the above applications require centimeter accuracy in terms of the positioning information and therefore make use of SiReNT (network) RTK.

As for the utility mapping, this application requires only sub-meter accuracy and therefore uses (network) DGPS. The Public Utilities Board (PUB) is the biggest user of SiReNT DGPS for asset Tracking and monitoring.

Besides these applications, SiReNT also plays a role in scientific research. An example of this is the incorporation of the monitored atmospheric parameters (such as the Zenith Tropospheric Delay (ZTD) and the Integrated Precipitable Water Vapor (IPWV)) into numerical weather models in order to improve Solar Irradiance forecasting.

1.3. Research objectives

1.3.1. Motivation

In order to enable and serve high-quality positioning solution applications, such as, but not limited to examples described before, and to protect SLA from claims against it, the SiReNT infrastructure included an IM component. This component is part of the used Trimble PIVOT (Progressive Infrastructure via Overlaid Technology), and one of its (main) tasks is to monitor the movement and/or quality of the GNSS CORS. For this (default) thresholds are applied to the IM displacement data or the so-called IM displacements. These thresholds have to be satisfied in order for the observation(s) to be considered reliable. More details on this can be found in chapter 4, and Appendix 1. The IM displacements from the monitoring engine that is selected for this purpose in SiReNT, are stored and presented to the infrastructure administrators/users.

This IM component and the information it generates, is not fully utilized and understood however. The infrastructure administrators find it tedious to go through all the information and different technical reports. Besides that, infrastructure users are also not able to use the IM, and/or it confuses them. This is the case as the presented IM information often is not very clear, overwhelming and/or very technical, and their understanding of the underlying fundamentals and algorithms limited. Most of the infrastructure users are only interested in how the errors will affect the achievable observation accuracy. The contributing and affecting factors are not clear or necessarily of concern to them. These factors, like the different types of atmospheric variations and delays, or multipath, often form a source of confusion (when included), as they are not always well understood.

SLA is therefore interested in developing an IM component/regime that possibly improves the integrity, and generates more intuitive information, that will be easier to understand and thus can be utilized more. First a better understanding is needed of the mentioned 'contributing and affecting factors'. Also, how can IM be performed, and how is it done around the globe (in several countries, including Singapore)? This theory study is needed as a good understanding of all this is limited. Note there has not been any previous research into this

topic by SLA.

This project does not only consist of a theory study, but is also backed by a data study. In this part, an attempt is made to find the answers to research questions that satisfy the TU Delft requirements, while at the same time providing valuable information/insights to SLA. It is for example not known whether the applied fundamentals and algorithms, that are incorporated within the Trimble PIVOT software, and applied in SiReNT, are indeed performing satisfactory, and ensuring the best possible performance. When talking about performing satisfactory, it means that a certain percentage (as per requirements) of IM displacements can be considered reliable, and are also not exceeding the thresholds. This is the same as the percentage of time where this is the case, as (in theory) the observations are logged every second. The Rover performance (and thus the quality of the correction data) is linked to this as well. Therefore, since this project is aimed at the IM performed in Singapore, the questions is how well is it been done here, and what is the observed integrity (in relation the default thresholds) over time? And how is this affected by sudden severe fluctuations in the relevant factors? How are the thresholds applied to the IM displacement data performing? It is believed by SLA that applying these thresholds to the IM displacement data from the RTK module, will enable one to control the Rover displacement data retrieved by the infrastructure user. The question is whether this is correct and whether these thresholds are applicable to the Rover displacement data in the first place. Besides that, are the SiReNT infrastructure and its CORS stable, or are there any trends visible in the stability and coordinates of these different CORS?

1.3.2. Objectives

A more intuitive IM regime is to be researched and developed. In this, the focus is on the CORS stability and positioning solution, especially on the way in which the IM information is visualized/presented. This IM regime should where possible, improve the current methodology. It should generate and visualize the IM information to the infrastructure administrators and infrastructure users in a way that is (relatively) easy to interpret, even when one lacks understanding of the fundamentals. A part of this project is therefore the analysis of the resulting IM reports and the information presented through the SiReNT Web App.

For all that, better understanding of IM is required, and the topics touched upon in section 1.3.1 should be covered. Based on this, it should be determined whether certain improvements/updates are required, in order to improve the network's performance. What these improvements/updates might entail exactly is expected to follow from the results of this research.

This graduation project will therefore consist of a literature study that will be aided by data processing, focused on the following research question:
What is the integrity of the SiReNT infrastructure (in terms of its stability and positioning solution quality), and what is needed to improve that, as well as the way it is monitored and visualized, in order to be more useful?

This includes the research sub-questions:

- *What, among other quality parameters, is integrity, and what is it with regards to GNSS based positioning systems?*

- *What are important degrading parameters/factors affecting the integrity of GNSS based positioning systems?*
- *What IM methods are available?*
- *What is being used in other countries?*
- *What is used in Singapore?*
- *How to use, improve, and communicate/visualize the SiReNT IM and its output?*

The sub-questions with regards to the data processing;

- *What is the impact of unusual fluctuations in the atmospheric information and/or the PDOP/number of tracked satellites on the IM displacement data, and what can be concluded from it?*
- *What thresholds to use in order to ensure that 99% of the IM displacement data is within the thresholds, and alert the user properly in case the network infrastructure is not necessarily providing trustworthy information?*
- *Are there trends in the IM displacement data and if so, what can be concluded from them?*
- *Is there a relationship between the IM displacement data and the Rover displacement data, and can the first be used in controlling the latter?*
- *How is the Rover performance affected by unusual fluctuations in the atmospheric information and/or the PDOP/number of tracked satellites on the IM displacement data, and what can be concluded from it?*
- *With regards to improving the redundancy within SiReNT, where to construct new CORS?*
- *How does a nearby earthquake event affect the SiReNT infrastructure?*

1.3.3. Approach and outline

The objective of this thesis is thus to answer the previous research questions. This is to be done in a clear fashion, thereby ultimately provide insights on improving the current methodology.

This is done by first researching the fundamentals; what defines integrity, what is it affected by, and how is IM performed (chapter 2). Besides that, the IM methods that are applied in several other countries, as well as in Singapore, are reviewed, in order to gain better and more detailed knowledge about what exactly is monitored and how can it be done (chapter 3). After this, the methodology that is applied in Singapore will be reviewed in more detail, alongside its output (chapter 4). The findings presented in the first few chapters, the so-called 'theory study', are discussed in chapter 5.

After gaining the appropriate knowledge and understanding, data is gathered, processed and presented (chapter 6-9). This includes IM displacement data and Atmospheric information. This is done in order to investigate the stability of the infrastructure, as well as the (possibly related) performance of the Rover. For the latter, a 'Rover' is deployed in the field, determining positioning solutions, while using the SiReNT correction information. This way the relationship between the output (in terms of northing, easting and height), the Rover displacement data, will be compared with the Trimble PIVOT Platform (TPP) RTK engine module (in VRS mode) output. This is one of the IM engine modules that is part of the TPP.

The aim in doing this is to determine a relationship between these outputs, in order to suggest appropriate warning and alert thresholds.

The specific way this is done, the *method*, is presented in chapter 6. Following this, all findings and data processing results with regards to the IM displacement data over a longer period of time, are presented and discussed in chapter 7. All findings and data processing results with regards to the Rover displacement data in relation to simultaneously recorded IM displacement data are presented and discussed in chapter 8. The findings and data processing results with regards to the construction of new CORS (more on this later), and a case study related to the impact of a nearby earthquake event, are presented and discussed in chapter 9.

Finally, from all the findings in this project, conclusions and recommendations are formulated in chapter 10, on how to possibly improve the integrity of the SiReNT infrastructure, and the way it is monitored, as well as the interpretability of/the visualization of the IM information.

-Theory study-

<div align="right">

2.

</div>

<div align="right">

Fundamentals

</div>

2.1. GNSS based Positioning system performance: system/quality parameters.

The performance of GNSS-based positioning systems is characterized by a set of quality parameters [14][15]. These quality parameters have to fulfill pre-set quality constraints in order to meet the desired requirements. Only in that case, the system is performing satisfactory and providing solutions that can be applied by the user(s). All these quality parameters are correlated as they all (indirectly) depend on the same factors (such as satellite geometry).

In general, the quality parameters are determined per specific time interval, or as an average over a certain time interval [15]. This is the case as the satellite geometry varies continuously over time. Besides that, sometimes satellites are temporarily unavailable due to for example failure and/or maintenance. The different quality parameters are *accuracy, precision, availability, integrity, reliability, continuity, capacity* and *redundancy*. All these parameters are described in greater detail below.

Accuracy

Accuracy is defined as the degree of correctness; that is, the closeness of the estimated parameter to the defined reference value or truth, at a given point in time or time interval [5][14][15][33] (for the visual representation see Figure 2.1).

The total error affecting the estimated parameter can be subdivided in several different error types, namely errors in the receiver or due to signal instabilities, weather influences and other physical changes in the propagation medium, as well as user related errors [5]. The latter are usually excluded in the accuracy specification of a system however. For GNSS applications, accuracy can be separated in the horizontal and the vertical dimensions [17].
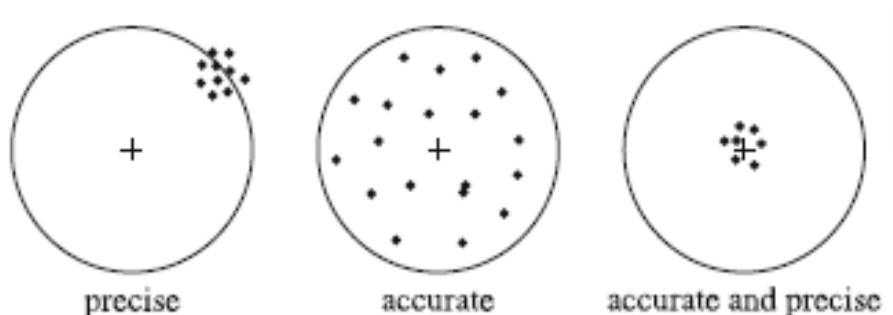
Figure 2.1: Visual comparison of the accuracy and precision of an observation [13].

Precision

Precision describes the quality of the observations; the spread or variance (the square of the standard deviation (σ)), and thus uncertainty in the estimated positioning solutions

[15][25][33] (for the visual representation see Figure 2.1). Precision is not to be confused with, and very different from accuracy. As the aim of using positioning systems usually is determining an unknown position rather than a known position, the accuracy of that positioning solution is not known. In that case, the uncertainty of that estimated positioning solution is an important indication of the quality of a certain device or system.

In relationship to GNSS positioning services, precision is usually expressed as a statistical measure of the performance of the system, as the system errors generally follow a known error distribution, accompanied by a confidence level in order to express the probability of that value [5][14][15]. Often applied is the 95% (2σ) confidence interval. This means that for any position solution, the probability that the positioning error is within the system's precision requirement is at least 95%. Other options are the 68% (1σ) and the 99,7% (3σ) confidence intervals.

Integrity

With regards to positioning solutions, integrity is defined as the measure of trust that can be placed in the correctness of the provided positioning information [15][17][26]. Generally included in this is the ability of the system to timely notify the user(s), in case the provided information is not fulfilling the preset quality constraints and exceeds set limits. In case the integrity is lost, (parts of) the infrastructure or the provided information should not be used.

Integrity can be lost either when the incorrectness of the used information is not being detected, or when the system fails in notifying the user within the 'time-to-alert' (TTA), after it is detected. Loss of integrity can happen at several levels; system level, operational environment level and user receiver level [26]. With sufficient redundancy available, the source of integrity loss can be identified and excluded, and positioning can continue.

Important parameters in this are [15][17][26]:

Figure 2.2: Visualization of correct and incorrect information, with regards to the Integrity Risk. The blue points and red points represent the observations for which $(\hat{x} - x) \leq AL$, and $(\hat{x} - x) > AL$, respectively. The integrity space (Ω_{AL}) is the space inside the circle, with x, the true value, in its centre.

- The TTA, in case a set limit is exceeded, the user has to be notified within a maximum given period of time.
- The integrity risk, defining the probability of providing incorrect or misleading information, such that the error exceeds the alert limit (AL), without being detected [17]:

$$(2.1) \quad Integrity\ Risk = P((\hat{x} - x) \notin \Omega_{AL} \cap No\ alert)$$

With $\hat{x}, x$ and Ω_{AL} representing the estimated value, the known value and the integrity space bounded by the AL's respectively. An error outside this space and thus exceeding the AL's (see Figure 2.2) should be detected and trigger a notification.

- The AL's define the maximum allowed position errors, in order for the provided information to be useful. These are usually specified such that the errors can be larger than the 95th percentile, however still within safe limits. This is defined in

correlation to the chosen (application specific) accuracy and integrity risk levels (related to the AL) [15].

- The minimum detection probability defines the minimum probability of an integrity loss to be detected successfully. From this parameter can be inferred how well measurement errors can be found.

Integrity is the complement of the probability of providing incorrect or misleading information:

(2.2) $Integrity = 1 - integrity\ Risk$ [17]

Continuity

Continuity is defined as the probability that the specified required system performance is maintained for a specific period of time, after commencing an operation in which the positioning information is used (POP: period of operation) [14][15][17][25]. This means that there are, and will be no interruptions within the POP without being scheduled. Hence the system is providing the user with trustworthy information in terms of accuracy and integrity. An important constraint in this, is that specified required system performance was available at the moment of commencing. In formula form this is given by [17]:

(2.3) $Continuity = P(\cap_{i=1}^{k}(No\ alert\ at\ i\ |\ System\ available\ at\ i = 1))$

with *i* and *k* representing the sample epoch and the total number of epochs in the specific time interval respectively. The '$System\ available\ at\ i = 1$' in this case, refers to specified required system performance being available at the moment of commencing. The continuity risk is defined as the probability that the specified required system performance will not be maintained throughout the intended POP (a measure of system unreliability) [15][25]. Note that in the geodetic community's terms reliability has another meaning however and can be divided into internal and external reliability [13][33][45]. Internal reliability, refers to the capability with which errors and anomalies in the data, and misspecifications of the used model can be traced. External reliability refers to the sensitivity of the positioning solutions to these errors, anomalies or misspecifications, in case they are not being detected.

Availability

Availability is defined as the percentage of time that the system is performing satisfactory and the provided information can be applied without issues (it is delivering the required quality), when required [5][14][15][26].

(2.4) $Availability\ (t) = t_{satisfactory}/t_{total}$

This is the case if accuracy, integrity and continuity requirements are satisfied. Availability is dependent on the environment within the specified coverage area (volume) and the technical capabilities of the system in use. The movement of the satellites with respect to the specific coverage area as well as the potentially large amount of time it takes to for example perform maintenance to the system or the satellites in case of failure, complicates and affects the availability. As just using observations might not be sufficient, the availability per specific coverage area at a certain time interval can be determined by designing and modeling the system, and analysing the simulation results versus the reality [25][26].

Coverage

Coverage is defined by the surface area (A_{total}) or volume in which the system is performing satisfactory and the provided information can be applied without issues ($A_{satisfactory}$), hence the positioning solution can be determined within the specified level of accuracy [5][14][15][25].

(2.5) $Coverage\ (m^2) = A_{satisfactory}\ /\ A_{total}$

The coverage of a GNSS system is dependent on things like the geometry of the system, the sensitivity of the used receiver, the atmospheric noise conditions, and the power levels and other factors affecting the availability of the signal (blocking, jamming, etcetera).

Capacity

Capacity is defined by the number of users that can use the GNSS-based positioning system at the same time [5][14][15].

Redundancy

Redundancy is defined as the availability of duplicates of critical elements and/or functions of a system or observations, so that there are more than the strict minimum. This in order to improve performance and reliability [14][33]. In a mathematical sense:

(2.6) $Redundancy = m - n,\ with\ n = rank(A), and\ m > n$

With m representing the observations, n the representing the unknown parameters to be estimated, and A representing the design matrix. Note that, for this to be true, the systems of observation equations must be of full column rank, meaning that all m must be linearly independent. In that case, when $m > n$, at least one solution exists (the system of observation equations is consistent). Redundancy will increase the level of reliability and is therefore recommended or even required at different levels (observation, system, user, etcetera) [32][43][45]. Having redundant receivers and DCC's will aid the reliability of the system itself, for example in case of an outage of some kind. Having redundant observations, due to for example using multi-constellation GNSS, multiple different signals, motion sensors and environmental sensors, will improve the precision of the positioning solution. It also enables one to check for errors. A systems robustness can be maximized by gathering as much information as possible in order to generate redundancy. This way the most reliable observations or an average can be selected for the data processing.

2.2. Important degrading parameters/factors

GNSS based positioning system performance is affected or disturbed by (a combination of) errors [14][23][25][26]. These consist of errors at *user and/or user equipment level, operational environment level* and/or *system level*. This can and will affect a GNSS based system and its positioning solution integrity. These error sources are more elaborately described in the following sections.

2.2.1. Important degrading factors at user and/or user equipment level

These degrading factors are caused by the end user and/or by the used equipment (receiver, receiver software etcetera) [25][26]. Degradation caused by the end user can be related to for example inadequate training, where degradation in the used equipment can be related to for example equipment overheating, power system outages or power fluctuations, processing algorithm errors and/or software incompatibilities.

2.2.2. Important degrading factors at operational environment level

These degrading factors are caused by interference (intentional and unintentional) and signal propagation properties [25][26].

Intentional interference
- Jamming: the GNSS signal is being jammed by interference with another signal, which overrides or conceals the GNSS signal [5][25][26]. In order for that to be possible, the jamming signal has to be powerful. This can be realized by generating a signal in or near the GNSS frequency bands.
- Spoofing: the GNSS receiver locks onto GNSS signals that are (appearing to be) valid [32][25][26]. Therefore, GNSS users can be misled by generating intentional interference through injecting a false, GNSS-like signal, resulting in significant positioning errors.

Unintentional interference
- Radio Frequency Interference (RFI): interference/signal disruption caused by external Radio Frequency (RF) sources, by transmitting signals in or near the GNSS frequency bands. Examples of such sources are Ultra-wideband Radar and communications, Broadcast television, Very High Frequency (VHF) signals, Personal Electronic devices and Mobile satellite services. This phenomenon can cause difficulties in tracking the GNSS signal.

Signal propagation related influences
- Tropospheric delay: The Troposphere is part of the lower Atmosphere (0-16 kilometer) [23] (see Figure 2.3). Tropospheric influences are caused by the changing humidity, temperature and atmospheric pressure within that layer. The Tropospheric delay
(~2.3-2.6 meter) is non-dispersive, hence it has the same impact on all signals. The troposphere consists of a hydrostatic (dry) part and a non-hydrostatic (wet) part [11][15][23][32]. The dry component (dry gases) comprises 90% of the Troposphere, and depends only on pressure. This part is responsible for the major part of the Tropospheric delay, however can easily be modelled. The wet component, dependent on the water vapor content, comprises the other 10%, and cannot be modelled very well. The latter is the case as the water vapor content changes rapidly. Tropospheric influences mostly affect the height component of the measurement and

do normally not vary much locally. Therefore, relative positioning with small baselines is preferred. For example, passing weather fronts generally cause difficulties, however, overall the Troposphere's variability is relatively low.

Figure 2.3: Visualization of the Atmospheric influences; the Tropospheric delay and the Ionospheric delay.

- Ionospheric delay: The Ionosphere is part of Earth's upper atmosphere (50-1000 kilometer) [11][14][15] (see Figure 2.3). Here Extreme Ultra Violet (EUV) and x-ray photons from the sun causes the ionization of atoms and molecules. The resulting free electrons largely affect the speed and direction of the propagation of radio waves, and therefore can cause significant positioning errors. Therefore, it is very important to understand what is going on in the ionosphere. The amount of delay (: meters – tens of meters) is related to the amount of electrons present and the frequency of the radio wave. The amount of electrons present is represented by the Total Electron Content (TEC) [11][15][23][33]. This is defined as the total number of electrons integrated between two points (satellite and receiver in this case), along a tube with a squared cross section of 1 square meter. The larger this value, the more the radio signal will be affected. The Ionospheric activity is largely variable with the path traveled, solar activity (solar cycle (11 years), solar flares), time of year, season, time of day and location. For this reason, it is very difficult to predict or model the precise impact of the Ionospheric delay. The Ionospheric delay is dispersive and inversely proportional to the frequency (the higher the frequency, the less is the Ionospheric effect and vice versa). The intensity of the Ionospheric activity can be represented by TEC maps and/or the I95 value.

- Multipath: the arrival of the incoming GNSS signal at different times, due to obstructions by and/or due to reflection off nearby structures or other reflective surfaces [14][15][26][32] (see Figure 2.4). This way some of the incoming signals do not reach the receiver directly but arrive at the receiver slightly delayed as they travel farther. This can cause multipath interference. There are two types of multipath interference, constructive and destructive [15]. Constructive multipath interference occurs when the direct and indirect signals are in-phase and destructive multipath interference occurs when the signals are out-of-phase. This results in positive and negative ranging errors respectively.
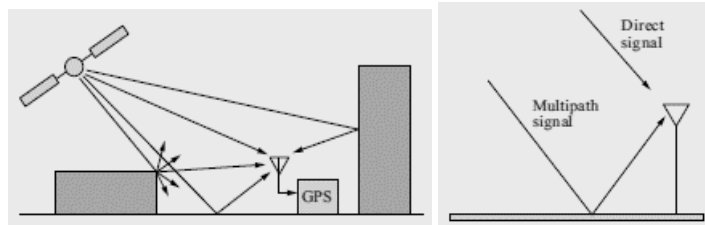
Figure 2.4: Visualizations of examples of multipath [32].

2.2.3. Important degrading factors at system level

System level degradation is caused by disturbances and/or variations that occur in the space segment, the ground segment and the interface between the two [25][26][32]. These degrading factors can cause excessive range errors.

- Satellite clock error: the used atomic clocks are very accurate, however subject to small inaccuracies over time (up to a millisecond), due to clock drift. This, in turn, causes a significant range error (up to several hundred meters) and needs to be corrected for.

- Orbit error: GNSS satellites travel in very precisely known orbits. These orbits are subject to (small) variations however. Similarly to a clock error, this causes a significant error in the determined position.

- Dilution Of Precision (DOP): which is related to the relative satellite-receiver geometry [11][15][32]. This affects the precision; when the satellites are clustered closely together or in one straight line, this results in a high DOP value and bad precision, where when they are widely spread/far apart, this results in a low DOP value and good precision. The Geometric Dilution Of Precision (GDOP) can be described by the combination of the PDOP and TDOP:
  - PDOP, the position (3D) dilution of precision (combination of HDOP, the horizontal dilution of precision and VDOP, the vertical dilution of precision).
  - TDOP, the time dilution of precision.

- Cycle slip: a cycle slip causes a discontinuity (jump or spike) in the locked, continuous carrier phase [11][15]. This will corrupt the carrier phase measurement, as the unknown ambiguity value from before and after the cycle clip will be different. In order for this to be repaired/corrected, a cycle slip detection algorithm, or a re-initialization is required. Cycle slips can be caused by obstructions, power loss, a failure of some kind, severe Ionospheric conditions or when the signal has a very low signal-to-noise (SNR) ratio.

- Antenna phase center offset and variation: not all the incoming GNSS signals do converge to the electrical center, within or outside of the antenna (antennas have no single well-defined phase center) [11][15]. This is dependent on the direction (elevation and azimuth) from which the GNSS signals are arriving, as well as on the intensity and carrier frequency of the GNSS signal. The electrical center is thus not constant, cannot be accessed, and also does not necessarily coincidence with the geometrical center.
  Therefore, a geometrical reference point is introduced on the antenna, where the vertical antenna axis of symmetry intersects with the bottom of the antenna [15]. The antenna center offset is the difference between the mean of the electrical phase center and this reference point and should be specified for each carrier frequency. The differences between the electrical phase center and the mean electrical phase center from individual observations are defined as the antenna phase variations. These deviations should be calculated in order to be corrected for. Note that when identical antennas are used and the baselines are relatively short, these antenna phase variations should cancel out, as they are identical [36].

Important degrading parameters / factors

User and / or user equipment level

Equipment overheating, power system outages, software incompatibilities etc.

Operational environment level

- *Intentional interference* Jamming, and spoofing
- *Unintentional interference* RFI
- *Signal propagation related influences* Tropospheric delay, Ionospheric delay, and multipath

System level

Satellite clock error, orbit error, dillution of precision, cycle slip, antenna phase center offset and variation

Figure 2.5: Schematic overview of the important degrading parameters/factors.

The Ionospheric delay, Tropospheric delay, orbit and clock errors, receiver noise and multipath are sometimes expressed as the User Equivalent Range Error (UERE), which is the square root of the sum of these parameters individually squared (: ~6-7 meter) [11][23]. In conclusion, there are numerous degrading factors (both intended and unintended) that need to monitored and dealt with (corrected for). This is one of the tasks of the reference network infrastructures, whose aim is to provide correction information that enables the determination of good quality positioning solutions. An IM component is required in order to ensure this indeed has been done sufficiently.

2.3. Integrity Monitoring

As defined at the start of this chapter, the integrity of a positioning system is the measure of trust that can be placed in the correctness of the information provided by this system. For the infrastructure user(s) it is very important to determine whether the positioning performance requirements, which are subject to the GNSS impact factors described in section 2.2, are met. If this is not the case, the system might not be providing trustworthy information. In that case, or when the integrity goes unmonitored, a notification (warning or alert) should be triggered as soon as possible. Some applications require these notifications more urgently than others; this is closely related to the type of application in which the reference network infrastructure is adopted. As mentioned before, utility mapping applications for example require sub-meter level accuracy, where applications such as autonomous vehicles, or flight guidance and control require a much higher standard (centimeter level) as structures and lives are dependent on it. Similarly, the ensuring of the quality of the information is more urgent in the 3D mapping projects as compared to the utility mapping.

In terms of the SiReNT infrastructure, the information is considered good if it can provide the user(s) with accurate (2-3 centimeter and 3-5 centimeter in the horizontal and vertical plane respectively) real-time positioning solutions at any time (independent of any circumstances). In this case, it can be used for all above-described applications, and serve as a solid IM foundation to improve upon.

In order to ensure information with good integrity, a stable GNSS-based positioning system is required. There are two main methods to monitor the stability of GNSS-based positioning systems (and its CORS). One is implementation at system level (external monitoring) and the other at user level (Receiver Autonomous Integrity Monitoring (RAIM)) [14][15][17][25][26]. These specific methods will be described in more detail in the following sections.

IM methods

System level - external monitoring	User level - Receiver Autonomous Integrity Monitoring (RAIM)
-> Ground-based vs. space-based	
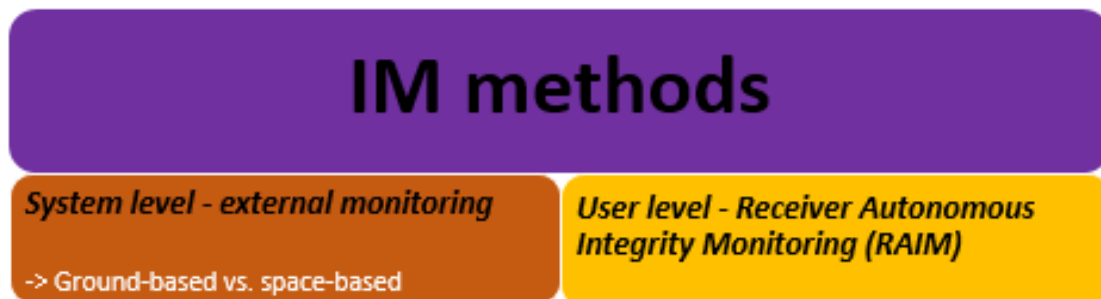
Figure 2.6: Schematic overview of the main IM methods

2.3.1. System level-external monitoring

This method uses the CORS of which the network consists, to continuously monitor the incoming signals and transmit information and corrections regarding any incorrect behavior [14][15][17][25][26]. One way in which this is done is by comparing the measured ranges with the ranges that are computed between the known locations of the satellites and these CORS (predictions). Another is by looking at the determined positioning solution itself; the baselines between the CORS can be measured and compared with the reference data. In case the measurement error is exceeding a certain pre-set threshold, it means a satellite has failed. The failing satellite is then excluded in order for the positioning to continue, assuming there are still sufficient satellites available.

When the measurement errors exceed the pre-set thresholds, the user(s) is/are to be warned within the TTA. A disadvantage of external monitoring is that it does not protect the system against local errors such as multipath. For this a combination with RAIM could be used (see section 2.4.2.)).

There are two types of external monitoring systems, ground-based and space-based systems [14][15][17][25].

Ground-based systems are usually employed in a more locally limited area, for example surrounding airports, in order to provide corrections for more stringent applications such as precision approach and landing operations. In this kind of networks, the information and corrections are broadcasted to the user(s) by the master station directly.

Space-based systems are usually employed in wider areas. These systems determine corrections regarding the satellite orbits, the satellite clocks, and the Ionospheric influence. In the space-based network, one or more geostationary satellite(s) is/are used (redundancy). In this case, the master stations relay the corrections and information to these geostationary satellites which in turn broadcast that to the user(s), along with the ephemerides and almanac information of these satellites themselves.

2.3.2. User level-Receiver Autonomous Integrity Monitoring

This method exploits observation redundancy in order to provide integrity [14][15][17][25][32]. This method is also known as internal monitoring, as the monitoring takes place within the receiver itself. It is aimed at detecting the existence of bad observations and the identification of the faulty satellite. For this, a statistical detection algorithm is used. Within this technique, it is first determined whether failure occurred. After confirmation, the observation (and thus satellite) that is failing is identified.

There are several types of algorithms including range comparison, residual comparison and position comparison [25][26]. The observations are either recorded per epoch individually (snapshot schemes) or involving observations from before a specific epoch (averaging/filtering schemes) [14]. In the latter method the last known range, residuals, position and velocity might have been used in order to predict the current observations. Preference for a specific method is usually based on computational complexity. Snapshot schemes are more often preferred as they do not assume anything regarding the motion of the receiver.

Whether this RAIM works (when used solely for determining a 3D positioning solution) depends on the number of satellites in range, assuming a good satellite geometry (if this is not the case, clearly more satellites are required) [14]:

- In case *less than 4* satellites are tracked, no 3D positioning solution can be determined in the first place, hence the user will not be affected by failure.
- In case *4 satellites* are tracked the determined 3D positioning solution will directly be affected. The error will not be detected however, and cannot be identified as all satellites will be used in determining this solution [25][26].
- In case *5 satellites* (redundancy of 1 satellite) are tracked however, the receiver is capable of detecting whether one of the tracked satellites is failing, resulting in large residuals in the positioning determination [25][26]. The failing satellite still cannot be identified however.
- In case *6 satellites or more* (redundancy of 2 or more satellites) are tracked, the receiver is capable of detecting, identifying and disregarding the failing satellites [25][26]:
    - When *exactly 6 satellites* are tracked, the failure detection and isolation (FDI) approach can be applied [14]. A special requirement for this approach is that no more than a single satellite can be failing at a specific instant of time however, as then there is not enough redundancy in the number of satellites.
    - When *more than 6 satellites* are tracked, the failure detection and exclusion (FDE) approach can be applied [14]. In this approach, a failing satellite does not have to be identified uniquely, which is a complex and elaborate task. Another positive point of FDE is that under it can deal with more than one failing satellite, even though the chance of that happening might be very low.

A summarizing overview of this is presented in Table 2.1.

One of the most well-known RAIM algorithms is the DIA (Detection, Identification, Adaptation) procedure [13][33]. This is a recursive procedure that is developed by the TU Delft. This procedure enables one to test different observation types simultaneously. Within this procedure systematic testing of observation errors, anomalies and failures (faults) takes place. This is done by hypothesis testing; a default model (the null hypothesis, H_0) is

considered versus alternative models (alternative hypotheses, H_a).

First, there will be a general test (Overall Model test) in order to check the validity of H_0. If its test statistic does not exceed a certain critical value, H_0 is accepted. However if it does, H_0 is rejected and the reason for the fault is identified. This critical value is based on the distribution of the test statistic, under the applied model (H_0 or H_a).

In the identification step a set of H_a's are considered one by one. These hypotheses are almost identical to H_0, involving small adaptations in the form of additional unknown parameters. These H_a are tested against the H_0 in order to find the most likely option (largest test statistic). Once the most

Table 2.1: Overview of RAIM possibilities following from the number of tracked satellites

No. of satellites	Possibilities
< 4	No 3D positioning solution can be determined.
4	3D positioning solution can be determined, however the failing satellite will not be detected.
5	3D positioning solution can be determined, the failing satellite will be detected, however cannot be identified.
6	3D positioning solution can be determined, the failing satellite will be detected, the FDI approach can be applied.
> 6	3D positioning solution can be determined, the failing satellite will be detected, the FDE approach can be applied.

likely H_a is determined, it is checked whether the critical value under H_0 and H_a are exceeded and not exceeded, respectively. If this is the case, this option is seen as most likely option and is accepted.

After the identification step, the fault still needs accounted for. This is done in the adaptation step, by applying the accepted model (H_a), in order to eliminate the faults.

This is then iterated, in order to make the system fault free (the system may contain multiple faults). The iterations continue until all faults are accounted for, or until the system ran out of redundancy (redundancy is what this algorithm is based on). Note that considering a large number of alternative hypotheses, involves a risk of incorrect detection. For further information, refer to [13][33].

RAIM is relatively cheap (compared to the System level-external monitoring), and could complement the external monitoring method, because [25][26]:

- It potentially could offer protection against Ionospheric influences and residual Tropospheric errors which might not be detectable by the external monitoring infrastructure;
- It works independently and regardless of the existence of any ground-based or space-based System level-external monitoring infrastructure;
- Its latency can be relatively short(er) (compared to the System level-external monitoring);
- It protects against local errors, such as multipath.

A big disadvantage of RAIM is that exclusion of satellites lowers availability. RAIM needs a minimum number of satellites and relies on the satellite geometry, therefore it is thus not always possible to apply RAIM. The increasing number of available GNSS constellations will increase the potential of RAIM, however.

<div style="text-align: right">

3.

</div>

Around the Globe

In order to gain a better understanding of the IM methods used in infrastructures similar to the SiReNT infrastructure, in this chapter first the methodologies adopted by the cadastral/mapping agencies in several other countries are reviewed. Following that, the methodology adopted for the SiReNT infrastructure is reviewed as well. The countries reviewed are the Netherlands, Australia (Victoria), Hong Kong, Malaysia, and thus Singapore. The choices with regards to the other countries are related to having personal contacts, their location and/or environment similarities.

3.1. Integrity Monitoring in the Netherlands

In the Netherlands, there are numerous different network infrastructures [43]. The Kadaster (Cadaster) for example, in collaboration with the Delft University of Technology (TU Delft), operates and maintains 40 CORS located throughout the Netherlands. These CORS are used by several agencies. The Cadastre itself provides surveyors of governmental authorities with a centimeter accuracy throughout the Netherlands in real-time, by operating and developing the Netherlands Positioning Service (NETPOS) infrastructure. This infrastructure is also used in observing the water vapour distribution by the Royal Netherlands Meteorological Institute (KNMI) [19][43].

Some of the NETPOS CORS are part of the AGRS.NL (Active GNSS Reference System) infrastructure as well [43]. This infrastructure provides the basis for the Geodetic infrastructure of the Netherlands and is used only for post-processing purposes (using the Bernese software [3]). Some of AGRS.NL CORS are providing data to the larger-scale IGS/EUREF Permanent GNSS Network (EPN) [43]. The EUREF is the Regional Reference Frame Sub-Commission for Europe.

Except for one, all CORS that part of the above infrastructures, are connected through a cable connection, as then it is not dependent on the availability of the cellular network. Currently, tests are being conducted with regards to using cellular or ADSL modems instead or as a backup.

The AGRS.NL/NETPOS infrastructures contain two independent, identical DCC's, where the incoming data gets assigned to one or the other, depending on availability. As for the receivers, different brands are used with overlapping coverage areas. This way, in case of failure of one of the specific brands, there are still enough CORS online to provide the user with proper ongoing quality.

IM

In the Netherlands, the stability of the small(er)-scale infrastructure is monitored using the relatively large(r)-scale infrastructure [43]. In the adopted approach the CORS of the latter are kept fixed, and the baselines between these fixed CORS and the observed locations (in

this case, the CORS that are part of the small(er)-scale infrastructure) are monitored continuously. By monitoring these baselines, it is ensured that the pre-set thresholds (with regard to the observed IM displacements) are not exceeded without issuing some type of notification (warning or alert). Following this method; the IGS infrastructure is used as fixed reference to monitor the EPN, which in turn is used (as fixed reference) to monitor the AGRS.NL infrastructure, which in turn is then used as fixed reference for monitoring the NETPOS infrastructure.

Besides the baselines with respect to the fixed reference CORS, the quality of the correction messages is monitored as well. This is done by using one (or more) Rover(s) and monitoring them continuously. The latter is done by permanently deploying actual Rovers specific locations, as well as by simulating them when and wherever they may be required, using the VRS mode. These Rovers, or so-called land meters, are programmed to restart every 15 minutes, fixing the solution and (re)measuring its location. This way it can be determined whether the system is working properly, by comparing the observations with the reference data.

On top of this, there is real-time monitoring of the power supplies and the raw data. If it is incomplete or including errors, it is fixed and if an observation is bad, then this will not be used. The AGRS.NL infrastructure even contains an extra data integrity check; the data is also checked for its completeness using the TEQC (Translation, Editing and Quality Checking) software.

Algorithms/software
As for the IM at observation level, in order to determine whether a certain observation is within the threshold, something similar to the DIA procedure from the TU Delft is applied [43]. This includes several statistical tests, such as the overall model test and the t-test. This goes for both the real-time software (GNSMART from Geo++) and the Bernese software [3]. Within the Bernese software specific inputs, like the Coordinate Reference System (CRS), precise satellite tracks, and other settings can be specified and changed, as well as what kind of output is required to be generated. Within this software outlier detection and quality control is applied. Note that when the preferred settings are applied, the software is assumed to be working properly, even though in the end it's a 'black box'.

IM visualization
In order to visualize the IM information (availability and usability) from the NETPOS infrastructure (and thus part of the AGRS.NL infrastructure) for the user, a dashboard (see Figure 3.1) is created, containing the following parameters [24]:
- The total number of users within a certain distance. If a hand phone is used then it will use a circle (0-35 kilometer, 35-60 kilometer, or 60$^+$ kilometer) around its location to find the number of users within that radius that got their fixed solutions (versus float), however in case a desktop is used, this circle will be centered around Amersfoort instead.
- Which CORS are up and running (have a fixed solution).
- Which (and how many) satellites are visible for all CORS simultaneously and have a fixed solution.
- The regional Ionospheric delay (the I95 value).
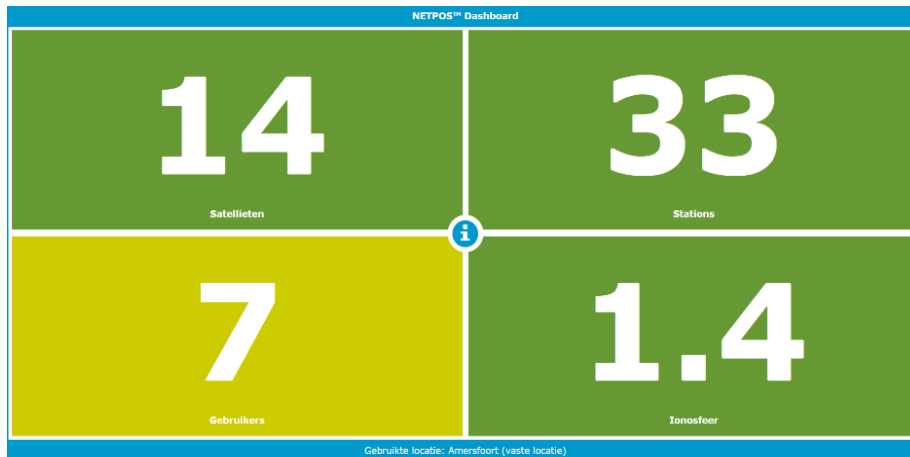
Figure 3.1: Figure visualizing the NETPOS dashboard in Real-Time [24]. The number of fixed satellites is presented in the upper left panel, the number of fixed CORS in the upper right panel, the number of connected users (fixed solution versus float solution) within a certain range of your position in the bottom left panel, and the Ionospheric delay (represented by the I95 value) in the bottom right panel.

The infrastructure administrators also have access to a real-time map, containing the same information, but then for the whole of the Netherlands. This is the case, as when issues arise, they need to know where what is happening in order to provide the right kind of service. The number of users per hour, as well as the history, is being logged so that this data can be requested and analysed afterward as well.

Regular checks
The AGRS.NL/NETPOS CORS are surrounded by stable control points that are used to check the CORS' stability (every 3-4 years), using theodolite, tachymeters and total stations. More specifically, this is done in order to check whether the CORS moves due to change in location and not the antenna with respect to the CORS itself. The latter can happen due to for example a change in setup or system instability. Note that after software updates slight changes in the observations often occur, however these are assumed to be improvements.

Certification
The AGRS.NL infrastructure is assumed to be very stable and therefore is used to annually verify the coordinates of other infrastructures in the Netherlands (06-GPS etcetera). The CORS of these infrastructures are then included in the AGRS.NL infrastructure, in order to get them certified and linked to the same reference system. In order to do this, 3-7 days of data is provided to the Cadaster. This certification verifies and shows that the specific coordinates are seen as truth and can indeed be used as a reference. On top of that, there is also a daily, post-processed, certification computation.

3.2. Integrity Monitoring in Australia (Victoria)

In Victoria, Australia, the State government in cooperation with the industry, academic institutions, and the community, has launched the statewide GPSnet infrastructure [1][6][42]. This infrastructure consists of over 20 CORS (relatively more concentrated in urban regions and less concentrated in the rural regions) and a DCC, and is been developed in order to provide homogeneous, consistent and reliable (network) RTK and DGPS data services for positioning and navigation purposes. This is aimed at different applications and users, such

as mining, precision farming, and surveying and mapping. Users of this infrastructure are provided with up to centimeter accuracy, dependent on the CORS baseline separation, equipment and techniques used. The infrastructure contains a variety of antennas and receivers, and is capable of storing the GNSS data for post-processing purposes.

IM

The stability and thus utility of the infrastructure is monitored in several different ways (in real-time and through post-processing), by Geoscience Australia. The stability of the CORS and its coordinates are monitored, with respect to several IGS CORS, over both short and long time periods.

Each GPSnet CORS also has the ability to monitor its performance and quality (in terms of the number of satellites tracked, SNR's, multipath etcetera).

Finally, the availability of the GPSnet CORS as well as the data streams is monitored, using a caster via an external NTRIP (Networked Transport of RTCM via Internet Protocol) monitoring service. NTRIP is the primary international standard for sending and receiving GNSS data such as correction streams, over the internet. In order to provide more than one client with GNSS data in real-time, more than one data stream is required. The NTRIP caster enables this and thus plays a critical role in GNSS infrastructures and real-time correction services. Therefore, the availability of the caster server and the NTRIP data streams is monitored continuously.

Geoscience Australia also operates the Australian Fiducial Network (AFN), contributing to the global IGS network, and providing a stable reference for monitoring GPSnet. Redundant facilities, for backup purposes, are in place in case something happens.

Software

In order to guarantee quality and reliability, this infrastructure is being monitored using purpose-written software. Within this monitoring method, there is a focus on two main aspects, the quality and integrity of the raw data, and the utility and stability of the infrastructure.

As for the first aspect, the raw data is pre-processed and analysed, and in case there are parts of the data missing, this is fixed. If an observation is corrupted, due to for example multipath, cycle-slips or latency, then that specific part of the data will not be used. This check is also done in order to check whether the GNSS receivers are working properly.

As for the second aspect, for this Trimble's Rapid Motion engine module, Network Motion engine module, and the Post Processing engine are used, to monitor the CORS stability internally (see Appendix 1 for more details on these specific engines). In this, the IGS precise ephemerides products (ultra-rapid and post-processing), Earth orientation, and velocity parameters are used.

IM visualization

The status of the specific CORS from the GPSnet infrastructure is visualized through a CORS interactive map (see Figure 3.2). In this map, the colour of the station markers represents the status of the specific CORS; green indicating that the CORS is online and healthy, yellow indicating that the CORS is online but that there is a problem, and red indicating that the CORS is offline. Besides that, here users can access other specific details of any CORS of interest, such as the health status, its location and the type of used equipment.
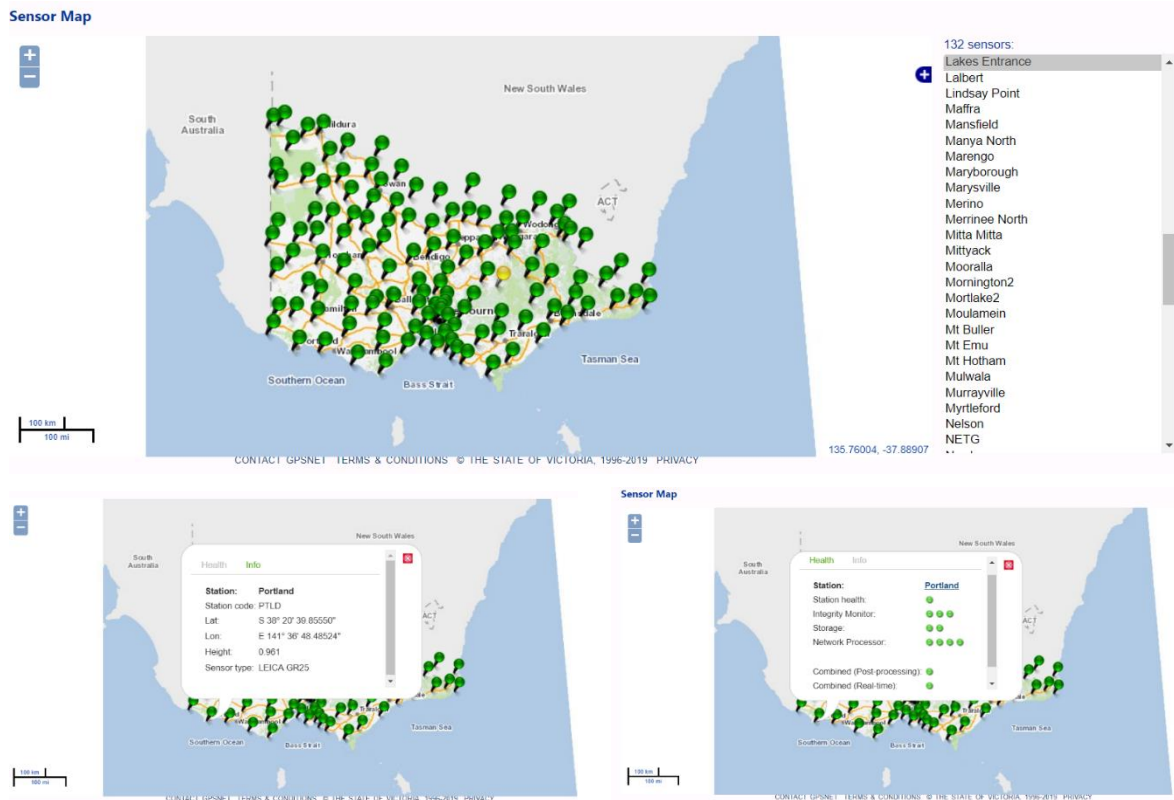
Figure 3.2: The GPSnet sensor map presenting an overview of the health of all the CORS (top) as well as the specific information and more detailed health information for a selected CORS (bottom left and right, respectively). Source: GPSnet website.

3.3. Integrity Monitoring in Hong Kong

In Hong Kong the Geodetic Survey Section of the Survey and Mapping Office of Lands Department developed and operates the Hong Kong Satellite Positioning Reference Station Network (SatRef), in order to provide (network) RTK and DGPS data services [20][31][48]. This network consists of eighteen evenly distributed CORS (10-15 kilometer apart), an IM station and a DCC. This distribution ensures that any user can access at least two CORS within a 10 kilometer radius, throughout most of Hong Kong.

These CORS are equipped with GNSS receivers and meteorological sensors. The CORS located on the hilltops are also equipped with tilt sensors. The meteorological sensors are installed to observe meteorological parameters for atmospheric analysis, such as the temperature, pressure, and humidity, where the tilt sensors monitor the stability of the CORS. Using this network results in a network RTK solution with centimeter accuracy and a DGPS solution with (sub-)meter accuracy. This is aimed at applications such as the real-time monitoring of deformation, as well as Precipitable Water Vapour (PWV) estimation, emergency services, navigation, and all sorts of surveying applications.

The data is transmitted through data lines, however the CORS contain backup modems, in case the network transmission fails. The historical data is archived in order for it to be available for the users upon request.

IM

In order to ensure the quality and reliability of these services, the network is continuously monitored. This is done in several different ways; by real-time monitoring the determined

29

(differential) correction data, the (high-precision) baselines, the transmission of the raw data from CORS to the DCC, and the system equipment.

The determined correction data is monitored by simultaneously using two of the CORS as Rover, in order to continuously carry out a network RTK survey by receiving the correction data. This way it can be determined whether the system is working properly in real-time, by
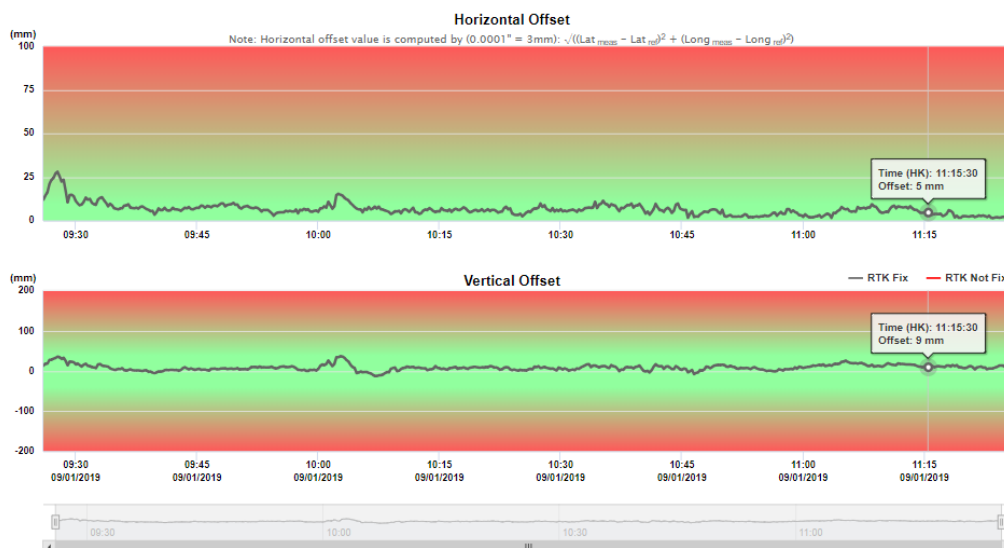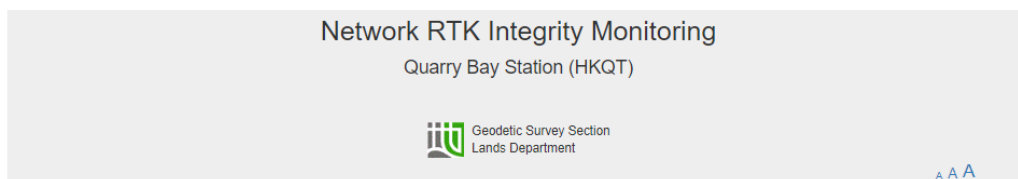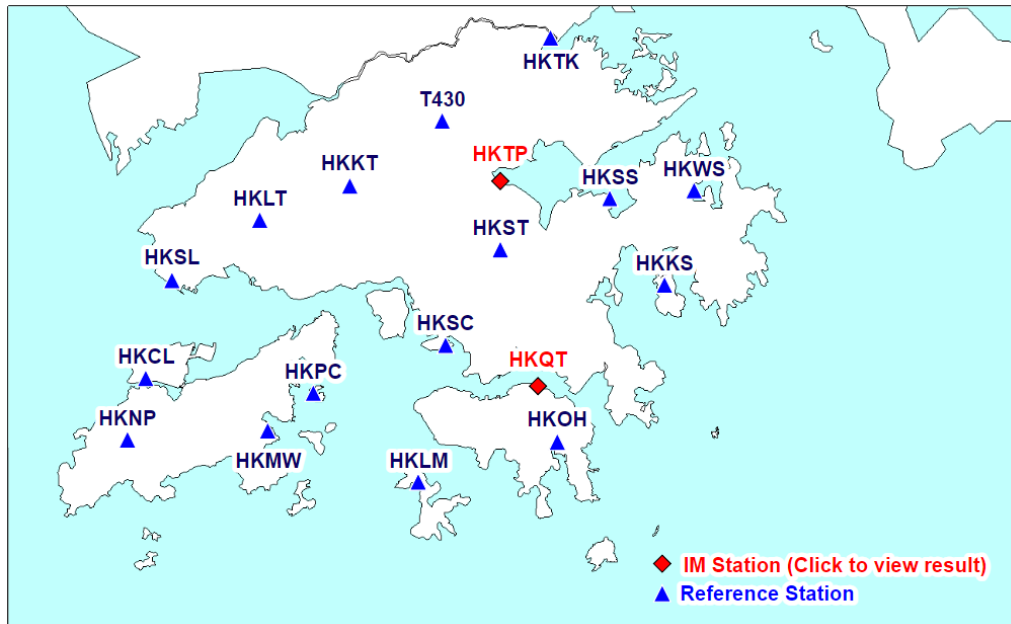
Figure 3.3: A map presenting the SatRef CORS in Hong Kong (top), and graphs visualising the Network RTK IM results as observed by one of the two IM CORS of SatRef; HKQT (bottom). These IM results are separated into two graphs, one for the offset in the horizontal plane, and one for the offset in the vertical plane. Source: SatRef website

comparing the observations with the reference data. Internally these observations are integrated to form a plane, in order to effectively monitor the performance of the network RTK system continuously.

The CORS are monitored weekly by using the surrounding CORS of the Asia-Pacific Reference Frame (APREF) as a stable geodetic reference. The baselines between each CORS and its 2 closest neighboring CORS are determined continuously. The baselines are used as input in a GNSS data quality control software for the visualization of the determined solutions, and in order to check the data integrity.

Besides that, the power supply for the CORS is monitored as well. Most of the SatRef CORS are equipped with Uninterrupted Power Supply (UPS) units to ensure that the CORS can work continuously and continue to do this for 4 days, even in case of any power failure. Whenever any failure occurs, the system will alert responsible officers immediately. Redundant facilities are in place, serving as backup, in order to allow fast recovery of service and lost data due to accidents.

Software

The Bernese software [3] is used, in order to perform high-precision post-processing of the GNSS data. For this, the IGS precise orbits are used.

The TEQC software is installed to monitor the transmission of raw data between SatRef CORS and the DCC in real-time. The software will indicate the time and duration for data lost, if any.

IM visualization

The main monitoring results and related status of the specific CORS, as well as the observations from the meteorological sensors, are visualized for internal use only.

The results from the continuous network RTK survey is accessible by the SatRef users, however (see Figure 3.3). This to give the user an indication of the quality of the correction data.

The IM displacement data observed by the 2 CORS, that are used for this, is visualised in two graphs, one for the offset (of the observation from the reference position) in the horizontal plane, and one for the offset in the vertical plane.

3.4. Integrity Monitoring in Malaysia

The integrity of the positioning system is as important as the accuracy of the position solution. The National Space Agency (ANGKASA) in collaboration with the University Technology Malaysia (UTM) therefore has developed the GNSS IM system for space-based positioning and navigation purposes in Malaysia [27][28]. This infrastructure includes 5 CORS, a DCC at ANKASA, and a processing center at UTM. Using this infrastructure results in a DGPS solution with (sub-)meter accuracy.

The infrastructure contains redundant parts, serving as a backup in order to ensure reliability.

IM

The aim of IM is to detect any possible causes for failure, such as satellite anomalies or anomalies in the transmitted GNSS signals or correction data, and alerting the infrastructure users in a timely fashion in case the monitored parameters exceed specified thresholds. The IM system can be subdivided into several levels; system-level, monitoring station-level and

user-level.

The system-level IM is based on the satellites, where monitoring the station-level IM is based on the CORS. The latter is aimed at processing and enhancing signal data at the CORS, in order to monitor its stability. The conducted method to determine the stability of the satellites as well as the CORS, is to compute the expected range between each of the CORS and the satellites. For this IGS's precise orbits are used as input. This predicted range is then compared with the observed range in real-time. This particular method favours extracting the satellite and signal anomalies, such as the multipath effect, the different kind of atmospheric delays, the receiver clock error, possible cycle slips, and any errors that might be included in the broadcast ephemerides. On top of that, the incoming raw data is monitored for completeness in real-time.

The user-level IM approach is aimed at monitoring the quality of the correction data. This is done by using some of the CORS as Rover, continuously carrying out GNSS pseudorange observations by receiving the DGPS correction data. This way it can be determined whether the system is working properly in real-time, by comparing the obtained observations with the reference data. All data is stored for post-processing purposes.

IM visualization

The information is visualized through a real-time dashboard application, according to the different levels. Included in this application is a map visualizing the health status of the CORS; green indicating that the CORS is online and healthy and red indicating the opposite. Through this application, the user can also access the specific details about the particular CORS, including the SNR, the sky plot and the GNSS elevation. Besides that, it also presents the satellite constellation status. Also included is the status of the user-level IM. Here the Rover, as well as the CORS (which is used as base station), are visualized in real-time, accompanied by the following:

- Time and date;
- Bassline length;
- Solution type (DGPS or RTK)
- Observations (northing, easting, and height, including standard deviations)
- Number of simultaneously tracked satellites.

3.5. Integrity Monitoring in Singapore

In Singapore the stability of the SiReNT infrastructure and its CORS is very important as well. As described in section 1.2, this infrastructure is operated and maintained by SLA. SLA also contributes to the global IGS network, by delivering data from the SNUS CORS. Any further general information can be found in this section as well.

IM

The IM of this infrastructure, and its CORS, is performed both in real-time and through post-processing.

The IM is done by monitoring the baselines, and displacements from the reference positions, as observed by the CORS, the completeness and transmission of the raw data from CORS to the DCC, and the system equipment.

Finally, just like with GPSnet CORS, the availability of the SiReNT CORS as well as the data streams are monitored, using a caster via an external NTRIP monitoring service. Similarly to

the infrastructures in the other countries, the SiReNT infrastructure contains redundant parts, serving as a backup in order to ensure reliability.

Software
For the network processing and in order to perform IM, the Trimble Pivot Platform (TPP) is adopted. A detailed analysis of this specific software package can be found in Appendix 1. Through this software package, the raw data is pre-processed and analysed, and fixed, in case there are parts of the data missing. If an observation is corrupted, due to for example multipath, cycle-slips or latency, then that specific part of the data will not be used. This check is also done in order to check whether the GNSS receivers are working properly.
For IM several engine modules are available depending on the required specifications (more on this in Chapter 4)**:** the Network Motion engine module, the Rapid Motion engine module, and the RTK engine module, and the Post-Processing engine module.
These engine modules are combined with an integrity monitoring module, which is linked to an Alarm Manager, in order to trigger notification (warning or alert) messages in case displacements or errors exceed pre-set thresholds.

IM visualization
Just like GPSnet, the status of the specific CORS from the GPSnet infrastructure is visualized through a CORS interactive map. In this map the colour of the station markers represents the status of the specific CORS; green indicating that the CORS is online and healthy, yellow indicating that the CORS is online but that there is a problem, red indicating that the CORS is online but unhealthy, and grey indicating that the CORS is disarmed (more information on this can be found in Appendix 1) and/or offline.
The observed displacements with respect to the reference position are also visualized, per CORS, in a scatterplot. Besides that, here users can access other specific details of the particular CORS, such as the health status, its location and the type of used equipment.
On top of what is visualized through the website, IM reports are being generated every three days. These IM reports include displacement charts, and scatterplots, as well as Statistical Point Overviews, per CORS. These reports are only presented to the network operators and infrastructure administrators and not to the infrastructure user(s) (see Appendix 2 for an example IM report).

For more details on how the TPP software package is used in the IM and what information is being visualized, please refer to Chapter 4 (and for a more elaborate review of the software package in general, see Appendix 1).

3.6 Concluding summary/overview
The different countries have quite some similarities in the way in which IM is performed, and the resulting information is presented/visualized. A summarizing overview of the most important details/findings is presented in Table 3.1.

Table 3.1: Overview is of the most important details/findings presented in this chapter, per country.

Countries	Specifics	Netherlands	Australia (Victoria)	Hong Kong	Malaysia	Singapore
IM	*External monitoring*	X	X	X	X	X
	RAIM					Possible
	Correction stream	X		X	X	Possible
	Other (power supply, connectivity, etc.)	X	X	X	X	X
Software	*Bernese*	X	X	X	X	
	GNSMART	X				
	TEQC	X		X		
	TPP		X			X
Redundant/backup facilities in place		X	X	X	X	X
Surrounding (IGS) infrastructure(s) used		X	X	X		
IM visualization	*Health status*	X	X	X (internal only)	X	X
	(Displacements of) Observations			X	X	X
	Atmospheric information (I95 value, temperature, pressure etc.)	some				X
	No. of users and their fix status, no. of simultaneously tracked satellites etc.	X			some	
Cooperation with other parties		X	X			
Regular checks using non-GNSS methods		X				

4.

SiReNT and the Trimble PIVOT Platform

As stated before, the stability of the SiReNT infrastructure and its CORS is very important. In this chapter, the way in which the TPP software package enables the IM of the CORS' stability of the SiReNT infrastructure, and the visualization of all information, is reviewed. The IM part of the TPP software package consists of several different Apps and modules, each with specific tasks, constantly working together in order to determine the quality of the infrastructure. First, the specific Apps and modules used in the IM (the 6th functionality, see section A.1.2) of the SiReNT infrastructure are reviewed. Besides this, an (optional) monitoring App, aimed at the determined positioning solution (by a Rover antenna), while using the SiReNT correction stream, is reviewed. Finally, the generated information as visualized through the TPP Web App is briefly discussed.

An overview of the Apps and modules discussed in this chapter is presented in Table 4.1. Note that the values presented in this table, are the values advertised by Trimble, hence they are probably the most optimal values as they are recorded under ideal circumstances. The values observed in reality might therefore differ from this. For more details on the TPP software package, including the Apps and modules described in this chapter, please refer to Appendix 1.

4.1. Controlling and IM

As described before, IM consists of multiple different parts, for example the satellites and their health, as well as the raw data, is continuously monitored by the GNSS receiver modules, and besides that the completeness of the correction data, the connectivity integrity and the integrity of the system equipment and the power supply are also monitored continuously. As for the IM of interest, the TPP software package provides *Trimble Integrity Manager (TIM)*, which provides real-time and post-processing engines to monitor the
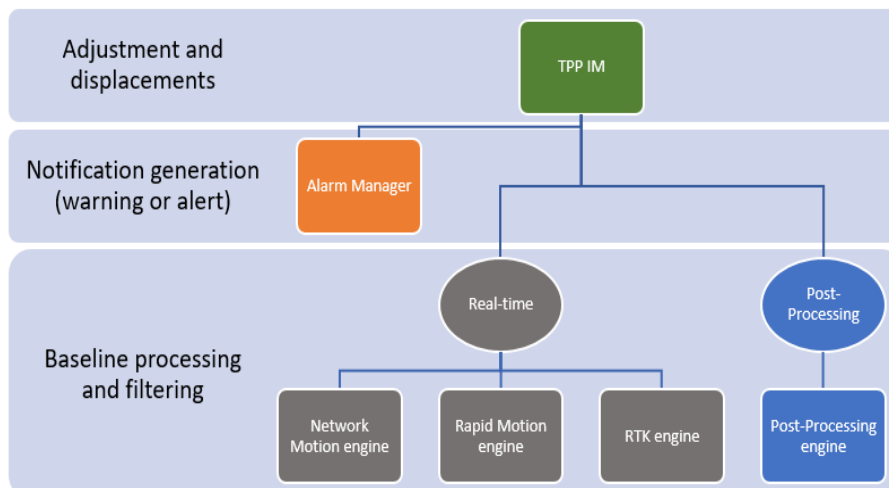
Figure 4.1: Schematic representation of the TPP IM of the CORS' stability.

movement and/or quality of the GNSS CORS with respect to one or more selected, fixed station(s), the real-time and post-processing engine modules to monitor the movement and/or quality of the GNSS CORS with respect to one or more selected, fixed station(s) (for a schematic representation, see Figure 4.1).

As mentioned in section 3.5, depending on the required specifications (see Figure 4.2) one can select from several baseline processing engine modules for IM purposes: the Network Motion engine module, the Rapid Motion engine module, the RTK engine module, and the Post-Processing engine module.
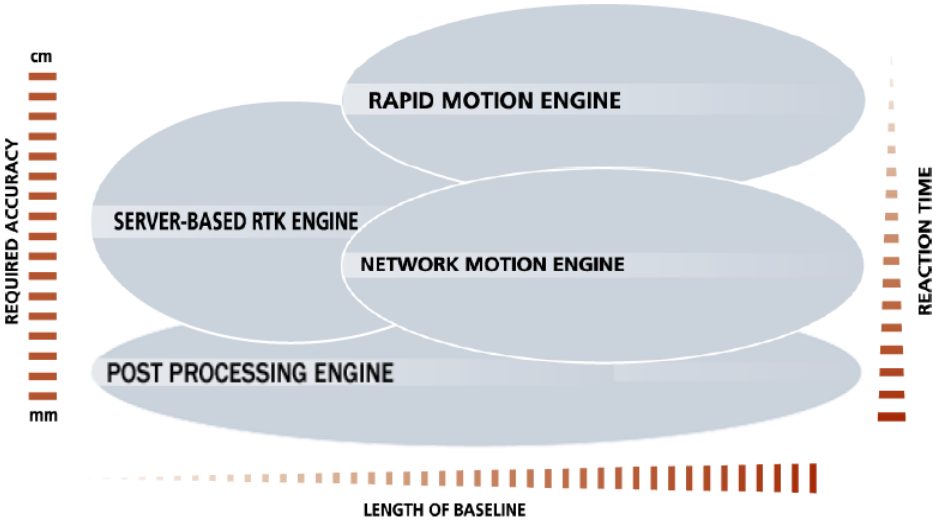
Figure 4.2: Visualization of when to use the different TIM engine modules, depending on the required accuracy, baseline length and reaction time [35].

The real-time engine modules are added under Synchronizer modules in order to make sure that the input data is synchronized and are able to run simultaneously [10][36]. Input to these engine modules are their ('true') reference positions and the raw data. Keep in mind that this raw data already has gone through the process described in section A.1.2 (see *'The TDC App (module: GNSS Receiver, RTO Single Station, Synchronizer)',* and thus has been analysed, checked, and corrected for errors already.

Using this information, baseline processing takes place. In this process, user-defined filtering methods can be applied in order to smooth and remove outliers from the determined position solutions. Whenever baselines are determined, redundant baselines can be used in order to get better results.

These engine modules are combined with the Integrity Monitor module in order to perform adjustments, and determine and display the displacements between the positioning solution and the known coordinates, in numerical and graphical form.

The workflow for the Post-Processing engine module is very similar, however stored raw data and rapid or final orbits are used as input for the baseline processing. The Integrity Monitor module is linked with the Alarm Manager to trigger notification (warning or alert) messages in case displacements or errors exceed pre-set thresholds. The so-called 'time-to-detect' is the actual time required for an engine module to detect motions/movements after an event has occurred. It is the minimum processing time required for each engine module for detecting a movement and consequently trigger such a notification [46].

The Alarm Manager can also be configured to trigger warning messages in case there are problems with any of the CORS in terms of a lost fixed solution.

Table 4.1: Overview of the different engine modules participating in the monitoring [10][30][36][38].

App-(Engine) Module	Aim	Reaction time (rt) & min. time-to-detect (mttd)	Scale	Products	Measurement accuracy
TIM-Post Processing	Static or Kinematic post-positioning.	Rt: slow (post-processing) mttd: 15 minutes (after starting the processing)	All scales	- Baseline components (dx, dy, dz) - Offsets from reference positions (ΔN, ΔE, Δh, Δ2D, and Δ3D) - Associated (co)variance matrices	1 mm
TIM-Network Motion	Detect (slow) deformation and counterchecks.	Rt: slow mttd: 3 hours (after ~24-hour convergence)	All scales	- Offsets from reference positions (ΔN, ΔE, Δh, Δ2D, and Δ3D) - Associated (co)variance matrices - Continuous information on the (accumulated) time used to determine each station.	10 mm (horizontal), 20 mm (vertical)
TIM-Rapid Motion	Detect deformations due to events such as earthquakes or landslides (with focus on the occasionally rapid movements (min. 2 cm/sec))	Rt: fast mttd: 1 second	All scales	- Offsets from reference positions (ΔN, ΔE, Δh, Δ2D, and Δ3D) - Associated (co)variance matrices.	2 cm/sec
TIM-RTK	Detect real-time movements.	Rt: fast mttd: 1 second	Small to medium scale (max. baseline length: 35 km) (Baselines mode) or all scales (VRS mode)	- Offsets from reference positions (ΔN, ΔE, Δh, Δ2D, and Δ3D) - Associated (co)variance matrices.	2 cm
TIM-Integrity Monitor	Compute network adjustment and displacements, and minimize applied corrections by detecting blunders and large errors.	-	-	- Updated positions over time - Data visualization - Alarm generation	-
TIM-Alarm Manager	Notify the user(s) in case thresholds are exceeded.	-	-	Notifications (warnings or alerts) (+ information mode)	-
TRI (Rover Integrity)	Determine the Rover performance; monitor correction information & Initialization performance	-	Within bounds of the network infrastructure	- Statistics (average offset, RMS, 1σ standard deviation). - Graphs	2 cm

Whenever the CORS positions are updated (periodically, for example to correct for known velocities), the estimation processes are reset and the processing sessions are restarted using the updated coordinates.

The Trimble Rover Integrity (TRI) can be adopted to monitor the performance of Rovers (through permanent Rovers or through using the VRS mode) that are deployed within the bounds of the GNSS reference network infrastructure while they take into account the incoming correction data [10][36]. The quality of this correction information can be measured based on the initialization (time-to-fix) and the quality of the positioning solutions. The time-to-fix is tested by periodically re-setting the Rover(s). It can this way also be used to specifically investigate the initialization performance. The quality of the positioning solutions can be measured by comparing the position solution resulting from each re-initialization at a known position, with the reference coordinates. There is no connection with the TPP IM that will trigger notifications (warnings or alerts). Note however that this App is currently also not in use in Singapore.

Side note

Note that SNPT CORS is used as a fixed reference, as it is centrally located and according to SLA belongs to the few most stable CORS in the infrastructure (moving lesser relatively to the other CORS).

Initially the SING CORS, also centrally located, was proposed as a fixed reference by SLA. This CORS is assumed to be even more stable as it is rock anchored in the Dairy Farm nature reserve. However, the SING CORS was not maintained by SLA and cannot always be accessed immediately in case of problems, hence the SNPT CORS is selected as a more convenient option. Due to the fact that the SNPT CORS is used as a fixed reference, its IM displacements should always be zero. Therefore, its observations are corrected for that. These corrections are also applied to the displacement data of the remaining CORS.

4.2. Data visualization

For visualization purposes, the Network and IM (related) information is divided into Network Information and Atmospheric Information. All this information is presented on the SiReNT Web App and accessible by the user(s), unless stated otherwise.

4.2.1. Network Information

The Network Information visualizes whether the specific CORS are online and providing the appropriate quality (dependent on the chosen engine), as well as the observed (displacement from the) positions of these CORS with respect to the reference position. This is represented by a sensor map and a position scatterplot respectively (for the timespan of one's choice). In this sensor map the colour of the station markers represents the status of the specific CORS; green indicating that the CORS is online and healthy, yellow indicating that the CORS is online but infected, red indicating that the CORS is online but unhealthy, and grey indicating that the CORS is disarmed and/or offline. Besides that, here users can access other specific details of the particular CORS, such as its location and the type of used equipment (see Figure 4.3). The presented scatterplot is generated by the Network Motion

Sensor Map

Health   **Info**

Station: **Loyang**
Station code: SLYG
Lat: N 1° 22' 21.44708"
Lon: E 103° 58' 18.00928"
Height: 51.158
Sensor type: TRIMBLE NETR9

Position Scatter Plot

Timespan: Last 24 hours ▼
Sensor: Loyang ▼
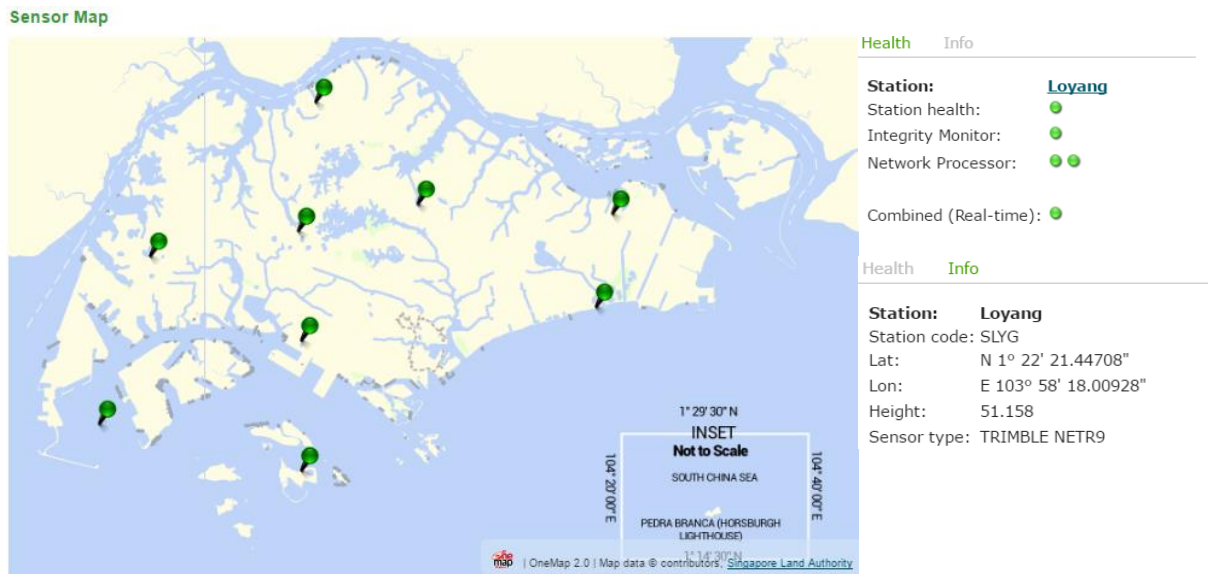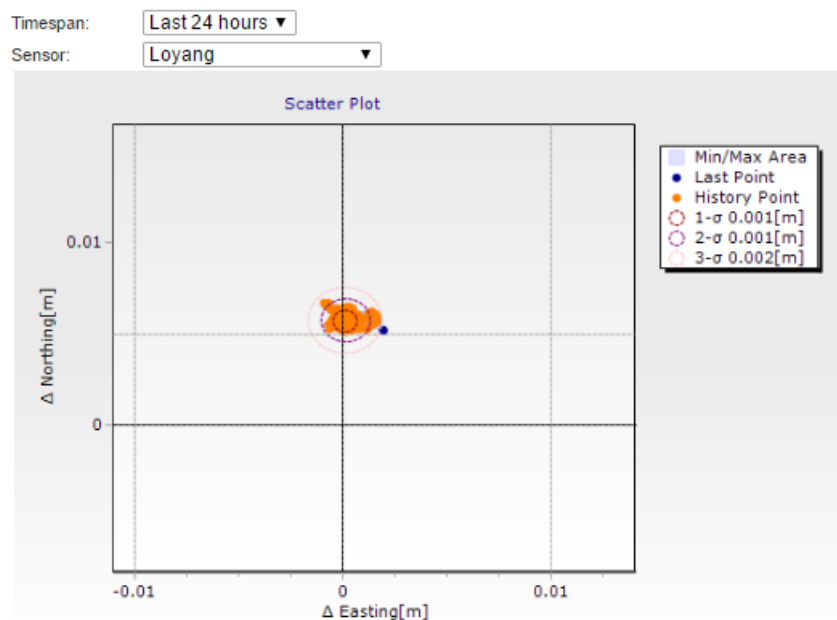
Figure 4.3: The SiReNT sensor map presenting an overview of the health of all the CORS (top left) as well as the specific information and health, for a selected CORS (top right), and a Scatterplot example, resulting from the Network Motion engine (bottom). Source: screenshot from TPP Web App.

engine module as that generates the most stable results. IM reports including these scatterplots, but also Statistical Point Overviews and displacement charts are generated every 3 days, visualizing the different parameters (ΔN, ΔE, Δh, Δ2D, and Δ3D), per CORS. These reports are only presented to the network operators and infrastructure administrators and not to the infrastructure user(s) (see Appendix 2 for an example IM report). Note that in the IM reports the SNPT CORS is omitted, as this is the fixed reference. Besides that, the SING CORS and the SNSC CORS were down during the specific period presented by the example IM report, hence they are omitted as well. Besides that, the included charts for the SLYG CORS are empty, just because the SNSC CORS was down [49]. Why this is the case, and what is the underlying relationship is not understood

Note that In the charts the notification (warning or alert) limits are included, however sometimes invisible due to the used range of the y-axis. This range is dependent on the maximum and minimum displacement during this period. Optional to include are the number of tracked satellites, PDOP values, (3σ) error envelope, and the linear trend of the data.

When these charts would present data over a longer period, they could be used when looking into possible trends over time. However, the IM reports generally span a period of 3 days. Also, since there is only a record of just over a year for most CORS (in the current configuration), the available data might not be representing the trend properly at this point in time.

This data can also be extracted in the form of an excel datasheet, presenting all the different parameter values alongside (co)variance matrix values.
When looking at the displacement graphs in the IM report, sometimes very large sudden displacements seem to occur. These anomalies are not (always) caused by observed motion, but can most of the time be related to breaks/disruptions in the data flow, atmospheric conditions, actual physical movement at the site, multipath, obstructions, and satellite geometry. When this occurs for longer than 60 seconds, this engine module needs to converge again. This process takes time and is usually visible in the graphs. This way it is (often) possible to conclude from the graph whether a certain anomaly was caused by actual motion or something else.

4.2.2 Atmospheric Information

Atmospheric Information presents the different atmospheric parameters related to the earlier described atmospheric errors (Ionospheric delay and Tropospheric delay). These parameters include the I95 value, the Ionospheric Residual Integrity Monitoring (IRIM) index and the Geometric Residual Integrity Monitoring (GRIM) index, the IPWV, the ZTD values, and the TEC values.

Table 4.2: The different I95 regions and their impact on GNSS observations

I95

The I95 value represents the Ionospheric activity accompanied by its expected influence on the relative GNSS positioning solutions (both (network) RTK and DGPS) [36][39]. This value is determined hourly from Ionospheric corrections of all satellites at all SiReNT CORS. All CORS that are part of the same network, hence all SiReNT CORS, will thus show the same I95 value [39]. The determined value is the 95% value, as the worst 5% of the data is rejected, hence the name 'I95'. This value is

Value	Ionospheric disturbances
0-2	Negligible
2-4	Weak Ionospheric disturbances
4-8	Strong Ionospheric disturbances
8>	Very strong Ionospheric disturbances
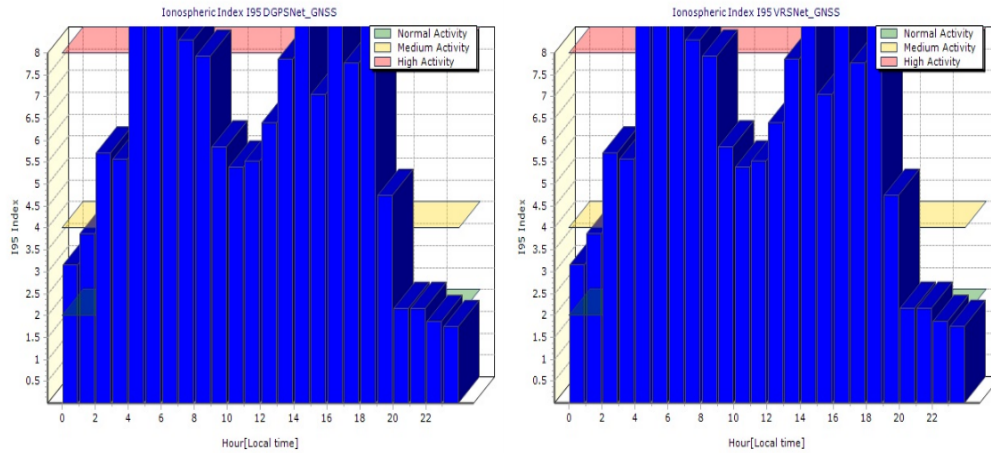
Figure 4.4: An example of the I95 value per hour from DGPS (left) and Network RTK (right), as presented through the TPP Web App. Source: screenshot from TPP Web App.

visualized in a real-time graph, see Figure 4.4. The different I95 regions and their impact on GNSS observations are visualized in Table 4.2. In chapter 7 and 8, the impact of the Ionosphere (represented by the I95 value) is analysed further in combination with IM displacements recorded at the same time.

IRIM/GRIM

The two largest factors affecting the performance of the Rover(s) that are using the SiReNT infrastructure are the differential Ionospheric residual errors and geometric errors between the SiReNT infrastructure and the Rover(s) [36][39]. The first are related to the Ionospheric activity and the latter are related to the Tropospheric activity and orbit errors, and together they are called the Network Processing residuals. Knowing the impact of these residuals would aid and improve the Rover(s) performance.

The Network Processor module attempts to remove the linear parts of these residuals by applying (Ionospheric and geometric) corrections to the raw data, during the network processing [36]. However as both the Ionospheric and geometric conditions are variable, these residuals cannot be considered to be entirely linear. This means that the non-linear part of the residuals will remain in the correction message sent to the Rover(s). The IRIM and GRIM indicate how much the Ionospheric and geometric impact factors, respectively, differ from a linear spatial variation.

The Network Processor module attempts to predict these Network Processing residuals by omitting the CORS of interest from the interpolation and comparing the observations at that CORS with the interpolation results, for all satellites. This way, the Network Processor accumulates hourly RMS values of all CORS (except those CORS forming the edges of the infrastructure), for the Ionospheric part as well as for the geometric part. It computes the 95% interpolation uncertainty value, where the worst 5% of the data are rejected. The highest then remaining values per hour are displayed through the TPP Web App, as IRIM and GRIM, respectively (see Figure 4.5). In these figures, this information is visualized for the SiReNT infrastructure as a whole. Note that this information is presented separately for DGPS and VRS as well. In the graphs, a value of 0.00 meters represents no predicted impact, and a value beyond 0.50 meters represents the highest predicted impact.
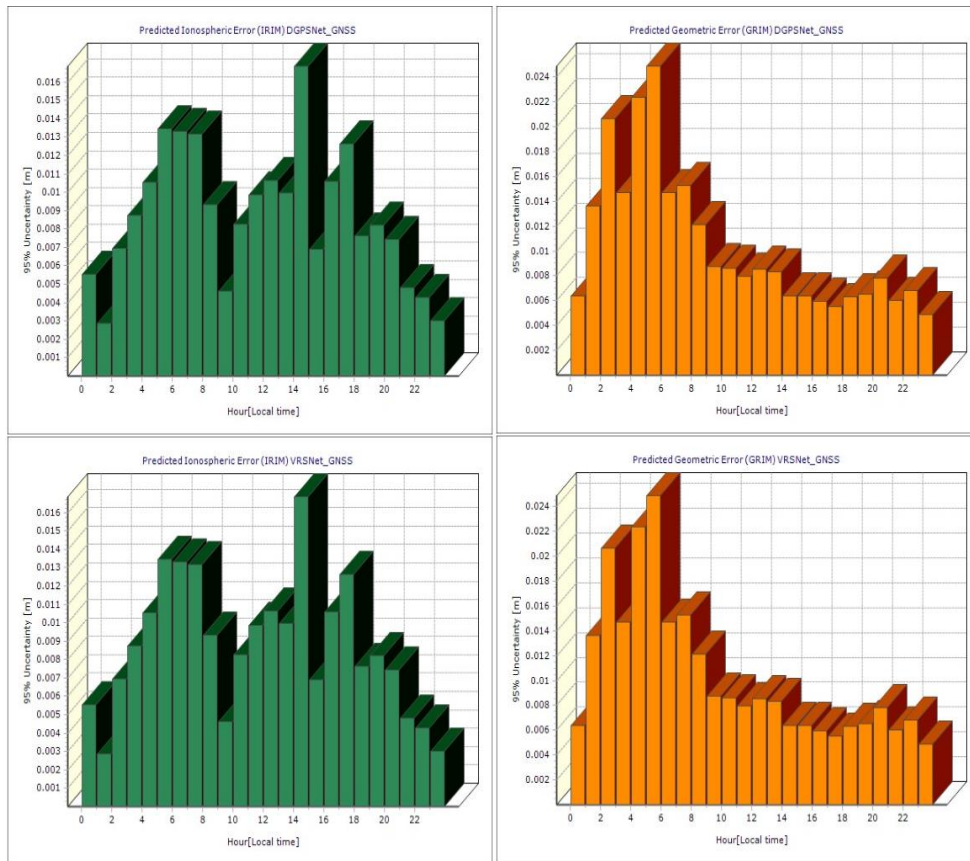
Figure 4.5: Graphic overview of the IRIM (in green) and the GRIM (in orange) per hour, as presented through the TPP Web App, both resulting from DGPS (top) and Network RTK (bottom). Source: screenshot from TPP Web App.

The CORS forming the edges of the infrastructure are excluded, as interpolation cannot be performed (only extrapolation) to those CORS. Therefore, the Network Processing module cannot estimate the non-linear residuals at these CORS (see CORS A, B, and C in the example infrastructure in Figure 4.6). Therefore, in the SiReNT infrastructure,

the RMS values for both contributions are accumulated, per hour, for the SNPT and the SNUS CORS respectively (as mentioned before, the SING CORS is not part of the network processing). From that the values for the infrastructure as a whole are determined. In section 5.2.1 the IRIM/GRIM indexes are analysed further and compared to simultaneously recorded IM displacements.
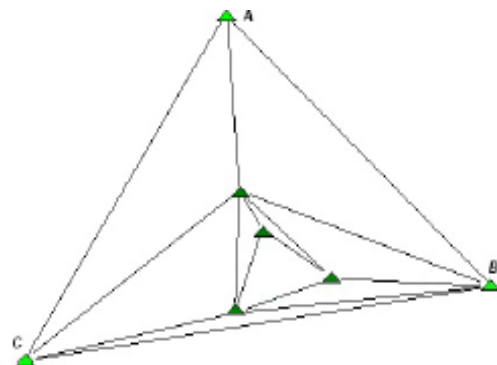
Figure 4.6: An example infrastructure; in this case the non-linear residual errors cannot be estimated (by interpolation) for the CORS at its edges (A, B and C) [31].

TEC

As described in section 2.2.2., free electrons largely affect the speed and direction of the propagation of radio waves, and therefore can cause significant positioning errors. The number of these free electrons present between the specific satellite and receiver are

represented by the TEC value. Therefore, this TEC value and its distribution are derived using the observations from all satellites to all CORS, and can be visualized in a contour map and a surface (animation) map (see Figure 4.7). In the contour map, each contour colour represents a specific TEC value, where in the surface map the different TEC values are represented by different colours as well [36]. This colour scale goes in 20 steps from blue (low) to red (high).

These maps enable the user(s) to check the current and past TEC status. In order to visualize the TEC value in the most suitable way (dependent on the user(s) requirements and the conditions at that time), different viewing properties can be chosen. The uppermost TEC value specifies the range that is expected and is to be displayed. During a period with relatively little activity, a relatively lower maximum (smaller range) can be used for visualization purposed, compared a period with high activity. There are three (range) options available:
- Low: 0-50 millimeter
- Medium: 0-100 millimeter
- High: 0-150 millimeter

Note that the map area extends beyond the bounds of Singapore, and thus the SiReNT infrastructure. This is the case as the PIVOT calculates the TEC values for the sub-ionospheric point. This is the perpendicular projection of the Ionospheric pierce point, the intersection of the station-to-satellite vector and an Ionospheric layer (seen as a shell) representing

Figure 4.7: Graphic overview of the TEC within the infrastructure, as presented through the TPP Web App; the contour map (top), the surface map (middle), and zoomed in on the surface map (bottom). Note that the orange dots represent the location of the SiReNT CORS; not a certain TEC value. Source: screenshot from TPP Web App.

the TEC of the ionosphere, onto the earth's surface. Users are enabled to use the zoom function in order to get a more general or detailed overview. The axes of the map represent the Longitude and latitude values for your reference.

Again, the network operator also has the opportunity to specify and change the grid size as well as the number of adjacent piercing points used for interpolating the value of a grid cell.

The default is set to 100 points and 15 points respectively. Increasing these numbers would improve the quality of the representations, however affect the computation speed.

IPWV & ZTD

The real-time IPWV Map represents the IPWV value at the CORS' locations (see Figure 4.8, top). This value is derived from the observations at these locations. Clouds (precipitation & water vapor) can affect radio waves, hence a low IPWV value is preferred. The colour scale for IPWV values consists of 20 steps from blue (low value) to orange (high value) [36].

In order to visualize the IPWV value in the most suitable way (dependent on the user(s) requirements and the conditions at that location and time), different viewing properties can be chosen. The uppermost IPWV value specifies the range that is expected and is to be displayed. In regions or during a period with relatively little Tropospheric humidity, a relatively lower maximum (smaller range) should be used for visualization purposes, compared to in a dry region or during a dry period. There are three (range) options available:
- Low: 0-15 millimeter
- Medium: 0-30 millimeter
- High: 0-60 millimeter

Besides this, the IPWV values (in millimeter) can also be visualized and inspected in a contour map and a surface map (animation) in real-time and for the past (see Figure 4.8, middle and bottom respectively). Users are enabled to use the zoom function in order to get a more general or detailed overview. The axes of the map represent the Longitude and

Figure 4.8: Graphic overview of the IPWV (in mm) within the infrastructure, as presented through the TPP Web App; the map representing the IPWV at the CORS' locations (top), the contour map (middle), and the surface map (bottom). Note that in the middle and bottom image the orange dots represent the location of the SiReNT CORS; and not a certain TEC value. Source: screenshot from TPP Web App. Note that these maps are not generated at the same time.

latitude values for your reference. The network operator also has the opportunity to specify and change the grid size; a higher number of grid points will result in a better and smoother interpolation, however a lower number might improve the computation speed. The default is

set to 100 points. The number of CORS used for interpolation specifies the number of CORS that are used for interpolating the value of each grid cell. Increasing this number would improve the quality of the representation, however it would also affect the computation speed. The default settings (all CORS) results in the quality of the images of Figure 4.8. The ZTD is highly related to the IPWV. The ZTD is the mapping of the Slant Total Delay (STD, the delay along the line-of-sight, between the satellite and the receiver) to the zenith direction.

The users can visualize and inspect the IPWV value (in millimeter), and the ZTD (in millimeter) as well as the contributing atmospheric parameters such as temperature (in °C), pressure (in mbar), and relative humidity (in %), in CORS specific charts and in overall condition charts.

The first type of chart enables the comparison of atmospheric conditions per selected CORS, where the latter enables the comparison of a specific parameter value between the different CORS.

When doing that, one can see that all these parameter values are very variable, already on a daily basis. However, as one

Figure 4.9: Examples of the CORS specific charts (top and middle) and the condition chart (bottom). The CORS' specific charts in this case are visualizing temperature and pressure over time (top), and the IPWV and ZTD over time (middle). The condition chart (bottom) is visualizing the ZTD over time, for all CORS. Source: screenshot from TPP Web App.

would expect since Singapore is relatively small, the simultaneously recorded parameter values are quite similar for all stations. Figure 4.9 visualizes an example of some of these charts.

5.

Discussion theory part

As one could have read in the previous chapters, there is a number of system/quality parameters of interest when working with GNSS methods (accuracy, precision, availability, integrity, reliability, continuity, capacity, and redundancy). A number of degrading factors (both intended and unintended) are affecting these parameters, hence the GNSS signals. These factors require continuous monitoring and correcting for. This is one of the tasks of the reference network infrastructures, whose aim is to provide correction information that enables the determination of accurate and precise positioning solutions (through for example the modeling the impact of the different degrading factors throughout the infrastructure, and in this case thus throughout Singapore).

In order to ensure that the infrastructure is stable and the provided (correction) information indeed is complete, correct and sufficient, an IM component is required. Besides the infrastructure's stability and the quality of the provided (correction) information, the satellites and their health, the raw data, the connectivity integrity and the integrity of the system equipment and the power supply are to be continuously monitored as well. IM in general, and IM of the stability of GNSS-based positioning systems (and its CORS) in Singapore is discussed in this chapter.

5.1. IM in general

The focus of this research is on the IM of the stability of GNSS-based positioning systems (and its CORS), and the provided (correction) information. The first can be subdivided in system level (external monitoring), and user level (RAIM). Both IM methods serve the same task; to notify (warn or alert) the assigned person(s), within the TTA, when the system might not be providing trustworthy information, or when the integrity goes unmonitored.

Through using the system level method, the system is monitored as a whole, meaning that the observations from all CORS are processed and verified centrally. Through this method (redundant) baselines can be generated between the different CORS, in order to compute network adjustments. This way large(r) scale infrastructures can be used to monitor (sub-)infrastructures of a relatively smaller scale, for example using the Bernese software [3]. For example, surrounding IGS CORS could be used as a stable external infrastructure to monitor the SiReNT infrastructure. This does not have to be done continuously, but merely as a double check at a regular interval, weekly for example.

Having a high amount of computing power would be good for certain applications, for example, those that demand that the user is to be informed of a loss of integrity within seconds. Hence this would require an external monitoring system, even though developing

and maintaining them is costly.

As mentioned however, RAIM (the user level method), might be sufficient for other applications or could be used to complement the external monitoring infrastructure. RAIM protects against multipath, Ionospheric influences and residual Tropospheric errors which might not be detectable by the external monitoring infrastructure. On top of that, including RAIM could be utilized to check the quality of the correction data.

The IM of the Rover performance in terms of positioning solution (and thus the quality of the correction data), could be done by determining and monitoring the displacements of the Rover or thus by using RAIM. Another indicator of the Rover's performance is the (re-)initialization time. This should therefore be monitored as well.

Having collaborations in place with academic/research institutions and the community might aid the reliability and quality of the infrastructure. This way it also becomes more clear what is required by the community and on top of that, research is usually aimed at developing better and newer methods, using the latest equipment and techniques.

As for the ways in which the IM information is presented, for clarity purposes it is good to visualize only the essential information, as too much information might only confuse the system user(s). More on this in the following sections.

5.2. IM in Singapore

In Singapore the external monitoring method is used, applying the TPP software (also used for the network processing). This software package includes a number of Apps, all working together to provide a complete solution. For a complete overview see section A.1.1, in Appendix 1. The fact that it consists out of numerous different Apps and modules, all with specific tasks, but through one common platform, means that it can be specifically determined where lies the cause of a certain error, may it occur. This is very convenient, however sometimes it might be difficult to keep a clear overview.

All or a selection of these Apps work together smoothly, through one platform, to provide the user with the required information. This information needs to be monitored (to keep its quality in check), for which the software includes an IM component. This component also monitors other involved aspects (power supply, connectivity, stability of the infrastructure, etcetera). The monitoring and correcting of the raw data is not a part of this however. This, as well as the estimation of the systematic errors, and the determination of the Ionospheric and Tropospheric models, predictions and corrections, is done separately. Note that there is no feedback from the IM component involved in the network processing, where there perhaps should be. Based on the IM output, the provided correction stream could be adjusted and/or weights could be assigned to the different CORS in order to get the best results possible.

Redundancy
Based on this study one could conclude that in Singapore, RAIM can be used to complement the currently adopted IM method (external monitoring). By using a combination of these different methods, one can have the best of both, with on top of that extra redundancy. The latter is the case as the results from the individual receivers (RAIM) can be verified against the results from the infrastructure and vice versa.

A way to generate even extra redundancy, would be the simultaneous use of different algorithms, for example, range comparison, residual comparison and position comparison. This way the results from the different algorithms, which are obtained simultaneously, could be compared and checked against each other.

Another way in which the redundancy can be improved, is by the construction of more CORS. During this project it is therefore also determined at what location these new CORS should be constructed in order to aid the SiReNT infrastructure in the best way possible. The results are presented and discussed in section 9.1.

Installing mixed brand facilities (such as CORS and a DCC) would help as well. A good start is to install different equipment brands throughout Singapore, such that ultimately there is an evenly distributed infrastructure in Singapore, consisting out of several different equipment brands. At this moment all equipment used in the SiReNT infrastructure is provided by Trimble. Therefore, in the worst case scenario, if Trimble instruments temporarily will go out of order due to an update or some error, etcetera, the whole SiReNT infrastructure will be down. This situation clearly is unwanted and should be avoided at all times.

Redundancy - side note
The Indian Regional Navigation Satellite System (IRNSS) could also play a role in increasing the redundancy (the system and observation redundancy). The IRNSS is a new stand-alone regional navigation system developed by the Indian Space Research Organization (ISRO), under the operational name of NavIC (Navigation with Indian Constellation) [32][34][41]. The constellation will comprise of 7 satellites; 4 geosynchronous orbit (GSO) satellites (in 2 different planes) and 3 geostationary satellites. These satellites have an orbital period that is equal to the rotational period of the Earth. The geostationary satellites are positioned at the equator, at 32.5º E, 83º E and 131º E and their orbits are parallel to the equator and therefore appear to be stationary with respect to the Earth's surface [41]. The 2 geosynchronous orbits are inclined and cross the equator at 55º E and 111.75º E respectively, and move in an 8-shape with respect to the Earth's surface. This system will thus provide coverage in Singapore (103.51º E). Its navigation signals will be broadcasted on a frequency band that is used by several other constellations as well (in the L-band).

Therefore, this can be a very useful addition to the GNSS that are currently being tracked by SiReNT. Using IRNSS should not cause any interference, as Code-Division Multiple Access (CDMA) is used, resulting in all unique signals being assigned unique codes.
Having redundancy is essential if you want to maintain a reference network infrastructure with a good reliability and integrity.

5.2.1. The Trimble PIVOT Platform

TPP IM – choice of engine modules
In order to monitor the movement and/or quality of the GNSS CORS (with respect to one or more selected, fixed station(s)), this IM component provides Real-Time and Post-Processing engine modules. All engine modules serve their own specific purposes. Based on interest, a certain engine module could be chosen.

As for SLA, since they are mostly interested in the stability of the infrastructure, the Network Motion engine module should be sufficient. Instead of having the baselines radiated out from the selected fixed CORS, having baselines between all CORS (the individual CORS being interconnected), will increase the redundancy however. As verification and when very accurate results are required, the Post-Processing engine module, using the final orbits, could be adopted. For the specific monitoring of rapid movements, such as earthquake events and such, the Rapid Motion engine module should be used. The RTK engine module falls between the Network Motion engine module and the Rapid Motion engine module, both in terms of reaction time and accuracy (see Figure 4.2). This engine module does therefore not necessarily serve a specific purpose for SLA, when the other engine modules are already in place.

SLA was under the impression that by applying certain thresholds to the output of the RTK engine module, the Rover performance could be controlled. In that case, this engine module could have been used for that particular purpose. This is not the case however, more on this later. Due to this, and since the objective of the IM component is already covered by the other (engine) modules, the RTK engine module can be seen more as an extra add-on. The Rover Integrity Module could be of great interest to SLA however. This module can be used to take care of the Rover performance IM, which is one thing that SLA is interested in. There is no connection to the IM component from this module however. Adding such a connection would enable the infrastructure administrator to monitor the Rover performance throughout the infrastructure, in Real-Time. For this either VRS or (some of) the CORS, simultaneously acting as Rover, distributed throughout Singapore, could be used.

TPP IM-Choice of fixed reference
As mentioned, the movement and/or quality of the GNSS CORS is monitored with respect to one or more selected, fixed station(s). In Singapore the SNPT CORS is selected for this purpose, because of its central location and as it is supposedly one of the (relatively) more stable CORS of the SiReNT infrastructure. The latter could not be investigated however, as due to this CORS being used as a fixed reference, there is no data available (its position shift is set to zero). Since this is the case it cannot be confirmed that this indeed is the most stable CORS of the SiReNT infrastructure. This could/should be confirmed regularly using a stable external infrastructure, like for example the IGS network (see section 5.1). This IGS network infrastructure has a long record of stable, traceable position time series and is therefore suitable to use as reference network infrastructure.
The SNPT CORS and the SING CORS are indeed the CORS that are the most centrally located in Singapore however. When zooming in on their specific locations, the SING CORS seems to be a better option, as it is rock anchored. However since the SING CORS is not maintained by SLA and therefore cannot always be accessed immediately in case of problems, the SNPT CORS (not rock anchored, but on top of a building with a large foot print) seems to be the best option in Singapore, assuming that it indeed is one of the (relatively) most stable CORS of the SiReNT infrastructure.

TPP – atmospheric information
The TPP monitors, models, visualizes, and records several atmospheric parameters, in order to provide a better solution. These parameters, which might possibly affect the GNSS signals, are also visualized in the Web App, for a better understanding. These parameters are briefly discussed here.

I95

The I95 value is an important indicator of the activity of the atmosphere. Firstly, as mentioned, the SiReNT infrastructure determines the I95 value from both DGPS (DGPSNet) and Network RTK (VRSnet). The difference between the I95 values resulting from these two are very small, hence it is not understood why these are visualized separately. After inspection it is determined that for example during the whole of September 2016, the maximum difference is below 0.2 and the average difference over the whole month is $2.29*10^{-4}$. These are only small differences and therefore not clearly visible in the presented graphs. Hence only one graph is presented everywhere in this project, in which the average of the two (DGPSNet and VRSNet) is visualized over several months (01-09-'16 till 30-01-'17).

When looking at the daily variations, such as visualized in the example in Figure 4.4, one can conclude that overall there is (some) dependence on the time of the day. Generally, the Ionospheric activity is lowest around midnight and highest around noon (just before and after); it increases during the morning, with increasing solar intensity. This makes sense as with increasing solar intensity, the amount of EUV and x-ray photons from the sun, which are causing the ionization of atoms and molecules, are increasing as well. At noon there often seems to occur a small dip in the Ionospheric activity, after which it increases again during the afternoon. Later on, towards the early evening hours and at night this activity decreases again. An interesting thing to note is that the activity during the afternoon is often stronger as compared to the activity during the morning. This agrees with the data visualized in Figure 7.2 (top).
Why their often is a dip at noon, and why the during the afternoon the maxima often is higher this is likely to be related to the impact of (daily) variations in the solar intensity. Why this is the case is not quite understood,

When looking at the I95 values during the whole period (see Figure 7.2, top), one can also see that these are quite variable. Especially at the start (and in the first half) of this data set relatively more (very) high I95 values occur, where in the second half of this dataset circumstances improve and the (very) high I95 values are almost no longer observed.
The circumstances on some other dates (which are not included this dataset range) are investigated as well, via the TPP Web App. These graphs look like the example in Figure 4.4. From this investigation it turns out that during the months May - July, the Ionospheric activity is generally higher as compared to during the months November - December; towards the end of the year the maxima generally are getting a bit lower. Seasonal variations in the solar intensity thus play a role as well.

From this dataset the percentage of I95 values that was within the individual, specific regions, during this period is determined to be:

- I95 =< 2:   18.36%
- 2 < I95 =< 4:   36.43%
- 4 < I95 =< 8:   38.34%
- 8 < I95:   6.87%

Note that through the TPP Web App (see example in Figure 4.4) only values below the value 8 are presented, possibly because most of the time the I95 values are below this value; in

this whole period 93,13% of the I95 values are below 8. Having I95 values close to, or exceeding 8 means that the Ionospheric activity is very strong. If this is the case, it is very likely that displacement magnitudes are affected.

IRIM/GRIM

Similar to I95 value, there are only very small differences between the values for DGPS and VRSnet, which are therefore not clearly visible in the presented graphs. After inspection it is determined that for example during that September 2016, the maximum difference between the two are less than $1.19*10^{-5}$ and $1.36*10^{-5}$ meters for the IRIM and GRIM respectively. As for the average difference over the whole month; these values are less than or equal to $3.43*10^{-9}$ and $9.24*10^{-8}$ meters for the IRIM and GRIM respectively.

These are only small differences and therefore not clearly visible in the presented graphs. Hence again only one graph is presented in this research, visualizing the average of the two, see Figure 7.2 (top). These graphs show a lot of variability throughout the period that is visualised in the graphs (: 01-09-'16 – 30-01-'17); no clear trend over time.

When looking at the IRIM graph specifically, one can see that in the first half of this data set relatively more (very) high values occur, where in the second half of this dataset circumstances improve and the occurring maxima are generally (much) lower (similar to the I95 graph). One would expect these IRIM variations to show (some) resemblance to the I95 variations, as both are related to the Ionospheric activity. This resemblance is partly there, mainly when very high I95 values were recorded, relatively high IRIM values were recorded coincidently.

Hence it turns out that this factor is affected less by (abrupt) variations in the solar intensity, and therefore is of lesser use as an indicator of the Ionospheric activity.

When looking at the GRIM graph specifically, one can see that this dataset differs from the previous two (only the largest GRIM values seem to show some coincidence). The GRIM values show mostly their own independent behavior, and vary quite randomly over time. When looking at the GRIM graph one can also see that, dissimilar to the I95 graph and the IRIM graph, there is not much difference between the first half and the second half of this dataset. This is understandable, as this parameter is more related to the Tropospheric activity and orbit errors. The latter varies randomly throughout the year for example, and is not affected by any daily or seasonal variations.

TEC

The TEC value is another parameter that is related to the (intensity of the) Ionosphere and its expected impact. This parameter could be used for monitoring space weather impacts, and is therefore an interesting parameter for researchers in that particular field. The TPP does not present this parameter in a graphs form, only through the map overview(s). This parameter does not change much throughout the extent of Singapore (as Singapore is very small) however, so the question is whether it is necessary to visualize this parameter through a map, instead of just a graph/value.

ZTD, IPWV, Relative humidity, pressure and temperature

In general, with increasing temperature, the capacity of a given volume of air to contain water vapor increases, hence the ratio of water vapor versus air (the relative humidity) decreases, and vice versa with decreasing temperatures.

As for the atmospheric pressure, normally it will increase with increasing temperatures. However, as the atmosphere is not a limited space, air expansion can take place, resulting in a decreasing density of air. This will cause the (warm) air to rise up, while reducing the atmospheric pressure at the surface. These parameters together contribute to the IPWV and thus the ZTD, which trends are very similar, other than the difference in units.

Due to its location, the island does not have 4 clear seasons. Instead, Singapore has 2 seasons, the wet season and the dry season. Overall the weather is always relatively similar however and therefore it is expected that the atmospheric conditions do not vary much. It often rains at the end of the afternoon for example, even during the dry season and independent of the temperature. This agrees with the data; in general, besides some daily variations, there is not really a (seasonal) trend visible in the Tropospheric information. Note however that there is not yet a long SiReNT record available. Also note that Singapore is relatively small and therefore the weather conditions recorded at the different CORS are quite similar.

TPP – Web App/Dashboard
For clarity reasons only the information that is minimally required in order to give a good overview of the current circumstances should be presented through the (Web) App, in a straight-to-the-point manner.

It would still be good to include an overview/sensor map of the quality of CORS as is currently is done through the TPP (Web) App (see Figure 4.3). This way the user(s) can easily see what is the status of the infrastructure and its individual CORS.
The related scatterplots and graphs however only will confuse the infrastructure user and possibly generate the idea that the SiReNT infrastructure is unstable. Therefore, these should be omitted from the (Web) App that is meant for the public. These could be interesting for the infrastructure administrator however, as one can easily select a certain time period and see how the stability of a CORS was at a certain point in time. This enables an infrastructure administrator to investigate specific observations/time periods more closely. As for the information to be presented in the graphs, it suffices to just present the IM displacement data per component (ΔN, ΔE, and Δh), as these values form the $\Delta 2D$ and $\Delta 3D$ results. A good addition could be to add colours to the observations, based on when they were recorded (for example per x hours). This enables one to visualize the quality of these last x hours.
Besides that, it would be convenient if the graphs and the scatterplots are linked, such that if one were to select a certain observation in the scatterplot, this observation will also light up on the specific graphs.

Something that is missing from the specific information and health overview per CORS (see Figure 4.3), is its fix status (fixed solution versus float solution). Hence this would be a good addition.
Other additions, that could be convenient (mainly for job planning), could be to present the current Pollutant Standards Index (PSI) and weather in the different parts of Singapore, but especially the forecast for both.
This could all be done using the same base map (see Figure 5.1), thereby making it easier for the user to access and compare the different kinds of information

In addition to this, a dashboard, such as the NETPOS Dashboard, should be generated. The homepage of this dashboard should be visualizing several parameters, all in real-time. This would enable the (end-)user to see what is the current status with regards to all these parameters, in one view. One would however also be able to access further information related to these parameters, by selecting the one of interest.
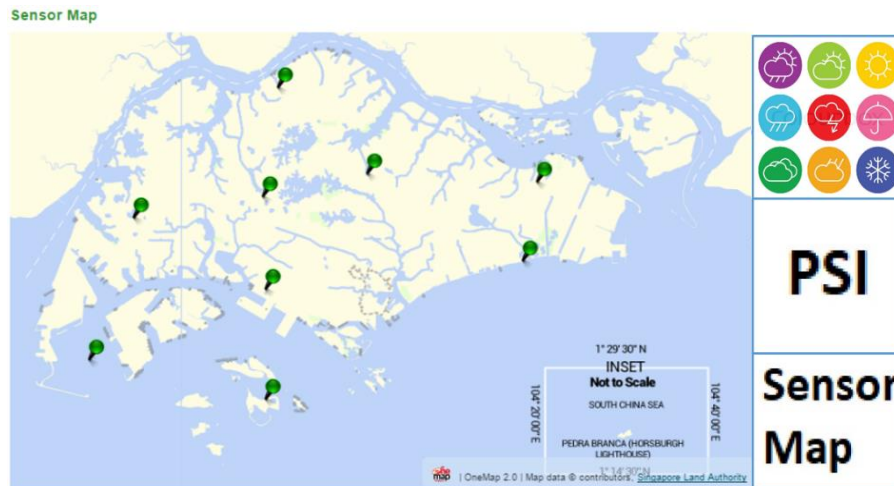
Figure 5.1: An option for the future sensor map, integrated with the weather and PSI forecast. The option of one's selection is visualized on the map, at the arbitrary locations, or per region of Singapore. In this example the sensor map is visualized.

With regards to the information presented through this dashboard, communicating the following is believed to be sufficient and useful:
- The number of tracked satellites, where by selecting the part of the dashboard presenting this parameter, one can access a skyplot centered at your location. The background colour of the part presenting this parameter could be used to indicate whether it is a good, reasonable or bad situation, depending on the number of fixed satellites in relation to the number of tracked satellites. This way conclusions can be made about the satellite availability/visibility at that location, at that particular time.
- The number of connected users, where by selecting the part of the dashboard presenting this parameter, one can access the number of Rovers which have a position fix, and the number of Rovers that do not, within a certain range from your location, or per region in Singapore. This way the user(s) can easily see how many Rover(s) have fixed their solution and how many did not. The background colour of the part presenting this parameter could be used to indicate whether it is a good, reasonable or bad situation, depending on this ratio. This way conclusions can be made about the quality of the provided correction stream, at that particular time.
- An indication of the Ionospheric delay (for example through the I95 value, perhaps in combination with the TEC value), as this is the largest factor affecting the GNSS signals. The background colour of the part of the dashboard presenting this parameter could be used to indicate whether it is a good, reasonable or bad situation, depending on this value. By clicking on this part, one can access the related chart. This enables one to view the last few hourly values, in case there is an interest in that.

For this, even if both are required for processing purposes, there is no need to visualize the DGPS and the VRS results separately. This because the DGPS mode values are very similar to the VRS mode values, hence only one chart is needed for visualization purposes (see section *'Atmospheric information'*).

It is not necessary to present the TEC parameter separately to the general infrastructure user. This parameter might be too technical for the average infrastructure user, and is only of interest for specific purposes (like monitoring space weather). It does not add extra value to the already presented indicator of the Ionospheric delay.

- The GRIM index/predicted geometric error (see Figure 4.5), indicating how much the geometric impact factor differs from a linear spatial variation. This will give the user an indication of the geometric error that is or could be remaining in the correction message sent to the Rover(s). Hence this is a parameter that is of major interest to the user(s). Partly based on this, decisions can be made on whether or not continue surveying at that point in time.

  The background colour of the part of the dashboard presenting this parameter could be used to indicate whether it is a good, reasonable or bad situation, depending on this value. By clicking on this part, one can access the related chart. This enables one to view the last few hourly values, in case one is interested in that. For this parameter, it also suffices to show only one chart as the differences between the DGPS and the VRS mode values are small enough to be neglected for visualization purposes.

- The Rover performance (the initialization time (time-to-fix) and the quality of the positioning solutions) using the Rover Integrity module. This Rover performance could be represented by a colour, to indicate whether it is a good, reasonable or bad, based on a combination of the time-to-fix and the quality of the positioning solutions (green for when both are good, yellow for when one is good, and red for when none are good). The time-to-fix could for example be considered good if under x seconds (with x being a representative value for Singapore, more on this later), where the quality of the positioning solutions could considered to be good if they are satisfying an accuracy 2-3 centimeter and 3-5 centimeter in the horizontal and vertical plane respectively.

  Note that this performance will be determined under relatively ideal circumstances (since CORS will be used as Rover; CORS all have a good skyview and are situated at relatively stable locations) at that point in time, and therefore only serves as an indicator of what is possible. The initialization times (or an average of them) in (near) real-time/during the last hour could be determined, per Rover. By generating a plane through the Rovers, or by interpolating the observed values, an indication of the possible Rover performance anywhere in Singapore could then be determined. Note that due to the small size of the country, the differences throughout Singapore are not expected to be very big however. Therefore tests will have to be conducted in order to see whether this is indeed the right approach, or whether it is sufficient to determine one value per wind direction, or perhaps even just one value only, representing the whole of Singapore.

  Both a scatterplot/chart for the quality of the positioning solutions, and a chart for the time-to-fix, could be included. This could then be accessible by selecting the part of the dashboard presenting this parameter.

  Based on this, one can conclude whether or not it would be a good time to start/continue a survey.

All other data does not need to be presented to the infrastructure (end-)user, and might only cause confusion.

An example of how the dashboard could look like, is visualized in Figure 5.2.

The value range to which what colour should be assigned depends on the specific parameter. What would be the optimal ranges for the different parameters would have to be further researched and discussed. For example, for the Ionosphere, when using the I95 value, the ranges could be set to green for I95<4, yellow for 4<=I95<8, and red for I95>=8, where for the quality of the tracked satellites could be represented by the PDOP value, green for PDOP<4, yellow for 4<=PDOP<=7, and red for PDOP>7.

The information button in the center should link the user with further information on how to interpret the dashboard.

Figure 5.2: Example of what the SiReNT Dashboard could be looking like, based on the 5 parameters: the number of tracked satellites, the number of users, the GRIM (in cm), the Rover performance, and an indication of the Ionospheric delay. In the visualized situation all parameters are satisfying the set limits.

5.2.2. IM reports

IM reports – general

The IM results are presented to the infrastructure administrator through auto-generated IM reports on a regular basis. These reports present the IM displacement data from the Network Motion engine module. This is the engine module that is mainly aimed at monitoring the stability of the infrastructure.

Apparently, when a CORS is down, it is automatically excluded from these reports. For clarity reasons it would be better to still include any CORS that is down, accompanied by the reason for it being down. Even in case it would only be down for a certain part of the period, this should be indicated. This would give a more complete overview, and one would know what is going on with all CORS during the period that is presented by the IM report.

It is not understood why the charts belonging to the SLYG CORS would be empty, just because the SNSC CORS is down. This should be looked into and solved.

IM reports – time period
These IM reports, including statistical point overviews and displacement charts, resulting from this engine module are generated every 3 days. This is means a lot of reports are generated on a yearly basis, consisting of limited data. The IM reports are more meant to present an overview of the infrastructure's IM results. It would be sufficient to do this for example weekly, or even monthly, depending on when the data reduction algorithm starts working on the data.

IM reports – components
As for the information to be presented in the IM reports, just like through the (Web) App, it suffices to just present the IM displacement data per component (ΔN, ΔE, and Δh), as these values form the $\Delta 2D$ and $\Delta 3D$ results. The latter are currently presented as well, but do not add any valuable information to the results per component (if the 2D or 3D result is exceeding a threshold, then so would at least one of the horizontal or vertical components, see Appendix 3).

IM reports – chart specific
As for the IM displacement graphs themselves, in all these reports the used vertical axis ranges are based on the data itself. Hence they are different in the different reports. It would be good to use a non-variable y-axis, with default limits, such that the IM displacement data can be easily compared, even if it is in different reports. When chosen large enough, it will also always include the (different) thresholds. This would enable the system administrator to easily see whether thresholds have been exceeded, and if so, when.

IM reports – scatterplots
The included scatterplots do not serve much purpose in the reports, in the way they are presented. It can be an easy tool to see whether the CORS has been stable, however, in the report one cannot differentiate between data from different time periods. Hence it serves merely as an overview of the whole period. It would be more interesting if the different days could be colour coded for example, or assigned different signs. If not, these current scatterplots can be omitted (the same data is already presented in the graphs as well), thereby reducing the presented number of graphs/plots. If the infrastructure administrator wants to access the scatterplots specifically, one can do so through the Web App.

IM reports – statistical point overview
The Statistical Point Overviews would/could be interesting if the values actually represented reliable observations, and not the maxima and/or minima from anomalies in the data. The mentioned anomalies are often caused by the fact that this engine module needs to converge again. This process takes time and is usually visible in the graphs as a sudden relatively large displacement. While this happens, this engine module should not record data as per usual, as these relatively large displacements can be very confusing. Instead an indication of the fact that a re-initialization is taking place, could be included. This data, which are in fact outliers, should not be used for the generation of the Statistical Point Overview and the trend determination. The information which the scatterplots present, such as the 1σ, 2σ, and 3σ values, could be added to these Statistical Point Overviews as well. That would make this overview more complete, especially when adding a comparison with the same parameters determined from long term data.

- The percentage of displacement data per month, excluding the data recorded during the (re-)initialization, that was/relative number of observations that were reliable dependent on the applied thresholds AND at the same time inside these thresholds. This is part of the *availability* described in section 2.1, as the observations are logged with an equal interval. This means that this parameter equals the percentage of time that the recorded observations are satisfactory, which is one of the requirements for the system to be performing satisfactorily as well.
  In order to determine whether the observations/displacements were reliable, the earlier described method adopted by the TPP can be used.
  Included in this could be a comparison to results from the past, over different timespans (1 month, 1 year, etcetera) and/or per specific timespan, for example in the form of a bar graph (see Figure 5.3). This would provide the infrastructure administrator with a clear overview of the IM performance of the different CORS per timespan, and it could easily be seen whether a specific CORS is behaving similarly, better, or worse, as compared to the past.
- The quality of the correction information provided to the Rover, measured based on the initialization time (time-to-fix) and the quality of the positioning solutions. The latter could be added in the form of displacement graphs and Statistical Point Overviews.
- Another possible addition is the difference between the trends determined from the specific time period which the report is presenting, and the overall trend (determined from the whole dataset). This could provide a clear indication of whether something changed/is different during that particular time period.

These reports, or any IM displacement data for that matter, are meant for the infrastructure administrators, and should not be shown to the infrastructure user, as they might not fully understand it, and jump to a wrong conclusion.
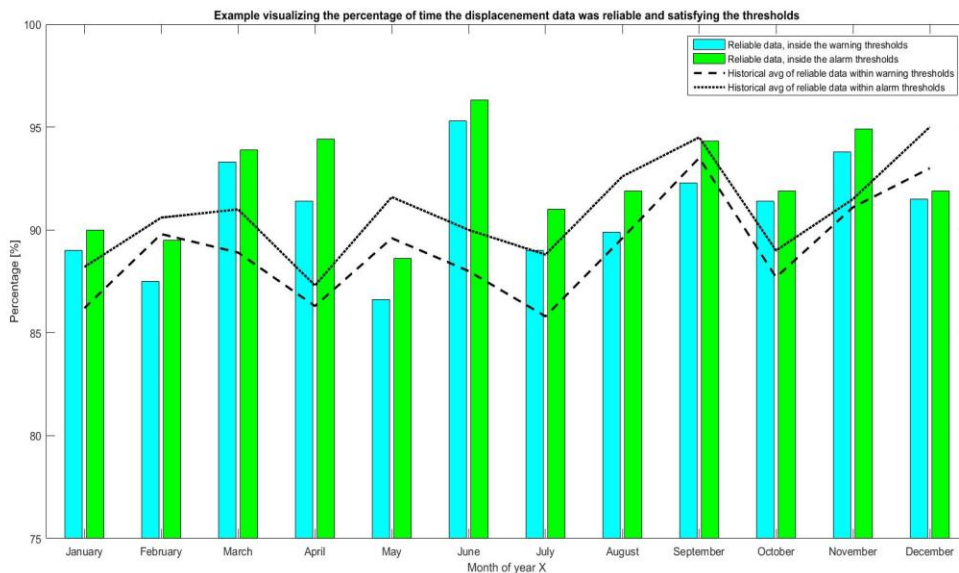
Figure 5.3: An example visualizing the percentage of displacement data was reliable and satisfying the applied thresholds (warning threshold and alarm threshold), as compared to the past. Similar graphs could be generated for each CORS.

-Data Study-

6.

Trimble Pivot data processing

Now that we know how IM is taken care of in several countries, including Singapore, it is interesting to know how well it is been done in the latter; what is the integrity of the recorded observations over time? How is this affected by fluctuations in the relevant factors? Are there any trends visible in the stability and coordinates of the different CORS? Are the thresholds applied to the IM displacement data sufficient? As described before, the default thresholds used in the TPP IM of the CORS' quality are the result of testing performed by Trimble under ideal circumstances. Therefore, they are not necessarily perfectly applicable to each and every CORS worldwide. Remember, it is believed by SLA that applying these thresholds to the IM displacement data from the RTK module, will enable one to control the Rover displacement data retrieved by the infrastructure user. The question is whether this indeed is the case.

The ultimate aim is to find out if, and in that case, how, the integrity, and the way it is being monitored can be improved. One way in which the current methodology already can be improved is through adding extra CORS, that consist of hardware of other brands. This would increase the overall redundancy within the infrastructure, thereby improving its performance and reliability. These CORS can also simultaneously be used at Rover. In order to serve SiReNT best, it should be determined where exactly these CORS should be constructed.

One of the tasks of the IM component is to notify (warn or alert) the user in case that is required. So far no notification related to the positioning solutions was triggered however, even though they do not always meet the required quality (following from feedback from the user(s)). This might be related to a mix-up of settings or a wrong understanding, where the notification mode was left unticked during a service configuration. This all could be fixed, in which case it is important to know whether there is a relationship between the IM displacement data and the Rover displacement data (and thus whether applying thresholds to the IM displacement data can be used to control the Rover displacement data). If there is indeed a relationship between these datasets, then it would be interesting to know what thresholds would be adequate in ensuring a good (accuracy of 2-3 centimeter and 3-5 centimeter in the horizontal and vertical plane respectively) and continuous quality of the Rover displacement data. If there is no relationship between these datasets, it is important to find out what the thresholds actually do apply to, and still, and how they are performing. For example, in case they do apply only to the IM displacement data itself; what percentage of the IM displacement data is within the applied thresholds.

To answer all these questions, first the stability of the network infrastructure itself and its individual CORS, in relation to the atmospheric information, PDOP values and the number of tracked satellites, are analysed. Besides that, the relationship between IM displacement data and Rover displacement data is investigated. Part of this is the relationship between those

data sets and the atmospheric information, PDOP values and the number of tracked satellites. Lastly, the most suitable positions at which new CORS should be constructed, as well as the effects from the August 13th, Magnitude 6.5, Sumatra Earthquake event, are determined.

The specific way in which the data gathering and processing are done is presented in section 6.1. The different datasets and results from the data processing are presented and discussed in chapters 7,8 and 9, after which the recommendations and conclusions are formulated in chapter 10.

6.1. method

The specific tools used in these analyses can be found in the Appendices.

The steps taken are as follows:

Step 1: Obtain and analyse the IM output (ΔN, ΔE and Δh with respect to SGEOID09) from the RTK engine module over a longer period of time in order to find possible trends and/or determine the percentage of measurements over this period, where the CORS were supposedly providing trustworthy (reliable) information (according to the default thresholds).

This analysis is done per CORS and the logging interval to be used for this is hourly (related to the limiting logging interval on which it depends). If logging intervals in the dataset differ from this, resampling is required. Later on in this investigation, the impact of using other thresholds (as compared to the default thresholds) is looked into, and discussed as well.

To be part of this analysis is the possible relationship between the displacements and the atmospheric information (IPWV, I95, IRIM/GRIM etcetera), PDOP values and the number of tracked satellites.
Remember that all the used IM output is relative to the SNPT CORS (the fixed reference), hence its observed displacements are 0.

For this, the IM output from the TPP RTK engine module in baseline mode will be used, as these observations will have a similar accuracy (RTK accuracy) as Rover observations. Besides that, out of the available datasets, the data from this engine module is assumed to be resembling Rover observations the best (the VRS mode was not in use during this period).

Step 2: Obtain and analyse RTK Rover observations (northing, easting, and height with respect to SGEOID09) over a known location, using the provided SiReNT VRS correction information. Two types of observations will be obtained simultaneously; continuous observations and observations where the Rover will be (re-)initialized regularly (every 300 seconds). For the latter, the TPP TRI module will be adopted.
The continuous Rover displacement data will be used in the investigation into the possible correlation between the estimated positioning solutions and the IM displacement data, where the reinitialized Rover displacement data will be used in order to determine the performance in terms of (re-)initialization; the duration of the convergence.

The logging interval to be used for the continuous observations is 15 seconds, where the logging interval to be used for the reinitialized observation is 5 seconds. If the logging intervals differ from required logging intervals, resampling of the data is required.

The reason for these logging intervals to be different is related to the specific aim of the different datasets (continuous observations versus reinitialized observations).

The logging interval of the continuous observations is to match the logging interval of the IM displacement data that it is correlated and compared with, which is 15 seconds.

In order to determine the (re-)initialization time accurately however, a logging interval of 15 seconds is insufficient. A sampling interval of 5 is chosen, as during the trial testing the reinitialization time mostly exceeded 5 seconds. Using this sampling interval is therefore believed to be sufficient in order to provide a good idea of this performance factor. Besides that, a smaller sampling interval would result in even larger datasets, which means it would be increasingly more difficult to handle.

The results are compared with the fluctuations in the atmospheric information (IPWV, I95, IRIM/GRIM etcetera), PDOP value and number of tracked satellites during this period. Note that this will only be providing an indication, however, as these datasets all have a larger sampling interval.

In order to obtain the Rover displacement data, a Trimble Zephyr antenna on a secure location (rooftop of GPSlands' (GPSL) building) is used, in order to simulate a Rover being deployed in the field. This antenna is part of a permanent reference station and therefore assumed to be stable. In this case, the observations are also forwarded to a Trimble R10, via a re-radiating kit. This way the Trimble Zephyr antenna can simultaneously serve as a Rover. Because of the costs and company regulations involved in this, the data collection will be done for only a limited number of days. In order to get a more reliable result, this timespan should be much longer, however from this one can develop a first idea about a possible correlation between the Rover displacement data and the IM output from the TPP RTK engine module. In the processing of the different datasets, MATLAB will be used.

Step 3: Determine the displacements of RTK positioning solutions resulting from the Rover with respect to the known coordinates (ΔN, ΔE, and Δh). If required, the positioning solutions have to be converted to northing, easting and height with respect to the Singapore Height datum first (using the SiReNT Web App).

The coordinates of the GPSL reference point are:
- 1° 20' 58.28509 N → 36848.984 m (northing)
- 103° 50' 26.12450 E → 28809.243 m (easting)
- 53.014 m (ellipsoidal height) → 43.082 m (height with respect to SGEOID09, corrected*)

*Corrected in order to take into account the difference between phase centers of the two antenna's (Trimble Zephyr Antenna versus Trimble R10) being: 0.146 m.

Step 4: Collect the data from the TPP RTK engine module in VRS mode (ΔN, ΔE, and Δh), of the same dates and compare this with the continuous Rover displacement data resulting from *Step 3*. This can be done by determining the correlation between this Rover displacement data and the IM displacement data from the (used) CORS.

To be included in this analysis are the atmospheric information (IPWV, I95, IRIM/GRIM etcetera), PDOP value and number of tracked satellites during this period. This way it can be analysed if, and in that case, how all these affect the Rover displacement data (and thus Rover performance).

Step 5 (extra): Determine where extra CORS and/or Rovers should be constructed for the best overall coverage.

The main aim of this research project is to advise on how to aid and/or improve the integrity, as well as the IM and its output, with regards to the SiReNT infrastructure. The first part can be done by improving the redundancy and reliability of the infrastructure as a whole, which in turn can be done by the construction of more CORS. Therefore, the most suitable locations for these CORS are determined.

Step 6 (extra): Obtain, compare and analyse the IM displacement data (ΔN, ΔE, and Δh with respect to SGEOID09), from the RTK engine module in baseline mode, the Rapid Motion engine module and the Network Motion engine module, during the August 13th, magnitude 6.5, Sumatra Earthquake event.

To be part of this is the analysis of the atmospheric information (IPWV, I95, IRIM/GRIM etcetera) and PDOP or number of tracked satellites during this period, and how these possibly affect the IM displacement data.

6.2. Data analysis: data & results of data processing

Following the methodology described in section 5.1 thus provides us with the following datasets/products:

- *IM displacement data and atmospheric information, from the RTK engine module in Baseline mode*, over a longer period of time.
- *IM displacement data and atmospheric information, from the RTK engine module in VRS mode*, over a smaller period (~2 weeks).
- *Rover displacement data (both continuous data and data with regular (re-)initializations)*, over the same period (~2 weeks).
- *Map visualizing the best locations for the construction of new CORS.*
- *IM displacement data and atmospheric information, from the RTK engine module in Baseline mode, the Rapid Motion engine module and the Network Motion engine module* on the August 13th, magnitude 6.5, Sumatra Earthquake event.

7.

Trimble PIVOT data analysis part I
IM displacement data

This chapter is about the IM displacement data from the RTK engine module in Baseline mode, and atmospheric information, that was recorded over a longer period of time. Using the results presented in this chapter, the integrity of the IM displacement data recorded by the SiReNT infrastructure is determined, based on the default thresholds. Also, the impact of unusual fluctuations in the atmospheric information and/or the PDOP/number of tracked satellites on the IM displacement data is investigated. In this, the main focus is on the timing of these events. Besides that, from the results in this part also can be concluded whether there are trends in the IM displacement data and if so, what can be concluded from them. Finally the thresholds, and whether they are sufficiently filtering out the above-mentioned impacts, in order to ensure that at least 99% of the reliable data is within these thresholds (without throwing out too much data, that is not likely to be affected by these impacts).

In this chapter first all related results are presented (see section 7.1), followed by the discussion of these results (see section 7.2).

7.1. Results

As expected the datasets contain several different time intervals, varying from every few seconds to hourly, depending on for example the data type (I95, IPWV, horizontal displacements, vertical displacements etcetera) and the data reduction algorithm, hence resampling was required.

As described briefly in section 3.5, and more elaborately in Appendix 1, the TPP software package can use the (default) thresholds in order to trigger warnings and alerts. These thresholds are then also used to disarm the integrity monitoring system (for that specific CORS). When talking about disarming the integrity monitoring system, it means that the option to trigger warnings of alarms is disarmed (for the specific thresholds, see Table A.1.2). In that case the observations are no longer considered to be reliable.

The impact of applying these thresholds to the displacements is investigated. This is done per CORS, per component (northing, easting, and height), showing varying displacement magnitudes. This is then combined with the atmospheric information, PDOP values and number of tracked satellites.

The focus of this project is on the separate components as almost always whenever these are simultaneously satisfying their specific thresholds; the 2D and 3D observations will as well, see Appendix 3.
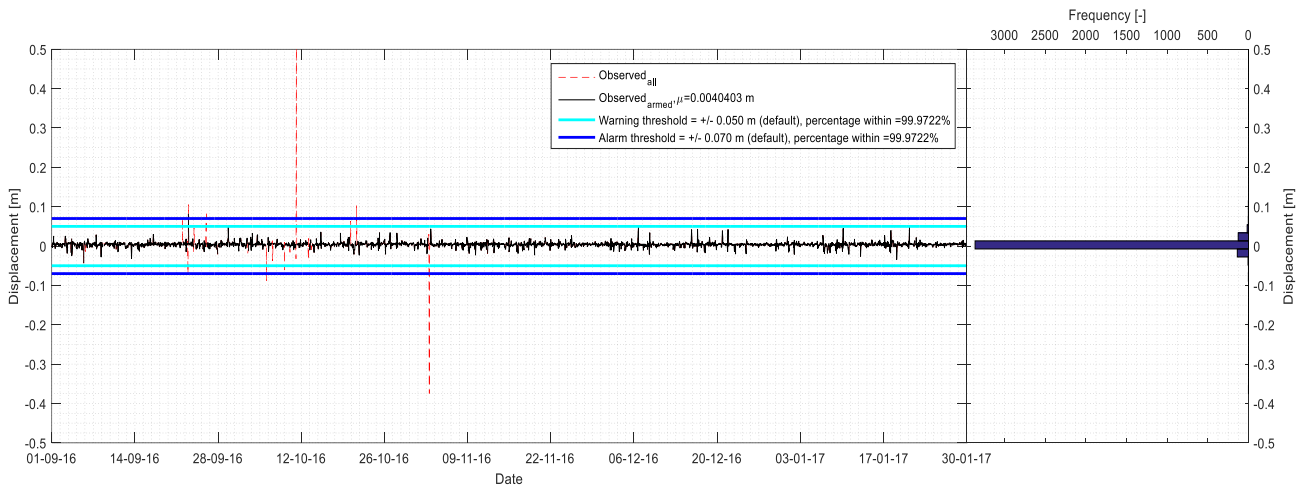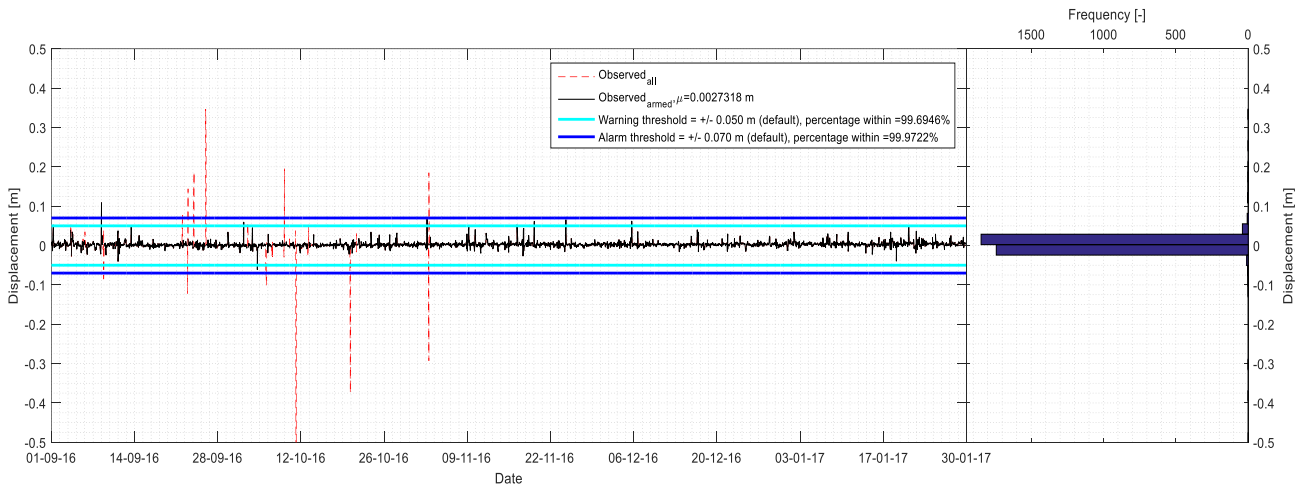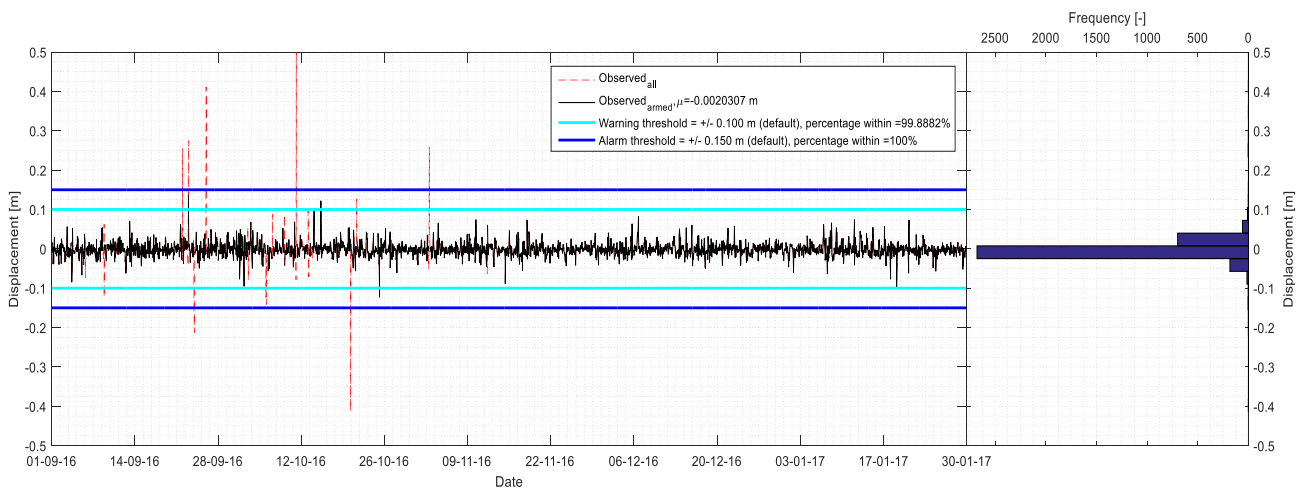
Figure 7.1: Graphs visualizing the displacements in the northing direction (top), the easting direction (middle), the height (bottom) as observed by the SLYG CORS (period: 01-09-'16 – 30-01-'17). For a more detailed explanation of the graphs, see '7.1 Figures/Tables explained'.
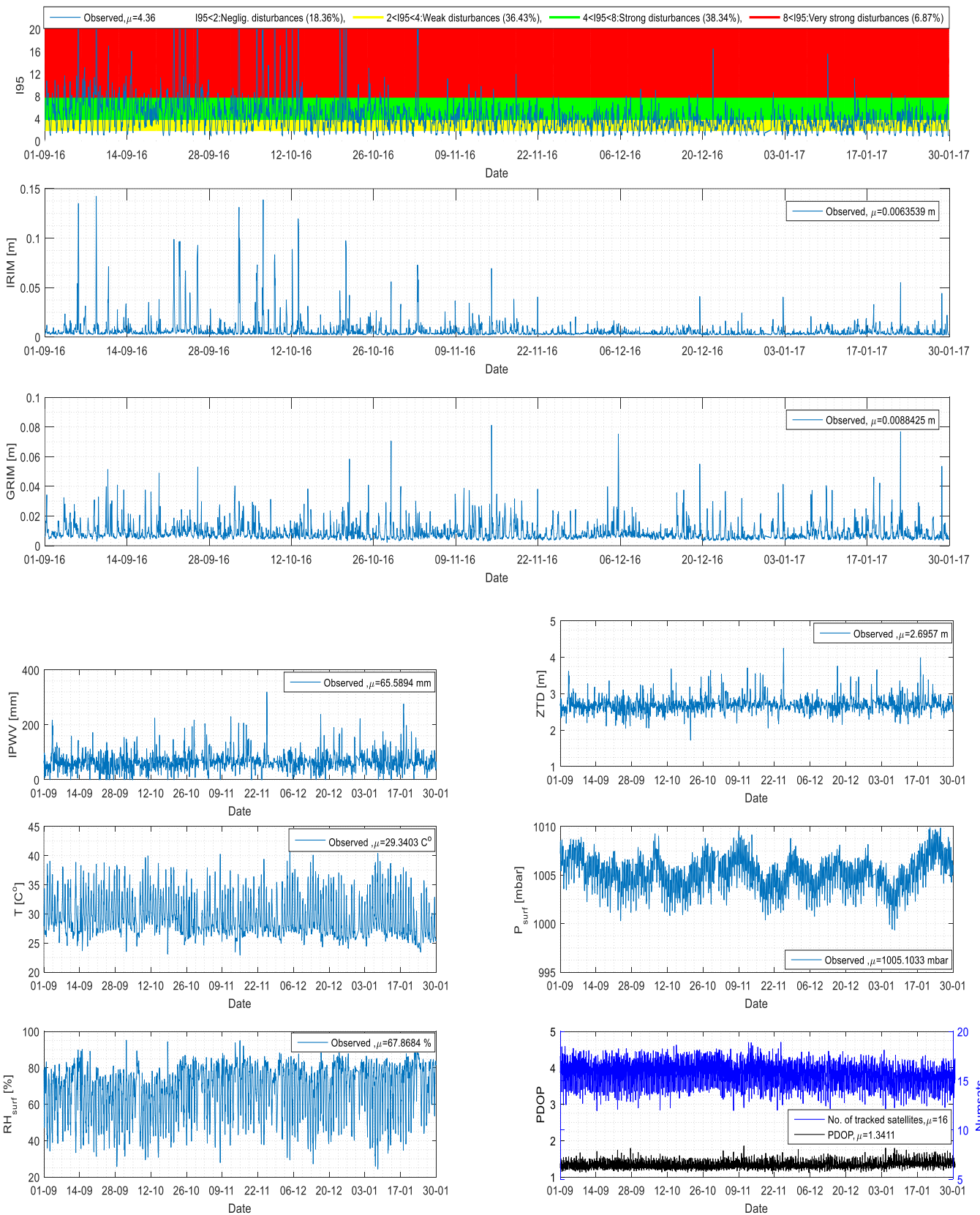
Figure 7.2: Graphs visualizing the I95/GRIM/IRIM values (top) as observed by SiReNT, and the Tropospheric information, PDOP values and number of tracked satellites (bottom) during this period, as observed by the SLYG CORS (period: 01-09-'16 – 30-01-'17). For a more detailed explanation of the graphs, see '7.1 Figures/Tables explained'.

By comparing the IM displacement data to the default thresholds, it is first determined what percentage of data would have caused the system for a specific CORS to have been disarmed (observations were unreliable) in case the thresholds were applied. From this follows the percentage of observations that were supposedly reliable. After that the percentage of supposedly reliable observations that were between the warning and alert thresholds respectively, is determined. Examples of the resulting graphs (in this case for the SLYG CORS) can be found in Figure 7.1. In this figure both the supposedly unreliable (red dashed) and the supposedly reliable data (black) is plotted, in order to visualize when the observations were reliable and when they were not. These results are compared to the simultaneously recorded Ionospheric and Tropospheric circumstances, which are presented in Figure 7.2. The TEC values are not included in this, as they could not be provided. This is not problematic however, as the I95/IRIM values are believed to act as a good indicator of the impact of the Ionosphere.

The data for most CORS in this dataset contains data over ~5 months and is the longest dataset that is available for this project. Therefore, this dataset is also used to determine possible trends in the stability and coordinates of the different CORS, with respect to the SNPT CORS. For this only the data that was supposedly reliable, is used. After confirming the reasonability of the trend approximations, the estimated trends are presented in Table 7.1, alongside with 2 maps (Figures 7.3 and 7.4) visualizing the horizontal and vertical motion of the SiReNT CORS, with respect to the SNPT CORS, respectively. Note that this is thus not the absolute motion of the CORS. To simply apply interpolation between the CORS in order to generate an overview of the motion everywhere in Singapore seems inconclusive. Hence in these maps only the motion at the CORS is visualized, as these are the only locations where the motion is known.
The ways the reasonability check of the determined trends is performed are described in Appendix 4. Keep in mind that the data recorded by the SNSC CORS and the SING CORS is from a much shorter period however, due to data connection problems.

The graphs for the SLYG CORS are thus presented in Figures 7.1 and 7.2, where the graphs for all CORS can be found in Appendix 5. Note however, that in this Appendix the Figurelayout is different; here the horizontal components and the vertical component in combination with the Tropospheric information graphs are presented in two separate figures. Also, here the SiReNT I95/IRIM/GRIM graph is presented individually.
An overview of all the results can be found in Table 7.1. More details on what all the figures visualize and the Table present is explained in the subsection '7.1 Figures/Tables explained'.

7.1.1. IM displacement data from the RTK engine module in baseline mode

First of all, in general it is mainly the red dashed time series that exceeds the thresholds (see Figure 7.1, and Appendix 5). This is as expected since these are the moments where the observations supposedly were unreliable, and the system for that CORS would have been disarmed, if the default thresholds would be applied. In that case, these observations would have been seen as outliers and filtered out by the TPP software. It comes clear from the graphs that this happens several times during this period. Most graphs also show (some) black (supposedly reliable) displacements exceeding the thresholds, some even with

magnitudes larger as compared to the supposedly unreliable displacements. This is possible, as large displacement magnitudes do not necessarily also have 3σ standard deviations that are exceeding the pre-set thresholds. Hence the determined positioning solutions (and thus displacements) can still be determined to be reliable (see appendix 1 for more details).

As one would expect, the displacements in general are sometimes negative and sometimes positive, there are no clear patterns visible on this time scale. Also, when comparing the time series per component (northing, easting, and height) one can conclude, that when observing a large displacement magnitude in one of the components, it often means the simultaneously observed displacement magnitudes in the other components are relatively large(r) too. This makes sense as when an observation is affected by something, it is unlikely that only one of its component is affected.

When looking at the (large) displacements (that are exceeding the thresholds), one can see that the usually the northing component shows the least of these occurrences, followed by the easting component, and finally the height component. Generally, the magnitudes of the displacements in horizontal components are quite similar, but smaller as compared to the magnitudes of the displacements in the height component.

Most of the relatively large displacements are occurring during the first half of the data sets. Several of the dates at which these were recorded by the different CORS are coinciding (depending on the length of the time series); for example, September 1st, 6th, 9th, 11th and 26th, October 9th, 12th, and 21st, and November 3rd, and 11th. It comes clear from the graphs that the data reliability improves (less red displacements, and less displacements exceeding the thresholds) towards the second half of the time series.

When looking at the mean magnitude of the 3D displacements (see Table 7.1), it turns out that the mean displacement for the SRPT CORS is the smallest (closest to zero), followed by SLYG, SING, SNSC, SNYU, SSMK, SSTS, and SNUS in ascending order of magnitude.

Table 7.1: Mean magnitudes of 3D displacements per CORS.

CORS	mean [m]
SLYG	0.0052
SNSC	0.0140
SNUS	0.0324
SNYU	0.0153
SRPT	0.0032
SSMK	0.0255
SSTS	0.0302
SING	0.0061

From the results presented in Table 7.2 (and Graphs in Appendix 5) can be concluded, that during this period, the IM displacement data recorded by the SNSC CORS was the most reliable. After that comes the SING CORS, followed by the others (their reliability differs less than 0.3 %). When looking at the percentage of reliable observations that were within the specific thresholds, one can see that the SLYG CORS was doing best, followed by SRPT, SNSC, SING, SNYU, SNUS, SSMK, and SSTS, in descending order.

Note that the SSTS CORS was affected by a data disruption, resulting in small data gap, on October 10th.

7.1.2. Ionospheric information

The I95/IRIM graphs present the values for the SiReNT infrastructure as a whole (see Figure 7.2, and Appendix 5). In the graphs, one can see that these values vary quite a bit as well, including some large magnitudes throughout the time series.

Table 7.2: Overview of all results, per specific component. For a more detailed explanation of what is presented in this graph, see '7.1 Figures/Tables explained'.

Northing

CORS	Mean [m]	System armed [%]	Armed observations within warning threshold [%]	Armed observations within alert threshold [%]	Trend [m/y]
SLYG	0,004	98,53	99,97	99,97	-0.0007
SNSC	0,0006	100	99,75	100	0.0032
SNUS	-0,0018	98,58	99,58	99,86	-0.0011
SNYU	0,0002	98,53	99,72	99,94	-0.0022
SRPT	0,002	98,61	99,78	99,97	-0.0024
SSMK	-0,0059	98,36	99,19	99,67	0.0007
SSTS	-0,0017	98,32	99,32	99,82	0.0004
SING	-0,0061	99,84	99,68	100	0.0157

Easting

CORS	Mean [m]	System armed [%]	Armed observations within warning threshold [%]	Armed observations within alert threshold [%]	Trend [m/y]
SLYG	0,0027	98,53	99,7	99,97	0.0072
SNSC	0,0071	100	99,88	99,94	0.0153
SNUS	0,0042	98,58	99,86	99,97	0.0012
SNYU	0,0038	98,53	99,89	100	0.0004
SRPT	0,0008	98,61	99,94	100	-0.0006
SSMK	-0,0005	98,36	99,86	100	0.0047
SSTS	0,0068	98,32	99,82	100	-0.0029
SING	0,0005	99,84	99,68	100	0.0359

Height

CORS	Mean [m]	System armed [%]	Armed observations within warning threshold [%]	Armed observations within alert threshold [%]	Trend [m/y]
SLYG	-0,002	98,53	99,89	100	0.004
SNSC	-0,012	100	99,88	99,94	0.005
SNUS	-0,0321	98,58	99,5	99,95	0.0007
SNYU	-0,0148	98,53	99,56	99,97	0.0093
SRPT	0,0024	98,61	99,83	99,94	0.0091
SSMK	-0,0248	98,36	98,44	99,89	0.0005
SSTS	-0,0294	98,32	99,43	99,47	0.0041
SING	0,0004	99,84	100	100	0.0542

In the I95/IRIM graphs the number of occurrences of these values as well as the overall magnitudes are getting smaller towards the second half of the time series however. One can see that the few largest I95 values are occurring mainly during September and October, for example on September 6th, and 9th, between September 23th-26th, October 9th-13th, and October 20th, but also on November 3rd, and some slightly smaller, but still relatively large values, as compared to most, on December 22th and January the 11th. Interesting to note is that the relatively large values usually were recorded during the second half of the day. Another thing to note is that these relatively large values often suddenly occur. Hence from now on, these will be referred to as sudden severe fluctuations (keep in mind that we are dealing with hourly values here, however).

Table 7.3: Overview of the number of I95 observations per specific region in percentages.

SiReNT I95

Value	Disturbance	Percentage
0-2	Negligible	18.36%
2-4	Weak	36.43%
4-8	Strong	38.34%
8+	Very strong	6.87%

An overview of the percentages of the number of observations per I95 region is presented in Table 7.3. The largest I95 values often (not always) coincide with large values in the IRIM graph.

7.1.3. Tropospheric information, PDOP, and number of tracked satellites

When looking at the Tropospheric information and the observed PDOP/number of tracked satellites in general, one can see that all graphs fluctuate quite a bit (see Figure 7.2 (bottom), and Appendix 5).

Other than a few sudden large values (further on referred to as sudden severe changes) in the IPWV/ZTD graphs and a minor change in the surface pressure trend (on January 1st), no unusual variations occur in the graphs.

The recorded temperature and relative humidity are negatively correlated; the graphs show a mirrored kind of behavior. This means that when the temperature is relatively high, the relative humidity is relatively low and vice versa. This is in agreement with what is described before, in section 5.2.1 (*TTP - ZTD, IPWV, Relative humidity, pressure, and temperature*). The overall (spread of the) temperature and relative humidity differ somewhat depending on the CORS' location.

For most CORS, the PDOP and the number of satellites gradually increase and decrease, respectively, from January 5th onward. This relationship between the PDOP and the number of tracked satellites is expected, as when the number of tracked satellites decreases, the number of satellites that could improve the relative geometry decreases too. This is likely to result in an increasing PDOP.

As for the SING CORS, something interesting happened with the PDOP and the number of satellites suddenly increase and decrease, respectively, on January 23rd, after which they suddenly return to the usual values on January 24th. Other than that, the recorded PDOP and number of tracked satellites do, other than some relatively slightly more extreme values, not show unusual variations, and behave as expected.

It seems as if there is a diurnal variation in the recorded PDOP values/number of tracked

satellites. During the mornings (even though not very clear) there are often maxima in the recorded PDOP value and minima in the number of tracked satellites.

The GRIM graph (see Figure 7.2, and Appendix 5) does not show much difference between the first and the second half of the time series; the recorded values also show no direct relation to the recorded I95/IRIM values. The largest GRIM magnitudes are recorded on October 20th, and 30th, on December 5th, and 19th, and on January 24th.

7.1 Figures/Tables explained

The displacement graphs per component (figure 7.1, top: northing, middle: easting, and bottom: height) visualize:

- The supposedly reliable observations in black;
- The supposedly unreliable observations in red (dashed line);
- The warning threshold in cyan;
- The alert threshold in (dark) blue.

The bar graphs included on the right are visualizing the frequency of the occurrence of a certain range of displacements (all). This way it can easily be seen that the observations are normally distributed around the mean. The percentage of supposedly reliable observations, that satisfied the specific thresholds (warning and alert), is presented in the legends.

The SiReNT I95/IRIM/GRIM graph (figure 7.2, top) present these respective parameters in blue (Note that these are values for the infrastructure as a whole). The I95 graph is presented at the top, the IRIM graph in the middle, and the GRIM graph is presented at the bottom. Note that in the I95 graph the different regions are visualized by the colours assigned to these regions (see Table 4.2):

- White: negligible Ionospheric activity;
- Yellow: weak Ionospheric activity;
- Green: strong Ionospheric activity;
- Red: very strong Ionospheric activity.

The percentage of I95 values which were within these specific regions is presented in the legend at the top of the graph.

The Tropospheric information graphs (figure 7.2, bottom) visualize the observed parameters (IPWV, temperature, relative humidity, ZTD and the atmospheric pressure) in blue, where in the bottom-right graph, the PDOP value is visualized in black together with the number of tracked satellites in (dark) blue.

All graphs, per CORS, are presenting data from the same time period, enabling comparison of the different data types.

Table 7.1: This table presents the mean of the reliable 3D displacements during this period, per CORS.
The cells in this table are also coloured depending on the value it contains. In general, the lighter the colour of the cell (with ultimately white) is, the closer the value is to zero, and vice versa.

Table 7.2: This table presents the IM displacement data related results (from left to right):

- The mean of the supposedly reliable displacement data;
- The percentage of the supposedly reliable displacement data from this CORS (dependent on the computed 3σ standard deviations exceeding the disarming threshold);
- The percentage of supposedly reliable observations which were within the warning thresholds;
- The percentage of supposedly reliable observations which were within the alert thresholds;
- The trend in the supposedly reliable displacement data.

The cells in this table are coloured depending on the value it contains. In general, the lighter the colour of the cell (with ultimately white) is, the better the value, and vice versa. In the columns containing the mean displacements three colours are used (negative: green, 0: white, and positive: yellow). In the columns containing the percentages, two colours are used, ranging from dark shades of green for the lowest percentages to lighter shades of green for the higher percentages. In the columns containing the determined trends, three colours are used (negative: red, 0: white, and positive: purple). This way it easily can be seen whether, according to this data, a certain component is perfect (white) or less good (increasing darkness of colours).

Table 7.3: This table presents the percentages of the I95 values per specific region, during this period (for the SiReNT infrastructure as a whole).

Table 7.4: This table presents an overview of the dates where there were supposedly unreliable IM displacements (represented by u), or reliable IM displacements, exceeding the default thresholds (represented by r), together with the dates on which there were sudden severe fluctuations in the Ionospheric/Tropospheric activity and/or GRIM value, or a combination of the two. Sudden severe fluctuations in the Tropospheric activity are represented by salmon pink, sudden severe fluctuations in Ionospheric activity are represented by orange, and a combination of both is represented by brown. Note that this overview is done per day.

7.1.4. Comparison

Most of the relatively large displacements are occurring during the first half of the data set (more specifically during September and October). Besides that, the I95/IRIM values are relatively higher during this period as well. Therefore, the IM displacement data from these two months, in combination with the Ionospheric information and the Tropospheric information, the PDOP and the number of tracked satellites, that stood out, are analysed further. This means that the SNSC CORS and the SING CORS are excluded from this analysis, as from these CORS there is only limited data available.

A comparison of the specific dates during these months, on which IM displacements were supposedly unreliable, or reliable but exceeding the default thresholds, with the dates on which there were sudden severe fluctuations in the Ionospheric/Tropospheric activity and/or GRIM value, is presented in Table 7.4. When talking about severe fluctuations, it means that the change in the parameter value exceeds
All related graphs can be found in Appendix 6 and 7, for September and October, respectively. For a more detailed explanation of the specific graphs, see 'Appendix 6 and Appendix 7 Figures explained'.

From the information presented in Table 7.4, it can be concluded that whenever there were both sudden severe fluctuations in the Ionospheric activity and in the Tropospheric activity and/or GRIM value, this always coincided with unreliable IM displacement data. This was recorded by all of the CORS on September 11th and 22nd, and on October 3rd, 6th, 7th, and 13th.

Whenever there were sudden severe fluctuations in the Ionospheric activity only, this also almost always coincided with unreliable IM displacement data, and sometimes with reliable IM displacement data exceeding the default thresholds, as well.
The dates on which it coincided with the unreliable IM displacement data, was recorded by all of the CORS on September 6th, 9th, 23rd, 24th, and 26th, and October 9th, 11th, 12th, and 20th. Note that on October 10th, the unreliable IM displacement data only was recorded by 3 CORS.

The dates on which sudden severe fluctuations in the Ionospheric activity coincided with reliable IM displacement data exceeding the default thresholds, was recorded by all of the CORS on September 9th, and one/some of the CORS on September 23rd, 24th, and 26th, and October 12th.
On September 15th, all CORS recorded sudden severe fluctuations in the Ionospheric activity, but no coinciding unreliable IM displacement data, or reliable IM displacement data exceeding the default thresholds.

Sept. Day	1	2	3	4	5	6	7	8	9	10	11	12	13	14	15	16	17	18	19	20	21	22	23	24	25	26	27	28	29	30
SLYG				u		u			u r		u											u	u r	u			u			
SSTS	u r	u		u		u		u	u r		u			r								u	u	u	u r		u			r
SSMK	u r	u		u		u			u r		u			r						u		u	u	u r	u r		u			r
SRPT		u	r			u			u r		u											u	u	u	u		u			r
SNYU	u r	u		u		u		u	u r		u			r								u	u	u	u r		u			r
SNUS	r					u			u r		u											u	u	u	u		u			r

Oct. Day	1	2	3	4	5	6	7	8	9	10	11	12	13	14	15	16	17	18	19	20	21	22	23	24	25	26	27	28	29	30	31
SLYG		u				u	u		u	u	u	u	u	u	r					u	u				r						
SSTS		u	r			u	u		u		u	r	u	u						u	u										
SSMK		u				u	u		u	u	u	u	u	u						u	u					u					
SRPT		u				u	u		u		u	u	u	u						u	u										
SNYU		u				u	u		u		u	u	u	u						u	u										
SNUS		u				u	u		u	u	u	u	u	u						u	u										

symbol/ colour	meaning
u	Unreliable IM displacement
r	Reliable IM displacement exceeding threshold
	Sudden severe fluctuations in the Tropospheric activity and/or GRIM value
	Sudden severe fluctuations in the Ionospheric activity
	Sudden severe fluctuations in the Ionospheric activity and Tropospheric activity and/or GRIM value

Whenever there were only sudden severe fluctuations in the Tropospheric activity and/or GRIM value, this also coincided with unreliable IM displacement data a few times. This was recorded by most of the CORS on September 4th, and by all of the CORS on October 14th, and 21st.

There are a few occurrences where this coincided with reliable IM displacement data exceeding the default thresholds, as well. This was recorded by one/some/half of the CORS on September 4th, 14th, and October 4th, 15th, and 25th.

Besides that, there were also unreliable IM displacements and reliable displacements exceeding the default thresholds, when there was no record of sudden severe fluctuations in the Ionospheric activity and Tropospheric activity and/or GRIM value. This was recorded by all/most of the CORS on September 1st, 2nd, 28th, and 30th, and by one/some of the CORS on September 8th, and 21st, and October 26th.

There was one day on which there was a sudden severe fluctuation in the Ionospheric activity, however not coinciding with any unreliable IM displacements or reliable IM displacements exceeding the default thresholds. This was recorded by all of the CORS on September 15th.

Like that there are also days where sudden severe fluctuations in the Tropospheric activity and/or GRIM value were recorded, however not coinciding with any unreliable IM displacements or reliable IM displacements exceeding the default thresholds. This was recorded by all/most of the CORS on September 18th, 19nd, 25th, and 27th, and October 2nd, 4th, 5th, 15th, 25th, 28th, and 29th, and by one/half of the CORS on September 4th, 14th, and October 4th, 15th, and 25th.

Based on this several percentages can be determined. An overview of these is presented in Table 7.5.

During these two months, on 24.59% of the days, a severe fluctuation in the Tropospheric activity and/or GRIM value were recorded, where on 20.00% of those specific days, this coincided with unreliable displacements, and on 33.33% of those specific days, this coincided with reliable displacements exceeding the thresholds.

Besides that, on 18.03% of the days, a severe fluctuation in the Ionospheric activity was recorded, where on 90.91% of those specific days, this coincided with unreliable displacements, and on 45.45% of those specific days, this coincided with reliable displacements exceeding the thresholds.

On 9.84% of the days during these months, a severe fluctuation in both the Ionospheric activity and the Tropospheric activity and/or GRIM value were recorded. On all those specific days, this coincided with unreliable displacements, where on none of them it coincided with reliable displacements exceeding the thresholds.

On 47.54% of the days during these months, no sudden severe fluctuations were recorded, yet on 20.69% of those specific days unreliable displacements were recorded, and on 6.90% of those specific days, reliable displacements exceeding the thresholds, were recorded.

Finally, on 36.07% of the days during these two months, nothing of the above was recorded (not included in the table).

Appendix 6 and Appendix 7 Figures explained

The SiReNT I95/IRIM/GRIM graphs (figure A.6.1 and Figure A.7.1, for September and October respectively) present these respective parameters in blue (Note that these are values for the infrastructure as a whole). The I95 graph is presented at the top, the IRIM graph in the middle, and the GRIM graph is presented at the bottom. Note that in the I95 graph the different regions are visualized by the colours assigned to these regions (see Table 4.2):

- White: negligible Ionospheric activity;
- Yellow: weak Ionospheric activity;
- Green: strong Ionospheric activity;
- Red: very strong Ionospheric activity.

The displacement graphs per component (figures A.6.2-7 (top) and Figures A.7.2-7 (top), for September and October respectively), visualize:

- The supposedly reliable observations in black;
- The supposedly unreliable observations in red (dashed line);
- The warning threshold in cyan;
- The alert threshold in (dark) blue.

The Tropospheric information graphs component (figures A.6.2-7 (bottom) and Figures A.7.2-7 (bottom), for September and October respectively), visualize the observed parameters (IPWV, temperature, relative humidity, ZTD and the atmospheric pressure) in blue, where in the bottom-right graph, the PDOP value is visualized in black together with the number of tracked satellites in (dark) blue.

All graphs, per CORS, are presenting data from the same time period, enabling comparison of the different data types.

When comparing it to the total number of days in this two-month period, it follows that on 4.92% of the days in this period, unreliable IM displacement data was recorded, simultaneously with sudden severe fluctuations in the Tropospheric activity and/or GRIM value, where on 8.20% of the days, the latter coincided with reliable IM displacement data exceeding the thresholds.

On 16.39% of the days in this period, unreliable IM displacement data was recorded, simultaneously with sudden severe fluctuations in the Ionospheric activity, where on 8.20% of the days, the latter coincided with reliable IM displacement data exceeding the thresholds.

on 9.84% of the days in this period, unreliable IM displacement data was recorded, simultaneously with sudden severe fluctuations in the Ionospheric activity, and the Tropospheric activity and/or GRIM value.

Finally, on 9.84% of the days in this period, unreliable IM displacement data was recorded without any coinciding severe fluctuations in the atmospheric information. On 3.28% of the days, this was the case for reliable IM displacement data exceeding the thresholds.

It is noted that besides the results presented in Table 7.4, there are also some other, more occasional, supposedly unreliable displacements, which are CORS specific (not for all CORS (simultaneously)), and generally have a smaller magnitude. Therefore, these have not been presented here, as to focus on the more obvious ones.

Table 7.5: An overview of how often certain events were recorded, individually or together.
An overview of how often certain events were recorded, individually or together.
The number of days on which sudden severe fluctuations in the Tropospheric activity and/or GRIM value, or in the Ionospheric activity, or a combination of both of these, or none of these, were recorded, is presented in the column with the different shades of blue. This is presented as a percentage of the total number of days in September, October, and those months combined (whole period I).
The number of days on which there was a record of at least one supposedly unreliable displacement (u), or at least one supposedly reliable displacement (r) exceeding the thresholds, is represented in the column with the different shades of red. This is presented as a percentage of the total number of days on which there was either a sudden severe fluctuation in the Tropospheric activity and/or GRIM value, or in the Ionospheric activity, or a combination of both of these, or none of these. This is again presented for September, October, and those months combined (whole period I).
Besides that, the total number of days where sudden severe fluctuations in the Tropospheric activity and/or GRIM value, or in the Ionospheric activity, or a combination of both of these, or none of these, were recorded, coincided with a record of at least one supposedly unreliable displacement, or at least one reliable displacement exceeding the thresholds. In this case it is presented as the percentage of the total number of days in this two-month period.
The darkness of the shades increased with increasing percentages.

This Table should thus be read as follows, for example, during September, on 20.00% of the days of the month, a severe fluctuation in the Tropospheric activity was recorded. During this particular month, 16.67% of those days, coincided with at least one supposedly unreliable displacement, where 33.33% coincided with at least one supposedly reliable displacement that exceeded the thresholds. This is presented in the same way for October, and for both months combined (whole period I).
As for the last two columns (whole period II), these should be read as follows, for the top row; on 4.92% of the days in this two-month period, there was a record of a sudden severe fluctuation in the Tropospheric activity and/or GRIM value coinciding with at least one supposedly unreliable displacement. On 8.20% of the days in this two-month period, a sudden severe fluctuation in the Tropospheric activity and/or GRIM value coincided with at least one supposedly reliable displacement exceeding the thresholds. The other rows read the same.

	September			October			Whole period I			Whole period II	
	# of days	u	r	# of days	u	r	# of days	u	r	u	r
Troposphere	20,00%	16,67%	33,33%	29,03%	22,22%	33,33%	24,59%	20,00%	33,33%	4,92%	8,20%
Ionosphere	20,00%	83,33%	50,00%	16,13%	100,00%	20,00%	18,03%	90,91%	45,45%	16,39%	8,20%
Both	6,67%	100,00%	-	12,90%	100,00%	-	9,84%	100,00%	-	9,84%	-
None	53,33%	31,25%	12,50%	41,94%	7,69%	-	47,54%	20,69%	6,90%	9,84%	3,28%

7.1.5 Observed motion

From the trends in the IM displacement data (see Table 7.1), the motion per year of all CORS is determined, with respect to the SNPT CORS (see the motion maps, Figures 7.3 and 7.4). All the position shifts are thus recalculated taking into account the estimated shift of this fixed reference. Hence, the motion of the latter is visualized in the maps as being zero. Note that this is therefore not the absolute motion of the SiReNT CORS. For the trend determination, only the supposedly reliable IM displacement data is used.

One can see that the observed (relative) horizontal movements are mainly directed eastward. Some are however more aimed to the north (SRPT, SING, SNSC, SSMK) and some more to the south (SLYG, SSTS, SNUS, SNYU). As for the observed vertical motion, except for SING and SNSC, all CORS either recorded very little movement, or a subsiding movement, with respect to the SNPT CORS.
The magnitudes of the observed motion are mostly in the millimeter range. The magnitude of the observed motion for the SING CORS is much larger as compared to that of the other CORS however.

Note that there are no clear seasonal or diurnal variations, nor anything clearly related to local differences such as signal blockage by structures, visible in the recorded IM displacement data.
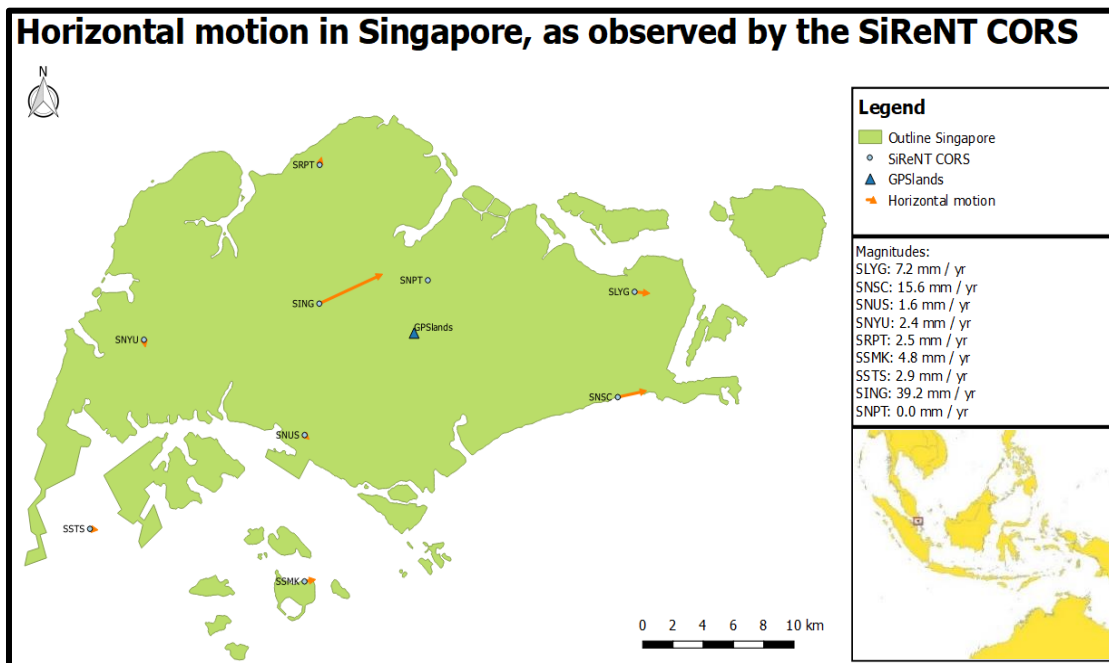

Figure 7.3: A map visualizing the horizontal motion, with respect to the SNPT CORS, as observed by the SiReNT CORS. The motion direction is visualized by the pointing direction of the arrows, where the magnitude is represented by its length, and is listed in the legend.
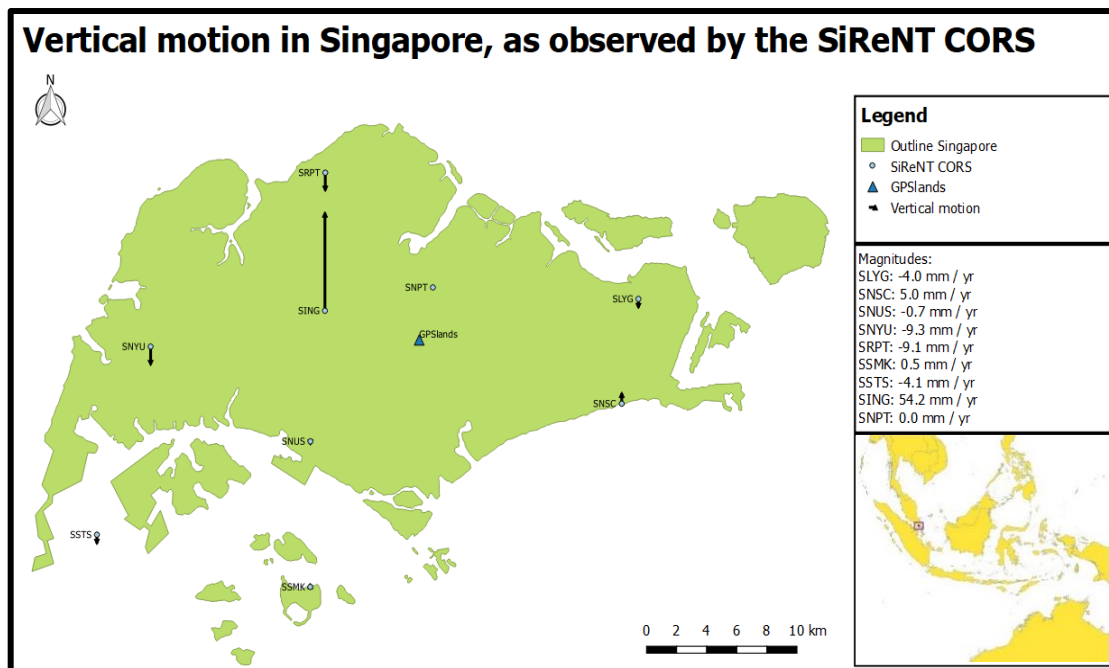
Figure 7.4: A map visualizing the vertical motion, with respect to the SNPT CORS, as observed by the SiReNT CORS. Uplift and subsidence is visualized with arrows pointing North (uplift) and South (subsidence), respectively. The magnitude of the motion is represented by the length of the arrows, and is listed in the legend.

7.2. Discussion

In this section, the datasets, as well as the results presented in section 7.1 are further discussed.

Resampling

In order to aid the analysis as well as to determine possible trends, all this data is resampled to hourly data, such that all observations from the different data types now have matching timestamps. This time interval is chosen to be hourly, as this is the largest time interval originally present in the data.

Resampling, especially if the time step into which is resampled is larger, usually means that information will be lost. To ensure that at all times actual real data is used, rather than a simulated or approximated data, this is not preferred. In this case that was a necessity however.

Data reduction

Firstly the data reduction should take place much later, and secondly, for this, a proper algorithm should be written or developed. This, so that the data reduction happens in a clear and consistent fashion, without throwing away too much relevant while at the same time keeping too much irrelevant data. In case there are too many observations in a certain timespan, these should be averaged in order to get the required number. At the moment there are numerous occasions where the data from a specific CORS is completely missing, where the data from other CORS is included several times per hour. The data from all CORS should be included once per particular timespan.

IM displacement data - differences between CORS
As comes clear from the presented IM displacement data, the magnitudes and directions of the recorded displacements, at a particular time, do differ per CORS. As their locations differ, the observed IM displacements per CORS were not expected to be identical. However, as Singapore is relatively small, they were expected to be more similar.
Because of Singapore's small size, the impact of the Ionospheric activity is assumed to be the same all around the country. Besides that, the different CORS are all equipped with the same, or at least very similar equipment. Hence, besides the fact that the GNSS signals observed by the different CORS have slightly differing travel times, the differences can be related to local differences, such as signal blockage by structures, affecting the skyview and causing multipath, and locally differing Tropospheric circumstances and/or weather variations.

Note that in terms of data reliability, the different CORS throughout Singapore behaved very similar however. Also, note again that all CORS are corrected for the displacements observed by the SNPT CORS.

IM displacement data - CORS reliability
As described before, the data cannot be used to check whether the SNPT CORS indeed is the most stable CORS. It can be used however, to order the other CORS in terms of stability (and reliability) (with respect to the SNPT CORS). From the results can be concluded that over the 5 months, both the SLYG CORS and the SRPT CORS where performing quite similar, and relatively better than the other CORS. After that follow SNYU, SNUS, SSTS, and SSMK in descending order. Note however that the mean displacement from the SNUS CORS does not agree with this, and is furthest away from zero. Based on the results, the SING CORS and the SNSC CORS were doing quite good as well. However, keep in mind that their datasets are very short, and therefore it is assumed that this is not a good representation of the stability (and reliability) of the respective CORS.
In order to get better results, longer data sets, that are unaffected by the data reduction algorithm, are required.

When looking at the components individually and comparing the (large) displacements (that are exceeding the thresholds), one can conclude that the height component usually is less reliable as compared to the horizontal components (see figure 7.1, and the figures in Appendix 5, 6, and 7). This could be related by the shape of the geometric ellipsoid that GNSS adopts. This ellipsoid does not always perfectly match the Earth's surface everywhere. On top of that, in the vertical plane, there are only satellites on one side, as compared to in the horizontal plane, where there can be satellites on both sides. Because of this, the impact of the Troposphere is normally also more severe on the vertical component then it is on the horizontal components.
When comparing the horizontal components, it turns out that the eastern component of the observations is reliable less often as compared to the northing component of the observations. Why this is the case is uncertain, however it could be that this is caused by the specific motion direction of the satellites. This possibly favors the northern component over the eastern component.

Comparison of IM displacement data with atmospheric information, PDOP value and number of tracked satellites (September-October 2016)

During this period several supposedly unreliable IM displacements were recorded. Besides that, there were also (relatively) large supposedly reliable IM displacements which were exceeding these thresholds. Sometimes the reliable displacements are (even) exceeding the unreliable displacements. Why the latter is the case is not quite understood, this is possibly related to the fact that whatever factor is causing this, is not properly detected by the IM system yet. Hence this should be further investigated.

When looking at the results presented in section 7.1, one can conclude that sudden severe fluctuations in the Ionospheric activity could very well be the main factor causing the IM displacements to be unreliable. Almost always, whenever there was a record of this, especially if coinciding with severe fluctuations in the Tropospheric activity and/or GRIM, unreliable IM displacements were recorded as well.

The only day on which this was not the case, was on September 15th. On that day the sudden severe fluctuations in the Ionospheric do not affect any of the CORS. Why only on this day, and not on others, is not quite understood.

Another interesting observation is that on October 10th, only three CORS (SLYG, SNUS, and SSMK) recorded coinciding sudden severe fluctuations in the Ionospheric activity and unreliable IM displacements, where the other CORS did not record anything. Singapore is small, and it is assumed that therefore the impact of the sudden severe fluctuations in the Ionospheric activity would affect all the CORS in a similar way. However, the magnitude of the unreliable IM displacement seems to be related to where these specific CORS are located (in terms of North versus South). Hence, when looking at the IM displacement graphs from these CORS (see Appendix 6, and 7), one can conclude that during this period, the impact of these sudden severe fluctuations in the Ionospheric activity was decreasing towards the northern parts of Singapore. This means that, even though this does normally affect all the CORS in a similar way, it also can only affect a select number of CORS, an/or the impact can vary depending on where the CORS are located, even though it is only several kilometers apart.

Note that the data from the SSTS CORS contains a data gap on this day, and thus it is not possible to say anything about this CORS with regards to this.

Note that the unreliable displacements are usually recorded during the second half of the day. This agrees with the timings of the sudden severe fluctuations in the Ionospheric activity presented in Table 7.4. These are usually recorded during the second half of the day as well (see graphs in Appendix 6 and 7). It turns out that on the dates and times where those were recorded simultaneously, the Ionospheric activity was suddenly extremely high (the IRIM values agree with this). As described before, I95 values between 4 and 8 already indicate strong Ionospheric activity (causing disturbances), where I95 values exceeding 8 indicate a very strong Ionospheric activity. The Ionospheric activity has an impact on the GNSS observations and can cause sudden relatively large displacements. Especially the extremely high values, exceeding 14, which most of the time even cause observations to be unreliable. Especially when the Ionospheric activity suddenly increases a lot, the observations are very likely to be affected, as the applied corrections (as part of the network processing) are no longer sufficient.

The sudden severe fluctuations in the Ionospheric activity being the main driving factor behind unreliable IM displacements, also agrees with the results presented in Table 7.5; on 90.91% the days (16.39% of the total number of days during this two-month period), where sudden severe fluctuations in the Ionospheric activity were recorded, unreliable IM displacements were recorded simultaneously as well. When looking at the days on which the sudden severe fluctuations in the Ionospheric activity coincided with sudden severe fluctuations in the Tropospheric activity and/or GRIM, this percentage even increases to 100.00% (9.84% of the total number of days during this two-month period).
On 45.45% of the days (8.20% of the total number of days during this two-month period), where there was a record of sudden severe fluctuations in the Ionospheric activity only, there were reliable displacements exceeding the thresholds recorded as well.

The fact that in the I95/IRIM graphs the number of occurrences of these values as well as the overall magnitudes are getting smaller towards the second half of the time series can be related to variations in the solar activity, following seasonal fluctuations. The GRIM graphs do not show any such variation and are more random. This is expected, as this factor is related to Tropospheric activity and orbit errors, which are assumed to take place at random, and without any seasonal fluctuations.

When taking a closer look at the relationship between the IM displacements and sudden severe fluctuations in the Tropospheric activity and/or GRIM, it turns out that there generally is less coincidence. When there were sudden severe fluctuations in the Tropospheric activity and/or GRIM, this coincided with a much lower percentage of unreliable IM displacements, only 20.00% (4.92% of the total number of days during this two-month period). With regards to reliable displacements exceeding the thresholds, on 33.33% of the days (8.20% of the total number of days during this two-month period) where there was a record of sudden severe fluctuations in the Tropospheric activity and/or GRIM, these were recorded simultaneously. The number of reliable displacements exceeding the thresholds is thus higher when coinciding with sudden severe fluctuations in the Tropospheric activity and/or GRIM (as compared to sudden severe fluctuations in the Ionospheric activity). The impact from this is thus filtered out less sufficiently, as compared to the impact of sudden severe Ionospheric activity (more on this further on).

Some of these IM displacements that are exceeding the thresholds, coincide with unusual spiky behavior in the IPWV/ZTD graphs. It is unclear what is the exact relationship between this spiky behavior and the IM displacement magnitudes, however. Also, the reason why the displacement magnitudes only are impacted sometimes (at other times nothing unusual is visible in the graphs) is not understood. One explanation could be that there is another, unknown factor, that is, in varying degrees, affecting both the Tropospheric information and the displacement magnitudes. That would explain why at times the different CORS recorded unusual behavior simultaneously. This could be the same factor, or related to the one that is causing (some of) the supposedly reliable IM displacements to be exceeding the supposedly unreliable displacements.
This could for example be due to re-initializations, after loss of connection. These parameters could also be affected by artefacts related to the Ionospheric activity (or errors in the determination thereof). Another explanation could be that the infrastructure attempted to correct the displacement data for the impact of whatever was affecting the observations, with varying results. This spiky behavior could also be related to the fact that the only data

available is the data that is affected by the data reduction algorithm (and/or resampling), and therefore misses important information. Before the resampling the different datasets had slightly differing time stamps, hence a differing timespan. Another possibility is the occurrence of a temporarily sudden change in Tropospheric circumstances, due for example intense weather episodes. However, there should then be a record of these, and on top of that, this should then also be visible in the pressure/temperature data. As this is not the case, it is not very likely that this behavior is caused by intense weather episodes. Note however that events like that are able to affect the observations in similar ways.

It of course also could be that this behavior occurred within a timespan which was just too small for the impact of it to be recorded by the IM displacement data. Hence, this could mean that the impact of the parameters representing the Troposphere information still is underestimated and that not only the extreme cases of suddenly increasing, very strong activity has a great impact on the GNSS observations. In order to find out more, further research is required.

As expected, there is some relationship between the Tropospheric information and the simultaneously recorded GRIM value. Some of these dates, like September 11th, 20th, and 26th, also match the dates on which relatively large I95 values/unreliable displacements were recorded. On other dates, like September 13th, October 22nd, and 29th, this is not the case however. Apparently, on these dates the observation were not affected either, showing that the impact related to a large GRIM value on the data reliability, if there is any, is much smaller as compared to the impact of sudden severe fluctuations in the Ionospheric activity.

The PDOP and number of tracked satellites do not really show unusual variations. Hence the impact from these on the simultaneously recorded IM displacement data cannot be analysed. The one sudden change in PDOP and number of satellites, as recorded by the SING CORS, on January 23rd-24th, does coincide with an unreliable displacement, yet it is unclear what caused this. This change only took place once, and its duration was quite long. Even though unlikely, it could be that something was covering part of the antenna for the whole time, causing a continuous signal blockage.

Default thresholds

As presented in the results, and discussed in chapter 8, there is no relationship between the IM displacement data and the Rover displacement data. Hence the applied thresholds cannot be used in order to control the Rover performance. Instead, these thresholds are merely aimed at monitoring the output of the engine modules themselves, and warning notifying the user(s) whenever necessary. That does not change their level of importance however.

In this project's analyses, the default thresholds are applied. This would have caused the CORS would have been disarmed a few times, while notifying the end user. Most of the time however (over 98%, see Table 7.2), all CORS would still have been armed (and thus recording reliable IM displacement data). Of this reliable IM displacement data, over 99% was within the thresholds, for all CORS.

Hence, one can conclude that if the default thresholds were to be applied, almost all unreliable observations (likely due to sudden severe fluctuations in the Ionospheric activity), would be filtered out, and the resulting data would satisfy the thresholds for over 99% of the time.

Under the assumption that the reliable IM displacements that were exceeding the thresholds were indeed affected by the sudden severe fluctuations in the Tropospheric activity and/or GRIM, one can conclude that these are filtered out less sufficiently. Note however that, as mentioned previously, it also is possible that both the displacement data and the Tropospheric information are affected by the same unknown factor. In that case, it could be that nothing is/was filtered out, but just that this factor affected all parameters in varying degrees.

Making the thresholds smaller does slightly improve that. It does however also result in more of the general IM displacement data being filtered out, even data that does not seem to be disturbed and cannot really be related to any of the mentioned causes (see Figure 7.5). This would mean that notifications would be pushed out several times a day, every day, and a lot of data would be considered unreliable. In case there is only limited data, like in the case of this research, this would mean that there will not be much reliable data left.
Perhaps, when having the original displacement data (without being affected by the data resampling algorithm), this would be less of a problem.
Besides that, if this is the same for the IM displacement data resulting from the Network Motion engine module (here the IM displacement data from the RTK engine module in Baseline mode is discussed), it would generate the idea that the SiReNT infrastructure is not very stable.
Bigger thresholds would result in the opposite; less data loss, however with the (main) disturbances filtered out much less sufficiently.
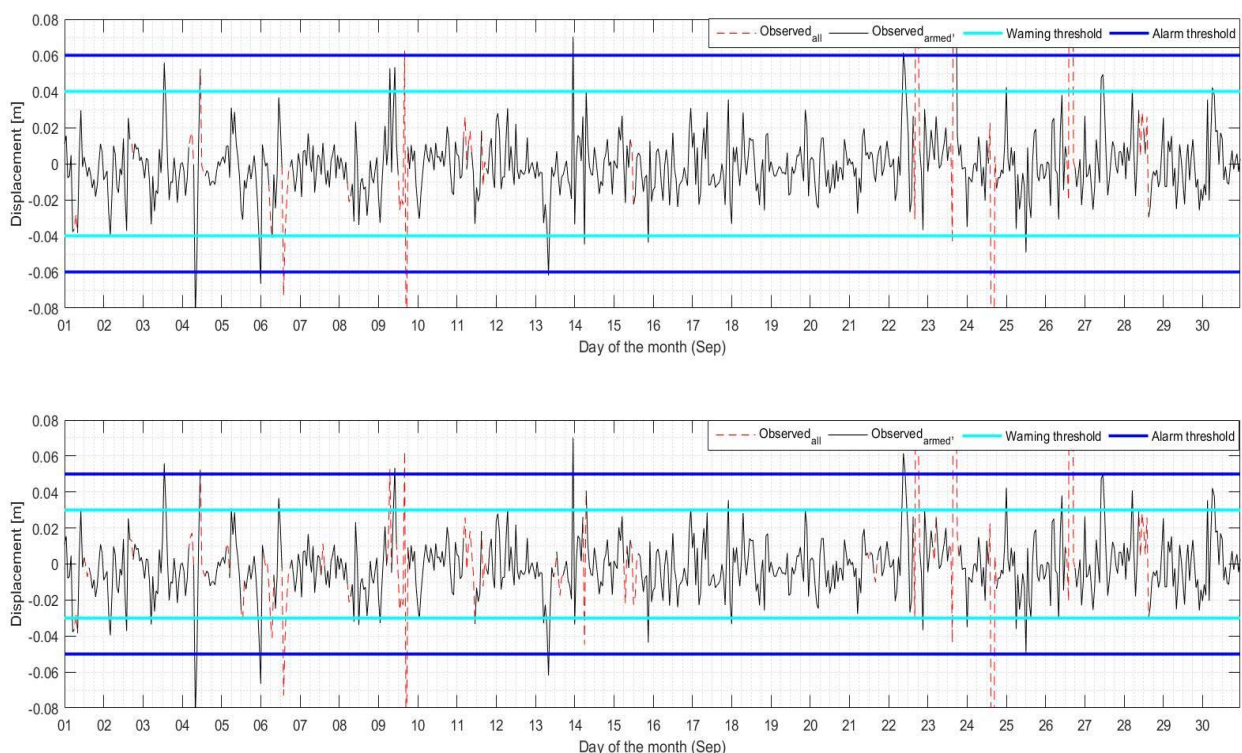
Figure 7.5: Graphs visualizing the height component of the SLYG CORS, when using tighter thresholds; a vertical warning and alert limit, of 0.09 m and 0.140 m, respectively (top), and a vertical warning and alert limit, of 0.08 m and 0.130 m, respectively (bottom).

The default thresholds are therefore considered to be quite a good trade-off (for the RTK engine module in Baseline mode); they filter out most of the main disturbances (especially the ones which are assumed to be related to sudden severe fluctuations in the Ionospheric activity), while minimizing the amount of data loss.

How this applies to the other engine modules is uncertain, as the thresholds can (and possibly should) be adjusted per engine module. This is the case as the aim and output of one engine module is independent from that of the other engine modules. Therefore, even though the default thresholds perform sufficiently with regards to the RTK engine module, there is a good possibility that this is not the case for other engines. Hence this should be further investigated.

Also, ways in which the disturbances can be filtered out better, without causing (much) reliable data loss, should be researched further. Perhaps it would be good to for example combine the IM displacement data with the Ionospheric information, as well as the Tropospheric information. An algorithm could be developed that could automatically find and confirm what is causing the displacement data to be unreliable, if it is determined to be unreliable, in Real-Time. Based on that it could be decided whether the observation indeed should be considered unreliable, and filtered out.

Trends and motion
From the trends in the data is the yearly motion of each CORS, with respect to the SNPT CORS, determined. One should realize that this is thus not the absolute motion.
In order to get reliable results, long datasets should be used. The maximum length of the available datasets for this research project was only 5 months however. The datasets from the SING CORS and the SNSC CORS were even shorter than that (around 1-2 months). Therefore, the results from these CORS can assumed to be even less reliable, relative to the results from the other CORS. It turns out that the displacement magnitudes for these specific CORS are relatively large, especially for the horizontal component. When disregarding the results from these CORS, the observed motion is predominantly a subsidence, while moving towards the (South-)East. Keep in mind that this is the motion with respect to the SNPT CORS however. The yearly motion of this CORS itself is unknown, hence nothing can be said about the absolute yearly motion.

Local differences are possible, especially in the vertical plane; local subsidence occurs throughout the world. The differences in the horizontal plane are somewhat more unexpected however, even though most of them are not even extremely large. The whole of Singapore (which is not very big in the first place) is located on one and the same continental plate (the
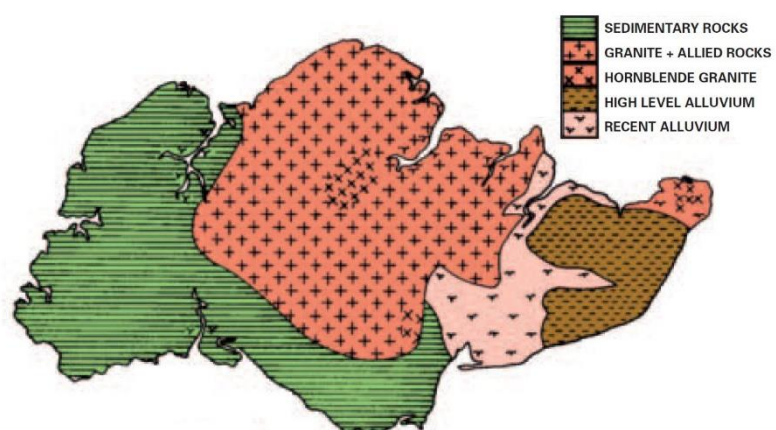
Figure 7.6: Simplified geological map of Singapore [4].

Sunda plate) [44]. Therefore, one would expect that all CORS observe horizontal speeds which are very similar to that of the SNPT CORS, hence resulting in corrected speeds of (close to) 0 mm/yr. This is not the case however, meaning that either there are indeed local horizontal movements ongoing, even in the horizontal plane, or that the data contains a discrepancy. The first could possibly be related to the fact that even though the whole of Singapore is located on one plate, the bedrock/subsurface is not the same everywhere [4] (see Figure 7.6); and different rock types behave differently. It also could indicate the presence of local fracturing/cracking/faulting however. Both would allow the differences in the observed motion pattern in the horizontal plane.

8.

Trimble PIVOT data analysis part II
Rover displacement data

This chapter is about the IM displacement data and atmospheric information, from the RTK engine module in VRS mode, in combination with the Rover displacement data, over a smaller period (~2 weeks). This Rover displacement data includes both continuous data and data with regular (re-)initializations. Using the results presented in this chapter, it is determined whether there is a relationship between the IM displacement data and the Rover displacement data, and if so, whether the first can be used in controlling the latter. The Rover performance itself will also be investigated and compared to the atmospheric information, in order to see how the first is affected by the unusual fluctuations in the latter. Again, the focus in this is on the specific timing of these events.

In this chapter first all related results are presented (see section 8.1), followed by the discussion of these results (see section 8.2).

8.1. Results

First of all, note that in this analysis the IM output of the RTK engine module in VRS mode (also with RTK accuracy) is used. Just like the Rover, the CORS are now using the VRS correction information to generate a positioning solution. Therefore, this is the engine module (out of all TPP engine modules) which is expected to have the most similar output to 'normal' RTK Rover observations, and thus is the most suitable to use in this analysis.

Note again that data gaps, usually caused by connection problems, occur randomly throughout the data sets.

Like before, it is first determined what percentage of the IM displacement data would have been unreliable in case the default thresholds were applied. Next, using the remaining data, the percentage of supposedly reliable observations which were between the specific thresholds, is determined. As before, the displacements are showing magnitudes which are normally distributed around the mean.

The largest displacements have been identified and are briefly analysed further in combination with the Ionospheric information, the Tropospheric information, the PDOP and the number of tracked satellites. Only SLYG, SRPT, SNSC, SNUS, and SING have been selected for this, as these are the most likely to participate in generating the VRS correction information to be used by the Rover (based on its location, see further on).

The TEC values are not included in this, as they could not be provided. This is not problematic however, as the I95/IRIM values are believed to act as a good indicator of the impact of the Ionosphere.

As mentioned before, an important part of this project is to compare the IM displacement data from the nearest surrounding CORS, to simultaneously observed Rover displacement data. For this the continuous Rover displacement data was recorded, by a Rover that also uses the VRS correction information. This VRS correction information is provided using a sub-network, consisting out of some combination of the nearest surrounding CORS. Therefore, the number of possible CORS is limited depending on the Rover location (see GPSlands' location in the motion maps of Singapore (Figures 7.3 and 7.4)).
In order to do a meaningful comparison with the Rover displacement data, this data is resampled such that the time stamp of the Rover displacement data matches the time stamp of the IM displacement data.

The continuous Rover displacement data is used, not only to find possible relationships (correlations) with the IM displacement data, but also to determine the Rover performance in terms of the quality of the positioning solutions. This is therefore also analysed, together with the Ionospheric information and Tropospheric information, PDOP values and number of tracked satellites, as observed by the specific mentioned CORS.

Besides continuous Rover displacement data, re-initialized Rover displacement data was also recorded. This data is used in order to determine the Rover performance in terms of the (re-)initialization time. The latter is compared with the same Ionospheric information and Tropospheric information, PDOP values and number of tracked satellites.

The Tropospheric information, PDOP values and number of tracked satellites are visualized per CORS, together with the (re-)initialization time data of the Rover. This is also accompanied by a Figure presenting the I95/IRIM/GRIM graphs. This enables easy comparison of the different types of data. Note that the graph visualizing the (re-)initialization time data of the Rover is thus the same in all figures.

The results presented in this section are further discussed in section 8.2. An overview of all the CORS related results from this chapter is combined in Table 8.1, enabling an easy comparison.

Note that there was a data recording disruption between July 12th 5 pm - July 13th 2 am, resulting in a data gap in all datasets. This is related to a SiReNT server update (and corresponding issues).

8.1.1. IM displacement data from the RTK engine module in VRS mode.

When looking at the IM displacement graphs (see Figure 8.1 and Appendix 8), one can see that the displacements in general are sometimes negative and sometimes positive, without clear patterns in it. Similar to before, one can conclude that when observing a large displacement magnitude in one of the directions, it often means the simultaneously observed displacement magnitudes in the other directions are large too. As mentioned in the previous chapter, this makes sense as when an observation is affected by something, it is unlikely that only one of its component is affected.
When looking closer, one can see that during this period there are (only) a few dates on which series of relatively large(r) (often partly supposedly unreliable) displacements
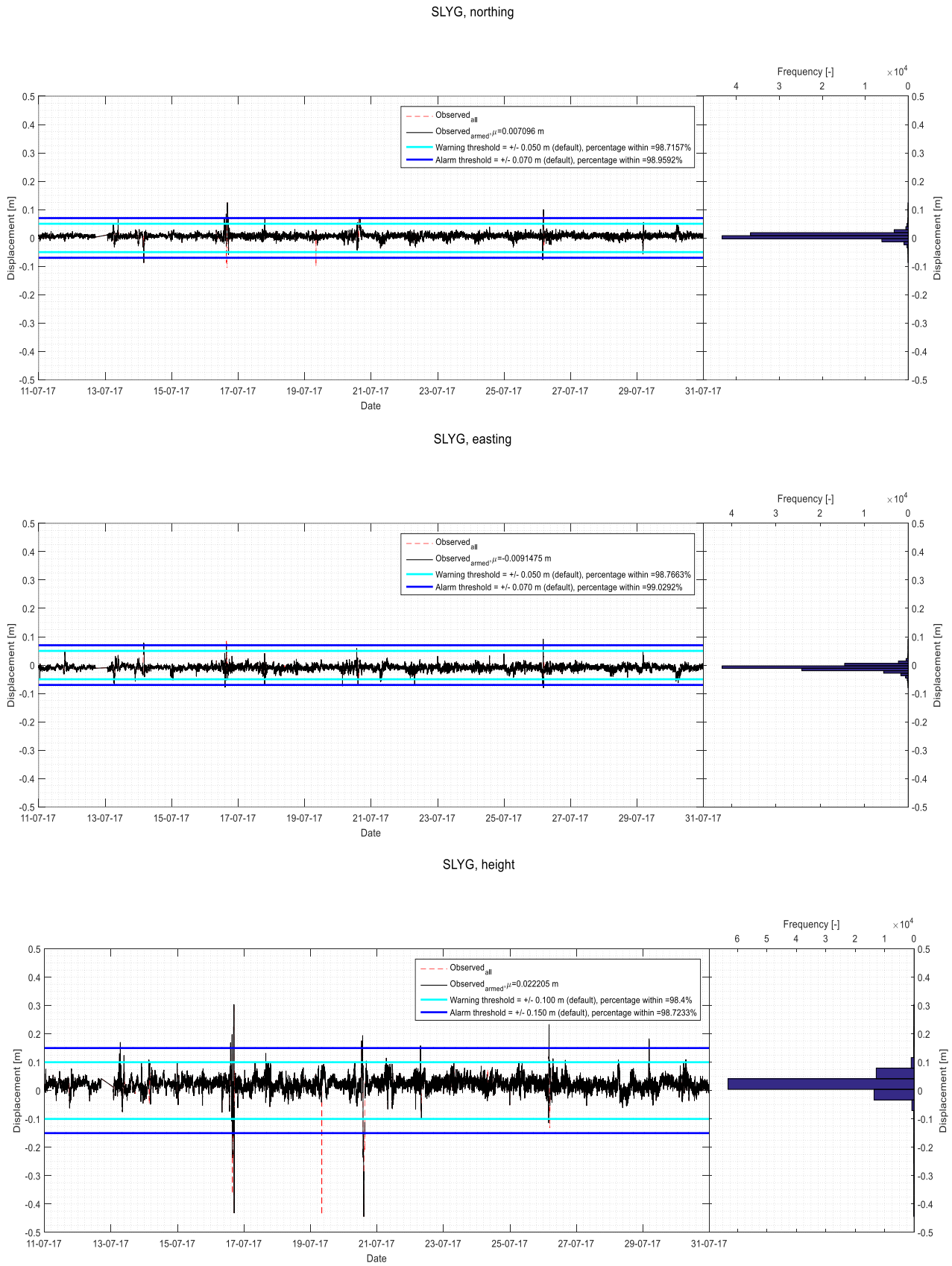
Figure 8.1: Graphs visualizing the displacements in the northing direction (top), the easting direction (middle), the height (bottom) as observed by the SLYG CORS (period: 11-07-'17 – 31-07-'17). For a more detailed explanation of the graphs, see '8.1 Figures/Table explained I'.

Table 8.1: Overview of all results combined, per specific component.

Northing

CORS	Mean [m]	System armed [%]	Within warning threshold, when armed [%]	Within alert threshold, when armed [%]	Correlation (Pearson) with Rover
SLYG	0,0071	99,09	98,72	98,96	0,0075
SNSC	0,0207	97,67	96,93	97,45	0,0067
SNUS	0,0055	99,88	99,79	99,82	-0,0158
SRPT	0,0013	99,16	98,99	99,13	0,0058
SING	-0,0023	96,28	96,03	96,2	0,0007

Easting

CORS	Mean [m]	System armed [%]	Within warning threshold, when not disarmed [%]	Within alert threshold, when not disarmed [%]	Correlation (Pearson) with Rover
SLYG	-0,0092	99,09	98,77	99,03	-0,0394
SNSC	-0,0171	97,67	96,86	97,44	-0,0506
SNUS	-0,004	99,88	99,7	99,8	-0,0167
SRPT	-0,0076	99,16	99,07	99,15	-0,0193
SING	-0,0066	96,28	96,02	96,19	0,0431

Height

CORS	Mean [m]	System armed [%]	Within warning threshold, when not disarmed [%]	Within alert threshold, when not disarmed [%]	Correlation (Pearson) with Rover
SLYG	0,0222	99,09	98,4	98,72	0,0082
SNSC	-0,0004	97,67	97,08	97,41	-0,0258
SNUS	-0,007	99,88	99,72	99,81	-0,0036
SRPT	0,0261	99,16	98,69	99,07	0,0022
SING	0,015	96,28	95,52	96,19	0,0214

8.1 Figures/Table explained I

The *IM displacement graphs* per component (Figure 8.1, top: northing, middle: easting, and bottom: height) visualize:

- The supposedly reliable observations in black;
- The supposedly unreliable observations in red (dashed line);
- The warning threshold in cyan;
- The alert threshold in (dark) blue.

The bar graphs included on the right are visualizing the frequency of the occurrence of a certain range of displacements (all). This way it can easily be seen that the observations are normally distributed around the mean. The percentage of displacement data that satisfied the specific thresholds (warning and alert), while the data was supposedly reliable, as well as the mean of the data are presented in the legends.

All graphs are presenting data from the same time period, enabling comparison of the different data types.

Table 8.1: An overview of all the results per CORS, per component (top: northing, middle: easting, and bottom: height), as presented in section 8.1. This Table presents (from left to right):

- The mean of the supposedly reliable displacements;
- The percentage of observations that were supposedly reliable (dependent on the 3 sigma values exceeding the thresholds);
- The percentage of supposedly reliable observations which were within the warning thresholds;
- The percentage of supposedly reliable observations which were within the alert thresholds;
- The (Pearson) correlation coefficient between the IM displacement data and the Rover displacement data.

The cells in these table are again coloured depending on the value it contains (with respect to these values for the other CORS); again in general, the lighter the colour of the cell is, the better the value, and vice versa.
In the columns containing the percentages, two colours are used, ranging from dark colours for the lowest percentages to ultimately white for the highest percentages. This way it easily can be seen whether according to this data, a certain component is perfect (white) or less good (increasing darkness of colours). All cells in the last column have been assigned about the same colour because all these values are in the same range, which is far from good (see Appendix 11 and 12, for the correlation graphs).

Table 8.2: This table presents the mean of the reliable 3D displacements during this period, per CORS.
The cells in this table are also coloured depending on the value it contains. In general, the lighter the colour of the cell (with ultimately white) is, the closer the value to zero, and vice versa.

occurred. Therefore, the focus of the analysis will be on what happened during these dates, especially the reoccurring ones; July 14th, 16th, 20th, 26th, and 29th. Besides that, for all components, there are only a few displacements just exceeding the thresholds.
Note that just like before, however more prominently and more often in this case, the magnitude of the relatively large supposedly reliable displacements exceeds the magnitude of these supposedly unreliable displacements. As explained in the previous chapter, this is possible, as large displacement magnitudes do not necessarily also have 3σ standard deviations that are exceeding the pre-set thresholds. Therefore the displacements can still be determined to be reliable (see appendix 1 for more details).

When looking at the components individually and comparing the displacements (see Figure 8.1, and the figures in Appendix 8), one can conclude that the height component often has the largest displacements. The displacements in the horizontal plane are much smaller and there does not seem to be much difference between the specific components in terms of the displacement magnitudes.

From the results presented in Table 8.1 (and Appendix 8) can be concluded that for this engine, during this period, the IM displacement data recorded by the SNUS CORS was the most reliable. After that follow SRPT, SLYG, SNSC, and the SING, in descending order of reliability.

When looking at the percentage of reliable observations that were within the specific thresholds, one can see this is following the same order.

When looking at the mean magnitude of the 3D displacements (see Table 8.2), it turns out that the mean magnitude for the SNUS CORS is the smallest (the closest to zero), followed by SLYG, SING, SNSC, and SRPT in ascending order of magnitude.

Table 8.2: Mean magnitudes of 3D displacements per CORS.

CORS	mean [m]
SLYG	0.0251
SNSC	0.0269
SNUS	0.0098
SRPT	0.0272
SING	0.0165

An example from the resulting graphs is presented in Figure 8.1, for the SLYG CORS (the graphs for all CORS can be found in Appendix 8), and explained in the subsection '8.1 Figures/Table explained I'.

8.1.2. Ionospheric information

The I95/IRIM graphs present the values for the SiReNT infrastructure during this period as a whole. In the graphs one can see that these values vary quite a bit, and that there are only a few I95 values with large magnitudes. One can see the few largest I95 values occurring on July 16th (afternoon), 17th (morning), and 20th (afternoon). The largest I95 values often (not always) coincidence with relatively larger values in the IRIM graph (see July 16th (afternoon), 17th (morning), and 20th (afternoon)) however not vice versa (see July 26th (afternoon) for example).

The resulting graphs are presented in Figure 8.2, and Appendix 9, and explained in the subsection '8.1 Figures explained II'.

8.1.3. The Tropospheric information, the PDOP and the number of tracked satellites.

When looking at the Tropospheric information and the observed PDOP/number of tracked satellites recorded by these CORS, one can see that all graphs fluctuate quite a bit. Besides the (daily) variations/fluctuations, one can see a few interesting things occurring. There are some unusual values/relatively (large) sudden changes recorded (by all CORS) during the period July 12th-13th, 26th-27th, and on July 30th (minor). Other than that not many unusual variations occur in the graphs recorded by these CORS.

The recorded GRIM again show no direct relationship to the recorded I95 values. Interesting to note is that some of the relatively larger GRIM magnitudes seem to coincide with relatively larger IRIM magnitudes or disruptions in the behavior of the IRIM values, however. The largest GRIM magnitudes are recorded on July 14th, 26th, and 30th (minor).
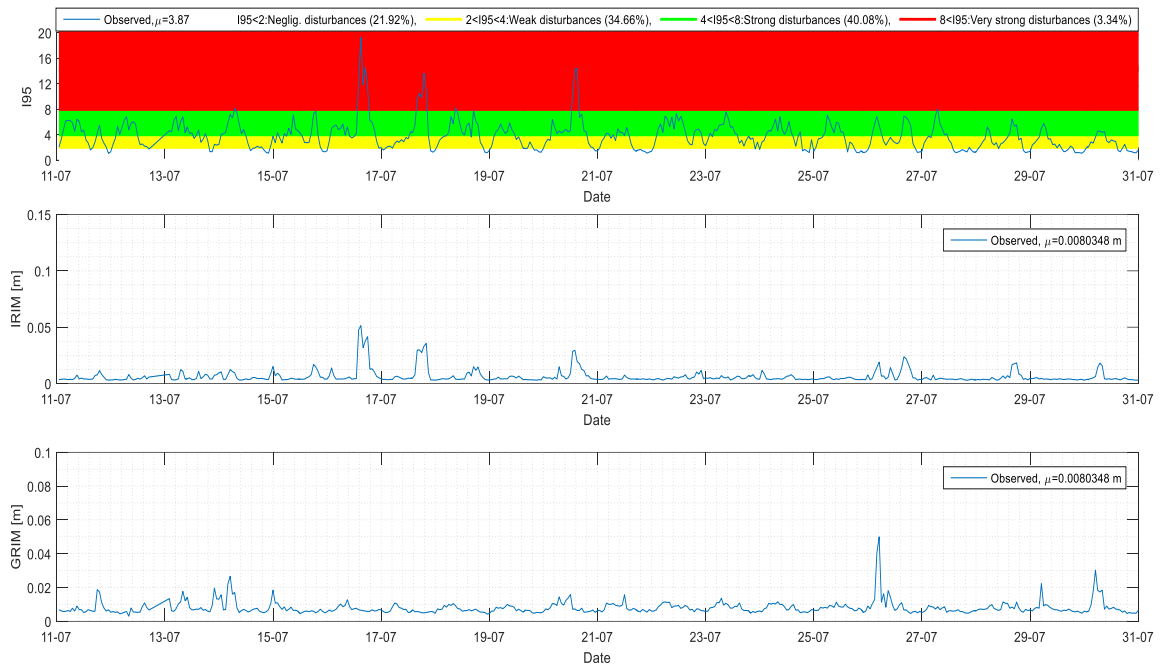
Figure 8.2: The I95/IRIM/GRIM values as observed by SiReNT (period: 11-07-'17 – 31-07-'17). For a more detailed explanation of the graphs, see '8.1 Figures explained II'.

SLYG
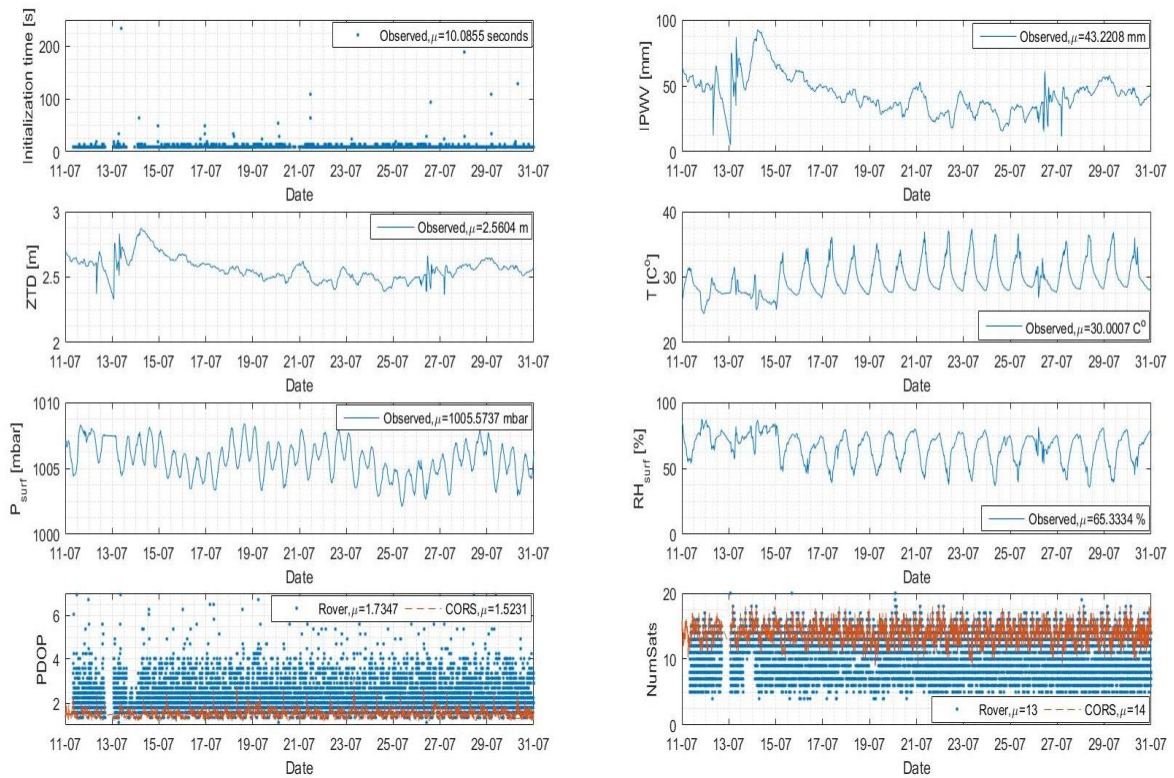
Figure 8.3: The (re-)initialization time, Tropospheric information, PDOP value, and the number of tracked satellites as observed by the SLYG CORS (period: 11-07-'17 – 31-07-'17). For a more detailed explanation of the graphs, see '8.1 Figures explained II'.

As for the PDOP and number of tracked satellites, from the graphs at the bottom rows of the figures can be concluded that, except for the SING CORS, all CORS observed a lower average PDOP/higher average number of tracked satellites as compared to the Rover. The spread of the PDOP/number of tracked satellites observed by the Rover in general is much larger as compared to that of the CORS however. It seems as if there is a daily returning variation, with maximum PDOP values observed during the mornings. At these moments (not very clear) there are often minima in the number of tracked satellites. Interesting to see is that on July 14th, the number of tracked satellites/PDOP value recorded by the Rover suddenly improves for a while, after which it returns to its old state.

The resulting graphs are presented in Figure 8.2, and 8.3, and Appendix 9, and explained in the subsection '8.1 Figures explained II'.

8.1.4. Re-initialized Rover displacement data
In most of the re-initialized Rover displacement data, one can clearly see the peaks of the (re-)initializations at a regular interval (mostly every ~300 seconds), see Figures 8.4 and 8.5. This (re-)initialization did not always go as planned however, sometimes it took even up to 10 minutes (~600 seconds) for it to take place, or did not take place at all. The (re-)initialization time or so-called time-to-fix itself, during this period is recorded by the TPP to be mostly 2-8 seconds. This (re-)initialization time is also determined from the data itself, using the information on whether the determined positioning solution was a 'Float' or a 'Fixed' solution, and the knowledge that (usually) whenever a (re-)initialization was taking place, a sudden (major) unusual displacement occurred, after which the data returned to its original state. Keep in mind that the data that is used for this, has an interval of 5 seconds. This means that the minimum (re-)initialization time that is determined this way, is at thus least 5 seconds, as this (unfortunately) means that (re-)initialization times below 5 seconds could
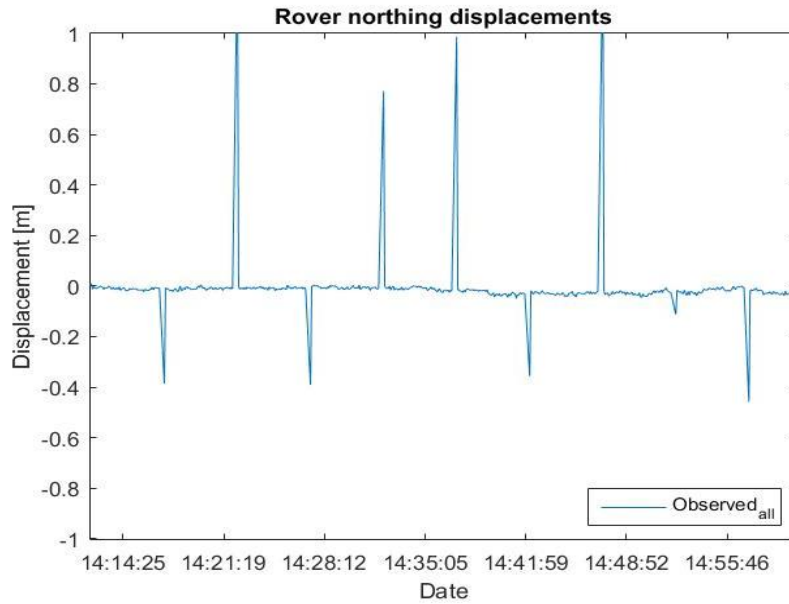
Figure 8.4: An example snapshot of the (re-)initialized Rover data while the (re-)initializations took place at regular intervals of ~300 seconds. For the complete time series, see Figure 8.5.

not be detected. This could be the cause of data gaps in the (re-)initialization time graph. On top of that, it also means that the resulting values are ranges of (re-)initialization times (minimum-maximum), rather than a specific value.
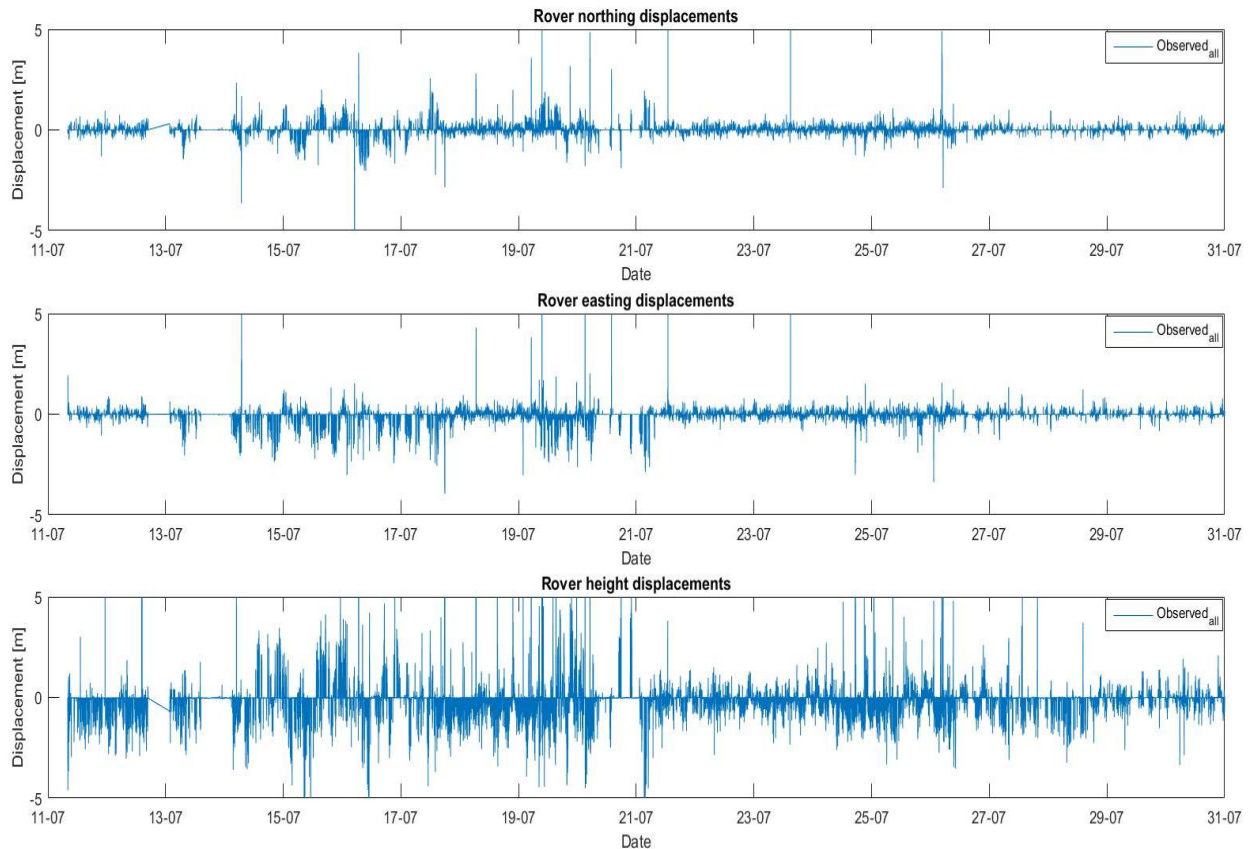
Figure 8.5: The (re-)initialized Rover data, showing the peaks of the (re-)initializations.

Rover performance ((re-)initialization time)

(Re-)initialization time [s]

■	0-9 (90.58%)
■	10-14 (8.45%)
■	15-19 (0.21%)
■	20-24 (0.11%)
■	25-29 (0.11%)
■	30-34 (0.11%)
■	35-39 (0.03%)
□	40-44 (0%)
■	45-49 (0.05%)
■	50-54 (0.03%)
□	55-59 (0%)
■	60+ (0.34%)
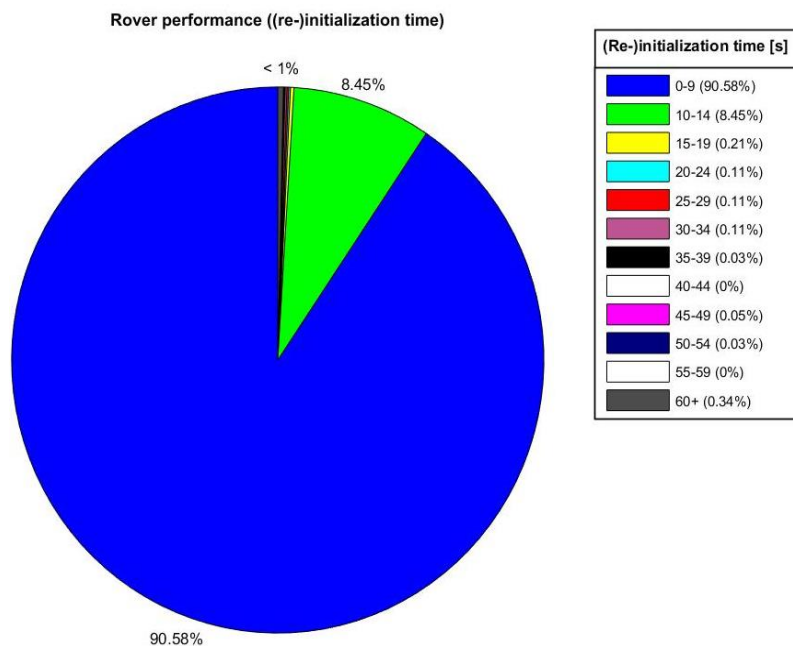
Figure 8.6: Pie chart of the Rover performance ((re-)initialization time.

From the results can be concluded that during this period the (re-)initialization time was mostly between 0-9 seconds (90.58%) (see Figure 8.6). There is also a substantial amount of times where the (re-)initialization time was taking 10-14 seconds (8.45%). These occurrences happened quite randomly throughout the dataset. Only very few times per day the (re-)initialization time exceeded 14 seconds (0.97%). Interesting to note is that the latter did not happen multiple times in a row. The longest individual (re-)initialization times occurred on July 13th, 21st, and 28th (see Figure 8.3). The magnitude and direction of the displacement at the time of the (re-)initializations varies quite a bit throughout this period (see Figure 8.4). Comparable to the IM displacement data, overall the Rover displacement data displacement magnitudes in the height component are larger as compared to the displacement magnitudes in the horizontal components. The manner in which the magnitudes vary is quite randomly, although the height component recorded more negative displacements at these times as compared to positive displacements. For the horizontal components, there is not so much difference between the number of negative and positive displacements.

The resulting (re-)initialization time durations are thus visualized together with the Tropospheric information, PDOP value and number of tracked satellites, as observed by the nearest surrounding CORS. This enables easy comparison of the different data types. An example from the resulting graphs is presented in Figure 8.3.

8.1.5. Continuous Rover displacement data

First of all, note that one can find (large) data gaps in the continuous Rover displacement data (See Figure 8.7). These gaps are independent of the gaps in the (re-)initialized data and can be related to data connection problems, causing the logging to stop. When this occurred, the logging had to be restarted manually. The size of these gaps varies as this loss of data connection occurred randomly and was not always noticed straight away by the vendor.

Besides that, the datasets contain several different time intervals, varying from a few seconds to 15 seconds. Therefore, all this data is resampled to data with matching time intervals of 15 seconds. Note that in order to do a more detailed comparison a smaller time interval is required, however in this case we are limited by the largest time interval. Even though the chosen time interval might not be frequent enough for the use of for example
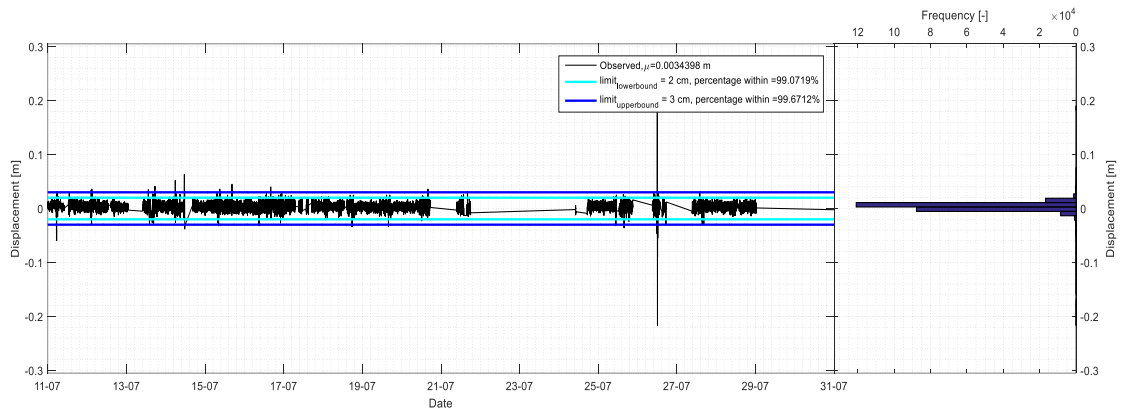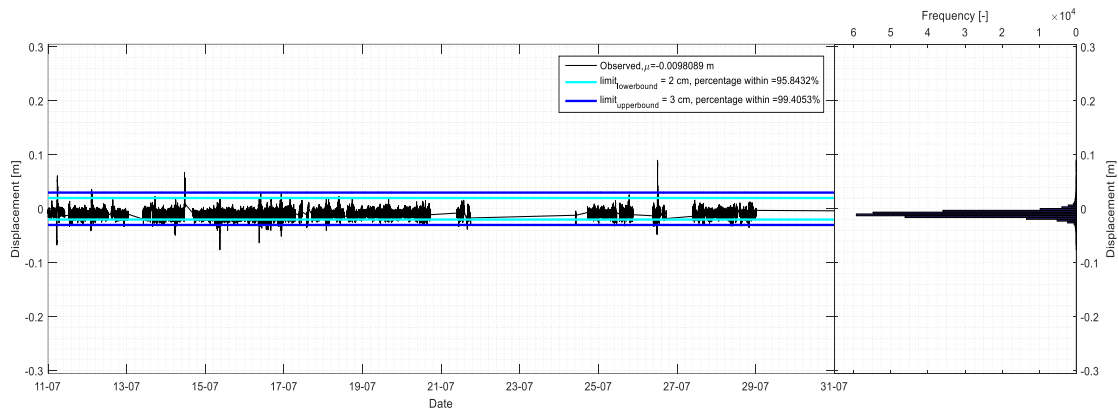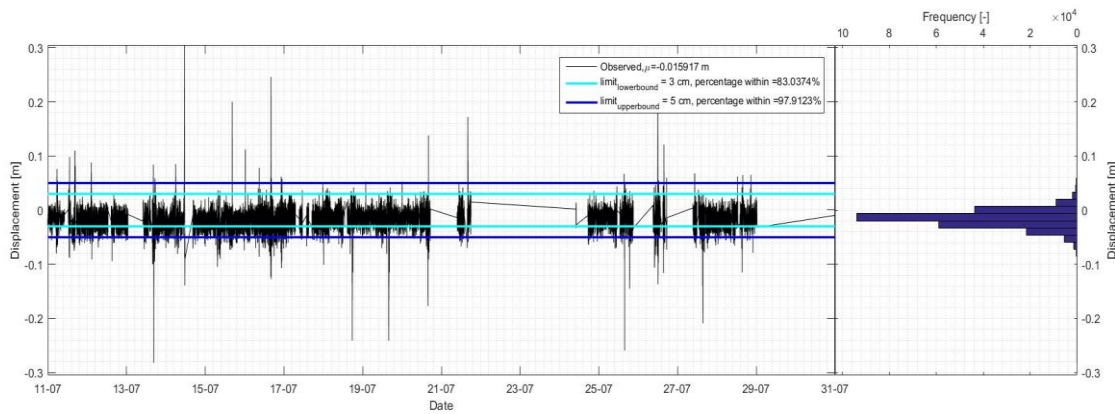
Figure 8.7: Graphs visualizing the Rover displacement data; in the northing direction (top), the easting direction (middle), the height (bottom) (period: 11-07-'17 – 31-07-'17). For a more detailed explanation of the graphs, see '8.1 Figures/Table explained III'.

autonomous vehicles, it should be sufficient for finding and analyzing the possible relationship between these IM displacement datasets and the Rover displacement data; it is believed to provide a basic understanding which can be developed further in the future.

As for the data analysis, similar to the IM displacement data, it is first

Table 8.3: Overview of the Rover results, per specific component (see Figure 8.7). The lower (upper) bound of the required accuracy was 2 (3) cm and 3 (5) cm in the horizontal (vertical) plane, respectively.

	Mean	Within lower bound [%]	Within upper bound [%]
northing	0,0034	99,07	99,67
Easting	-0,0098	95,84	99,41
height	-0,0159	83,04	97,91

determined what (horizontal accuracy: 2-3 centimeter, vertical accuracy: 3-5 centimeter) (see Table 8.3). Alongside this, the mean displacement value is determined as well. The latter can give the reader a first idea regarding the performance of the Rover in terms of accuracy (through the displacement of this mean value, from zero).

When looking at the displacement data, one can see that the observed displacements in general are again quite variable, however without any clear patterns in it. Just like in the IM displacement data, when observing a relatively large displacement magnitude in one of the components, it often means the simultaneously observed displacement magnitudes in the other components are relatively large too. As mentioned previously, this makes sense as when an observation is affected by something, it is unlikely that only one of its component is affected.

During this period the displacement magnitudes where exceeding the thresholds multiple times. For the horizontal components, the graphs do show a few relatively large(r) displacements on July 11th, 14th, 15th and 26th. For the height component this happens more often however; (almost) daily.

Similar to the IM displacement data, the Rover displacements are showing magnitudes that are normally distributed around the mean.

When looking at the components individually and comparing the displacements, one can conclude that the displacements in the height component are the largest. The displacements in the horizontal plane are much smaller, and there is not much difference between the specific horizontal components in terms of displacement magnitudes.

The continuous Rover displacement data is used to determine possible correlations between the Rover displacement data and the IM displacements. This analysis is done per component as it is understood by SLA that the default threshold applied to the IM displacements in the TPP software are/can be used to control the Rover displacement data. For this to be possible, there has to be some kind of relationship between the different components of the IM displacement data and the Rover displacement data. In order to find whether there is such a relation, the (Pearson) correlation coefficient is determined and visualized by plotting the Rover displacement data versus the IM displacement data. The latter is thus done per specific component. More information about the correlation coefficient and how it is computed, can be found in Appendix 10. The results per CORS, are analysed below.

The resulting graph from this section is presented in Figure 8.7. figures and tables from this section are explained in the subsection '8.1 Figures/Table explained III'.

8.1.6. Correlation between IM displacement data and Rover displacement data

As mentioned before, the CORS' IM displacements have been plotted against the Rover displacements (using the matching time stamps), and the correlation between these two has been determined. The resulting correlation coefficients for the SLYG CORS (see Table 8.1 and Figure 8.8) are (very) close to zero. This is the same for the other CORS (see Table 8.1 and Appendix 11).

The shapes of the generated point clouds can be generalized as (something resembling) a diamond shape, mostly centered around or close to zero. This means that most of the time, the larger the magnitude (negative or positive) of the CORS' (Rover's) displacement is, the closer the Rover's (CORS') displacement (for that same component) is to zero. Most values are densely distributed around the center.

The point clouds for the horizontal components seem more compressed (meaning that horizontal tips are further apart than the top and bottom), as compared to the point clouds belonging to the height component (more similar width and height at the center). This is mainly due to the chosen limits of the axis however. These are chosen this way in order to be able to see as much detail as possible. Specific things and observations that do not agree with the previous or need further specification, are described per CORS below.

On top of the point clouds visualizing the amount of correlation, the 3D displacement, together with the Rover displacement data, is visualized for each CORS as well. Both the complete data sets and zoomed-in subsets are visualized in the bottom panels of the respective figures (see Figure 8.8 and Appendix 11). From this can also be concluded that the observed behavior in the two data sets is very different, for all CORS. Also, the displacement data for the CORS is spread out a bit more as compared to the Rover displacement data.

96

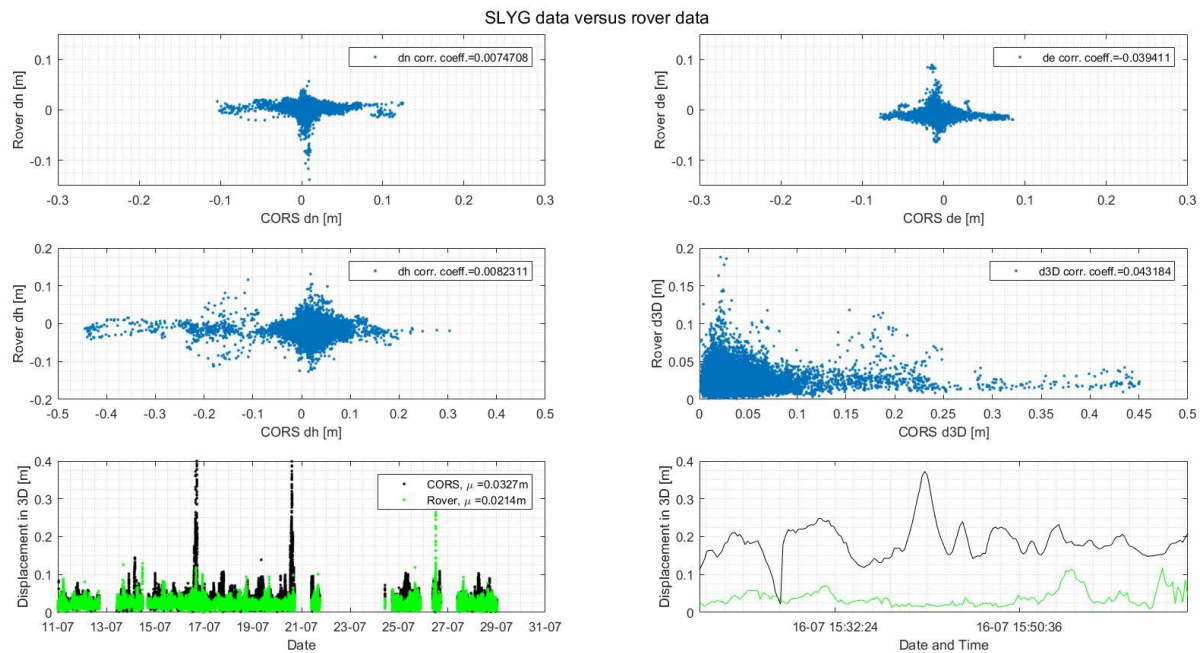Figure 8.8 and the figures in Appendix 11 and 12) are visualizing the correlation between the IM displacement data and the Rover displacement data, and graphs visualizing the displacements in the 3D component, for both the Rover and the CORS (period: 11-07-'17 – 31-07-'17). The first are visualized in the upper and middle panels (; northing: upper left, easting: upper right, height: middle left, and 3D: middle right), and the latter is visualized in the bottom panels (; complete displacement data: bottom left, and zoomed in; bottom right).

Table 8.4: Overview of the Correlation Coefficients resulting from applying certain thresholds (; 0, 0.05, 0.10, 0.15, 0.20, and 0.25 meters, respectively). The cells in these table are again coloured depending on the value it contains. Positive values are assigned the colour red, where negative values are assigned the colour blue. In general, the lighter the colour of the cell is, the better the value, and vice versa. This way it easily can be seen whether according to this data, a certain component is perfect (white) or less good (increasing darkness of colours).

SLYG

Here, based on the correlation coefficient, the northing component shows the least correlation, followed by the height component and then the easting component. The shapes of the point clouds generally follow the description above.

For the northing component, the left and right tip are stretched out slightly further as compared to the tip toward the top. For the easting component, the left and right tip are stretched out slightly further as compared to the tip toward the bottom. The tip toward the bottom and top, for the northing and easting component respectively, are more similar to the horizontal components. This means that the positive (negative) magnitudes of the Rover displacements are relatively less small for the northing (easting) component, as compared to the Rover displacements in the opposite direction and the CORS displacements.

Figure 8.8: Graphs visualizing the correlation between the SLYG IM displacement data and the Rover displacement data, and graphs visualizing the displacements in the 3D component, for both the Rover and the CORS (period: 11-07-'17 – 31-07-'17). The first are visualized in the upper and middle panels (; northing: upper left, easting: upper right, height: middle left, and 3D: middle right), and the latter is visualized in the bottom panels (; complete displacement data: bottom left, and zoomed in; bottom right). For a more detailed explanation of the graphs, see '8.1 Figures/Table explained IIII'.

For the height component, it is more shaped like a diamond shape, however with an extra (smaller) point cloud on its left side. It could also be seen as if the left tip of the diamond shape widens out again and ends less pointy as well. That means that the CORS displacements for this component are relatively more negative. Besides that, for the negative CORS displacements, ranging between -0.1m and -0.45m, there is a range of different magnitudes of Rover observations (which are not necessarily) close to zero.

SRPT
Here, based on the correlation coefficient, the height component shows the least correlation, followed by the northing component and then the easting component. The shapes of the point clouds generally follow the description above. Some things to note are the relatively longer tips towards the right and down for the northing component, and slightly longer tips towards the left and top for the easting component. This means that for the northing component, the negative Rover (positive CORS) displacement magnitudes are relatively larger, especially when the CORS (Rover) displacements are (close to) zero), where in the easting component this is the opposite. For the height component, these numbers are more similar.

SNSC
Here, based on the correlation coefficient, the northing component shows the least correlation, followed by the height component and then the easting component. The shapes of the point clouds generally follow the description above, however a lot less distinct for this specific CORS. The CORS displacements are spread out wider as compared to the Rover displacements. Other things to note are the relatively longer tips towards the right and down for the northing component, and longer tips towards the right and top for the easting component. This means that for the northing component, the positive Rover (negative CORS) displacements magnitudes are relatively larger (especially when the Rover (CORS) displacements are (close to) zero). For the easting component, both the positive Rover and positive CORS displacement magnitudes are relatively larger. For the height component, the tips towards the left and right are relatively more spread out, meaning that the CORS displacements are more spread out (larger positive/negative magnitudes) as compared to the Rover displacements.

SNUS
Here, based on the correlation coefficient, the height component shows the least correlation, followed by the northing component and then the easting component (the latter two being quite similar). The shapes of the point clouds generally follow the description above. Some things to note are the relatively longer tip towards the bottom for the northing component, and a slightly longer tip towards the top for the easting component. This means that in the northing component, the positive CORS displacement magnitudes are relatively larger, where in the easting component this is the opposite (especially when the Rover displacements are (close to) zero). In the height component, these numbers are more similar.

SING
Here, based on the correlation coefficient, the height component shows the least correlation, followed by the northing component and then the easting component (the latter two being quite similar). The shapes of the point clouds generally follow the description above. Some

things to note are the relatively shorter tip towards the top for the northing component, and a slightly shorter tip towards the bottom as well as a longer top to the left, for the easting component. This means that for the northing component, the negative Rover displacement magnitudes are relatively slightly smaller (especially when the CORS displacements are (close to) zero), where for the easting component this is the opposite. As for the CORS displacements, for both the northing and easting components the negative displacement magnitudes are slightly larger (especially when the Rover displacements are (close to) zero). In the height component, the tips towards the left and right are relatively more spread out, meaning that the CORS displacements are more spread out (larger positive/negative magnitudes) as compared to the Rover displacements.

Concluding remarks

The correlation of only the relatively large(r) IM displacements specifically, with the Rover displacements, was also/further investigated. This is done by progressively filtering out the IM displacements of which the 3D displacements where below certain thresholds (; 0, 0.05, 0.10, 0.15, 0.20, and 0.25 meters, respectively). Hence, now only the (relatively) large IM displacements, that are exceeding these thresholds, and Rover displacements with matching timestamps, are used in the correlation determination. Note that these thresholds have nothing to do with the thresholds with regards to IM, that were discussed previously. The results for the SLYG CORS are presented in Table 8.4, and the related figures, as well as the figures from all other CORS can be found in Appendix 12.

When looking at the results for the SLYG CORS, one can see that only for the Eastern component the correlation coefficient steadily increases in magnitude. For the other components, and the 3D displacements, this is not the case. For all these, random changes in the magnitude as well as the sign (positive versus negative), were observed.

For most other CORS the same sort of random behavior is observed for all components when progressively increasing the applied thresholds (see Figure 8.9).

Note again that in the graphs in figures in Appendix 12, the 3D Rover displacements are again very different from the 3D CORS displacement.

Table 8.4: Overview of the Correlation Coefficients resulting from applying certain thresholds (; 0, 0.05, 0.10, 0.15, 0.20, and 0.25 meters, respectively).

Threshold	Correlation coefficients				# of obs.
	dn	de	dh	d3D	
-	0,0075	-0,0394	0,0082	0,0432	43896
>0.05	-0,0225	-0,0619	0,0236	0,1242	5112
>0.10	-0,1289	-0,1184	-0,0185	-0,0296	798
>0.15	-0,0413	-0,1501	-0,1359	-0,2281	469
>0.20	0,0242	-0,3404	-0,1445	-0,1542	254
>0.25	0,1980	-0,4167	0,0594	0,3297	118
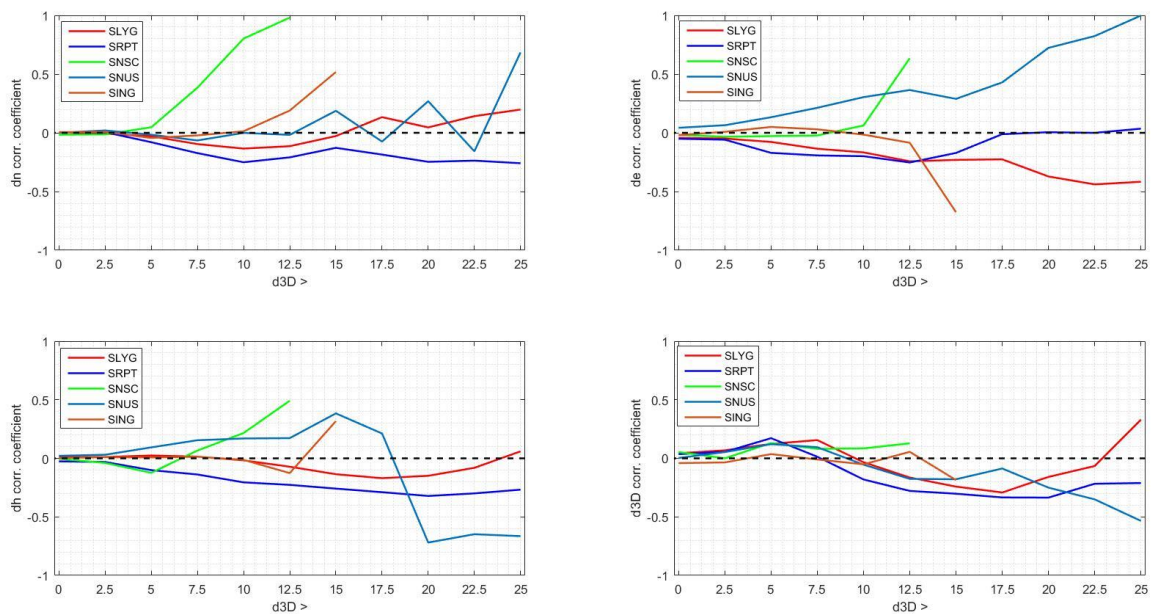
Figure 8.9: Overview of the Correlation Coefficients per component, resulting from applying certain thresholds, namely; 0, 0.025, 0.05, 0.075, 0.10, 0.125, 0.15, 0.175, 0.20, 0.225 and 0.25 meters, respectively.

8.2. discussion

In this section, the datasets, as well as the results presented in section 8.1 are further discussed.

IM displacement data and atmospheric information, PDOP and number of tracked satellites
When looking at the IM displacement data (see Figure 8.1, and the figures in Appendix 8), it seems as if the data was supposedly reliable most of the time. That is with regards to the default thresholds. Most CORS did simultaneously record (relatively) large displacements, on July 14th, 16th, 20th, 26th, and 29th. These displacements are often partly unreliable, especially the displacements on July 14th, and 16th. Overall the thresholds are exceeded quite often in this dataset, even over this relatively short period of time. The results from this dataset cannot be compared to those of the dataset from the previous section however, as the latter suffered data loss due to the data reduction algorithm and the resampling. Hence, the frequency of the observations used for this analysis is much higher, as compared to the previous section. Also, the engine module that is used in this context, differs from the one that was used in the previous chapter.

In this case, the dates on which relatively high Ionospheric activity was recorded (July 16th, 17th, 20th, and 26th), match only some of the above-mentioned dates (July 16th, 20th, and 26th). The relatively large GRIM values show some coincidence with the (relatively) large displacements in this case as well, on July 14th, and 26th. The Tropospheric information graphs (for all CORS) also show some unusual variations on these dates. Hence this shows that there (possibly) is a relationship between the Tropospheric information and the simultaneously recorded GRIM value, and the way in which the displacements are affected on these dates. It is not understood what causes the relatively large displacements on the

other dates however, or how/why some of the unusual variations in the Tropospheric information are observed simultaneously with unusual variations in the IM displacement data, while others are not.

It is likely, like before, that most of the (relatively) large displacements are caused by the (sudden increases in) Ionospheric activity, causing the applied corrections no longer to be sufficient. Some of these (relatively) large displacements can also be related to unusual variations in the Tropospheric information and simultaneously recorded GRIM. In general, it seems that the impact related to the GRIM value on the data is (much) smaller, as compared to the impact of the Ionospheric activity however.

The fact that the supposedly reliable displacements exceed the supposedly unreliable displacements, also shows that the applied thresholds are still performing insufficiently. As explained in the previous chapter, this seems the case especially when it comes to the impact of the Tropospheric activity. Note again however, that it also is possible that both the displacement data and the Tropospheric information are affected by the same unknown factor. In that case, it could be that nothing is/was filtered out, but just that this factor affected all parameters in varying degrees.

Note however, that not only the IM displacement data but also the different datasets themselves are affected by the re-initialization. This is clearly visible in the ZTD and IPWV graphs (see Figure 8.2 and Figures A.9.1-9.5), following the mentioned data recording disruption (between July 12th 5 pm – July 13th 2 am), for example. The SiReNT I95/IRIM/GRIM graphs are not affected much, however this could be due to the fact that these are hourly recorded parameters.

Interesting to note is the sudden temporary improvement in the number of tracked satellites/PDOP value, recorded by the Rover on July 14th. This occurrence is coinciding with unusual variations in the temperature and relative humidity, as well as a large increase of the ZTD and IPWV. What causes this and why it occurs only at that small period in time, and why it does not repeat itself, is unclear. If at a certain time on day x the number of tracked satellites/PDOP value suddenly improves, it would likely to be due to an improvement in the sky view. One would then expect that this would repeat itself the next day, however. This is not the case, hence there is more at play here. The fact that it looks like a major abrupt change is unusual as well. This could be due to a permanent signal blockage that suddenly is resolved, but only for a short period. Likewise, a sudden temporary drop in these parameters could be explained by a sudden temporary blockage of the antenna. Note that the latter is more likely as compared to the first however.

Besides that, except for the SING CORS, all CORS observed a lower average PDOP/higher average number of tracked satellites as compared to the Rover. This means that the sky view from the Rover was better as compared to the SING CORS, where for the other CORS this was the other way around. This could possibly be related to signal blockage by surrounding vegetation, which is only possible for the SING CORS. All other CORS are either on top of structures or (relatively) free from obstruction by vegetation.

One can conclude that the IM displacement data presented as part of this chapter do satisfy the thresholds less good. This could be due to the fact that the period over which this

displacement data was recorded, was much shorter, or because this displacement data was recorded by another engine module. Note that whatever the cause for this difference may be, the percentages presented in Table 8.1 were not used in this project, and presented merely for completeness. Therefore this was not investigated further.

Reinitialized Rover displacement data
When looking at the results related to the reinitialized Rover displacement data (see Figure 8.3, and the figures in Appendix 9), it is found that sometimes the (re-)initialization took very long to take place, or temporarily did not take place at all. This cannot be concluded from the graphs however, as a sudden large displacement is not a requirement for a (re-)initialization. Perhaps when there were no spikes visible, even the 'Float' solution was very good, or at least accurate enough (causing only (very) small displacements) to not show up in these graphs (due to the extent of the y-axis). Another reason for this to could be that at that time the vendor was tweaking the set-up, while the logging was still going on, and/or that the (re-)initialization actually took less than 5 seconds, not leaving a record.

The determined (re-)initialization time itself varies, however is mostly between 0-9 seconds. Note that based on this data it is unfortunately not possible to further distinguish between (re-)initialization times of 0-4 seconds and 5-9 seconds. This is the case as the logging interval is 5 seconds and therefore a (re-)initialization time that is logged once, could actually have taken anywhere between 0-9 seconds. There were also numerous times where this took 10 seconds or more. These (re-)initialization times occur quite randomly throughout the dataset. The longest (re-)initialization times occurred on July 13th, 21st, 28th. Except for the one on July the 13th, these occurrences, or any other of the relatively longer (re-)initialization times for that matter, do not clearly coincide with anything happening in the Tropospheric information graphs and/or the Ionospheric information graphs, however. In general, it is hard to find a relationship between the (re-)initialization times and the Tropospheric information graphs and/or the Ionospheric information graphs.
It could be that these are caused by a sudden change in satellite geometry, affecting the PDOP and the number of tracked satellites. This cannot be concluded from the graphs however, as nothing unusual is recorded at these times.

In order to get better results and a better understanding of the Rover performance in terms of the (re-)initialization time, further research is required, using 1 Hz data. That would enable one to see what is happening in greater detail, especially when zooming in on specific periods of interest.

Interesting to note is the fact that the height component recorded relatively more negative displacements during the (re-)initialization times. This means that while using a 'Float' solution, the determined range was often too long. This does not necessarily mean something, as we are talking about a Float solution, but it is still something to note. Overall the magnitudes of the displacements vary quite randomly throughout the dataset.

Continuous Rover displacement data
When looking at the results related to the continuous Rover displacement data (see Figure 8.7), one straight away notices all the (large) data gaps, especially during the second half of the dataset. Due to these, a lot of information was lost. This could and should have been omitted by the vendor, by monitoring the connection more closely.

In order to find out if there is a correlation between this Rover displacement data and the IM displacement data from the specific CORS, both datasets are resampled in order for them to have matching timestamps. This resampling (most probably) caused even more data loss.

The (relatively) large displacements occurring on July 14th, and 26th, could be related to the described fluctuations in the Tropospheric information and/or GRIM value. For the other (relatively) large displacements there is not really a clear relationship found. The impact of the Ionospheric activity on the Rover displacement data is less distinct. Besides that, the timings at which the (relatively) large displacements in the Rover displacement data occur, do not really match those of the IM displacement data. This is somewhat unexpected, as one could argue that the same delays/circumstances apply to both the Rover and the SiReNT infrastructure, as reference infrastructure, equally. Especially since the CORS and the Rover were both using the VRS method. Perhaps this is related to the fact that another type of antenna is used for the Rover, as compared to the antenna's used as CORS. This should not be the cause however. Another reason could be that perhaps there was some filtering applied (without knowing about it) to the observations recorded by the CORS', where this is not the case for the Rover displacement data.

As expected the horizontal components are (a lot) better as compared to the vertical component. For the displacements in the height component and the horizontal components, over 80%, and over 95%, respectively, is within the lower bounds. Over 97% of the displacements for all components are within the upper bounds. The average observations for all components are also well within the set lower bounds.

In conclusion, there is no (clear) relationship between the Rover displacement data and the recorded Tropospheric information and/or the Ionospheric information. Besides that, there also is no relationship between the IM displacement data and the Rover displacement data, in terms of the timing of the (relatively) large displacements.
Further investigation is required on this, in which higher frequency data should be used. This enables one to zoom in and look at the smaller timescale.

Correlation
It was understood/assumed by SLA that the default thresholds could be applied to the IM displacement data, in order to control the Rover performance. Even though there does not seem to be a relationship between the IM displacement data and the Rover displacement data, in terms of the timing of the (relatively) large displacements, this assumption is further investigated by determining the correlation between the continuous Rover displacement data and the IM displacement data from several CORS.

From the general shape of the resulting point clouds as well as the determined correlation coefficients it can be concluded that there is (almost) no correlation between the Rover displacement data and any of the IM displacement data of any of these CORS. There are slight differences in the resulting shapes and correlation coefficients, depending on the specific component and the CORS. These differences do not change anything about the results however, and the related points can possibly even be seen as outliers. Overall, the larger the absolute magnitudes of the CORS' (Rover's) displacement are, the smaller those of the Rover (CORS') are. Most points are distributed around the center, showing no correlation at all.

This does not improve when applying thresholds to the displacement data. For all CORS, the correlation coefficients for all components, as well as the 3D displacement, are generally varying quite randomly, both in absolute magnitude and sign (positive versus negative). The fact that less observations are available due to the filtering, means that the remaining observations are assigned a relatively higher weight as compared to without any filtering. This explains why the magnitudes of the correlation coefficients are generally higher when only using displacements over a certain threshold, as compared to when no threshold is applied.

The included 3D displacement graphs, especially the one that is zoomed-in, clearly confirm that there is very little to no correlation between the Rover displacement data and the IM displacement data from the different CORS'.

It could be that the datasets are individually affected by unique sources of noise, which in turn causes very little to no correlation. It is also possible that the resampling affected the data and caused a mismatch, thereby affecting the amount of correlation. However, since the resulting correlation results are so very low, that it is (very) unlikely that without resampling and/or with noise filtering there suddenly would be a lot of correlation.

Trimble PIVOT data analysis part III
Case studies

This chapter presents and discusses the results with regards to improving the redundancy within SiReNT (in terms of the construction of new CORS), and the case study on the August 13th, magnitude 6.5, Sumatra Earthquake event. The first can be found in section 9.1, and the latter in section 9.2.

9.1. Case study: Redundancy through extra CORS/Rovers.

As follows from section 5.2, the redundancy and reliability of the SiReNT infrastructure as a whole, in general, can be improved by the construction of new (extra) CORS. In this project the most suitable locations for this are determined. The results are presented in section 9.1.1, and further discussed in section 9.1.2.

9.1.1. Results

As for the construction of extra CORS, it was first determined what parts of Singapore are within a certain range of at least one of the existing CORS. From this can be concluded that almost the whole of Singapore is within 10 kilometer of at least one of the SiReNT CORS
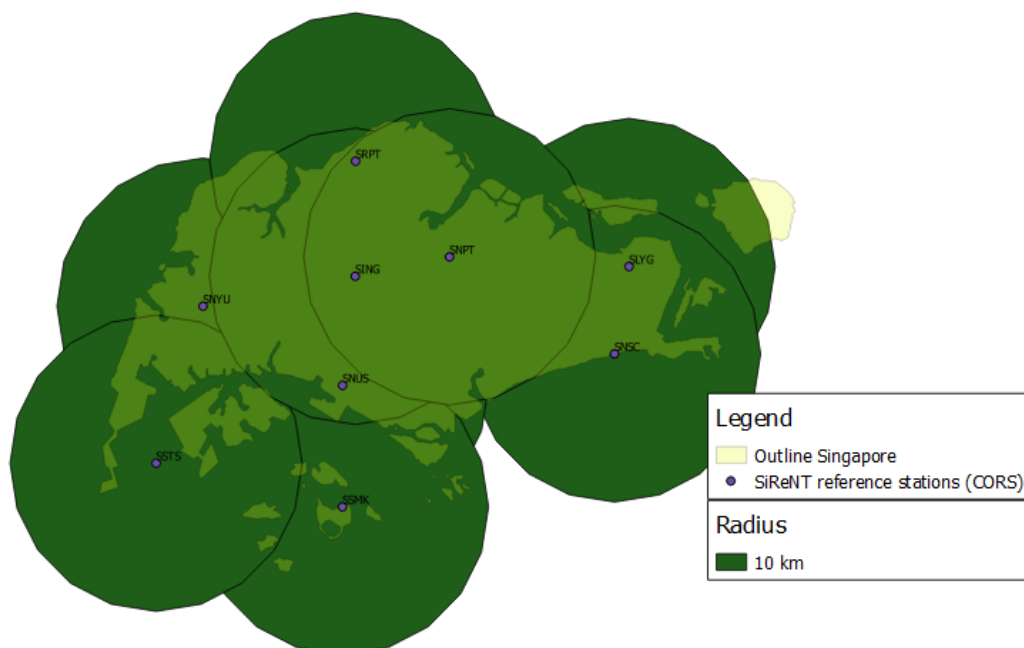
Figure 9.1: Figure visualizing what parts are within 10 km of at least one of the SiReNT CORS.

(see Figure 9.1). The baselines will thus always be short enough to be considered small baselines. Hence, for that reason there are actually no extra CORS required. Reducing the baseline lengths even more would not affect the observations negatively however, and it could possibly (even) cause improvements.
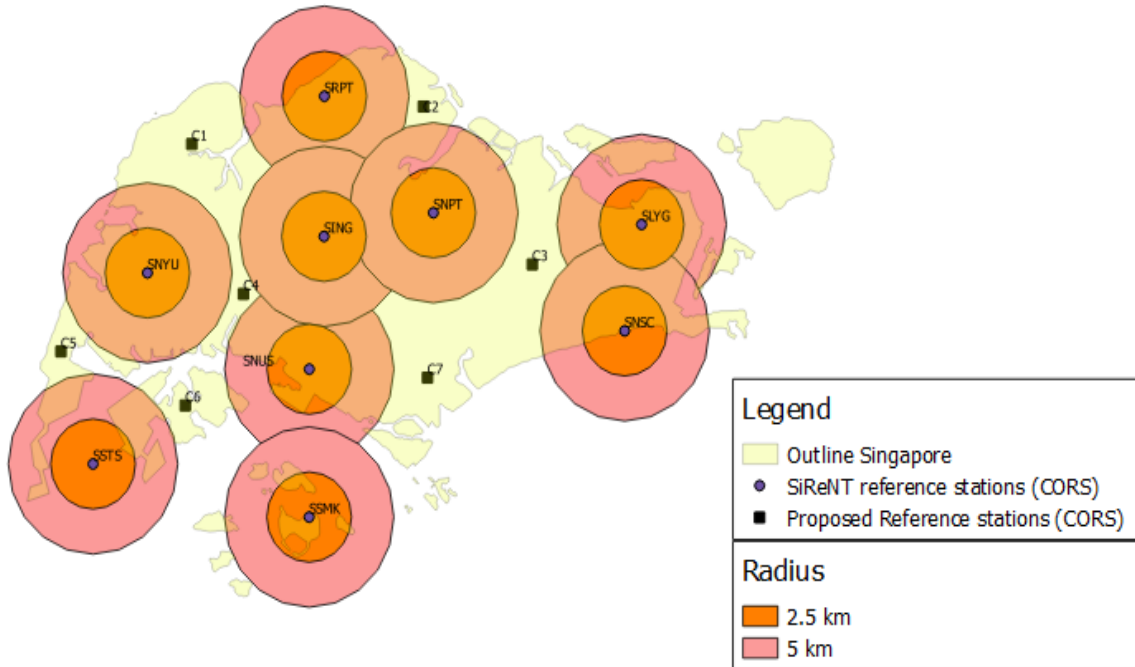
Figure 9.2: Figure visualizing what parts are within 2.5 km and 5 km of at least one of the SiReNT CORS. Based on that, the locations of the proposed CORS are determined.

It is also investigated which parts of Singapore fall within a radius of 2.5 kilometer, and 5 kilometer of the existing CORS. Based on that, the locations for the extra CORS are determined (see Figure 9.2). When including the new CORS, almost all of Singapore will be within 5 kilometer of at least one of the SiReNT CORS (see Figure 9.3).

This is accessory however, the main reason is to generate redundancy and at the same time enable the monitoring of the Rover performance around Singapore. The first can thus be realized by installing equipment of different brands at (or close to) the determined locations. These CORS, and/or already existing CORS can simultaneously be used as Rover (depending on their location). The latter can be used to monitor the Rover performance (and the correction information) throughout Singapore.

For this to be realised any of the CORS located inside a triangle (sub-network) of three other CORS could be used (assuming the VRS method is used). The aim is to have several such Rovers distributed throughout Singapore in order to provide a good indication of the Rover performance around Singapore. This can then be used as a benchmark, and to see if the infrastructure is performing as it is supposed to. The results presented in this section are further discussed in section 9.1.2.
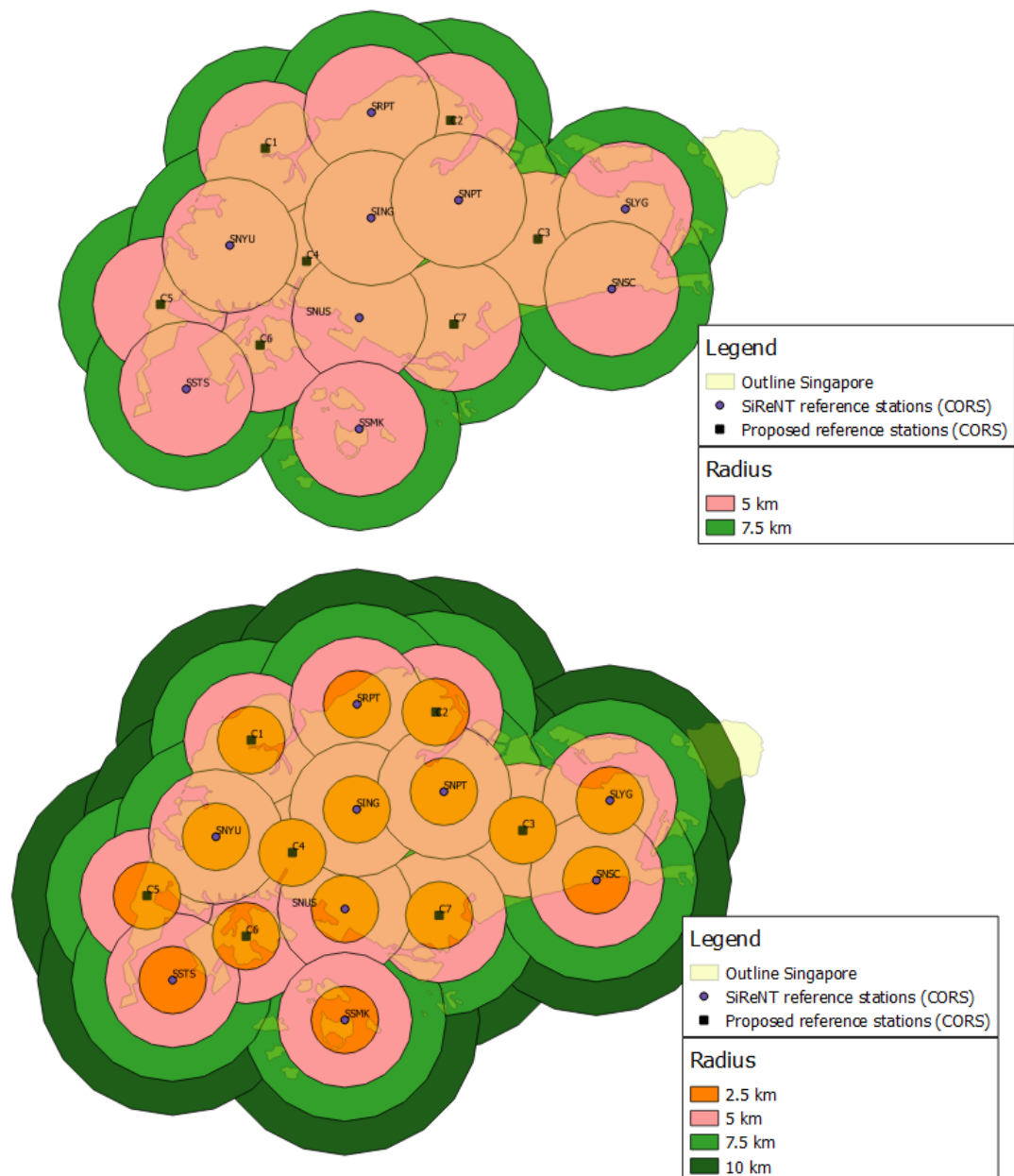
Figure 9.3: A map visualizing what parts of Singapore are within 2.5 km and 5 km of at least one of the CORS (including the proposed ones) (top), and what parts are within 2.5 km, 5 km, 7.5 km, and 10 km (bottom).

9.1.2. Discussion

Extra facilities are recommended, in case of failure for whatever reason. It would be good to have mixed brand facilities as well. The infrastructure can thus be improved by constructing more CORS, preferably with equipment of other brands. First of all, this results in reduced baseline lengths/an increased number of basslines between the CORS, and between the CORS and the Rover, independent of your location in Singapore.

Besides that, it also generates overlap of the coverage of the CORS (redundancy), now from different brands. Therefore, an issue that will put for example one of the brands temporarily out of order will not affect the whole infrastructure, but only a subset of it. The infrastructure can then continue to provide its services using the remaining CORS, which should still cover

the whole of Singapore. Also, the different CORS can be used to double check each other. The most convenient locations have been determined during this project, resulting in a distribution of CORS, such that independent of one's location in Singapore, one is always within 5 kilometers of at least one of the SiReNT CORS. This also means that there will always be multiple SiReNT CORS within 10 kilometer.

Some (or all) of these CORS, or already existing CORS can simultaneously be used as Rover. These then can be used to monitor the Rover performance (and the correction information) throughout Singapore. This is currently not being done, however would be a very good addition to what is currently in place.

9.2. Case study: The August 13th Sumatra earthquake event

On August 13th, at 11:08 am (Singapore time), a 6.5 magnitude event struck Sumatra [44][49]. This is an interesting case as by looking at the IM displacement data it can be analysed how the SiReNT infrastructure behaves in relationship to/is affected by an earthquake event taking place within the Asia-Pacific region.

In section 9.2.2. the IM displacement data on that date, for several engine modules, is presented. This includes IM displacement data from the Network Motion engine module (NME), the Rapid Motion engine module (RME) and the RTK engine module (RTKE) in baseline mode. Data from the other engine modules (the RTK engine in VRS mode and the Post-Processing engine) was also requested, however turned out to be incomplete and/or affected by the database reduction procedures too much to contain sufficient relevant data.

Like before, the IM displacement data is presented per CORS. First, it is determined what percentage of observations were supposedly unreliable (per engine) in case the default thresholds were applied. After that, using the remainder of the data, the percentage of supposedly reliable observations which were between the specific threshold is determined.

Examples of the resulting graphs (again for the SLYG CORS) can be found in Figure 9.4. Here both all displacement data and the supposedly reliable displacement data is plotted, in order to visualize when the system would have been disarmed.

These results are compared to the simultaneously recorded Ionospheric information, Tropospheric information, PDOP values and number of tracked satellites, which are also presented in Figure 9.5 (top and bottom respectively). The TEC values are not included in this, as they could not be provided. This is not problematic however, as the I95/IRIM values are believed to act as a good indicator of the impact of the Ionosphere. The graphs are explained in the subsection '9.2 Figures explained'. The graphs for all CORS can be found in Appendix 13.

Note that the SNPT CORS (as it is thus used as a fixed reference, meaning that its displacements are zero) and the SSTS CORS (as it did not record any data most of day) are omitted from this analysis. The results presented in section 9.2.1 are further discussed in section 9.2.2.

9.2.1. Results

IM displacement data

When looking at the displacement data of these CORS, one can see that during that day, just like any other regular day, the system per CORS would only be disarmed very few times, and only for some of the CORS. Besides that, there are only for some CORS displacements exceeding the thresholds, while the observations were supposedly reliable. In general, like before, the largest displacements were observed in the height component.

The focus in this section is on the Earthquake event at 11:08 am, however at that specific time, none of the CORS recorded an unusual displacement.

Ionospheric information

The I95/IRIM graphs present the values for the SiReNT infrastructure as a whole. One can see that this also was a relatively quiet day in terms of these values; there are no large spikes visible. The I95 values vary a bit, but are overall quite stable and mostly below 4, where the IRIM values are even more stable.

Tropospheric information, PDOP, and number of tracked satellites

When looking at the Tropospheric information and the observed PDOP/number of tracked satellites, one can see that all graphs for all CORS fluctuate in their usual manner. The PDOP and the number of tracked satellites do not show any unusual variations during this day. This, or similar behavior is recorded by all CORS.

The GRIM graphs present the values for the SiReNT infrastructure as a whole. One can see that this was also a relatively quiet day in terms of this value.
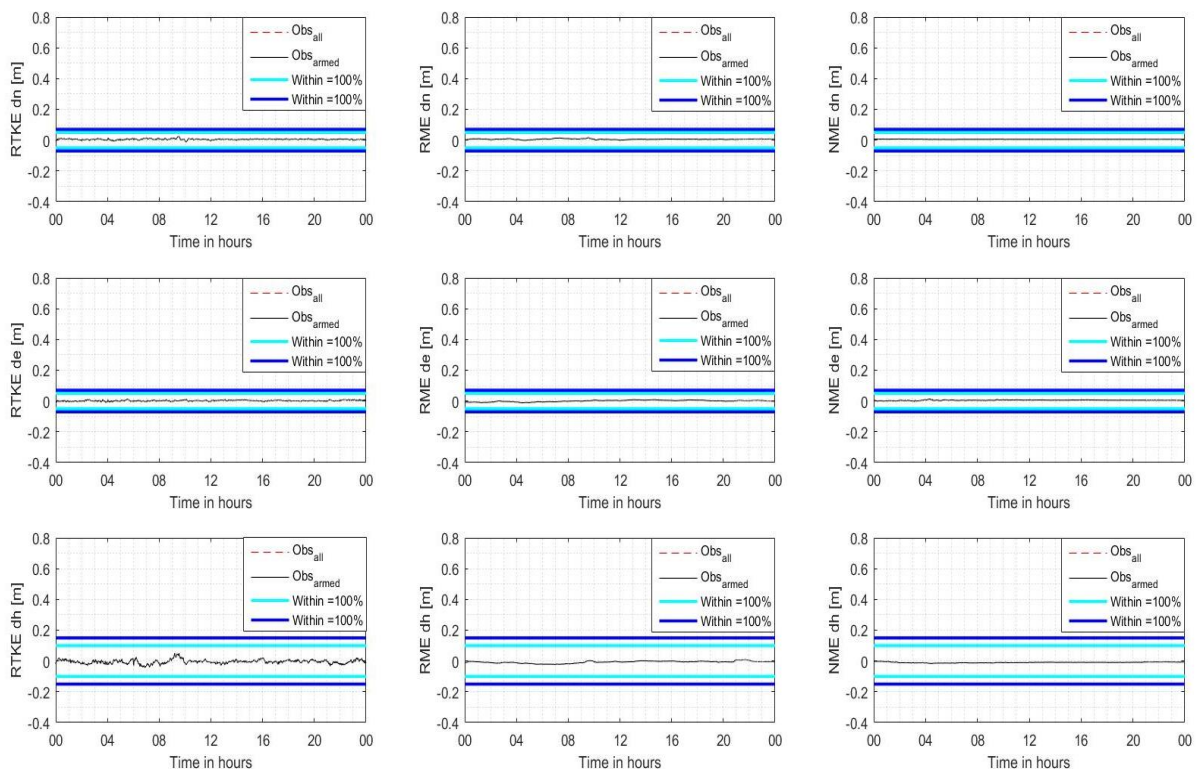
Figure 9.4: Graphs visualizing the IM displacement data for several engine modules (RTK engine module: left, Rapid Motion engine module: middle, and the Network Motion engine module: right) recorded on August 13th.

9.2 Figures explained

The displacement graphs per component, per engine module (Figure 9.4) visualize:

- The supposedly reliable observations in black;
- The supposedly unreliable observations in red (dashed line);
- The warning threshold in cyan;
- The alert threshold in (dark) blue.

The percentage of supposedly reliable displacements that satisfied the specific thresholds, as well as the mean of the supposedly reliable data are presented in the legends. The layout of Figure 9.4, is as follows:

	RTKE (baseline mode)	*RME*	*NME*
Northing displacements	RTKE dn	RME dn	NME dn
Easting displacements	RTKE de	RME de	NME de
Height displacements	RTKE dh	RME dh	NME dh

The I95/IRIM/GRIM graph (Figure 9.5, top) present these respective parameters in blue. The I95 graph is presented at the top, the IRIM graph in the middle, and the GRIM graph is presented at the bottom. Note that in the I95 graph the different regions are visualized by the colours assigned to these regions (see Table 4.2):

- White: negligible Ionospheric activity;
- Yellow: weak Ionospheric activity;
- Green: strong Ionospheric activity;
- Red: very strong Ionospheric activity.

The percentage of I95 values which were within these specific regions is presented in the legend at the top of the graph.

The Tropospheric information graphs (Figure 9.5, bottom) visualize the observed parameters (IPWV, temperature, relative humidity, ZTD, and the atmospheric pressure) in blue, where in the bottom-right graph, the PDOP value is visualized in black together with the number of tracked satellites in (dark) blue.

All graphs, per CORS, are presenting data from the same time period, enabling comparison of the different data types.

110
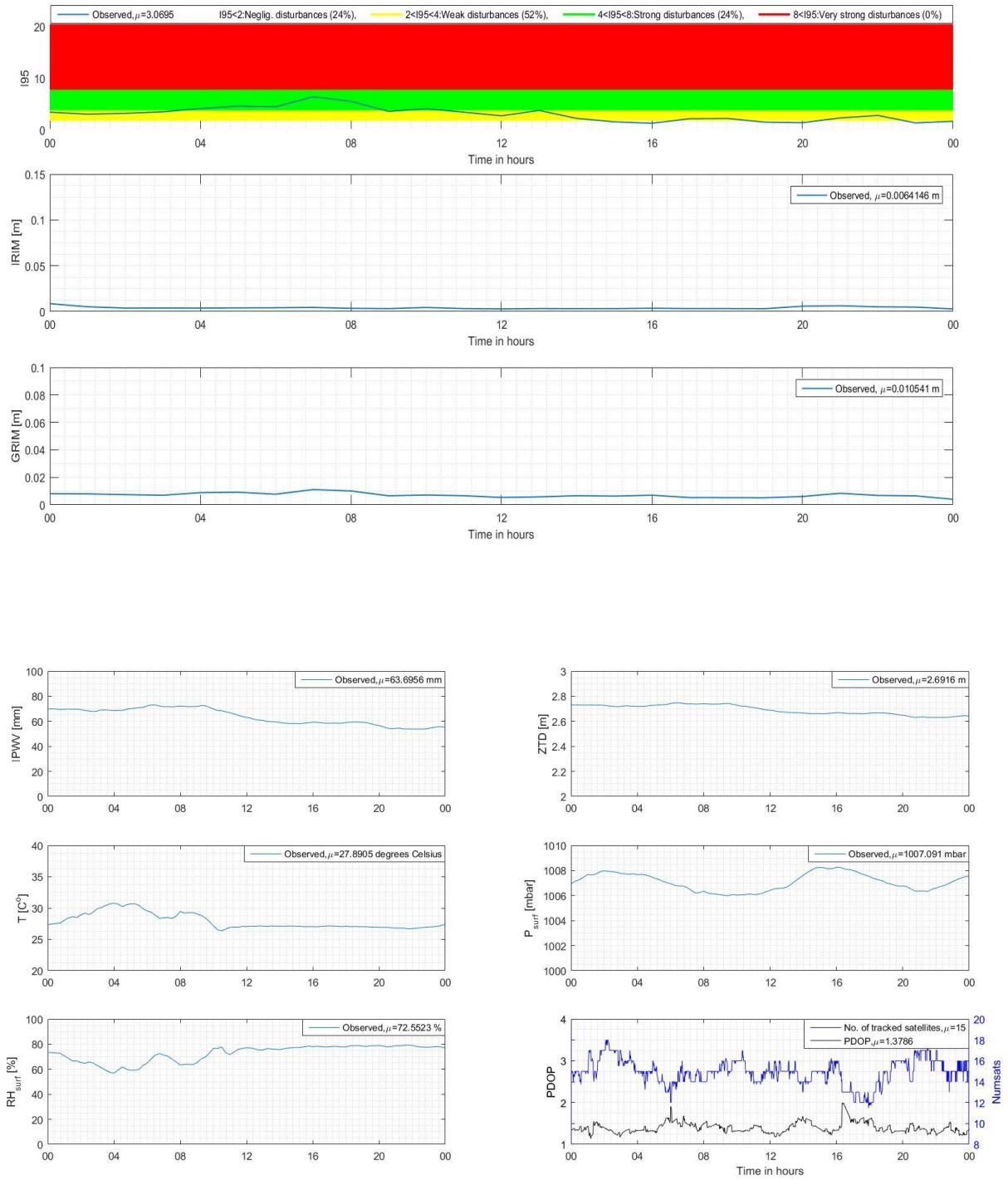
Figure 9.5: Graphs visualizing the I95/IRIM/GRIM (top), the Tropospheric information, PDOP value, and the number of tracked satellites (bottom) from the SLYG CORS.

9.2.2. Discussion

After comparing the IM displacement data from this period, to the Ionospheric information, the Tropospheric information, PDOP value and number of tracked satellites, one can conclude the following (confirmed with Earth Observatory Singapore (EOS)[47]).

The M6.5 earthquake in Sumatra on August 13th resulted in a ground motion which was too small to be observed by the SiReNT infrastructure (peak amplitude: less than 0.1 centimeter/second) (see Figure 9.6) [47]. That is why this event is not visible in the IM displacement data of any of the CORS. Besides that, during August 13th, there is not much striking happening in terms of suddenly changing atmospheric circumstances etcetera. The Ionospheric activity is fairly strong during most of the first half of the day, however this changes quite gradually. Therefore, it is concluded that during this day, the atmospheric circumstances are not causing obvious disturbances in the IM displacement data. The resulting displacement graphs for all CORS confirm this.
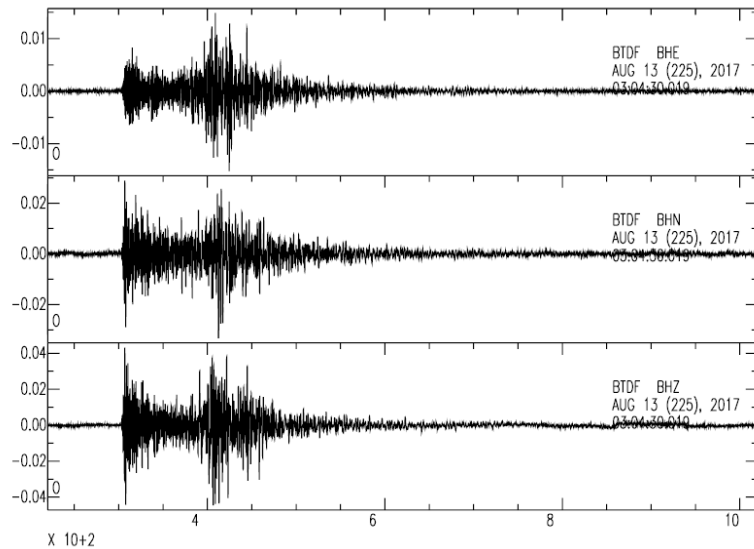
Figure 9.6: The M6.4 earthquake in Sumatra, as observed by a broadband seismometer [47]. In this figure the observed displacements [cm/s] are plotted for all components separately; easting: top, northing: middle, and height: bottom. The peak amplitudes of the observed displacements are less than 0.1 cm/s, which is far too small to be observed by the SiReNT infrastructure.

10.

Conclusions & recommendations

From all the findings presented in this report, conclusions and recommendations were formulated. This is done by first answering the research sub-questions, followed by the sub-questions related to the data processing, and finally the main research question.

10.1. Answers to the research sub-questions

These sub-questions were formulated in order to (first) gain fundamental knowledge about Integrity (and other quality parameters), and the way this parameter is monitored, as well as the factors affecting it. The answers to these sub-questions were found in Chapters 1, 2, 3, 4, and 5, and are presented in this section.

- *What, among other quality parameters, is integrity, and what is it with regards to GNSS based positioning systems?*
  Integrity is a measure of quality that can be expressed in terms such as honesty, sincerity, and trustworthiness. When it comes to GNSS based positioning solutions, integrity is defined as the measure of trust that can be placed in the correctness of the provided positioning information.
  An IM system monitors this, and is aimed at timely notifying the user(s) in case the provided information is not fulfilling the preset quality constraints and exceeds set limits. In case the integrity of the determined positioning solutions is lost, (parts of) the infrastructure or the provided information should not be used.
  The other quality parameters, with regards to positioning solutions, include accuracy, precision, availability, reliability, continuity, capacity and redundancy.

- *What are important degrading parameters/factors affecting the integrity of GNSS based positioning system?*
  The performance of GNSS based positioning system is affected or disturbed by (a combination of) errors. The impacts can take place on different levels; the user, or user equipment level, the operational environment level, or the system level.
  The first kind are caused by the end user and/or by the used equipment.
  The second kind are related to interference (intentional and unintentional) and signal propagation properties, and include jamming, spoofing, RFI, the Tropospheric delay, the Ionospheric delay, and multipath.
  The third kind are disturbances and/or variations that occur in the space segment, the ground segment and the interface between these two. These include satellite clock errors, orbit errors, a change in satellite geometry (affecting the PDOP and the number of tracked satellites), cycle slip, and antenna phase center offset and variation.

- *What IM methods are available?*
  There are two main methods to monitor the integrity (in terms of the stability of GNSS-based positioning systems (and its CORS)).

  One method is implementation at system level (external monitoring), using the CORS out of which the network consists, to continuously monitor the incoming signals and transmit information and corrections regarding any incorrect behavior. This can be done by for example looking at the determined positioning solutions, or directly at the determined ranges themselves.
  There are two types of external monitoring systems, ground-based and space-based systems. In the first, the information and corrections are broadcasted to the user(s) by the master station directly, where in the second, the master station relays this to one or more geostationary satellites which in turn broadcast that to the user(s), along with the ephemerides and almanac information of these satellites themselves.

  The other method is implemented at user level (RAIM), within the individual receiver(s) itself/themselves. For this type of monitoring there are several types of statistical detection algorithms available, including range comparison, and position and/or residual comparison. Note that the RAIM method is very dependent on the number of satellites in range, as well as the satellite geometry.

  These two methods, the external monitoring method and RAIM, can be either used individually and/or independently, or in some sort of combination, in order to complement each other. One's preferred choice depends on the type of application, as well as the environment.

- *What is being used in other countries, with regards to IM?*
  In the different investigated countries, several variants of the external monitoring method are applied by the cadastral/mapping agencies, in order to perform IM of infrastructures, similar to the SiReNT infrastructure. Usually this includes baseline and coordinate processing/comparison, both in real-time and through post-processing. The option to use RAIM to complement the external monitoring method is not utilized anywhere in the investigated countries.

  There are similarities as well; large(r)-scale network infrastructures surrounding small(er)-scale network infrastructures, are often used in order to monitor these network infrastructures. Most of these countries make use of the Bernese GNSS software to monitor their network infrastructure, using the IGS network and the precise satellite orbits.

  Besides the stability of the network infrastructure, things such as the raw data, the correction information, the system equipment, as well as the performance and quality of its CORS, are (often) monitored as well. Often the TEQC software is used to monitor the completeness of the data.

  When it comes to the visualization of the data, most countries present limited/specific information about the CORS to the public; such as its status and health, the used equipment and its coordinates. For this often a real-time interactive dashboard or map is used. Any additional information is usually visualized for internal use only.

On top of that, most, if not all countries, have backup/redundant facilities (usually consisting of equipment of a variety of brands) in place in order to ensure reliability. Sometimes regular checks are performed to check the stability of the CORS, using for example theodolite, tachymeters or total stations.

Important to note is the cooperation between State governments, the industry, academic institutions, and the community, that often takes place. This ensures that information provided by the network infrastructure is up to date/standard and suits the user's demands.

- *What is used in Singapore, with regards to IM?*
  In the SiReNT infrastructure, the TIM App is used to monitor the movement and/or quality of the GNSS CORS (the external monitoring method), where the TRI App could be used to monitor the Rover performance. The Trimble receivers used in this network infrastructure do also support RAIM, however this option is not utilized. The TPP also includes an Integrity Monitor module and an Alarm manager module. The Integrity Monitor module can be combined with one of the TIM engine modules in order to perform adjustments, and to determine and display the coordinate displacements. This component also monitors other involved aspects (power supply, connectivity etcetera), however not the raw data. That, as well as the estimation of the systematic errors, and the determination of the Ionospheric and Tropospheric models, predictions and corrections, is done separately. The Alarm Manager module can be used to trigger notification messages in case of problems, or when pre-set thresholds are exceeded.

  These Apps and modules are currently not utilized properly. Besides that, the SiReNT infrastructure is not monitored with respect to any other network infrastructure, and there are insufficient back-up systems in place.

  In terms of the visualization, users of the SiReNT infrastructure can access the so-called Network Information and Atmospheric Information. This includes specific information per CORS, the CORS' displacement charts and scatterplots, and the atmospheric information. Besides that, IM reports including Statistical Point Overviews and displacement charts are generated every 3 days and presented to the network operators/infrastructure administrators.

- *How to use, improve, and communicate/visualize SiReNT's integrity (in terms of its stability and positioning solution quality), IM and its output?*
  The use of the IM component and its output is clear; its ultimate aim is timely notifying the user(s) in case the provided information is not fulfilling the preset quality constraints and exceeds set limits. In that case (parts of) the infrastructure or the provided information should not be used. Also, the archived IM output can be used as proof of the ensured quality, for example against false claims.

  To ensure that the IM, with regards to the system's stability and positioning solution quality, is done properly, appropriate methods (including appropriate algorithms and thresholds) should be applied in the process. In this, there is room for improvements. The system and observation redundancy of/within SiReNT should also be increased. The IM of the network infrastructure and its CORS in the way it is been done at this point will only directly affect the CORS. Of course, in case the stability and positioning solution quality of the CORS is (very) bad, the Rover performance (using the VRS

correction stream indirectly resulting from these CORS) cannot be very good either. Ensuring good stability and positioning solution quality of SiReNT's CORS is therefore very important, however it is not enough.

The IM part of interest can also potentially be improved by establishing a connection between the Rover performance and the IM component. For this, the Rover performance has to be monitored, which can be done through employing the TRI App. Adding such a connection would enable the infrastructure administrator to monitor the Rover performance throughout the infrastructure, in Real-Time. Besides that, the output from the TRI App could then be compared to the IM data (RTK engine module in VRS mode for example) observed by the same instrument.

Note that at the moment of this research the TRI App seems to be an addition to the TPP with limited possibilities however. The resulting output is not as complete as the IM data and on top of that, it cannot be retrieved from the TPP.

It would also be good to actually use the IM output in the correction information generation; for example through assigning weights to the role that the output from a specific CORS plays in it, based on its IM output.

Furthermore, the surrounding IGS stations should be adopted as a stable fixed (external) reference to monitor the stability and positioning solution quality of the SiReNT infrastructure continuously or at a certain frequency, for example weekly. Besides this, in order to confirm the SiReNT CORS' (lack of) movement, control markers could be generated around them. This way the equipment's stability could be investigated by measuring their positions using precision instruments such as theodolites.

The number of tracked constellations and signals should be maximized in order to increase the availability and integrity of the GNSS service. This will in turn increase/improve the level of reliability and robustness of the SiReNT infrastructure. Therefore for example the IRNSS signals should be adopted as well.

In terms of what to visualize and how; only the necessary should be presented to the public, in a straight-to-the-point manner. The lesser, the better, in order to not confuse or overload the (end-)user with unnecessary information. A dashboard along the lines of the one presented in this report (see section 5.2.1) should be developed.

The complete output should be accessible by the infrastructure administrator however; in case it is required for further research/investigation.

The IM reports should be generated less often, as there is no need in having one every 3 days. On top of that, that way it is easier to compare the IM displacement data over a longer time (weekly or even monthly). The specific content and how it is presented in these reports should be updated as well, as to maximize their use and clarity. These reports should minimally include IM displacement charts, scatterplots, and statistical point overviews, however per component only. Updates, for example in terms of colour coding, should be applied in order for them to be easier to interpret. Possible additions to the report's content could include the quality of the correction information. Another option could be the percentage of the reliable displacement data that was simultaneously satisfying the applied thresholds, together with the average over previous years in the same months (as per Figure 5.3).

Besides that, for a complete overview, all CORS should be included. If during the period covered by the report any of the CORS were down, the presented information for this particular CORS should clearly indicate when and why this occurred.

Note that these reports, or any IM displacement data for that matter, are only meant for the infrastructure administrators.

10.2. Answers to the data processing sub-questions.

The sub-questions with regards to the data processing were formulated in order to develop an understanding with regards to what is monitored in SiReNT. The answers to these sub-questions are found in Chapters 7, 8 and 9, and are presented in this section.
The sub-questions with regards to the data processing;

- *What is the impact of unusual fluctuations in the atmospheric information and/or the PDOP/number of tracked satellites on the IM displacement data, and what can be concluded from it?*
  Firstly, note that the length of the datasets is quite short (~5 months), perhaps even too short to be able to say something meaningful about these impacts. Even though that is the case, an attempt has been made, and below this sub-question is answered with regards to the CORS.

  The different types of atmospheric information do show repeating diurnal variations but lack a clear seasonal trend over time. No clear repeating variations are visible in the IM displacement data however, not even diurnal variations; the observed displacements in general are quite variable, without clear patterns in it.

  The Ionospheric activity can cause sudden relatively large displacements, especially when (suddenly) extremely severe. The impact of those most of the time (even) would cause observations to be unreliable. Note however that if the default thresholds were to be applied, almost all of the supposedly unreliable observations that are related to sudden severe fluctuations in the Ionospheric activity (especially the relatively extreme cases), would be filtered out reasonably well.

  The exact relationship between the parameters representing the Tropospheric information, and the displacement magnitudes, is still not understood completely however. It is possible that the impact of (some of) these parameters still is underestimated, or that there is another, unknown factor, that is at times, in varying degrees, affecting both the Tropospheric information and the displacement magnitudes.

  The PDOP and the number of tracked satellites in general do not show much unusual behavior. Therefore, it is hard to say if/how these parameters affect the IM displacements. In order to find out more with regards to this and the impact of sudden severe fluctuations in the Tropospheric information, further research is required.

- *What thresholds to use in order to ensure that 99% of the IM displacement data is within the thresholds, and alert the user properly in case the network infrastructure is not necessarily providing trustworthy information?*
  The default thresholds used in the TPP IM of the CORS' quality are the result of testing performed by Trimble under ideal circumstances. Therefore, they are not necessarily perfectly applicable to each and every CORS worldwide.

  However, when applying these thresholds, it turns out that most of the time, over

98%, all CORS would still have been armed (and thus recording supposedly reliable IM displacement data). Over 99% of this displacement data was within the thresholds, for all CORS. Hence, one can conclude that if the default thresholds were to be applied, almost all supposedly unreliable observations would be filtered out, and the resulting displacement data would satisfy the thresholds for over 99% of the time. This leads to the conclusion that the current thresholds provide a reasonably good trade-off. Especially, since changing these thresholds would either result in an increasing amount of data loss on one hand, or a decreasing number of (main) disturbances to be filtered sufficiently on the other hand.

Note that this does not necessarily mean that the fact that the thresholds are concluded to be sufficient, also applies to the other engine modules. The thresholds can and probably should be adjusted independently, per engine module. This is the case as the aim and output of one engine module is independent from that of the other engine modules. Further research is required on this specific subject.

- *Are there trends in the IM displacement data and if so, what can be concluded from them?*
  When looking at the CORS observations presented in chapter 7, the observed motion relative to the SNPT CORS, is predominantly a subsidence, while moving towards the (South-)East. The yearly motion of this CORS itself is unknown, hence, so is the absolute yearly motion.
  The different CORS did observe differing horizontal movements however, which is an interesting finding (with regards to the CORS' stability). Assuming that there is no or very little relative movement, this could be caused by several factors (e.g. differing subsurface types, signal blockage, etcetera). Clear indicators for this are lacking however. Also keep in mind that the maximum length of the available datasets for this research project was only 5 months. If these the motion magnitudes and directions, resulting from these observations are correct however, action is required. In that case, the CORS should potentially be constructed at other locations instead.
  Hence this should be confirmed, for example by monitoring the SiReNT infrastructure with respect to the IGS infrastructure.

- *Is there a relationship between the IM displacement data and the Rover displacement data, and can the first be used in controlling the latter?*
  The thresholds cannot be used in order to control the Rover displacement data retrieved by the infrastructure user, as there is no relationship between these thresholds and the Rover displacement data. Even the IM displacement data from the RTK engine in VRS mode does not show a clear relationship, even though this engine module uses the same correction stream and therefore in theory should show at least some similarities. One could argue that this could be related to the impact of the resampling or noise etcetera.
  Either way, it turns out that the thresholds are aimed at monitoring the output of the specific engine modules themselves, rather than an indication of the resulting rover output being sufficient or not.

- *How is the Rover performance affected by unusual fluctuations in the atmospheric information and/or the PDOP/number of tracked satellites on the IM displacement data, and what can be concluded from it?*
  In this project, the Rover performance is divided into two parts; performance in terms of positioning solution (and thus also the quality of the correction data), and

performance in terms of re-initialization. For this continuous and (re-)initialized Rover displacement data is recorded, respectively.

The different types of atmospheric information do show repeating diurnal variations but lack a clear seasonal trend over time. No clear repeating variations are visible in the Rover displacement data however, not even diurnal variations; the observed displacements in general are quite variable, without clear patterns in it. Note that the length of the datasets is even shorter in this case.

When further comparing the results related to the Rover displacement data with the atmospheric information, it is found that there is no clear relationship between them (not in the relative (large) displacement magnitudes, nor in their timing); only (possibly) sometimes. It is possible that the times that the (re-)initialization took (very) long to take place, and/or the times where large displacements are recorded, are caused by a sudden change in satellite geometry, affecting the PDOP and the number of tracked satellites. This also cannot be concluded from the graphs, however.

In order to get better results and a better understanding of the Rover performance, further research is required, using 1 Hz data. The latter would enable one to see what is happening in greater detail, especially when zooming in on specific periods of interest.

- *With regards to improving the redundancy within SiReNT, where to construct new CORS?*
  Assuming that Singapore's sub-surface is stable, the new CORS, containing equipment of different brands, should be constructed on, or close to the locations visualized in Figure 9.3. That way, almost all of Singapore will be within 5 kilometers of at least one of the SiReNT CORS. These, and/or already existing CORS can then simultaneously be used to monitor the Rover performance (and the correction information) throughout Singapore.

- *How does a nearby earthquake event affect the SiReNT infrastructure?*
  The SiReNT infrastructure is at this moment not sensitive enough to record events such as the August 13th, M6.5 Sumatra Earthquake event. If this were to be something that should be recorded, other instruments, with greater sensitivity to movements, should be added to the infrastructure.

10.3. Main Conclusion

This research project was conducted in order to be able to answer the following main research question:
What is the integrity of the SiReNT infrastructure (in terms of its stability and positioning solution quality), and what is needed to improve that, as well as the way it is monitored and visualized, in order to be more useful?

In this section, the main conclusion of this research is presented, by answering this question. This conclusion is based on this report and the answers to the sub-questions presented in section 10.1-10.2.

The integrity (in terms of CORS' stability and positioning solution quality) of the SiReNT infrastructure is actually quite good. From applying the default thresholds, it follows that during the observed period, the IM displacement data was supposedly reliable for over 98% of the time. Applying these thresholds also results in almost all supposedly unreliable observations being filtered out. Over 99% of the remaining displacement data would be within the default thresholds. Hence, (at least) the default thresholds should be applied immediately. The impact of using different thresholds on the different engine modules should be investigated further (see section 10.4).

Improvements are required however, in order to get the IM displacement data to be reliable and at the same time within the thresholds, for 99% of the time or more, as well as to increase the reliability of the network infrastructure.

As a start, the overall redundancy should be improved. Several possibilities in which this can be done, have been described in this report. This will make the SiReNT infrastructure more robust and increase its reliability.

Also the way in which the integrity of the network infrastructure and its CORS currently is monitored could be changed (and by that, improved). As described, there are several ways in which this can be done, however all with as an important addition; the utilization of, and feedback from the Rover data. For this either several VRS or several of the CORS, simultaneously acting as Rover, distributed throughout Singapore, could be employed. For monitoring the performance of these Rovers, potentially the TRI App could be employed.

Since we are interested in the stability and positioning solution quality of the CORS, it would be better to monitor the IM displacement data from the Network Motion engine module. This module is specifically aimed at this. Note however, that like all options, this engine module still observes the motion with respect to the SNPT CORS.

Furthermore, the IGS infrastructure should (therefore) be adopted as a stable fixed reference as to monitor the SiReNT infrastructure as a whole. The SiReNT CORS should also be regularly investigated by measuring their positions with respect to surrounding stable control points, using precision instruments such as theodolites. This would also help one to confirm and better understand the observed (relative) motion of the SiReNT CORS.

In case there is any procedure (for data reduction for example) applied to the data, it should be ensured that this is done in a proper and consistent fashion.

In terms of what to visualize and how; only the necessary should be presented to the public, in a straight-to-the-point manner. The complete output should be accessible by the infrastructure administrator however, in case it is required for further research/investigation. The IM reports should be generated less often, its specific content and how it is presented in these reports, should be updated, as to maximize their use and clarity.

Besides this, further research could/would greatly benefit SiReNT, in improving its integrity (in terms of its stability and positioning solution quality) and IM. More on this in the next section. In relation to this, working more closely with academic institutions and the community, would be beneficial. That would also help in ensuring that the provided information/service is up to date/standard and suits the user's demands.

10.4. Recommendations for further research

Improving the current situation should be aided by ongoing research. First of all, when conducting further research, more observations should be taken, over a longer period of time, in order to generate more observation redundancy. This would also mean that more (different) circumstances would have been covered and (thus possibly) a more reliable result would have been obtained.

Different timescales and more frequent data
Other than that, besides looking at observations taken over a longer period of time, one should also zoom in and look at the observations on smaller timescales, for example daily or even hourly. This would enable one to perform a more detailed analysis. This goes for both the IM displacement data and the Rover displacement data.
Having this data would also enable one to better investigate the impact of factors such as the Ionosphere and Troposphere on the displacement data.

The thresholds, the (specific) impact of the external factors, and related (re)actions
Further research is also required into what exactly happens (besides triggering a notification) when the system is disarmed, and/or when the specific thresholds are exceeded. Currently, it is unclear whether there is anything in place which attempts to improve the situation in this case, in order to provide reliable data again, as soon as possible. On top of that, it should be investigated what happens for example if the observations exceed the specific thresholds, when the system already has been disarmed.

In terms of the specific thresholds, now their specific aim is determined, the value that is best suitable for these thresholds, per engine, along with their (dis)advantages should be further investigated. It is the question whether the same default thresholds are indeed applicable to all engine modules, as is done at this moment, as the aim and output of each engine module are independent from that of any other engine module. Hence it is expected that the thresholds to be applied are not the same either.
As part of this it should also be investigated in greater detail what is the impact of the different factors on SiReNT, and whether it is a good idea to for example combine the IM displacement data with the Ionospheric information, and the Tropospheric information, in order to improve the identification and filtering out of related unreliable observations. Also what causes the magnitudes of supposedly reliable displacements sometimes exceed the magnitudes of the supposedly unreliable displacements, should be investigated further.

Algorithms/methods and statistics
Research into the Minimal Detectable Bias, in order to find out what is the magnitude of the smallest error that can be detected with a certain level of confidence (for example 95% or 99%), using statistical testing. This parameter represents the actual integrity of the system and is of course linked to determining the correct threshold.

Research into a method/algorithm that can be specifically tailored to Singapore, especially if the determined Minimal Detectable Bias is not satisfying SiReNT requirements, even when the best threshold options are used.
In this (finding a method specifically tailored to Singapore) one could, or maybe even should, look both at, and compare, the results of external monitoring and RAIM, and combine them in some way.

It should also be investigated how exactly the feedback from the IM component can, and if used, should be utilized and applied in the network processing. Perhaps it could be used to for example assign weights to the CORS in the network processing, and correction determination etcetera.

Further research into how the TRI App could be maximally utilized is required as well.

Interference
Most SiReNT CORS are located at high(er) elevations, for example on top of buildings, and therefore, in theory, less sensitive to interference (due to the use of an elevation mask and choke ring antennas). It is clear, however, that interference can play a major part in affecting (the information provided by) an infrastructure. The next step, in improving the (integrity of the) infrastructure and the information provided by it, therefore would be to identify the possible impact/footprint of the different types of interference. This knowledge can then be applied in monitoring the IM displacement data, in order to mitigate the impact of these factors.

Appendices

Appendix 1: *The Trimble Pivot Platform (TPP)*

The general information about the SiReNT infrastructure can be found in section 1.2. In this Appendix the TPP, the software that is used in the network processing and the IM of the CORS' stability of the SiReNT infrastructure is reviewed more elaborately. First the TPP; its functionalities, Apps, and modules are briefly described in order to give one a general understanding of what this software package consists of. Next, the Apps and modules used in the IM of the SiReNT infrastructure (as presented in Table 4.1) are reviewed in more detail.

A.1.1. TPP: Apps and modules

SLA has employed the TPP for the network processing and IM of the CORS' stability of the SiReNT infrastructure. This technology utilizes one common platform for all Apps, such that its (combined) performance can be improved and its configuration simplified [10][36][37]. Besides that, now version consistency can be maintained across all involved Apps. Through the combination of the different Apps, with a wide range of capabilities, complete solutions can be created, dependent on the user's requirements.

This supposedly robust system is scalable to the application in which it is used, and is divided into separate services and applications, which can run on the same computer or spread over multiple computers. The TPP consists out of Infrastructure Apps which can be subdivided into Core Supporting Apps, Network Processing (and Dynamic Control) Apps, Earth Systems Apps, Monitoring Apps, and User Services Apps (see Figure A.1.1). All these Apps are briefly reviewed below, however note that in this research the focus lies on relevant Apps and modules, and that the ones in which there is no interest are omitted from this review.
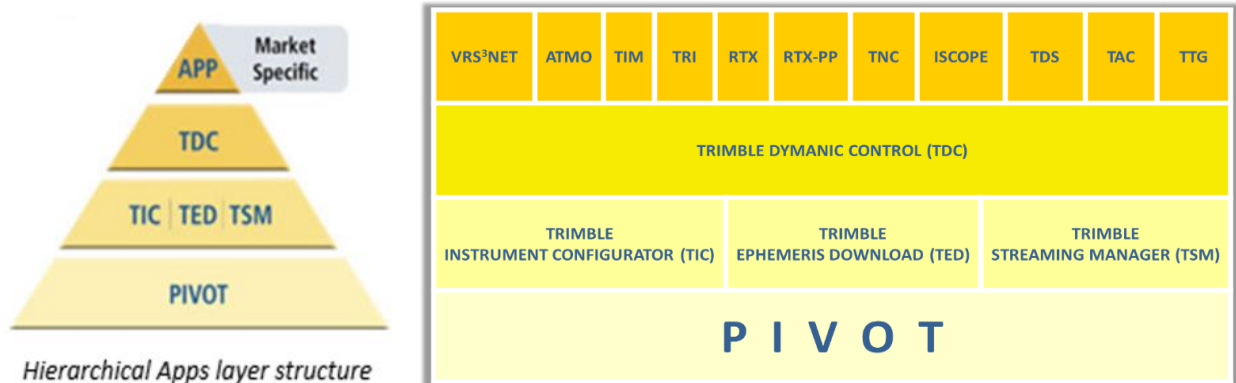
Figure A.1.1: The TPP hierarchical structure (left) and its Apps (right) [10]. From bottom to top: the TPP; its Core Supporting Apps (TIC, TED and TSM); its Network Processing and Dynamic Control App (TDC); and its other Network Processing App (VRS3Net), Earth System Apps (ATMO), Monitoring Apps (TIM and TRI) & User Services Apps (TNC, ISCOPE, TDS, TAC and TTG).

Core Supporting Apps

- Trimble Instrument Configurator (TIC): this App controls and runs the receivers and other high precision instruments in the network. It checks whether (and what number of) GNSS receiver modules are configured for, and capable of automatic data download and firmware updates.

- Trimble Ephemeris Download (TED): this App checks for, and downloads all relevant (precise) orbit information data and clock corrections, in order to make it

available for all applications using the TPP. This information is used to improve the geometric modeling and to check the quality of the used orbits. The registered orbit and satellite almanac information are continuously overwritten, in order to provide the user immediately with the best available information, even if the system has to be restarted.

- Trimble Streaming Manager (TSM): this App controls and manages incoming and outgoing data streams of any type. This is done through multiple different modules each with specific tasks related to receiving and transmitting, managing and storing the raw data.

Network Processing Apps

- Trimble Dynamic Control (TDC): this App monitors and manages all received data by the GNSS reference network, and generates, broadcasts (trough the Real-Time Output (RTO) module), and stores Single Station correction information. This is done through multiple device managers and modules that are part of the Core Supporting Apps, each with specific tasks related to configuring and monitoring the different connections, broadcasting the corrections and storing the received data.

- VRS³Net: this App generates, broadcasts and stores VRS correction information (Ionosphere and Troposphere) for centimeter accuracy positioning solutions within the bounds of the GNSS reference network infrastructure. Also used by the Reference Data Shop module (see below) to generate VRS data for Post-Processing purposes. In order to do this, this App is supported by the Trimble NTRIP Caster (TNC) App and the TDC App (and thus also the Core Supporting Apps).

The RTO (observations, corrections, positions etcetera) from these Network Processing Apps is taken care of by the RTO modules. There are 3 types of RTO modules:

 -RTO Single Station: used to forward data from a specific CORS to Rover(s) that connect to it, without the need to receive any input position.

 -RTO Multi Station: used to forward the observation data of the nearest, correctly operating CORS to the Rover. The provided Rover position is used in order to select the right CORS.

 -RTO Net: used for VRS network applications; a VRS is generated, using minimum 3 surrounding CORS, from which the applied network corrections (with RTK accuracy) are determined. For this, the Rover position(s) is/are required as input.

Earth Systems App

- Trimble Atmosphere (ATMO): this App is a VRS processing engine module that calculates the ZTD and the IPWV, and (optionally) the TEC values from the received, synchronized GNSS data (including weather information). This engine module works both in the real-time and in post-processing mode, using the previously stored observation data in that latter case. This App uses all the CORS from the SiReNT infrastructure.

Monitoring Apps

- Trimble Integrity Manager (TIM): this App provides real-time and post-processing engines to monitor the movement and/or quality of the GNSS CORS with respect to one or more selected, fixed station(s).

As described in section 3.5, this App can be combined with the Alarm Manager such that in case there is movement observed with a magnitude that is exceeding the set thresholds, the

user will be notified (warned or alerted). Depending on the required specifications (such as (maximum) time-to-detect and accuracy) one can select from several processing engine modules (see Figure 3.4); the Post Processing engine, the Network Motion engine, the Rapid Motion engine module and the RTK engine module (the different engine modules are reviewed in the next part). In order to perform its task, the TIM requires the TIC, TDC, and TED Apps, and in case the RTK engine module is ran in VRS mode, the TNC App as well.

- Trimble Rover Integrity (TRI): this App analyses the performance of permanent Rovers within the bounds of the GNSS reference network infrastructure while they take into account the incoming correction information. This can be done by periodically re-initializing the Rovers by resetting them. These measured performances represent the performance that should be observed by the field users. This App can also be used to specifically investigate the initialization performance. In order to do this, the TRI requires the TDC Apps. This also follows the system level-external monitoring method (see section 2.3.1); the determined positioning solution of the Rover in this case, is compared with the reference data, through the infrastructure.

User Services Apps

- TNC: this App manages the administration of multiple NTRIP Casters, and acts as communication center (of the infrastructure) towards the infrastructure user(s). It provides an overview of the status information of the to the Pivot platform connected users. This module distributes the correction information to the infrastructure user(s) in real-time

- iScope: this Pivot Web Application allows licensed users to (re)view the location of their connected Rovers in real-time, or follow the past sessions' trajectories, on the iScope Map. Note that because of performance reasons this map does not get updated automatically, but only after one clicks the refresh button.

- Trimble Data Shop (TDS): this App includes the Reference Data Shop module which enables the generation of GNSS reference data for either a CORS or a VRS position, for a desired observation interval. This data is then distributed to the infrastructure user(s).

- Trimble Accounting (TAC): this App enables the management of users and contracts (subscriptions, terminations and renewals), and provides relevant account information (on the number of registered users, per user: what company, the contact details, login, etcetera).

- Trimble Transformation Generator (TTG): this App allows adding transformation parameters and grid files to the correction data stream based on the RTCM standard. It includes the Transformation Generator module, which makes it possible to perform coordinate system conversions, by providing the necessary information (example: global CRS → local CRS at the Rover).

Note that for all Apps the more detailed information can be found in a list view, which is part of the details section in the TPP.

When categorizing the way in which the TPP monitors the IM of its CORS as one of the previously described methods (section 2.3) to monitor the integrity of GNSS-based positioning systems (and its CORS), then it can be concluded that these monitoring Apps and engine modules are implemented at system level (external monitoring (see section 2.3.1)); the determined positioning solution of the CORS itself, and the baselines between the CORS are measured and compared with the reference data.

Note that the GNSS receivers used in the SiReNT infrastructure do support RAIM however.

A.1.2. TPP: functionalities

The functionalities of the TPP can be subdivided in the following categories (containing their own Apps and modules that work together) [10][36]:

1. Data collection from the CORS
2. Data storage at the DCC
3. Data processing at the DCC
4. Transmission of real-time correction data to the user(s)
5. Generation of GNSS observation files for post-processing
6. System controlling and IM

The categories 1-5 combined provide the user with the Real-Time services (Figure A.1.3) and the Post-Processing services (Figure A.1.4). The way in which this works is reviewed in the following parts.

Real-Time Service

In order to provide the Real-Time service, the following Apps (and modules) are required:

- *The TDC App (module: GNSS Receiver, RTO Single Station, Synchronizer)*
  This/These receiver module(s) control and analyse the raw data received by the respectively connected receiver(s) by tracking the satellites and checking for errors, such as unhealthy satellites, data drifts, outliers or cycle slips, and attempt(s) to correct for it. Data which cannot be corrected for, is removed from the dataset. This analysis is conducted in combination with the antenna phase correction table, using the best available orbit information in order to correct for the antenna phase center offset and variation. The TPP technology uses per default satellites above an elevation angle of 10 degrees and broadcasted orbits, provided by the Ephemeris Manager module. The

Figure A.1.2: The baselines generated by the Network Processor; the baselines used in positioning solution determination represented in red (SING excluded), and the baselines used in the determination of the atmospheric parameters represented in blue (SING included). The reason why SING is excluded in the first, but included in the second, has to do with the fact that the SING CORS is not maintained by SLA and is not accessible at any time in case of issues. Source: screenshot from the TPP.

  receivers start tracking the satellites above an elevation angle of 5 degrees already however, to generate some space to properly track a specific satellite properly before using it.
  In case the Network Approach is used, the data is forwarded to the synchronizer in order to make sure that the timestamp matches and all the used data is observed at the same time. This data is then forwarded to the Network Processor (*VRS³Net App)*, where it is combined with the known positions of the CORS, in order to perform the Network Processing.

In case the Single Station Approach is used, the TDC App generates Single Station correction data, using the RTO Single Station module in order to forward this correction data to the NtripCaster module for it to be transmitted to the connected Rover(s).

- *The VRS³Net App (module: Network Processor (Storage), RTO Net)*
  This App is thus used in case the Network approach is used. During the initialization period the baselines between the CORS are processed by the Network Processor module (see Figure A.1.2), while it models and estimates systematic errors and generates the Ionospheric and Tropospheric corrections for both the Network RTK (VRS) mode and the Network DGPS mode, in real-time. This results in the Ionospheric and geometric (Troposphere and orbit) predictions and corrections. Included in this are the ZTD and TEC values. This output is reviewed in section A.1.4. Note that, as mentioned in the introduction, only 8 CORS are available for general use (and thus the network processing). All CORS are used with regards to determining the atmospheric parameters however.
  The RTO Net module combines and applies the incoming receiver data (from the Rover(s), through the NtripCaster module), in order to determine the VRS location and appropriate correction information. All this data is then forwarded back to the NtripCaster module and stored by the Network Processor Storage module.
  When activated, the Network Processor module has the ability to trigger notifications in case the Network performance is below the set thresholds or if there is a delayed network processing, a low number of satellites solved, or a processor (re-)initialization. This Network performance is computed per CORS as well as for the whole network, and it is based on the percentage of solved ambiguities (versus processed satellites) for the last 24 hours. As for the performance thresholds, by default this is set to 97% for the warnings and to 95% for the alerts.

- *The TNC App (module: NtripCaster)*
  The NtripCaster module serves as communication center and distributes the correction data (from the specific RTO module) to the Rover(s) and receives the receiver data from the Rover(s) in case they are using the Network approach.

- *The TAC App*
  At the Rover(s) the correction information is applied resulting in a centimeter to decimeter accurate positioning solution, depending on the technique that is used (DGPS versus RTK). Through this App it can be managed who is using the provided correction information.

Post-Processing Service
In order to provide the Post-Processing service, the following Apps (and modules) are required:

- *The TDC App (module: GNSS Receiver, Storage)*
  These receiver modules control, analyse and correct the raw data as previously described. This data is then stored straight away for Post-Processing purposes.

- *The TDS App (module: Reference Data Shop)*
  The Reference Data module uses the stored data to generate GNSS reference data of interest (output files for specific positions and/or periods).

- *The Trimble Web App in combination with the TAC App (module: Web application)*
  This Reference Data is forwarded to the user(s) over the Internet. Through the TAC App it can be managed who is using the provided correction information.
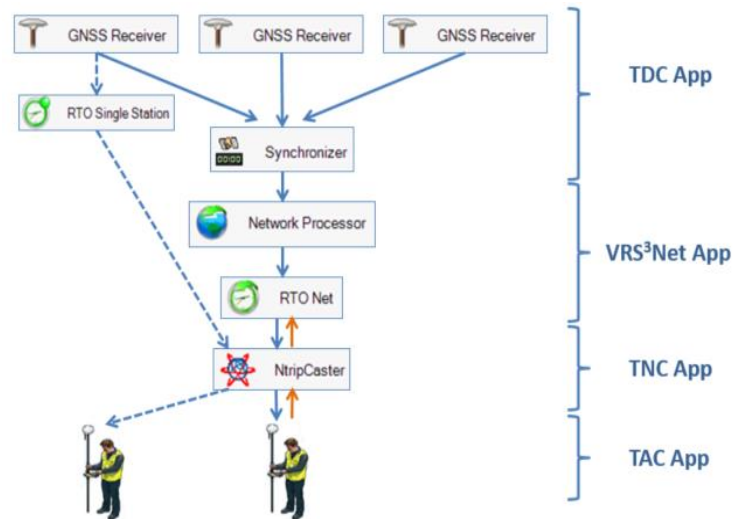
Figure A.1.3: Workflow of the Real-Time services provided by the TPP [10].
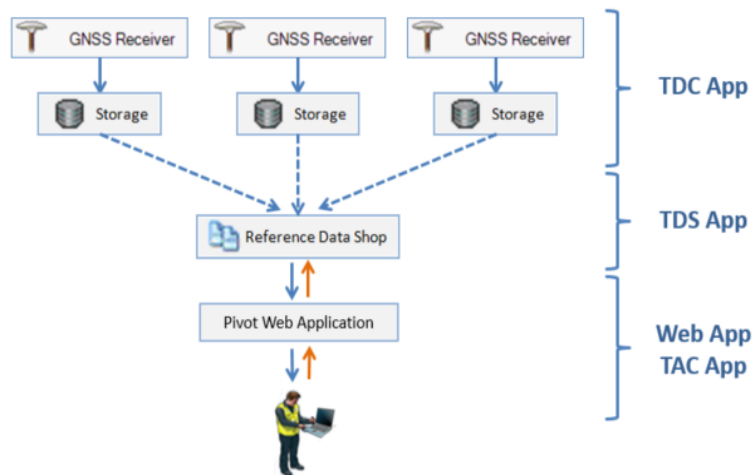
Figure A.1.4: Workflow of the Post-Processing services provided by the TPP [10].

A.1.3. TPP: IM

In this section, the Apps and modules that take care of the IM part of the TPP software package (presented in Table 4.1) are reviewed in more detail.

The TIM-Network Motion engine module

The task of this engine module is continuous analysis of the reference coordinates which allows the system to monitor long term motion and perform counterchecks for errors in these defined coordinates, as well as errors in the definition of antenna heights/types [10][36][38]. This is to keep the accuracy of the network in check.

This engine module determines the position differences (multi-station delta) of the CORS with respect to time [10][36].

In order to do that, this engine module determines the (current) baselines between the CORS' positions and the selected fixed CORS, which in this case is thus the SNPT CORS. These baselines are then compared to the reference baselines that are determined at the start of the processing session using the input reference positions. From this the offsets from their reference positions (ΔN, ΔE, Δh, Δ2D, and Δ3D) in meters, and associated (co)variance matrices, in meters squared, are determined and provided, alongside with continuous information on the (accumulated) time in epochs. An example of the resulting baseline plot is presented in Figure A.1.5.

Note that even though the SING CORS is excluded from the Network Processing, it is included in the IM baseline processing (see Figure A.1.2). There is no specific explanation for this. Besides that, note as well that in this engine module the baselines are radiated out from the selected fixed CORS to the remaining CORS, instead of having baselines between
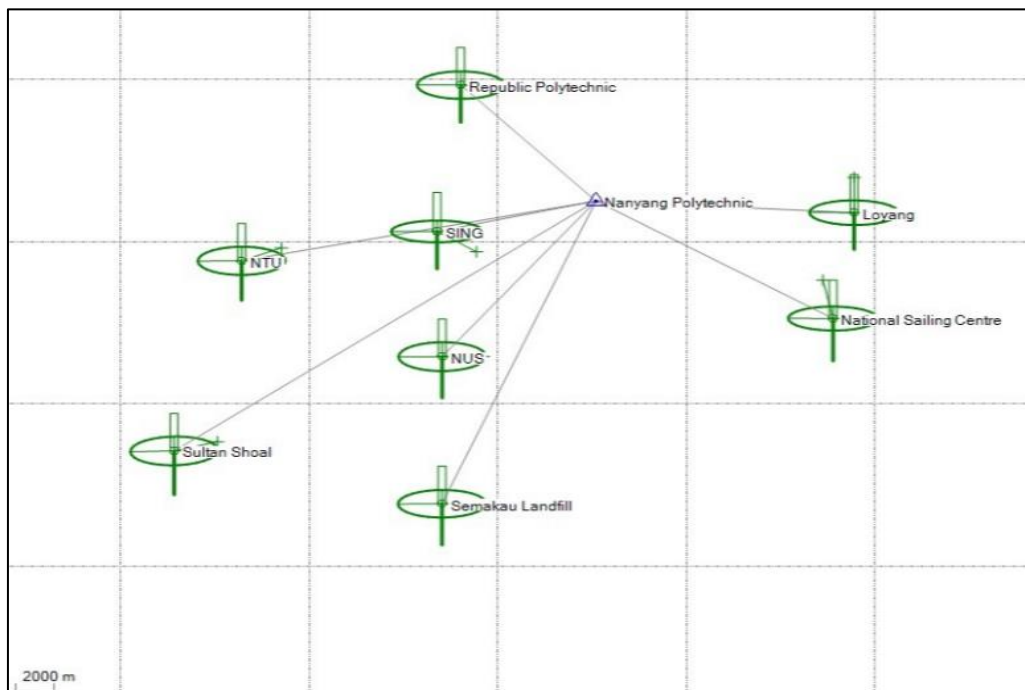
Figure A.1.5: Example of the baseline plot resulting from the Network Motion engine. The Network Motion engine module determines the (current) baselines between the CORS' positions and the selected fixed CORS. For the meaning of the graphical symbols in this visualization see 'The baseline plot graphical symbols explained'. Note that even though the SING CORS is excluded from the Network Processing (see Figure A.1.2), it is included in the IM baseline processing. There seems to be no specific reason for this. Source: screenshot from the TPP.

The baseline plots visualize the displacement of the positioning solutions with respect to the reference positions. The graphical symbols in these baseline plots have the following meaning:

- The blue triangle with the center dot represents the fixed CORS;
- The small circles in the center of the error ellipses (not always clearly visible) represent the reference positions of the CORS;
- The thin line starting from the small circles and ending with a cross, represent the deviations of the measured positions from the input positions, in the horizontal plane;
- The vertical solid lines, pointing up or down from the small circles, represent the measured height displacements;
- The error ellipses and the error height bar represent the 3σ standard deviation in North and East, and height respectively.

Note that these graphical symbols are scale independent and thus do not coincidence with the scale of the plot. this scale is configurable and depends on the smallest and largest values one expects. Using this, one can focus on a specific range of values one wants to observe. Per default the range starts at 0.005 meters and ends 0.3 meters. In case the maximum values for the displacements are exceeded, an arrow shows up at the end of the thin line. One can access the specific values by right-clicking the graphical symbols.

The Integrity Monitor module uses colors to display the status of CORS and baselines (here the 3σ standard deviations of the estimated positioning solutions determine its reliability):

- Green error ellipses, displacement indicators, and circles (station marks), meaning that the estimated positioning solutions (and thus displacements) are within all specified thresholds; the system is healthy.
- Green error ellipses and yellow displacement indicators (position and height) and error height bars, meaning that one or more of the computed displacements is exceeding the warning threshold but not the alert threshold, and the computed 3σ standard deviations are not exceeding the pre-set disarming threshold; the estimated positioning solutions (and thus displacements) are still reliable. In this case the CORS is infected and a warning is triggered (see Figure A.1.6). More on the specific thresholds later in this section, in '*The TIM-Alarm Manager*');

Figure A.1.6: An example figure of a situation where the CORS is infected. Source: screenshot from the TPP.

- Green ellipses and red displacement indicators (position and height) and error height bars, meaning that one or more of the computed displacements is exceeding the alert threshold, but the computed 3σ standard deviations are not exceeding the pre-set disarming threshold; the estimated positioning solutions (and thus displacements) are still reliable. In this case the CORS is unhealthy and an alert is triggered;
- Gray error ellipses, displacement indicators, and circles (station marks), meaning that the computed 3σ standard deviations are exceeding the pre-set disarming threshold, and the determined positioning solutions (and thus displacements) is (or may be) unreliable;
- Red circle (only) if there is no processed data available for that specific CORS.

The specific thresholds (warning, alert, disarming) are presented in Table A.1.1.

all CORS (the individual CORS are not interconnected). This is the case as, as described before, the integrity of the defined coordinates of the remaining CORS is monitored, and the delta's computed, with respect to the fixed CORS, and for that 1 baseline is sufficient. After the Ionosphere-Free combination is applied (to remove the Ionospheric delay by utilizing the availability of dual-frequency signals [23][32]) and the Tropospheric delay scale

factors are modelled/estimated, the determined position solutions and their (3σ) error envelopes typically converge with time.

In a reference network such as the SiReNT infrastructure it takes about 24 hours of processing for the positioning solutions to be reliable; a value within 10 millimeter and 20 millimeter of the true estimated value in the horizontal plane and the vertical plane respectively. The convergence of the (3σ) error envelope usually takes longer however (this cannot be explained for proprietary reasons). In general, the longer the engine module is running, the more reliable the positioning solutions will be. The minimum time-to-detect for this engine module is 3 hours and the IM displacement data is logged every 15 seconds. This engine module is recommended when one is interested in solutions being of high quality (millimeter accuracy) rather than fast [10][36][38]. The resulting scatterplot and charts of this engine module are currently chosen to be visualized as the output of the SiReNT Web App.

The TIM-Rapid Motion engine module

The task of this engine module is to monitor deformations, especially the occasionally rapid movements (2 centimeter/second or more), due to events such as earthquakes or landslides [10][36]. The rapid movements will be detected after every epoch (1 second), where the slow(er) movements will be detected later [10][36][38]. This is related to the fact that these movements, and hence the reaction to it, are slower. Therefore, the minimum time-to-detect for this engine module is: 1 second [38].

Because the rapid movements are detected rapidly, required alerts can be distributed rapidly as well, in case thresholds are exceeded, reducing the reaction time [10][36]. In this engine module, the IM displacement data is logged every 10 seconds. Note that in this engine module the Kalman filter is applied to estimate the position, velocity, and acceleration of the movement.

At the start of a session, this engine module will determine what CORS from this network are made available for processing. Next, the baselines between the known positions of these CORS are established, starting from the fixed reference. An example of the resulting baseline plot is represented in Figure A.1.7. Note that again, even though the SING CORS is excluded from the Network Processing, here it is included in the IM baseline processing (see Figure A.1.2). There is no specific explanation for this. In this engine module redundant baselines are used.

(see Figure A.1.9). During further processing, the (current) positioning solutions for the CORS are determined from the estimated baselines between the CORS. These are compared to their known reference positions, resulting in the offsets (ΔN, ΔE, Δh, Δ2D, and Δ3D) in meters, and associated (co)variance matrices, in meters squared.

Note that different models are used to calculate the (3σ) error envelope during the first hour and after the first hour. The first model is a rather negative model, however the second model does match the observation noise more closely. This causes a discontinuity in the displayed 3σ error values, after one hour. Why and what two models are used could not be shared by Trimble due to confidentiality reasons [46].

This engine module can be applied to networks of all scales. In order to improve the time-to-fix and the positioning solution accuracy, it is suggested to minimize the baseline length.

The TIM-RTK engine module

The task of this engine module is to determine CORS coordinates in real-time, with a measurement accuracy of 2 centimeter (RTK accuracy)[10][36][38]. There are two different modes in which this engine module is operating, the Baseline mode and the VRS mode

[10][36]. The time-to-detect for this engine module is: 1 second [38] and the IM displacement data is logged every 15 seconds [10][36].

When in Baseline mode it starts off in the same way as the Rapid Motion engine module; first the baselines between all the CORS' known positions are established, starting with the most central station (used as fixed reference). During further processing, in real-time, the (current) positioning solutions for the CORS are determined from the estimated baselines between the CORS. An example of the resulting baseline plot is represented in Figure A.1.7. In this engine module, the redundant baselines are used. In case one of the CORS is disabled/unavailable for more than 60 seconds, baselines from and towards it will be displayed as being paused.

When in VRS mode, the CORS positions are determined using the VRS correction data from the reference infrastructure. This method enables the user to determine the CORS' positions, using the provided correction stream.

In both modes the position solutions are compared with their reference positions, resulting in the offsets (ΔN, ΔE, Δh, $\Delta 2D$, and $\Delta 3D$) in meters, and associated (co)variance matrices, in meters squared. Note that even though the SING CORS is excluded from the Network Processing, it is included in the IM processing (see Figure A.1.2). There is no specific explanation for this. This engine module is recommended when a very fast (real-time) reaction time is required and RTK accuracy is sufficient.

Note that in the SiReNT infrastructure the Baseline mode is used, which means that it is only applicable within small or medium size networks (the baselines should not exceed 35 kilometer). The latter is of less concern if the VRS mode is used; can be used anywhere within the bounds of the VRS network (covering the CORS monitored with the RTK engine module).

The Alarm Manager is configured to also trigger alerts in case any CORS is operating with a lost fix (float) [36].
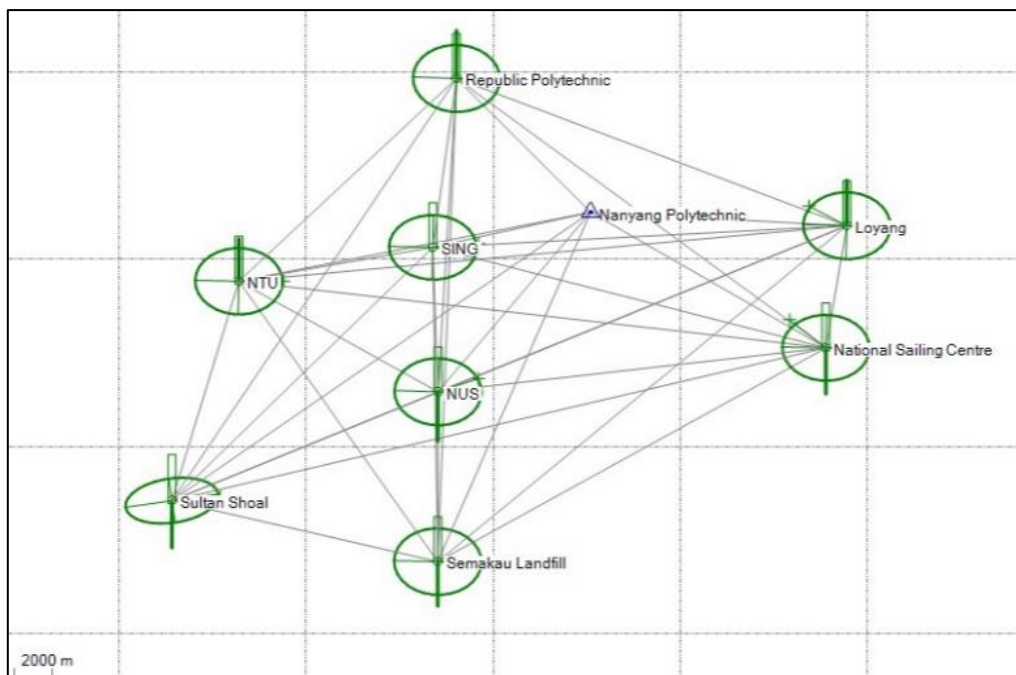
Figure A.1.7: Example of the baseline plot resulting from the other engine modules (the Rapid Motion engine, the RTK engine (Baseline mode) and the Post-Processing engine). For the meaning of the graphical symbols in this visualization see 'The baseline plots explained'. Note that even though the SING CORS is excluded from the Network Processing (see Figure A.1.2), it is included in the IM baseline processing. Source: screenshot from the TPP.

The TIM-Post-Processing engine module

This engine module enables one to perform Static or Kinematic post-positioning, using the stored raw data and rapid or final orbits as input [10][36]. Using these orbits may further improve the geometric modeling and hence the quality of the final result. The aim of this engine module is long-term drift determination and cyclical movement assessment. The time-to-detect for this engine module (after starting the post-processing) is: 15 minutes [38]. At the start of each processing session, the raw data is used to establish the baselines between all the CORS' known positions, with respect to the selected fixed station(s) in order to be used as reference coordinates [36]. Then, during these processing sessions, the position solutions of the CORS are determined (from the observations for all baselines) and compared to these reference coordinates. An example of the resulting baseline plot is represented in Figure A.1.7. In this engine module, the redundant baselines are used as well. When the static mode is used, this results in one stored position solution per baseline, however when the kinematic processing mode is used, this results in a stored position solution per baseline per epoch (hence several per session). When the latter is used there is an internally set limit to the number of CORS and the session duration as this process is very memory-consuming and results in a high number of results.

For each position solution the baseline components (dx, dy, dz), the offsets from their known positions (ΔN, ΔE, Δh, Δ2D, and Δ3D) in meters, and associated (co)variance matrices, in meters squared, are determined.

The processing is done with a session duration of one day (and a session delay of one hour) resulting in position solutions with accuracies of up to 1 millimeter (the most accurate engine module) [10][36][38]. This duration length is dependent on the baseline length(s). This engine module is therefore preferred in case positioning solution accuracy is much more important than the reaction time.

In addition to what is previously described, the Alarm Manager can be also configured to trigger notification (warning or alert) messages in case there are problems with any baseline in terms of lost fixed solutions [36].

The TIM-Integrity Monitor module

This is where the baselines and resulting positioning solutions from all the engine modules are received and the network adjustment and displacements are computed [10][36]. This module serves several purposes, such as position adjustment and update over time, as well as position and correction information output in the form of NMEA (National Marine Electronics Association) strings, data visualization, and alarm generation. Status messages regarding the latter, are currently displayed on the SiReNT Web App and distributed via emails and text messages.

By using the network adjustment functionality (least-squares adjustment) blunders and large (systematic) errors can be detected and the applied corrections applied can be minimized. In this adjustment at least one of the stations is required to be fixed (constrained), in order to provide reliable solutions. Then, while keeping one or more CORS fixed, adjustment of the remaining unfixed CORS can be performed, with respect to the fixed CORS.

By using the position update functionality, the positions can then be updated and improved according to the position solution offsets resulting from the network adjustments, after these are ensured to be correct. This can be done by using the last adjustment results or by using results over a certain interval. As described before, updating the positions resets and restarts

the engine modules.

The resulting information is stored as well as presented through the SiReNT Web App and reports, including charts and visualized in 2D maps and scatterplots [10][36].

As one can imagine the stored data will start piling up. Therefore, the TPP contains built-in procedures that reduce the database contents. This is done through averaging values over a certain time interval and by daily deletion of data older than a certain threshold. Therefore the historical data is limited accessible and thus not as detailed as it is at the moment it gets stored.

This module also contains some extra capabilities, such as axis rotation and velocity calculation. The axis rotation functionality could be used in specific cases where displacements of interest are not exactly coinciding with the direction of the Northing and Easting. In that case, the monitoring directions can be rotated per CORS individually, such that alarms are only triggered due to displacements exactly matching the direction of interest. The velocity calculation functionality is used to compute and visualize velocities using the observed position solutions.

The TIM-Alarm Manager module

This is an essential part of the TPP and the central point where all the notification (warning or alert) messages, and other messages in case the problem is solved, from the Integrity Monitor and other modules are received [10][36]. This includes multiple alarm conditions: such as for example lost connections, voltage exceeding threshold, no data from instrument etcetera. The Alarm Manager will combine and process these, and take (re)action and notify the appropriate user(s), according to what is configured. When it comes to the IM of the CORS' stability, there are three modes/levels that can be configured; the warning mode, the alert mode and the disarming (of the system) mode. A warning or alert will be triggered in case one more or more of the computed displacements is/are exceeding the warning or alert thresholds, respectively, without causing the computed 3σ standard deviations to exceed the disarming threshold. In that case the estimated positioning solutions (and thus displacements) are still said to be reliable.

Next to these two alarm levels there is thus a third option however, the disarming mode. Disarming the system takes place when the 3σ standard deviations exceed the pre-set disarming thresholds and the reliability of the result is too weak. In this case the observations should be seen as outliers and therefore will be filtered out, and besides this it does not result in any (re)action (the raw data is already corrected, or removed, and corrections generated, by the *TDC App* and the *VRS³Net App*), other than pushing out the mentioned notifications (warnings or alerts).

The default thresholds are visualized in Table A.1.1 (note that these are only applicable to the IM displacement data). These thresholds are

Table A.1.1: The default thresholds (TPP).

Warning Limit (Threshold Values)	
Northing:	0.050 meters
Easting:	0.050 meters
Height:	0.100 meters
2D:	0.070 meters
3D:	0.130 meters
Alert Limit (Threshold Values)	
Northing:	0.070 meters
Easting:	0.070 meters
Height:	0.150 meters
2D:	0.100 meters
3D:	0.180 meters
Disarm Limit (Threshold Value)	
3σ Northing:	0.050 meters
3σ Easting:	0.050 meters
3σ Height:	0.100 meters
3σ 2D:	0.070 meters
3σ 3D:	0.130 meters

the result of testing performed by Trimble under ideal circumstances, therefore they are not necessarily perfectly applicable to each and every CORS worldwide. One can configure and adapt the threshold values as per requirement. Note however that in SiReNT, the Alarm Manager currently is not in use for the described purpose.

Note that all engine modules in use are monitored independently. That means that when the IM displacements (or the related 3σ standard deviations) observed by a specific engine module are exceeding thresholds, this only will affect this particular engine module and not the others.

The TRI-Rover Integrity module

This App thus analyses the performance of Rovers within the bounds of the GNSS reference network infrastructure while they take into account the incoming correction data [10][36]. The quality of this correction information can be measured based on the initialization (time-to-fix) and the quality of the positioning solutions. From the latter statistics such as the average offset, the standard deviation, and the RMS, as well as graphs can be determined.

In order to determine the Rover integrity, one of the CORS can be used to simulate a Rover in the field, however this CORS should then be omitted from the CORS that are used by the Network Processor supplying the correction, unless it can perform both functions, independently and simultaneously.

The measured performances represent a measure of the performance that should be observed by the field users.

Appendix 2: *Example IM report*

Integrity Monitor Module

Company:	Singapore Land Authority
Operator:	N/A (scheduled report)
Address:	55 Newton Road #12-01
	Revenue House
	Singapore 307987
Creation Date:	9/1/2016 1:20:18 AM
Time System:	GPS time
Report Interval:	
Start Time:	8/29/2016 1:20:01 AM
End Time:	9/1/2016 1:20:01 AM
Duration:	3 Day(s), 0 Hour(s)

Configuration:

Name: IMNME_SNPT System: ITRF2005

Fixed Stations:

Station Name: Nanyang Polytechnic

    Station Code: SNPT

    Station ID: 10

    Reference Position X [m]: -1526243.0178

    Reference Position Y [m]: 6191002.6859

    Reference Position Z [m]: 152481.7527

    Reference Time: 9/13/2014 12:00:00 AM Tectonic plate: Eurasia

Monitored Stations:

Station Name: Loyang

    Station Code: SLYG

    Station ID: 9

    Reference Position X [m]: -1539524.1351

    Reference Position Y [m]: 6187726.7315

    Reference Position Z [m]: 151763.9247

    Reference Time: 9/13/2014 12:00:00 AM

    Tectonic plate: Eurasia

Station Name: NUS

    Station Code: SNUS

    Station ID: 14

    Reference Position X [m]: -1518382.6374

    Reference Position Y [m]: 6193173.4590

    Reference Position Z [m]: 142897.2098

    Reference Time: 9/13/2014 12:00:00 AM

    Tectonic plate: Eurasia

Station Name: NTU

    Station Code: SNYU

    Station ID: 11

    Reference Position X [m]: -1508025.2271

Reference Position Y [m]: 6195576.9694

Reference Position Z [m]: 148798.2633

Reference Time: 9/13/2014 12:00:00 AM

Tectonic plate: Eurasia

Station Name: Republic Polytechnic

Station Code: SRPT

Station ID: 12

Reference Position X [m]: -1519248.9586

Reference Position Y [m]: 6192545.5585

Reference Position Z [m]: 159624.0741

Reference Time: 9/13/2014 12:00:00 AM

Tectonic plate: Eurasia

Station Name: Semakau Landfill

Station Code: SSMK

Station ID: 6

Reference Position X [m]: -1518410.7300

Reference Position Y [m]: 6193331.3460

Reference Position Z [m]: 133831.3450

Reference Time: 3/19/2010 12:00:00 AM

Tectonic plate: Eurasia

Station Name: Sultan Shoal

Station Code: SSTS

Station ID: 13

Reference Position X [m]: -1504599.6287

Reference Position Y [m]: 6196617.2513

Reference Position Z [m]: 137086.2700

Reference Time: 9/13/2014 12:00:00 AM

Tectonic plate: Eurasia

Statistical Point Overview:

Minima Values of Monitored Points:

Point Name	Northing [m]	Easting [m]	Height [m]	2D [m]	3D [m]
Loyang	-0.1535	-0.5981	-0.6900	0.0004	0.0055
NUS	-0.0639	-0.3937	-0.4956	0.0001	0.0024
NTU	-0.0488	-0.3977	-0.4798	0.0000	0.0010
Republic Polytechnic	-0.0478	-0.4070	-0.4675	0.0002	0.0036
Semakau Landfill	-0.0492	-0.3982	-0.4825	0.0000	0.0043
Sultan Shoal	-0.1187	-0.4187	-0.4818	0.0001	0.0054

Maxima Values of Monitored Points:

Point Name	Northing [m]	Easting [m]	Height [m]	2D [m]	3D [m]
Loyang	0.0888	0.1240	0.1053	0.6158	0.9245
NUS	0.0804	0.2596	0.0749	0.3956	0.6341
NTU	0.0822	0.1263	0.0889	0.3994	0.6243
Republic Polytechnic	0.0824	0.1159	0.1023	0.4085	0.6208
Semakau Landfill	0.1030	0.6971	0.1509	0.7047	0.7207
Sultan Shoal	0.1491	0.9032	0.5706	0.9064	1.0149

Station Name: Republic Polytechnic
Displacement for component Northing:
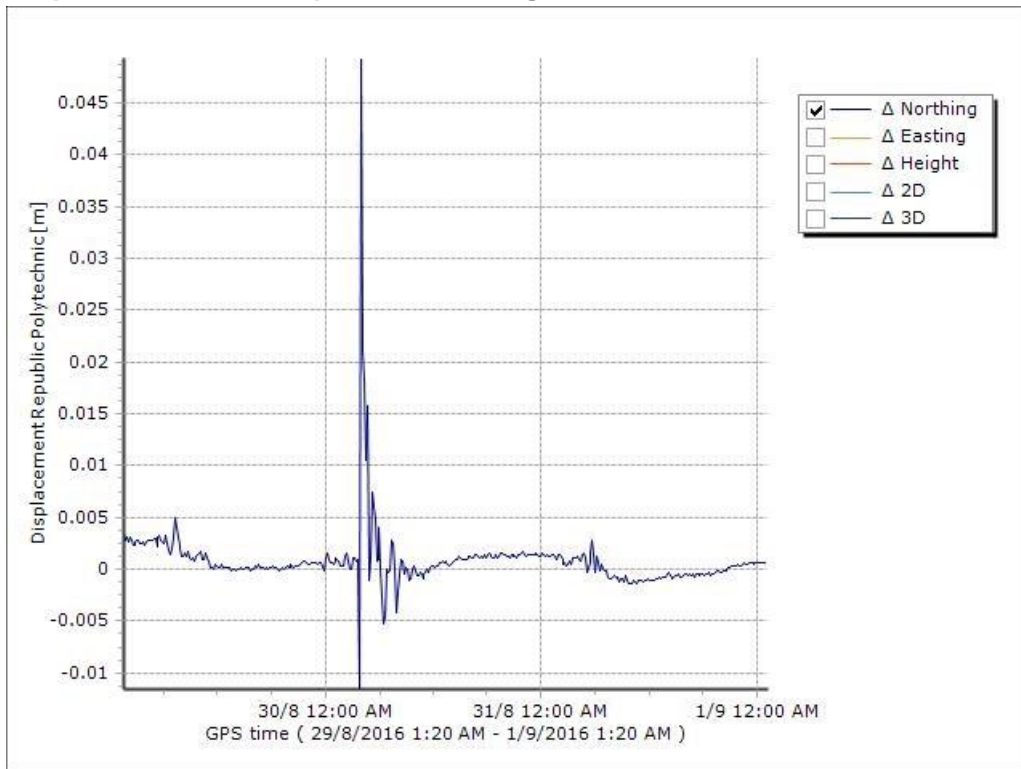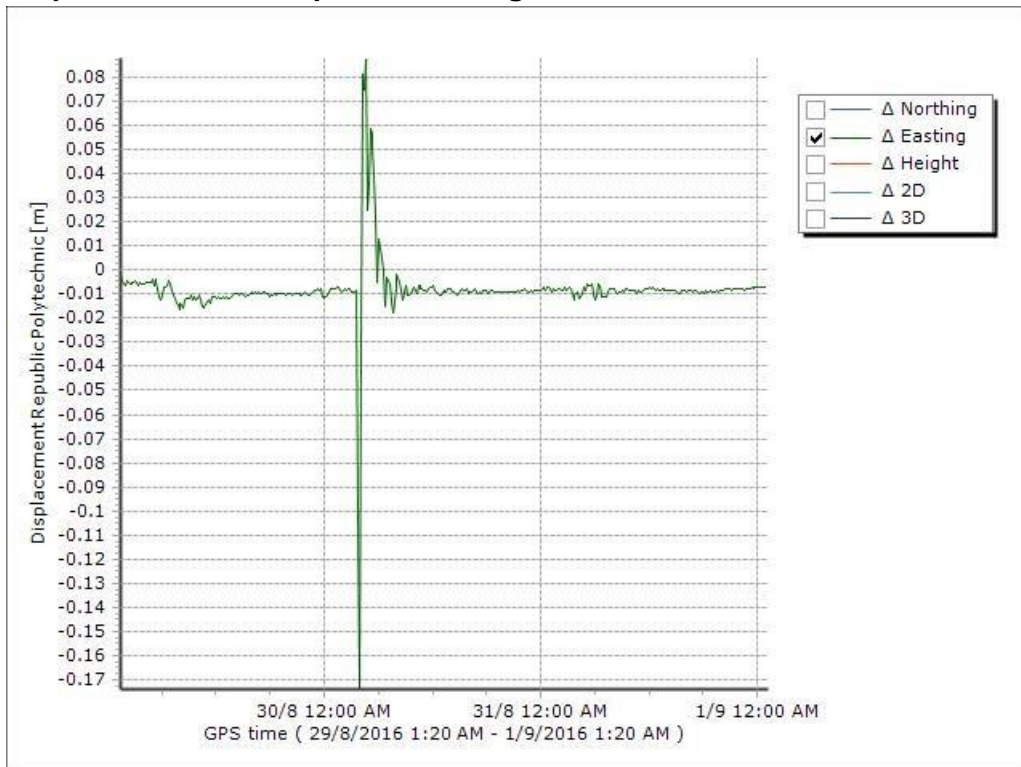
Displacement for component Easting:

Displacement for component Height:
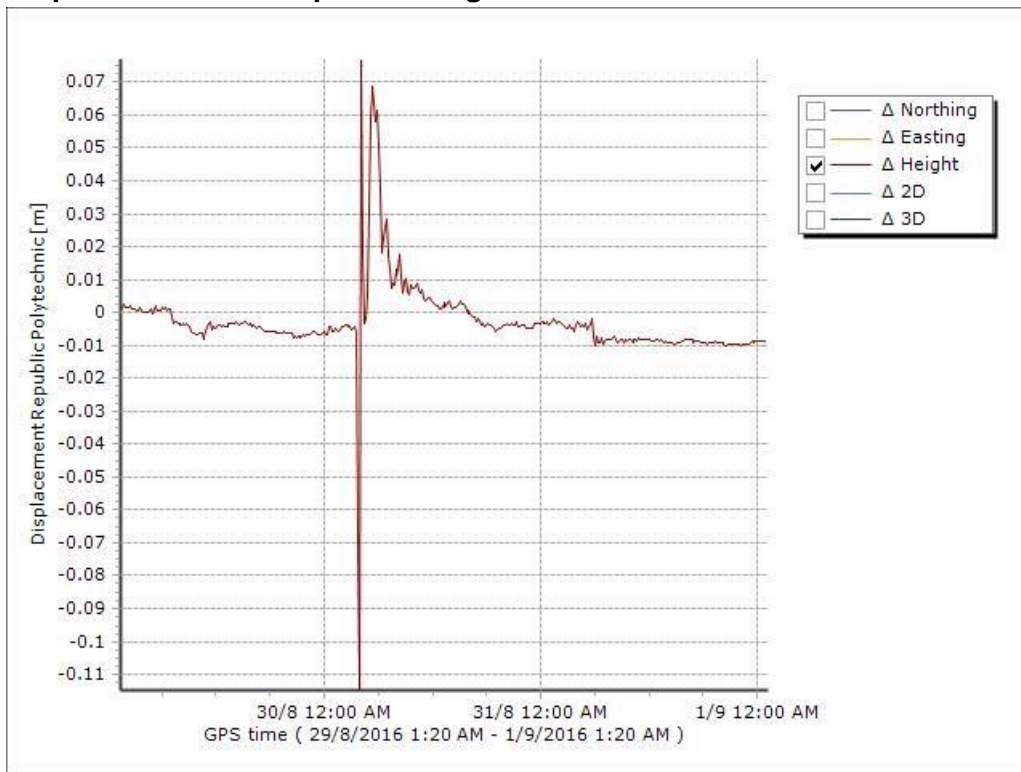
Displacement for component 2D:
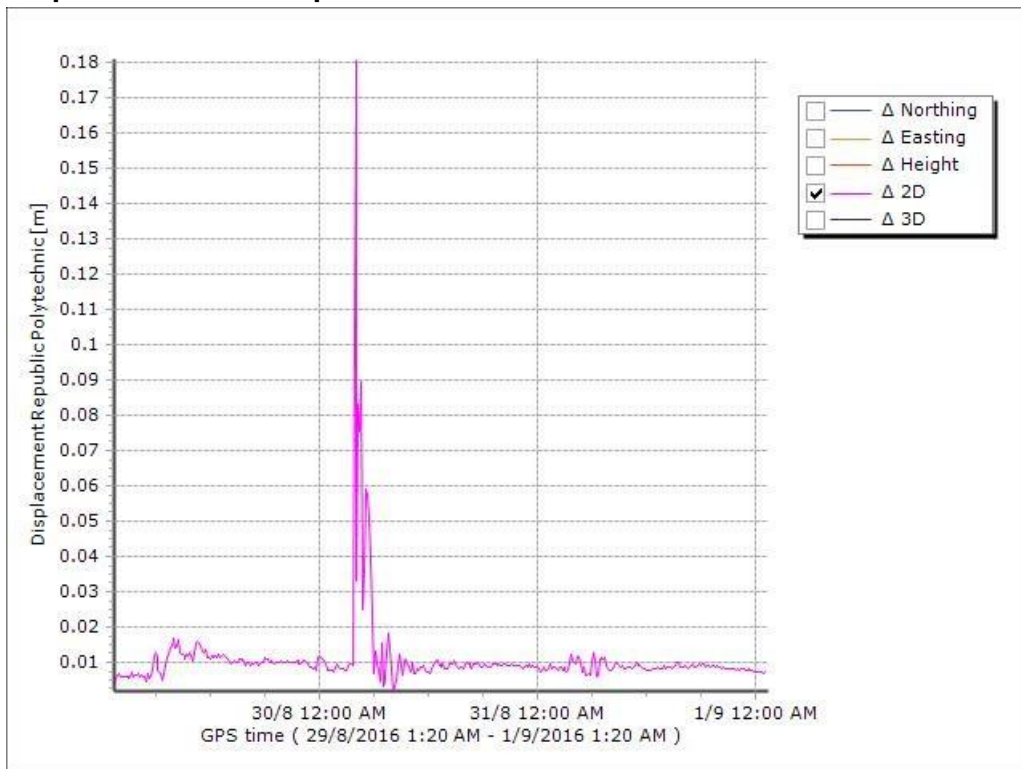
Displacement for component 3D:
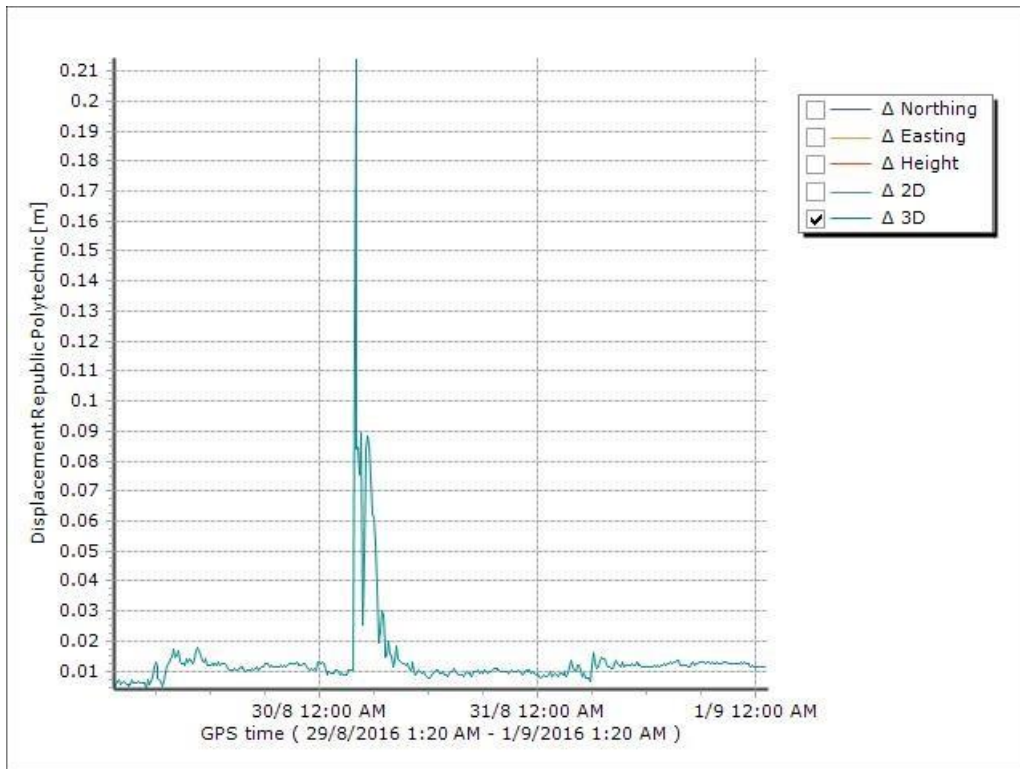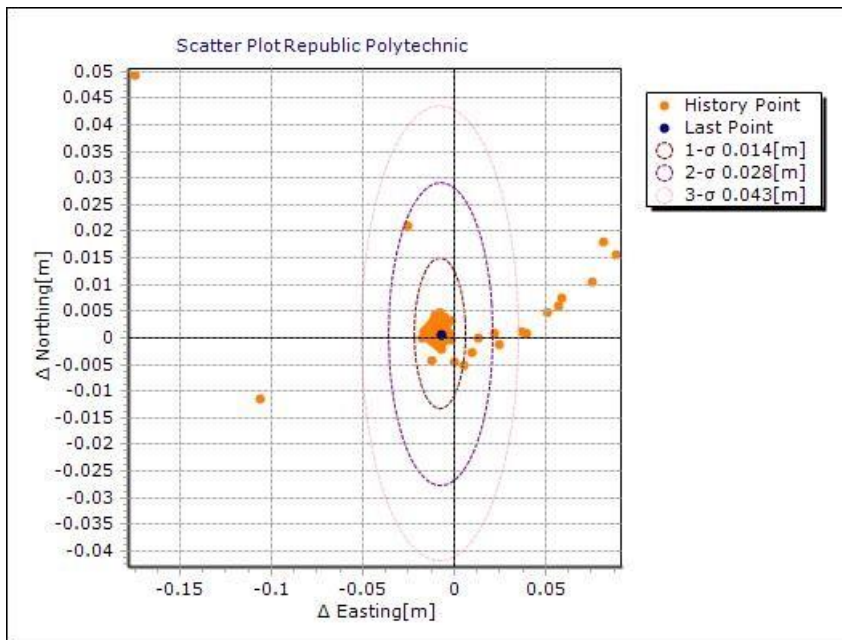
Scatterplot:

Station Name: Sultan Shoal

Displacement for component Northing:
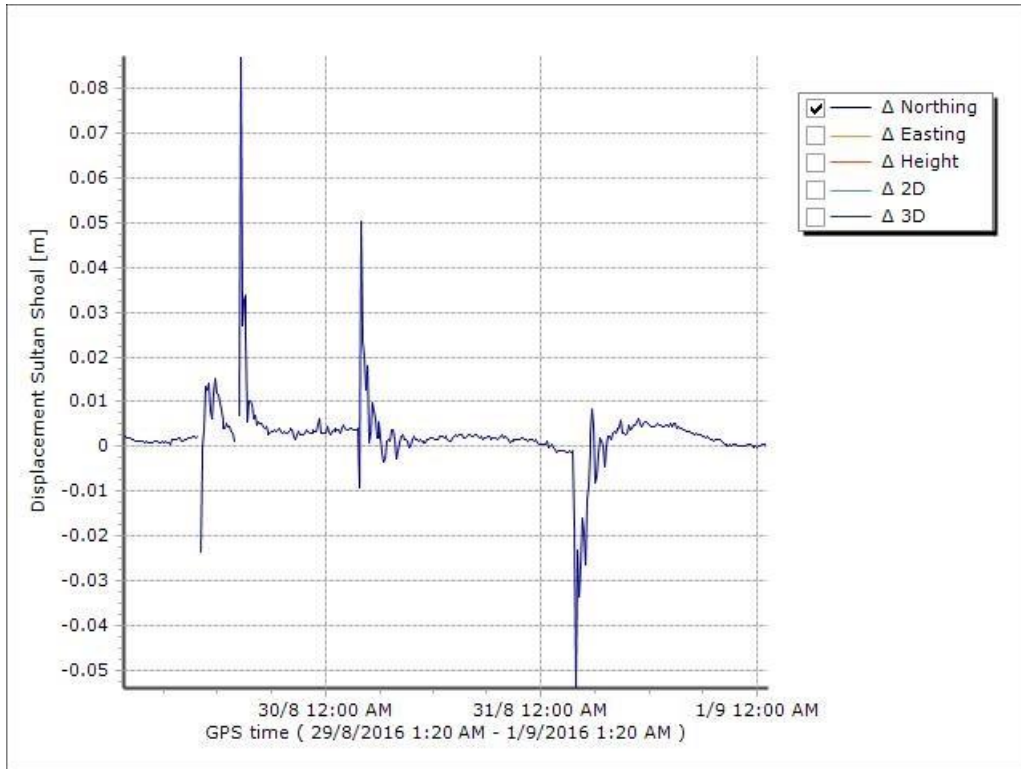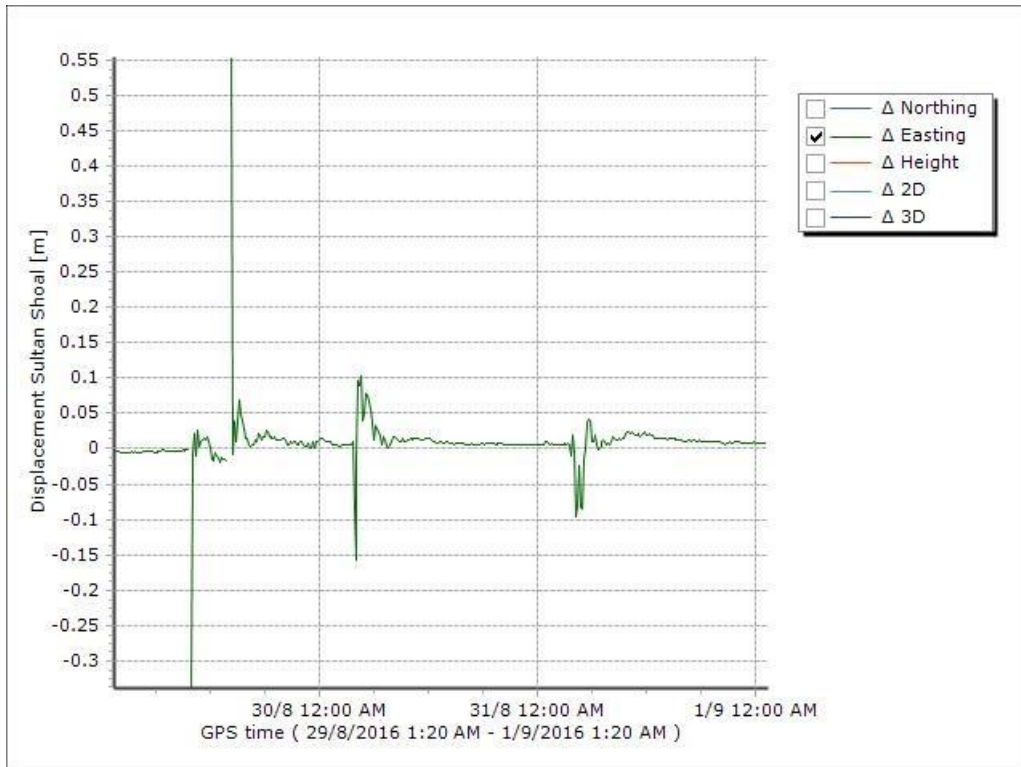
Displacement for component Easting:

Displacement for component Height:
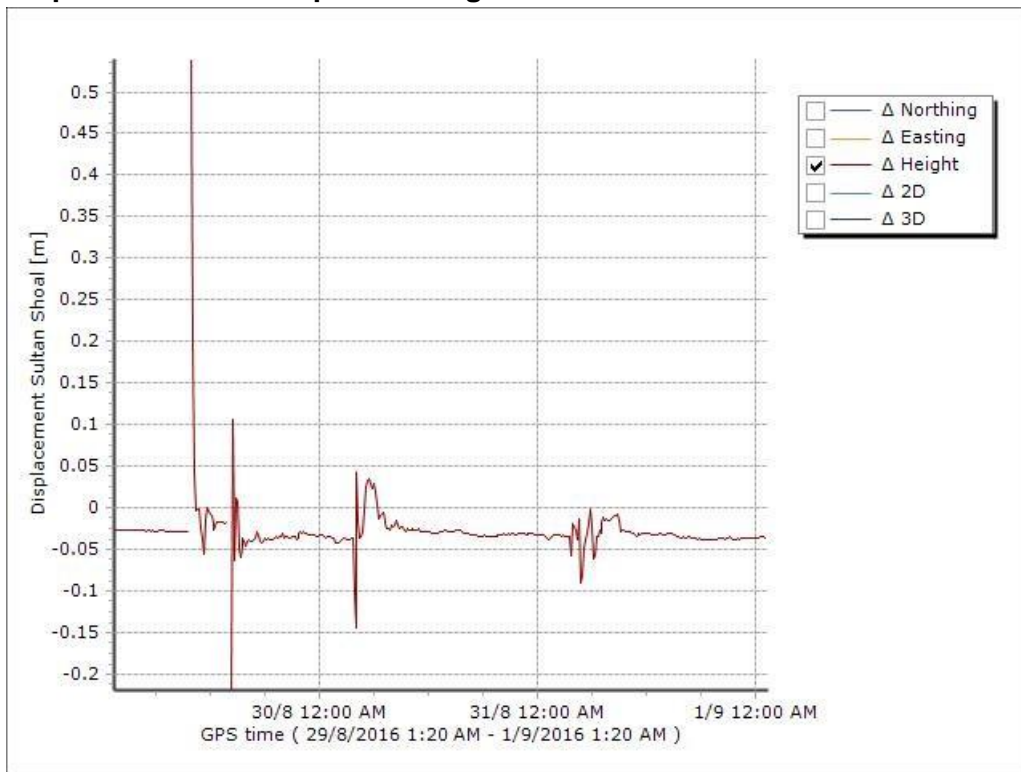
Displacement for component 2D:
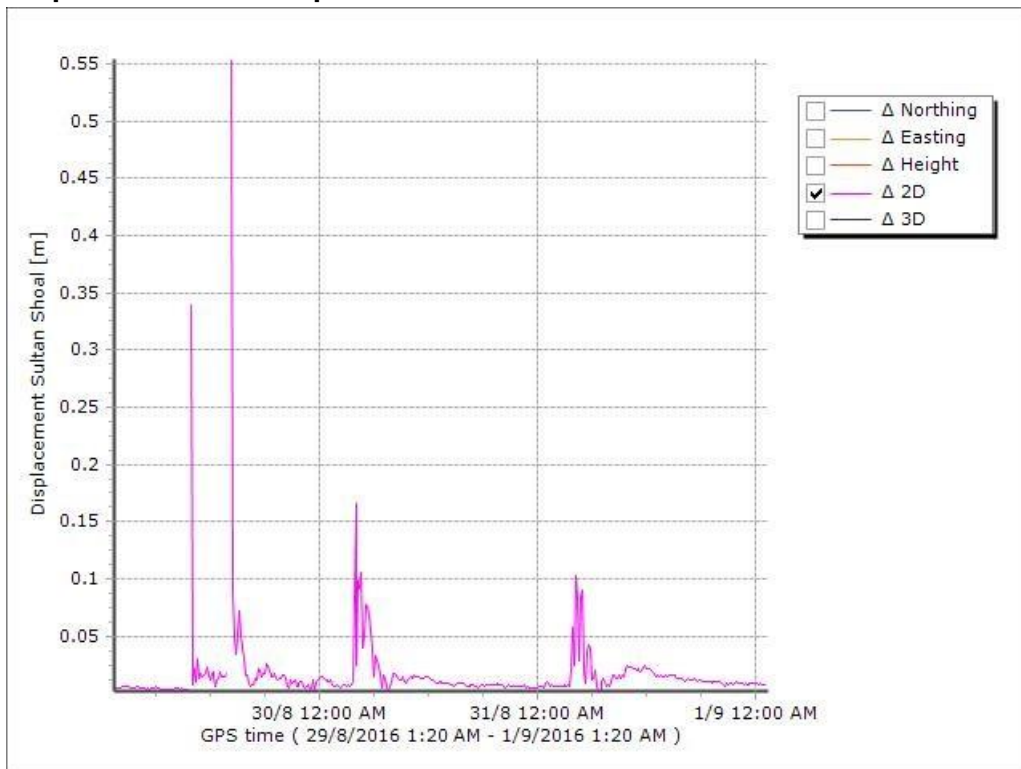
Displacement for component 3D:
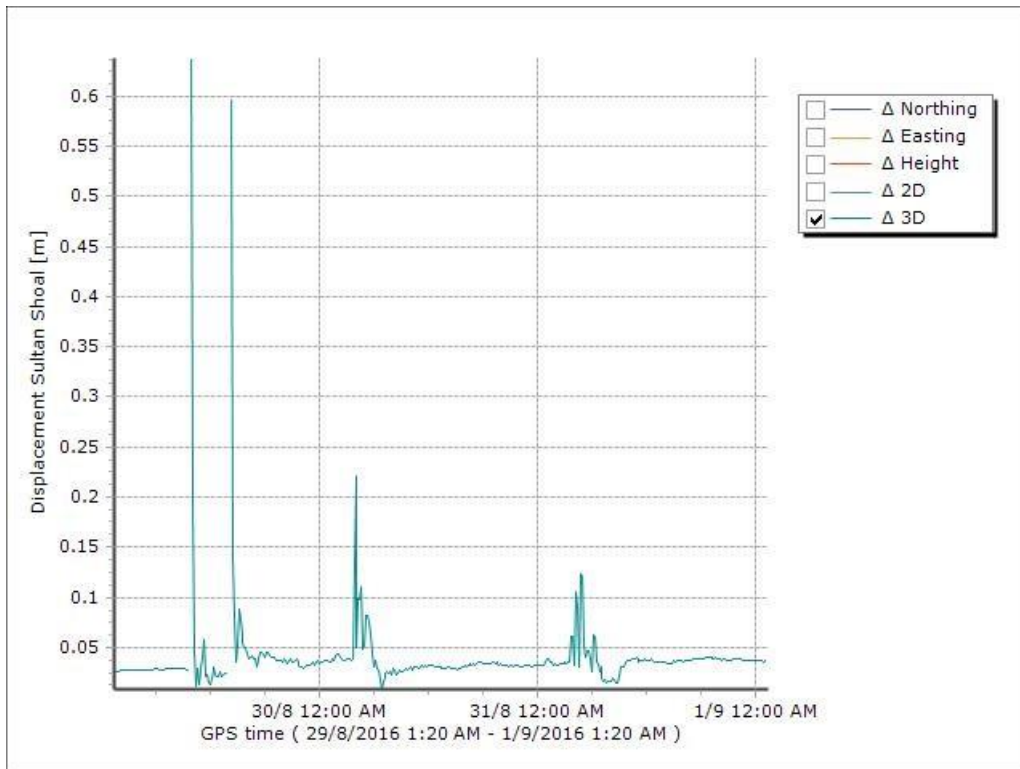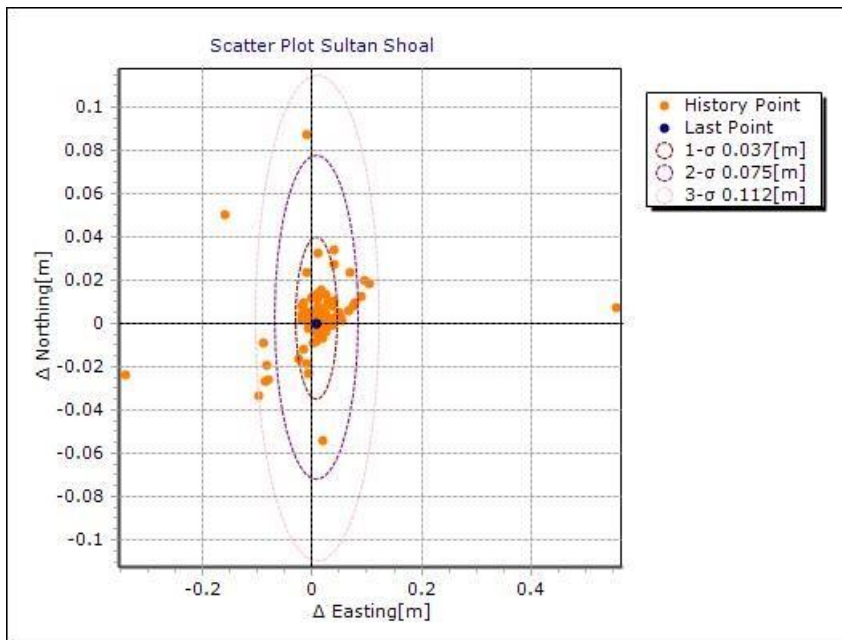
Scatterplot:

Station Name: Loyang

Displacement for component Northing:
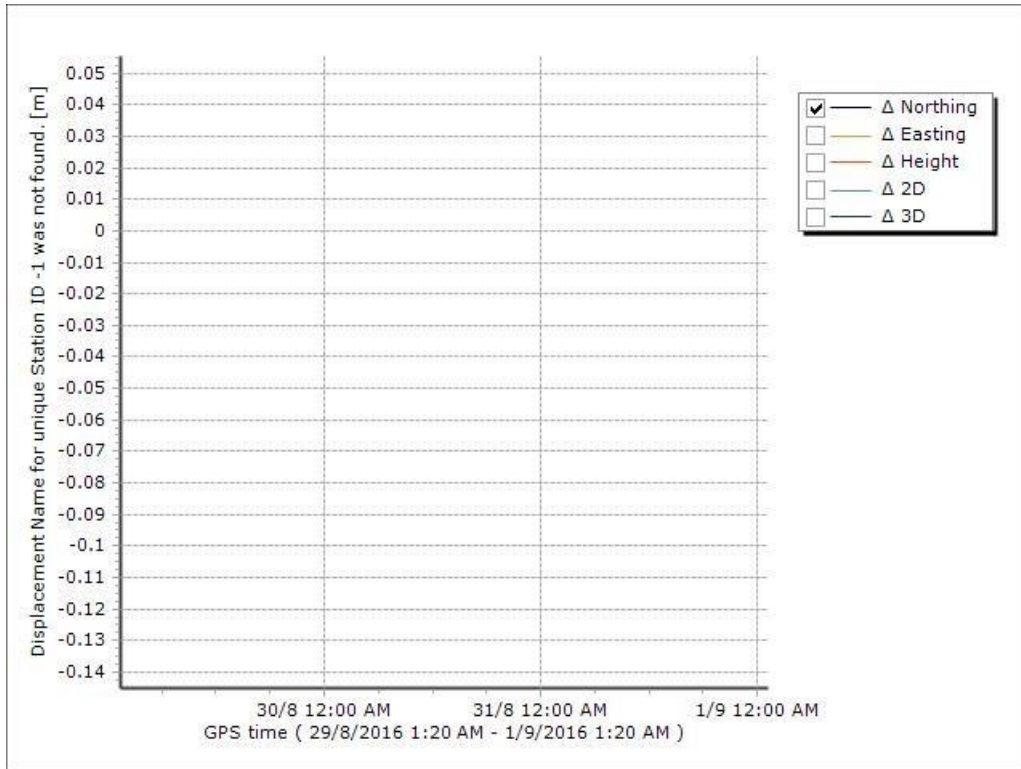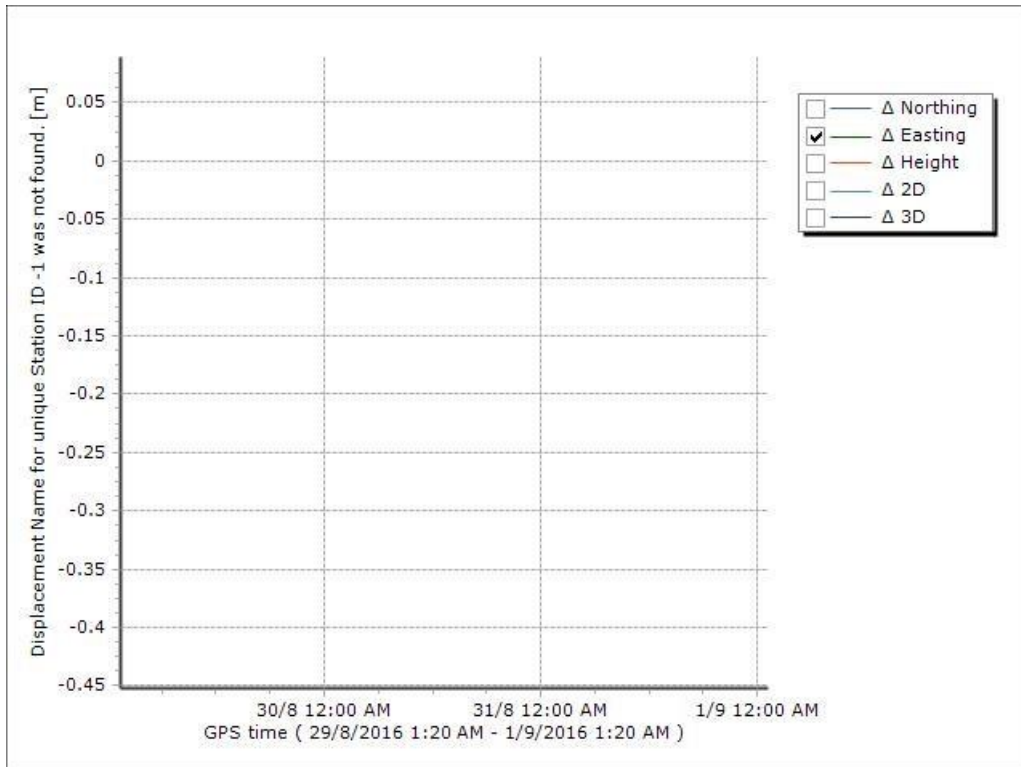
Displacement for component Easting:

Displacement for component Height:
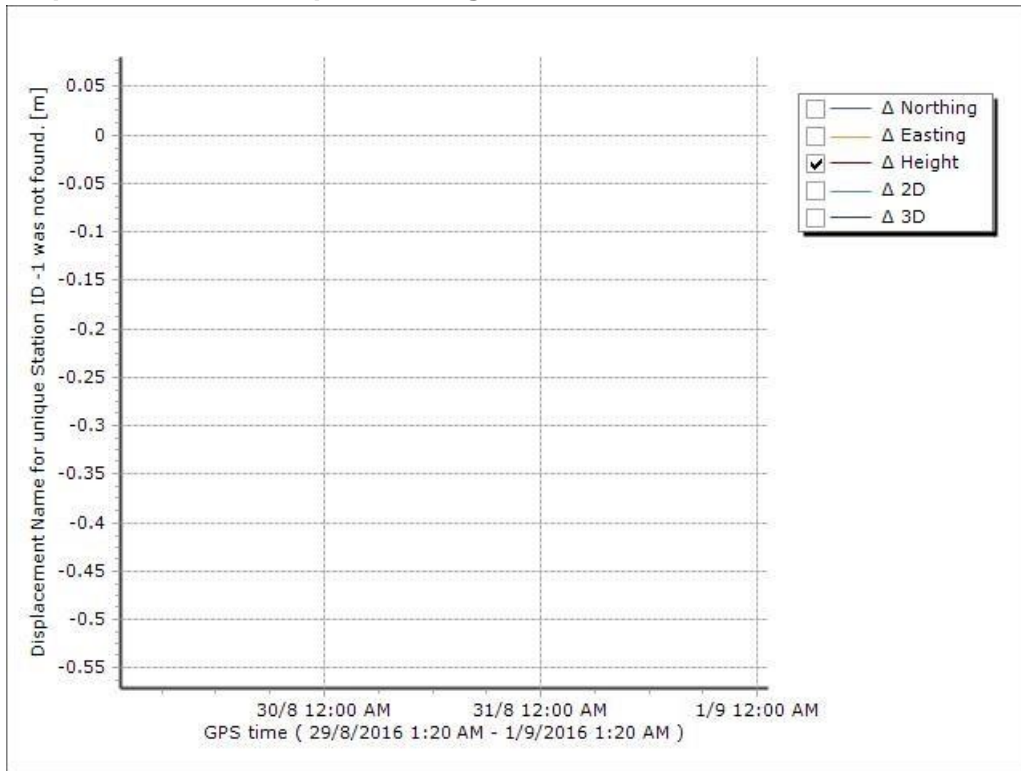
Displacement for component 2D:
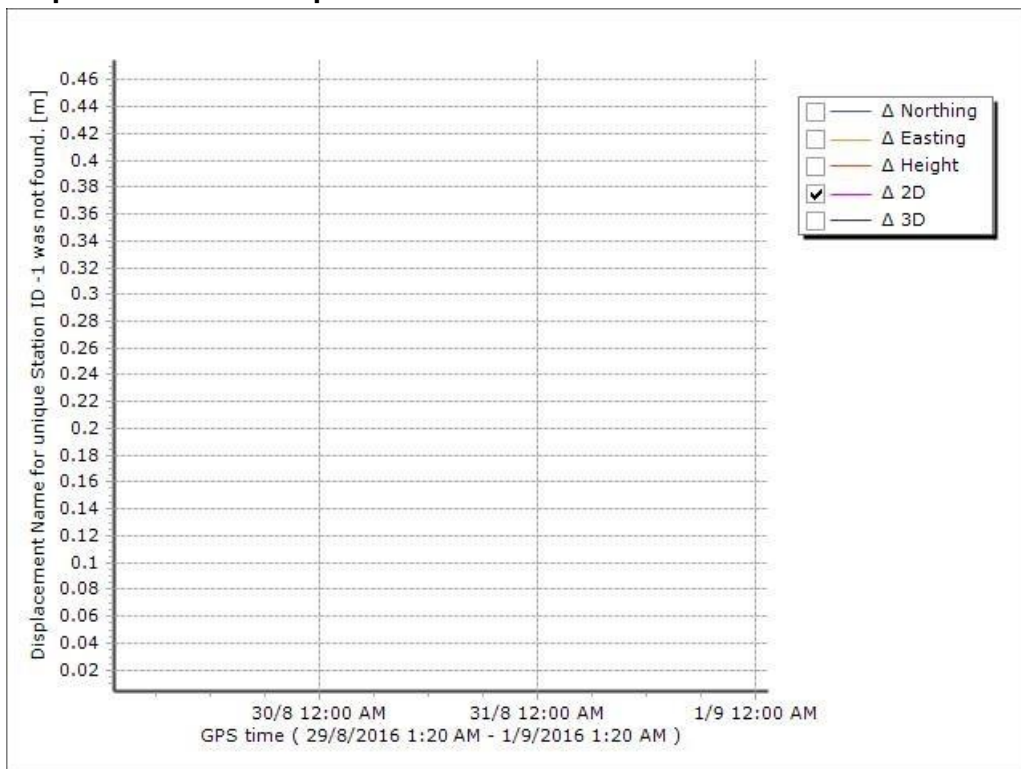
Displacement for component 3D:
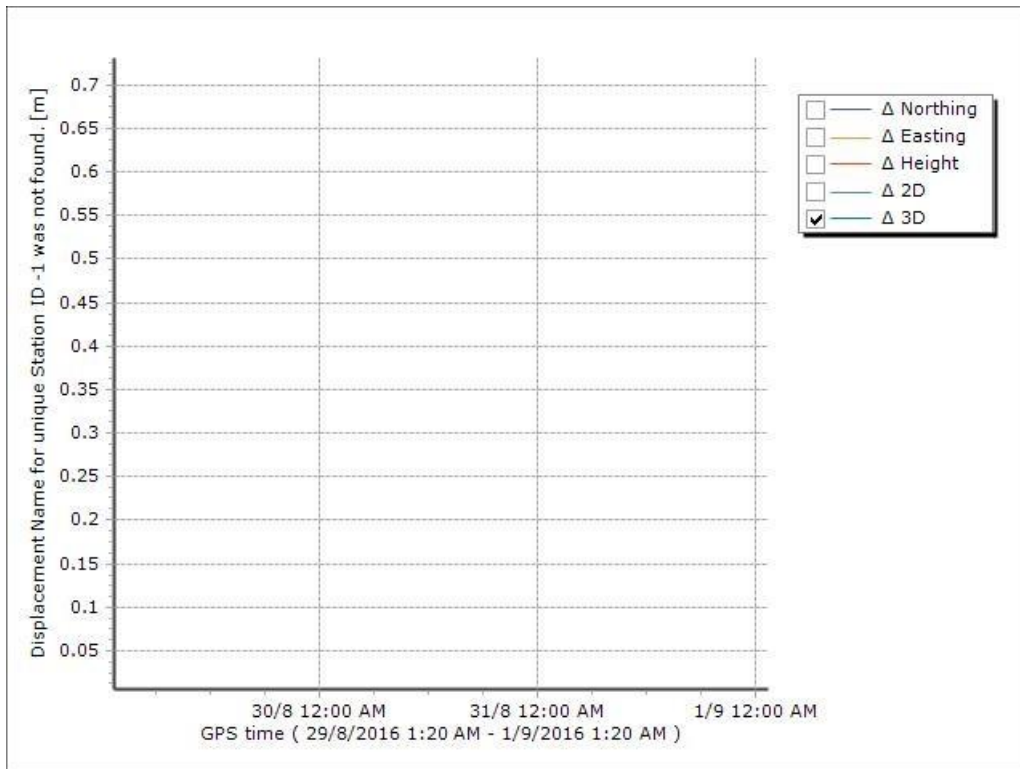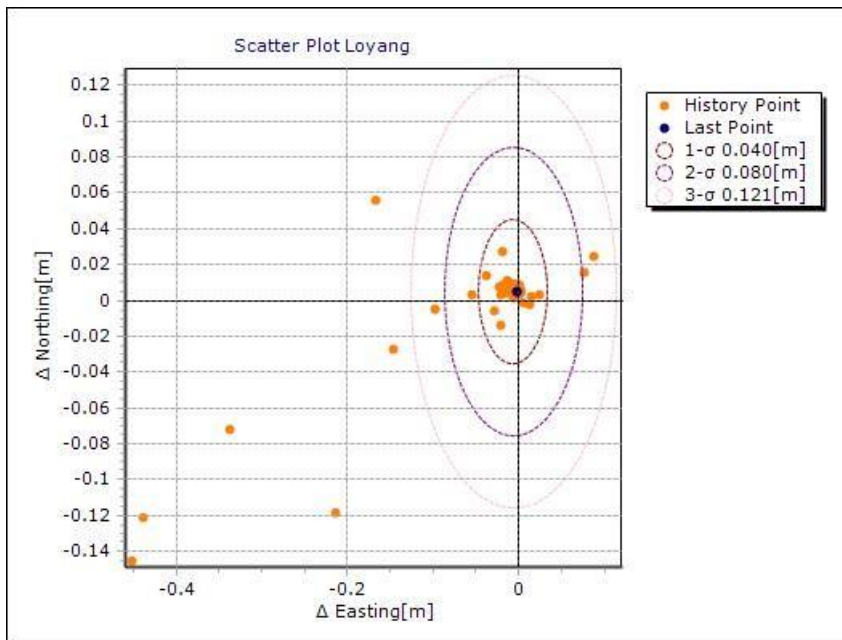
Scatterplot:

Station Name: NTU

Displacement for component Northing:
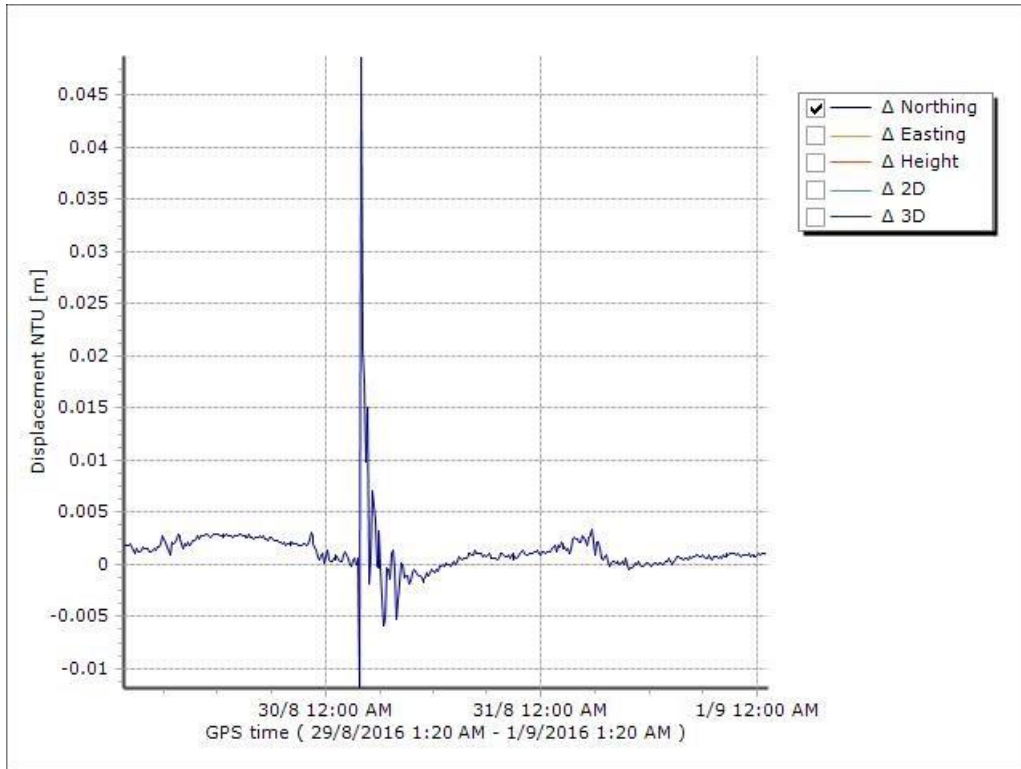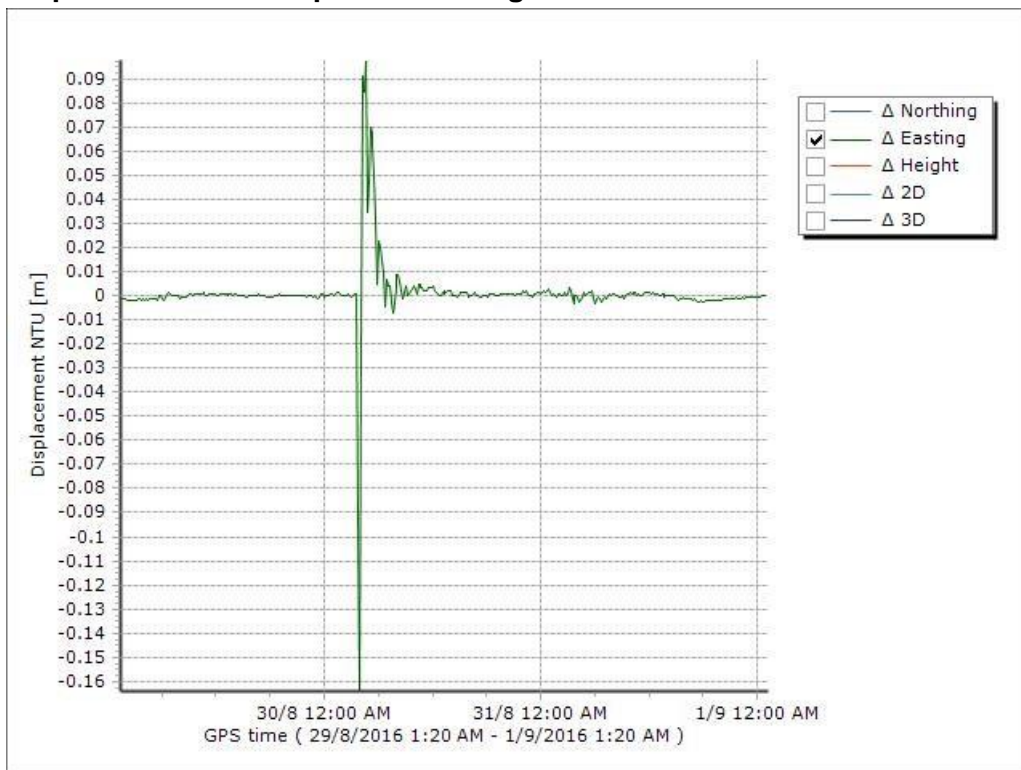
Displacement for component Easting:

Displacement for component Height:
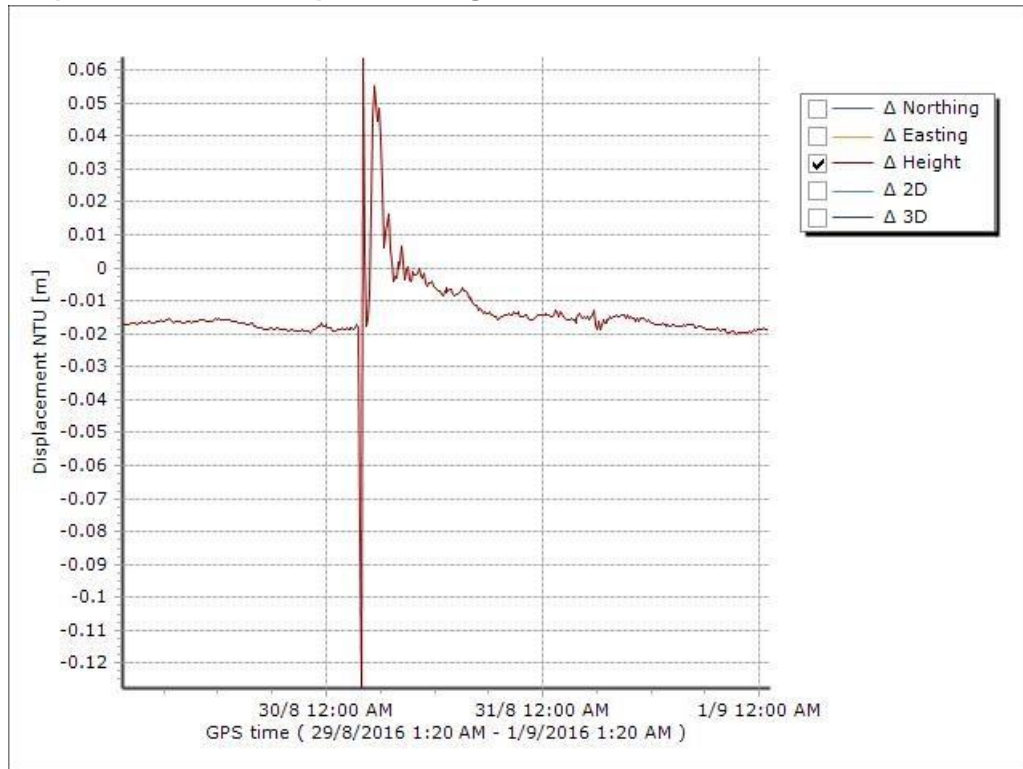
Displacement for component 2D:
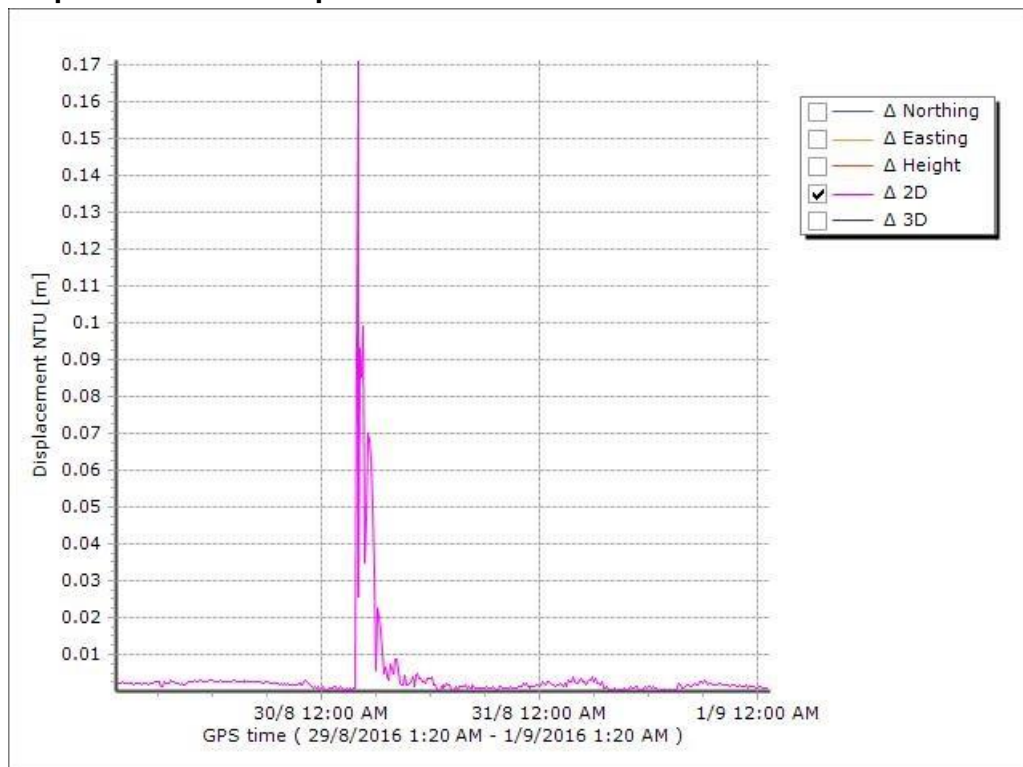
Displacement for component 3D:
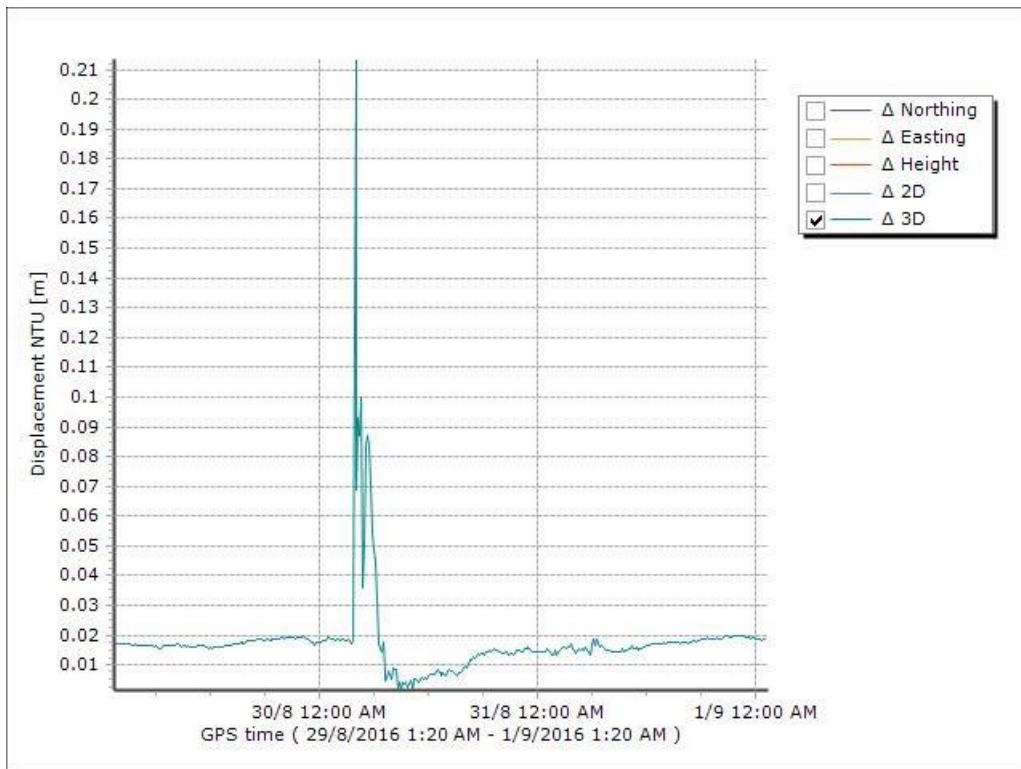
Scatterplot:
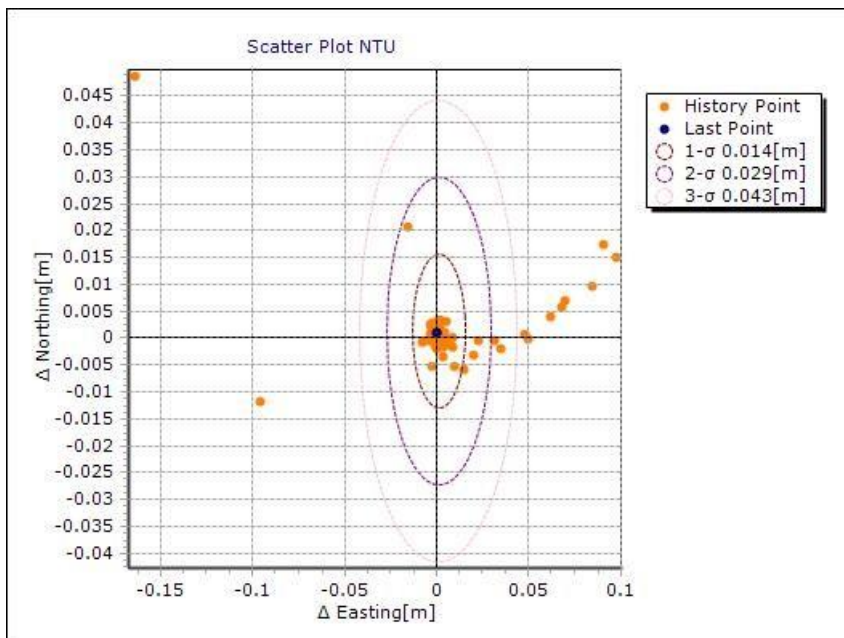
Appendix 3: *Proof that usually if the 2D or 3D result is exceeding a threshold, then so would at least one of the horizontal or vertical components.*

When the 3 sigma values of the observations do not exceed the specific disarming thresholds, the warnings and alarms will not be disarmed. In that case, if the maximum allowed displacements for all components are observed simultaneously it results in the following 2D/3D displacements. This is determined using both the warning and the alarm threshold values respectively:

- When using the Warning thresholds
$2D\ displ. = \sqrt{dn^2 + de^2} = \sqrt{0.05^2 + 0.05^2} = 0.0707\ m.$ *(2D Warning threshold = 0.070 m.)*
and
$3D\ displ. = \sqrt{dn^2 + de^2 + dh^2} = \sqrt{0.05^2 + 0.05^2 + 0.100^2} = 0.1225\ m.$
(3D Warning threshold = 0.130 m.)

- When using the Alarm thresholds
$2D\ displ. = \sqrt{dn^2 + de^2} = \sqrt{0.07^2 + 0.07^2} = 0.099\ m.$ *(**2D Alarm threshold** $= \mathbf{0.100\ m.}$)*
and
$3D\ displ. = \sqrt{dn^2 + de^2 + dh^2} = \sqrt{0.07^2 + 0.07^2 + 0.150^2} = 0.1797\ m.$
(3D Alarm threshold = 0.180 m.)

While most resulting displacements are (just) within the specific 2D/3D disarm thresholds that have been set, the resulting 2D displacement value is already exceeding the 2D warning threshold.
Hence, it turns out that while the warnings and alarms are not disarmed, the two horizontal components cannot have the maximum allowed displacement simultaneously without triggering a warning first (the 2D warning threshold might be too constraining).

Besides that, when thus the warnings and alarms are not disarmed, and the observed displacements for one component are near zero, for example 0.005 m., the second component is allowed to be:

$Maximum\ allowed\ displ. = \sqrt{Warning\ threshold_{2D}^2 - d_1^2} = \sqrt{0.07^2 - 0.005^2} = 0.0698\ m.$
and
$Maximum\ allowed\ displ. = \sqrt{Alarm\ threshold_{2D}^2 - d_1^2} = \sqrt{0.100^2 - 0.005^2} = 0.0999\ m.$

while not triggering a 2D warning or alarm, respectively.

In case of the 3D displacement, when the observed displacements for two of the components are near zero, again for example 0.005 m., the third component is allowed to be:

$Maximum\ allowed\ displ. = \sqrt{Warning\ threshold_{3D}^2 - d_1^2 - d_2^2}$

$$= \sqrt{0.130^2 - 0.005^2 - 0.005^2}$$

$$= 0.1298\ m.$$

and

$$Maximum\ allowed\ displ. = \sqrt{Alarm\ threshold_{3D}^2 - d_1^2 - d_2^2}$$

$$= \sqrt{0.180^2 - 0.005^2 - 0.005^2}$$
$$= 0.1799\ m.$$

while not triggering a 3D warning or alarm, respectively.

From this it can be concluded that displacement magnitudes like these, for (at least) one of the components, often trigger at least a warning and often an alarm even though the 2D/3D displacements are still within their respective thresholds. Therefore it can be concluded that if the displacements per specific component are all within the thresholds simultaneously; the 2D and 3D thresholds are usually satisfied as well (except for the 2D warning threshold, which might be too constraining).
However, when looking at it the other way around; satisfying the 2D/3D thresholds does not necessarily mean simultaneously satisfying the thresholds for all components too (see results).
Therefore, one can conclude that the 2D/3D displacements do not really add anything specific and thus are not required for triggering a warning or alarm or for (dis)arming the system. They could be monitored and analysed as a double check however.

Appendix 4: *Trends*

In order to determine the mean and the slope (trend) of the displacements, the least-squares method is adopted. In these estimations several harmonic parts are taken into account, because the signal is clearly not just a linear line, but contains several varying (harmonic) parts. These need to be estimated in order to approximate the possible trend as good as possible.

For this an iterative scheme is used, starting with up to 4-5 harmonic parts to be estimated (next to the mean and the trend). After each iteration, the reasonability of the approximations is checked and confirmed. When an approximation is not yet reasonable, another iteration is performed, reducing or increasing the number of harmonic parts to be estimated. This continues until the resulting trend approximations are determined to be reasonable. Whether this is the case is determined in two different ways:

- The first option is to look at the significance of the estimated harmonic components. If a specific estimate is very close to 0, then its significance is (very) low. In case the significance of a certain estimated component is (very) low, that specific component can be omitted, and thus less components are to be estimated.
  The final approximation, while using only the estimated components of high significance, is confirmed to be reasonable; to confirm the trend approximation to be reasonable, the significance of the estimated components should not be (very) low.
- The second method is to look at the formal variance of residuals. If the mean of these residuals is (close to) 0 (meaning that the standard deviation per estimate of the residuals is very similar to the formal variance of the residuals), the trend approximation is confirmed to be reasonable as well.

Example

As an example here the workflow for the trend estimation of the SLYG CORS northing is presented. Estimating 4 different extra harmonic parts next to the mean and the slope, results in: 0.0012 m (mean), 2.97e-06 m (slope), 0.0020 m (1), 0.0040 m (2), -4.08e-09 m (3) and 1.10e-12 m (4).

When looking at these results one can easily conclude that the significance of the latter two is so very small, that they can be omitted. In this case, the significance of the slope component is pretty small as well, however that is not very weird as the slope is not expected to be very large since Singapore is located on the Eurasian plate and assumed to be (quite) stable. Besides that, the significance of the slope component is still much larger as compared to the latter two. Also, the slope is what we are interested in, hence this cannot be omitted. This means that extra iterations are performed, estimating less components. After some trial and error, it was determined that 4 components should be used in this estimation, resulting in the following design matrix:

$$
A = \begin{bmatrix}
1 & t_1 & \cos(2\pi t_1) & \sin(2\pi t_1) \\
1 & t_2 & \cos(2\pi t_2) & \sin(2\pi t_2) \\
1 & t_1 & \cos(2\pi t_3) & \sin(2\pi t_3) \\
.. & .. & .. & .. \\
.. & .. & .. & .. \\
1 & t_n & \cos(2\pi t_n) & \sin(2\pi t_n)
\end{bmatrix}
$$

Next, the second method is used as a double check. For example, in this case, when following and using the results of method 1 (thus estimating 4 components only), this results in a value for the mean of the residuals that is indeed very close to zero: 1.48e-18 m. Therefore, it can be assumed that the resulting slope indeed describes the estimated trend in the data for this component well.

This workflow is applied to all (reliable) displacement data, resulting in a reduction of the number of estimated components to 4, like in this example. After applying these two methods the resulting trends are assumed to be as good as possible, resulting in the values presented in chapter 7 (Table 7.2 and the motion maps, Figures 7.3 and 7.4).

Appendix 5: *IM displacement data and atmospheric information, from the RTK engine module in Baseline mode*

SLYG

SLYG, northing
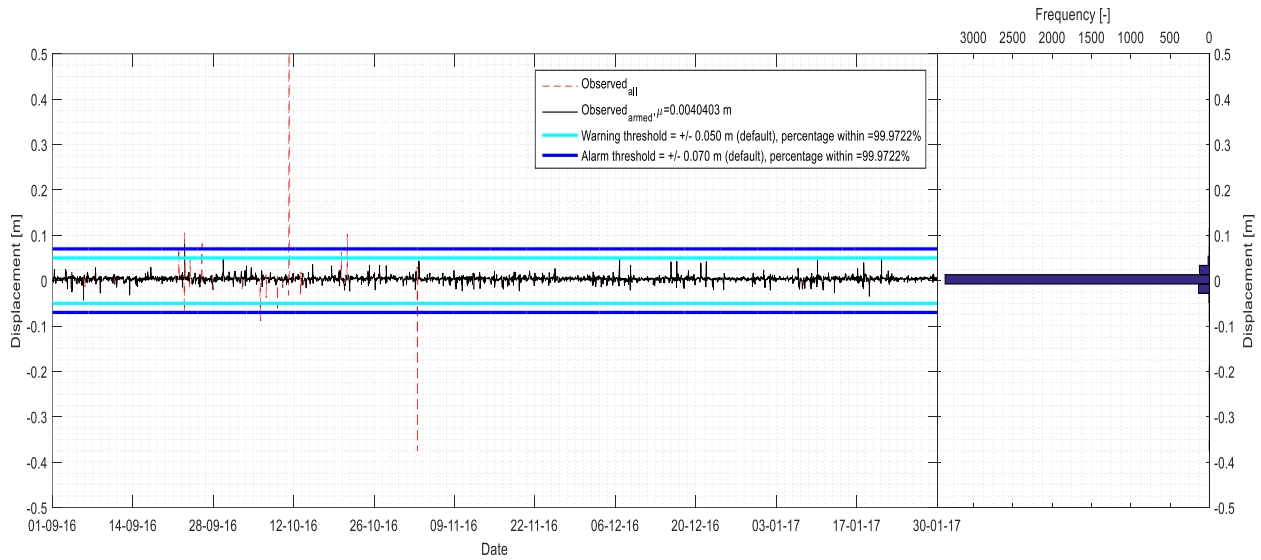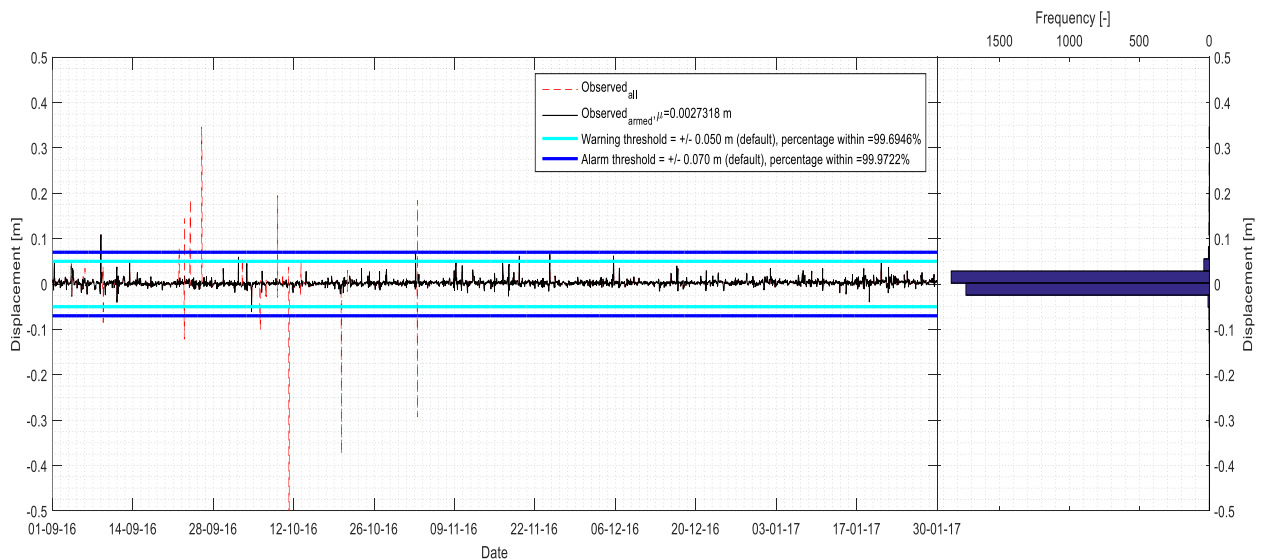
SLYG, easting

Figure A.5.1: Graphs visualizing the displacements in the northing component (top), the easting component (bottom) as observed by the SLYG CORS (period: 01-09-'16 – 30-01-'17).
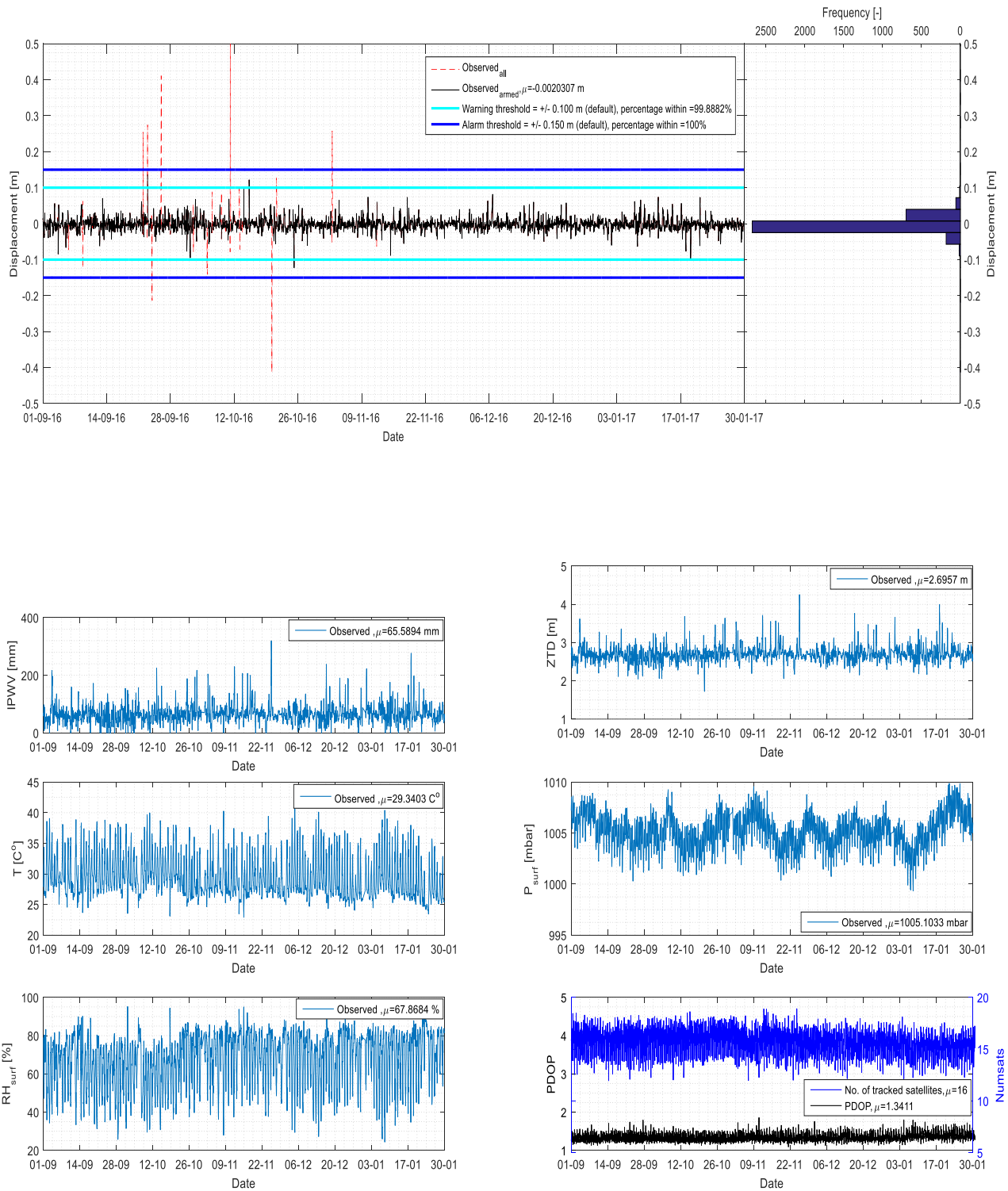
Figure A.5.2: Graphs visualizing the displacements in the height component (top), and the Tropospheric information, PDOP values and number of tracked satellites (bottom) as observed by the SLYG CORS (period: 01-09-'16 – 30-01-'17).

SSTS

SSTS, northing
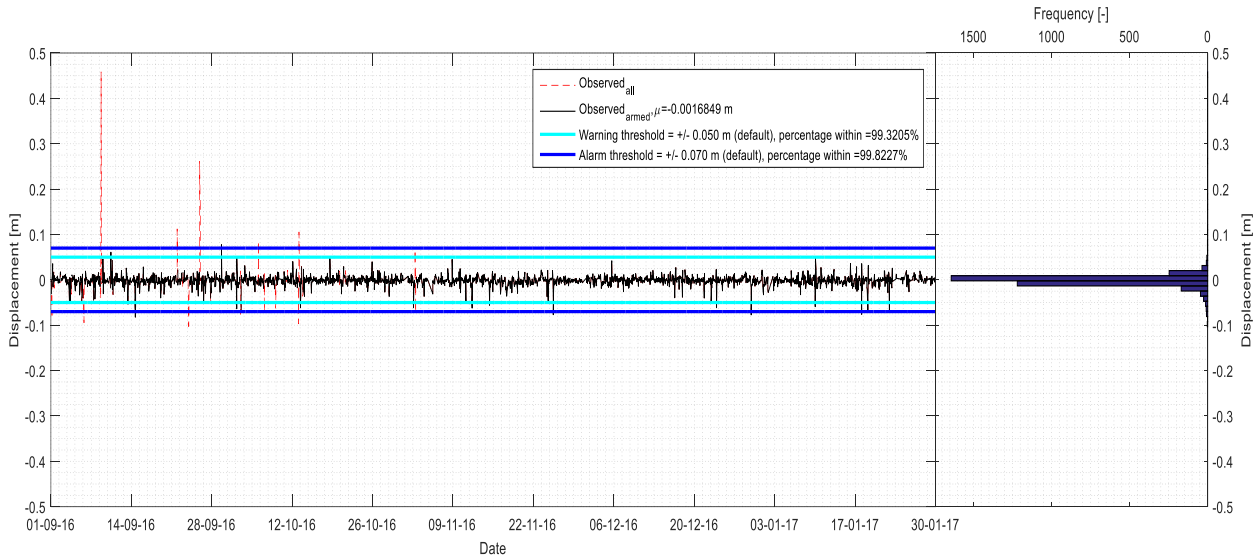
SSTS, easting
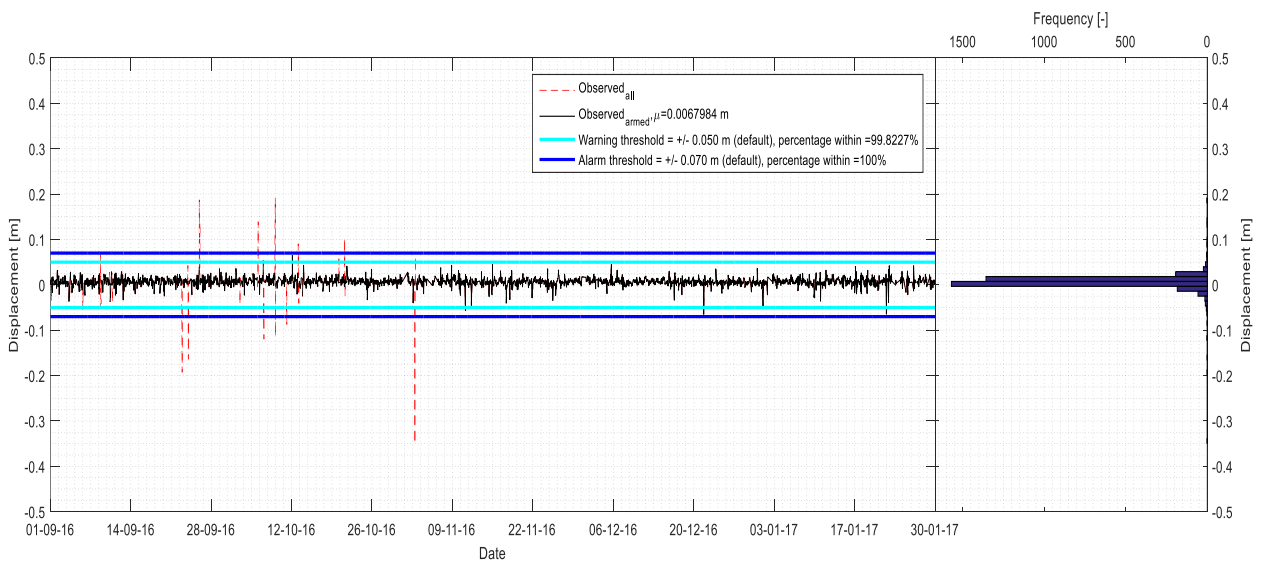
Figure A.5.3: Graphs visualizing the displacements in the northing component (top), and the easting component (bottom) as observed by the SSTS CORS (period: 01-09-'16 – 30-01-'17).

159

SSTS, height
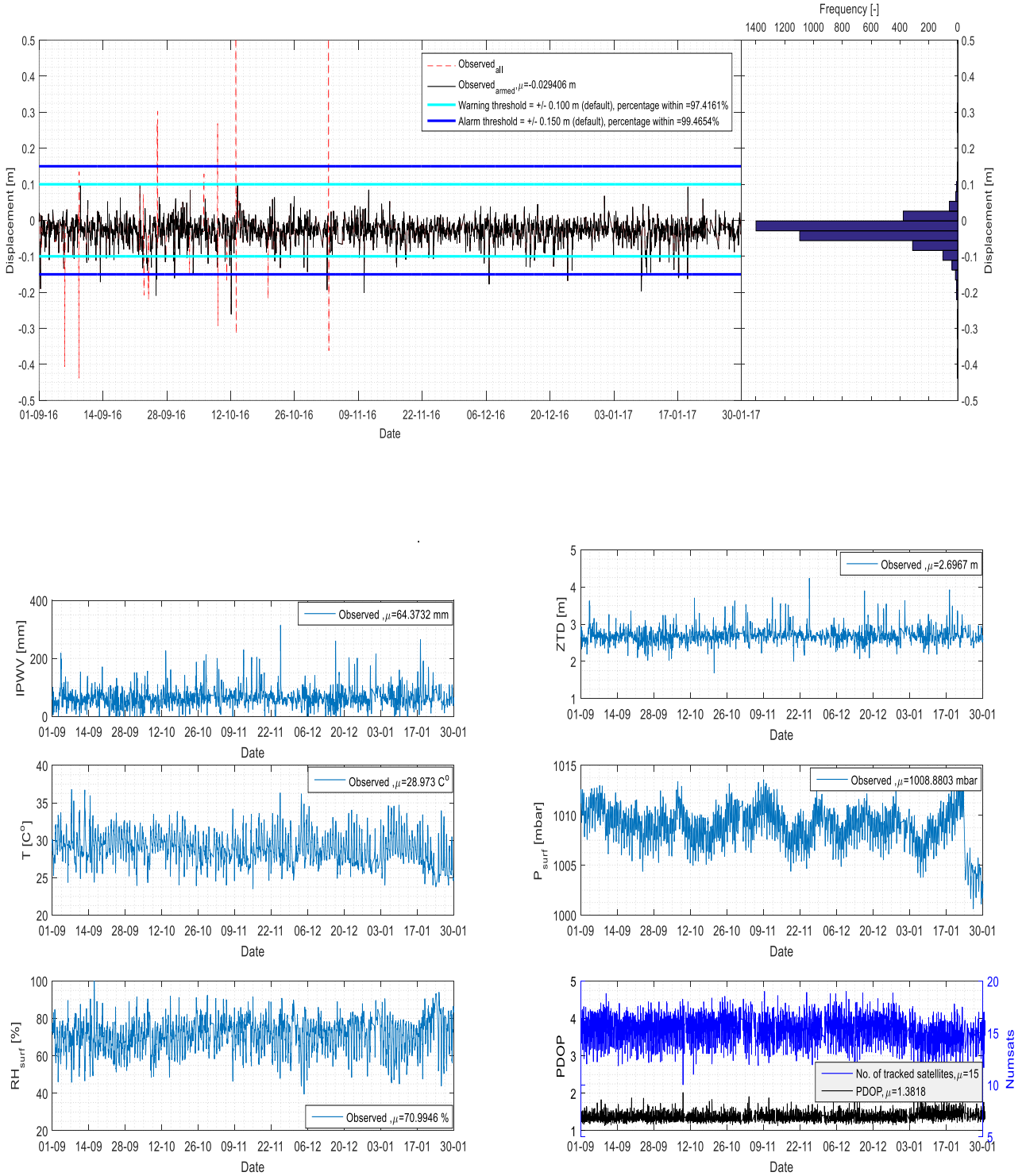
Figure A.5.4: Graphs visualizing the displacements in the height component (top), and the Tropospheric information, PDOP values and number of tracked satellites (bottom) as observed by the SSTS CORS (period: 01-09-'16 – 30-01-'17).
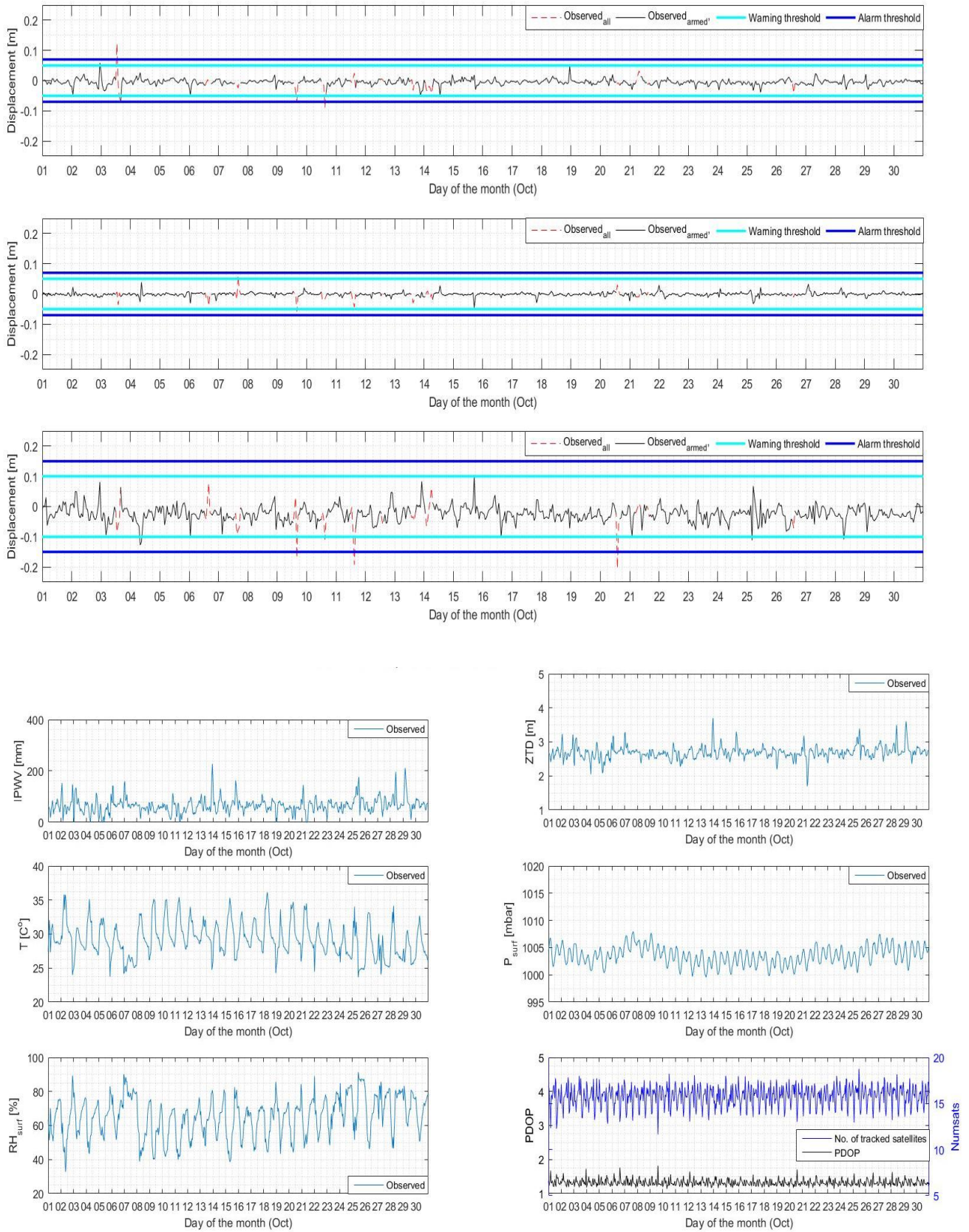
SSMK

SSMK, northing
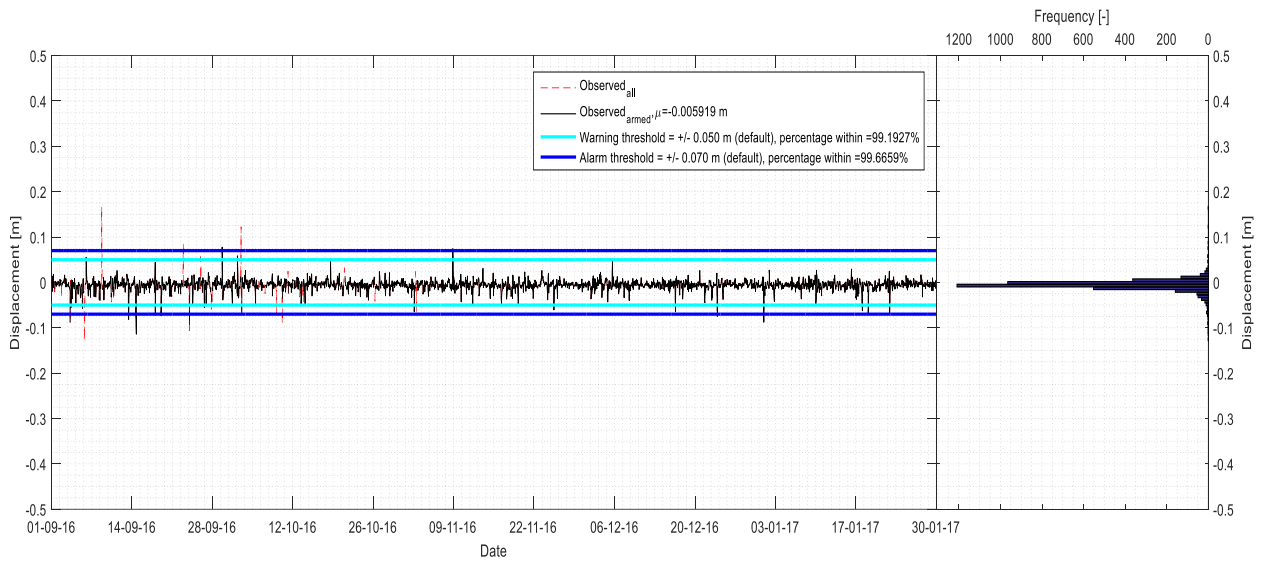
SSMK, easting
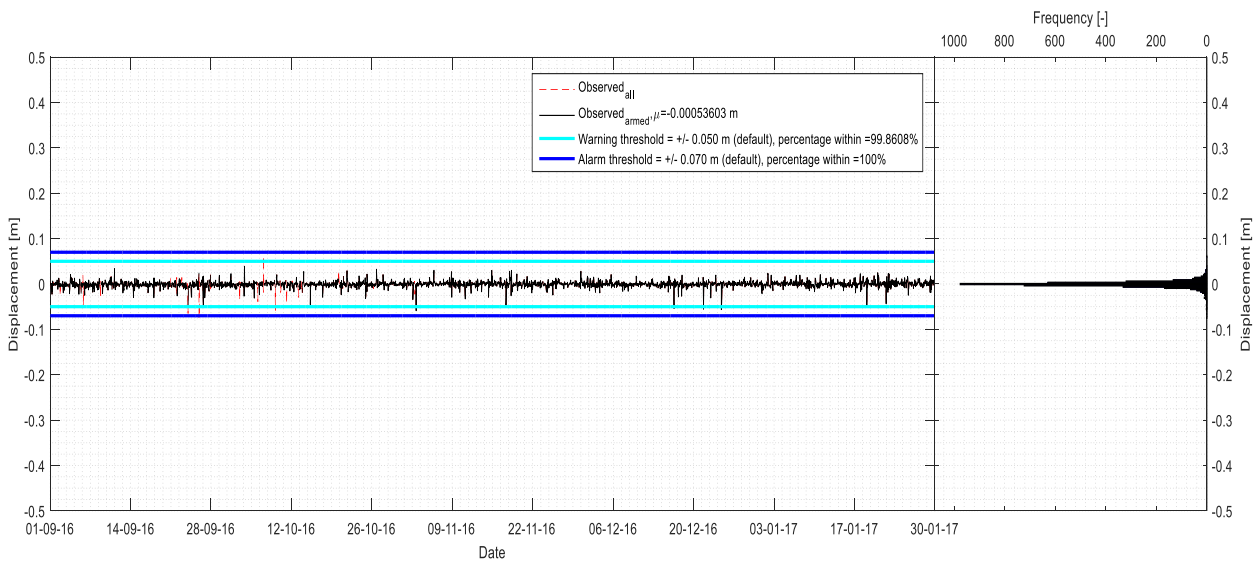
Figure A.5.5: Graphs visualizing the displacements in the northing component (top), and the easting component (bottom)
as observed by the SSMK CORS (period: 01-09-'16 – 30-01-'17).
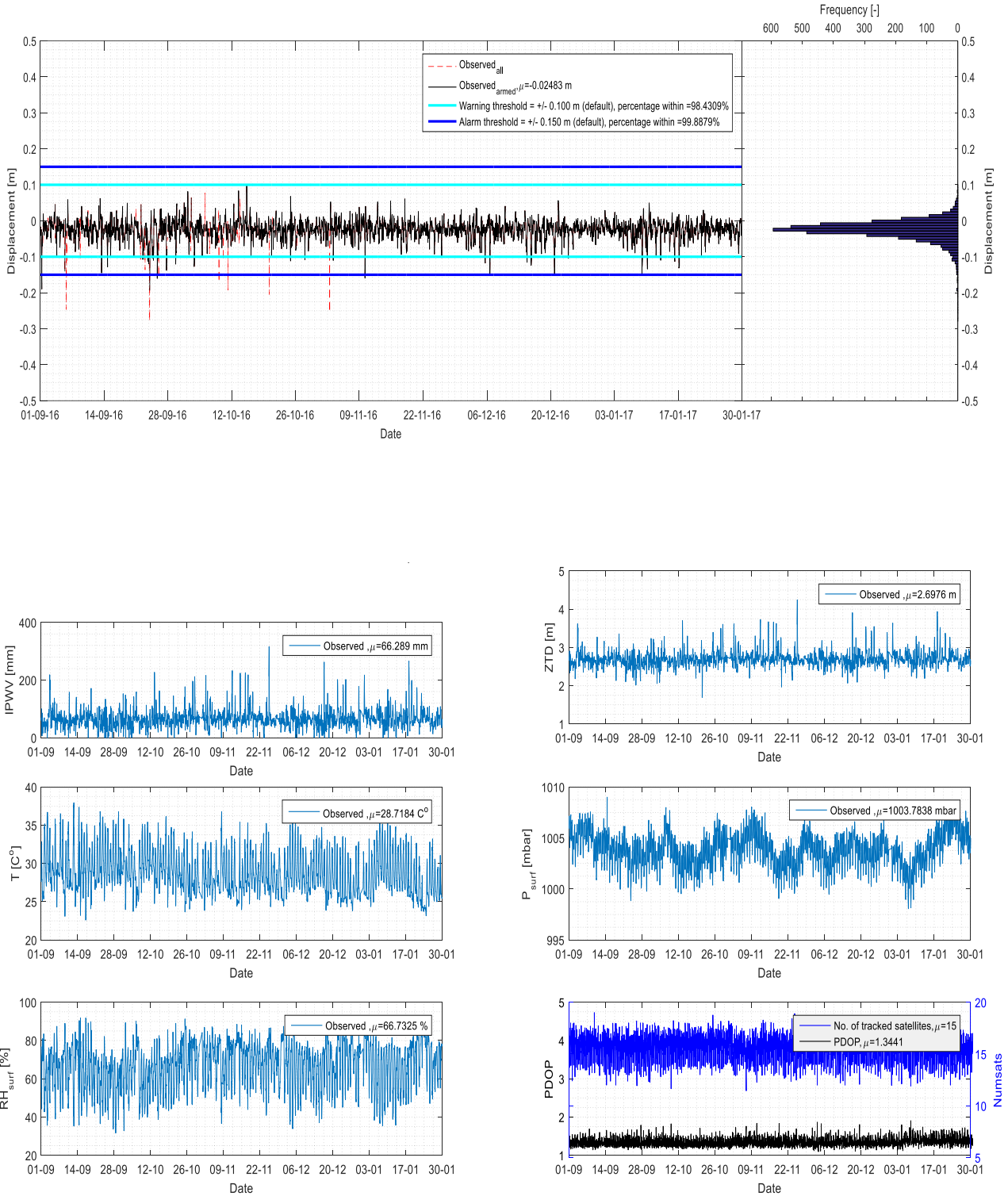
Figure A.5.6: Graphs visualizing the displacements in the height component (top), and the Tropospheric information, PDOP values and number of tracked satellites (bottom) as observed by the SSMK CORS (period: 01-09-'16 – 30-01-'17).

162
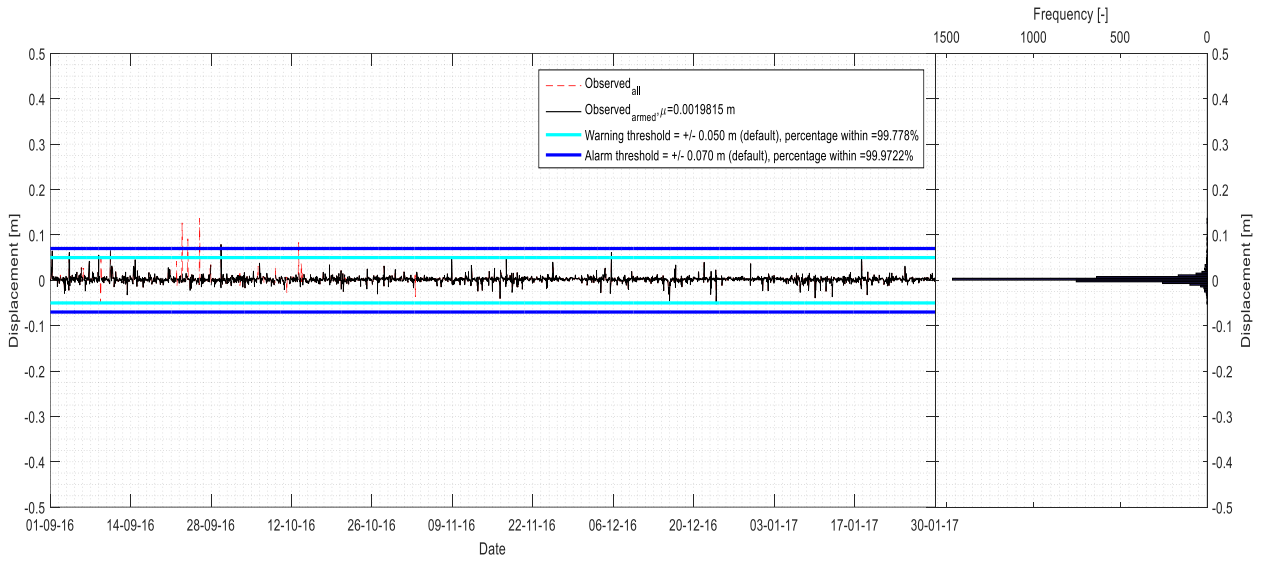
SRPT

SRPT, northing
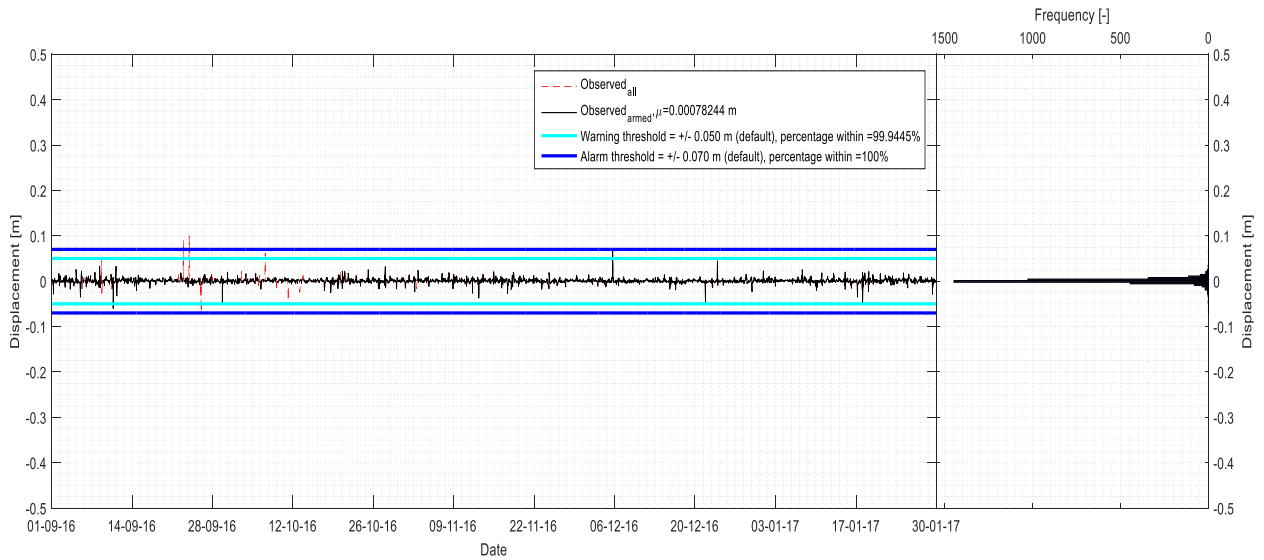
SRPT, easting

Figure A.5.7: Graphs visualizing the displacements in the northing component (top), and the easting component (bottom) as observed by the SRPT CORS (period: 01-09-'16 – 30-01-'17).
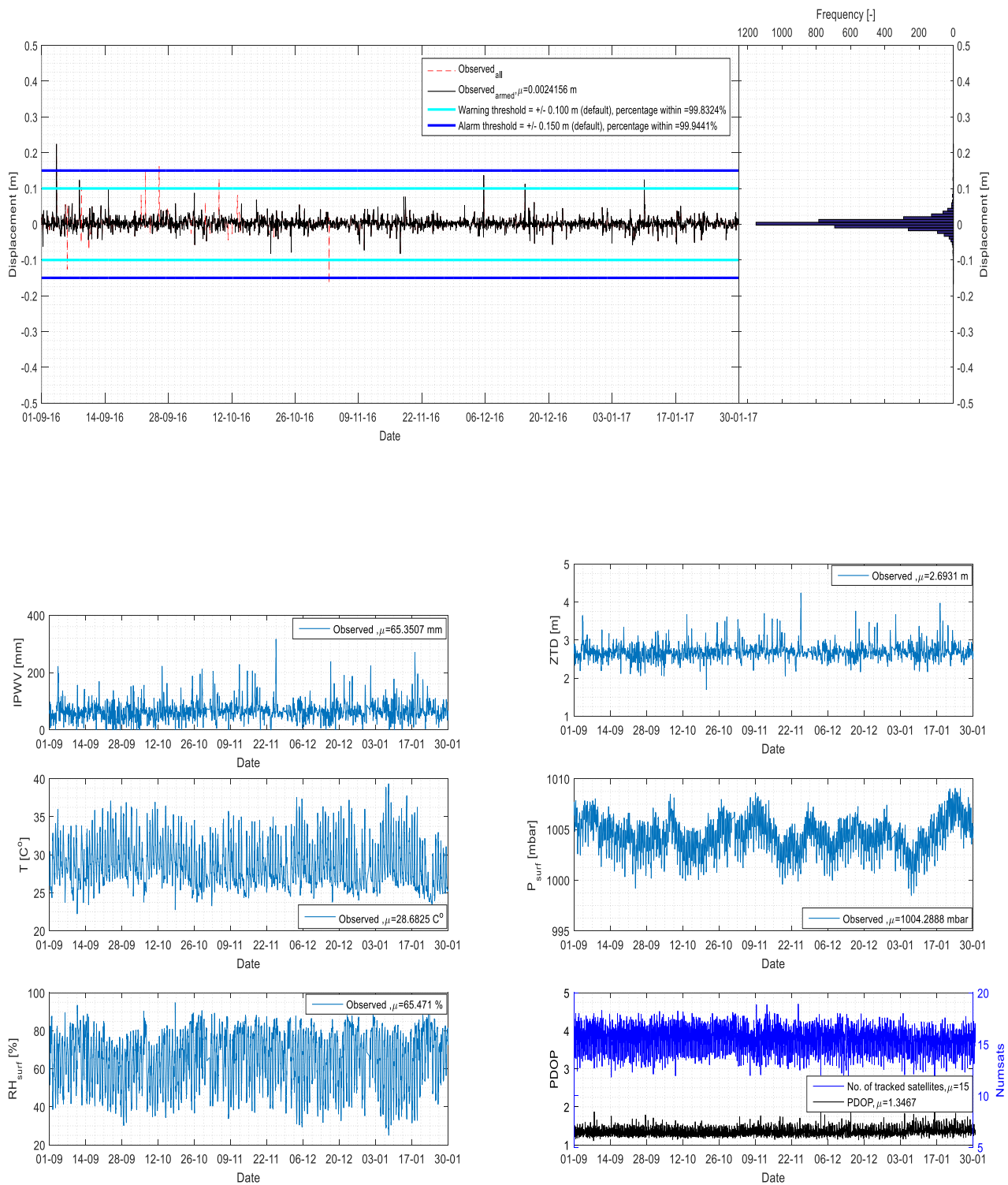
Figure A.5.8: Graphs visualizing the displacements in the height component (top), and the Tropospheric information, PDOP values and number of tracked satellites (bottom) as observed by the SRPT CORS (period: 01-09-'16 – 30-01-'17).
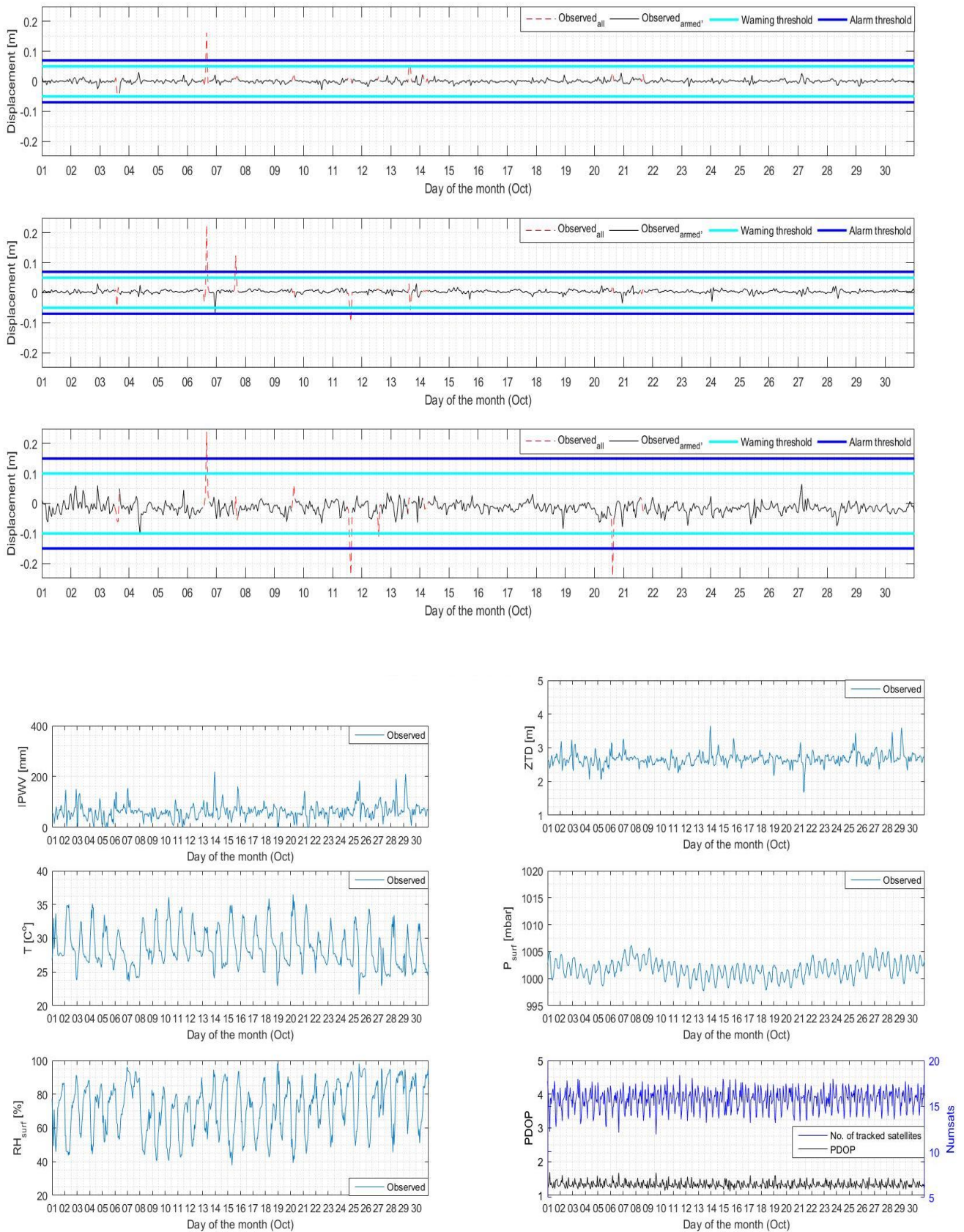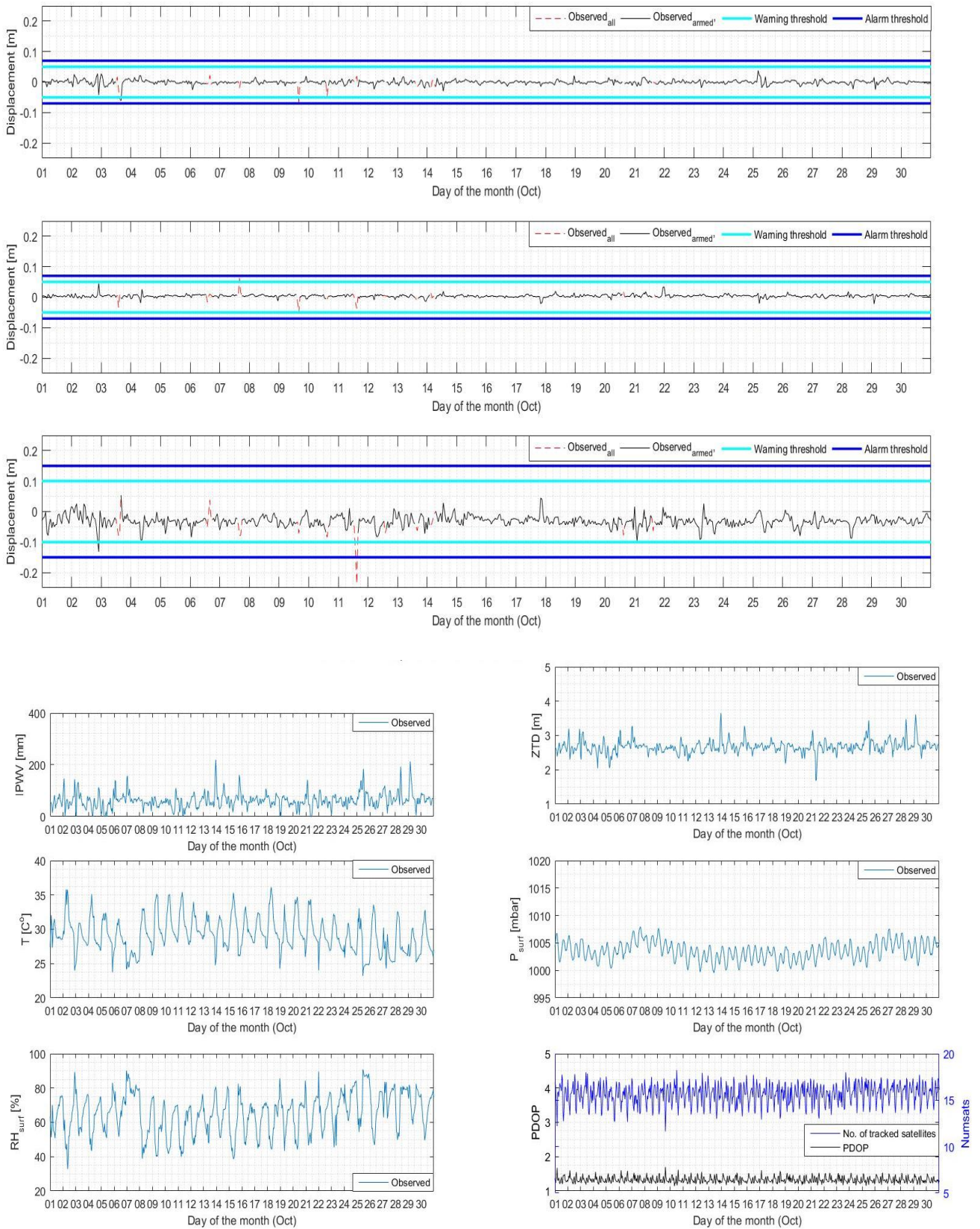
SNYU
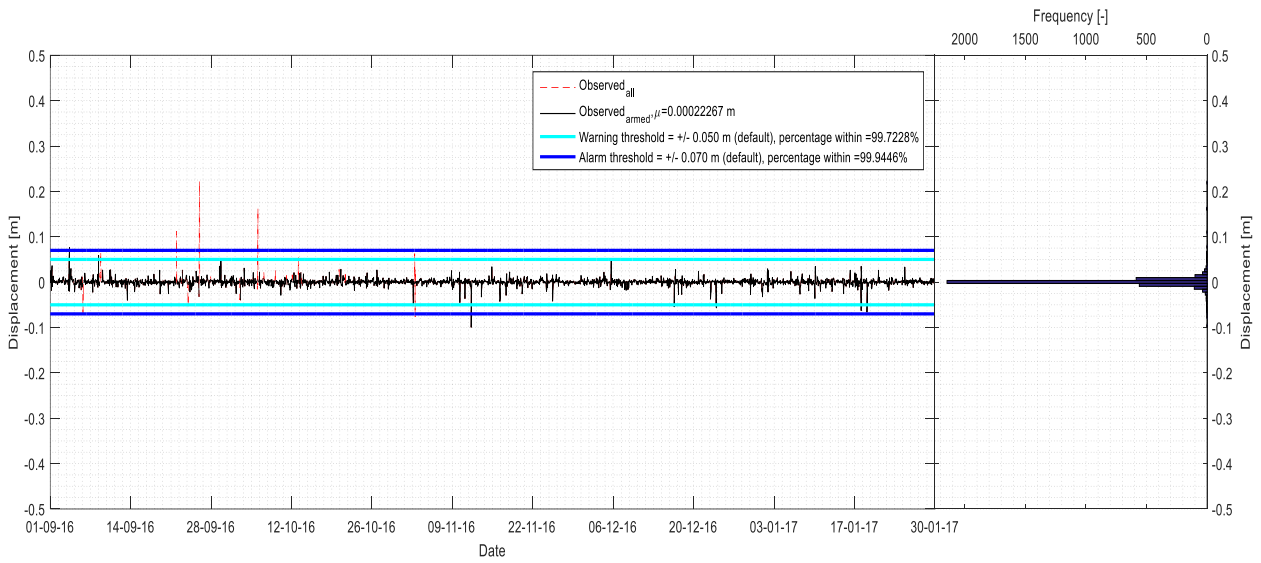
SNYU, northing

SNYU, easting
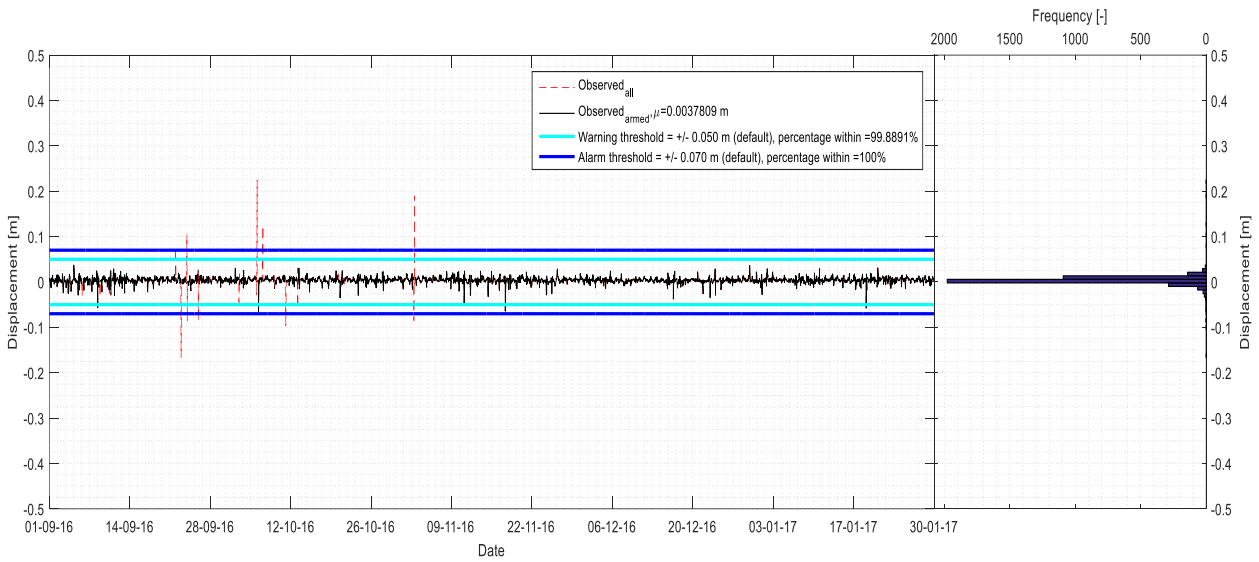
Figure A.5.9: Graphs visualizing the displacements in the northing component (top), and the easting component (bottom) as observed by the SNYU CORS (period: 01-09-'16 – 30-01-'17).
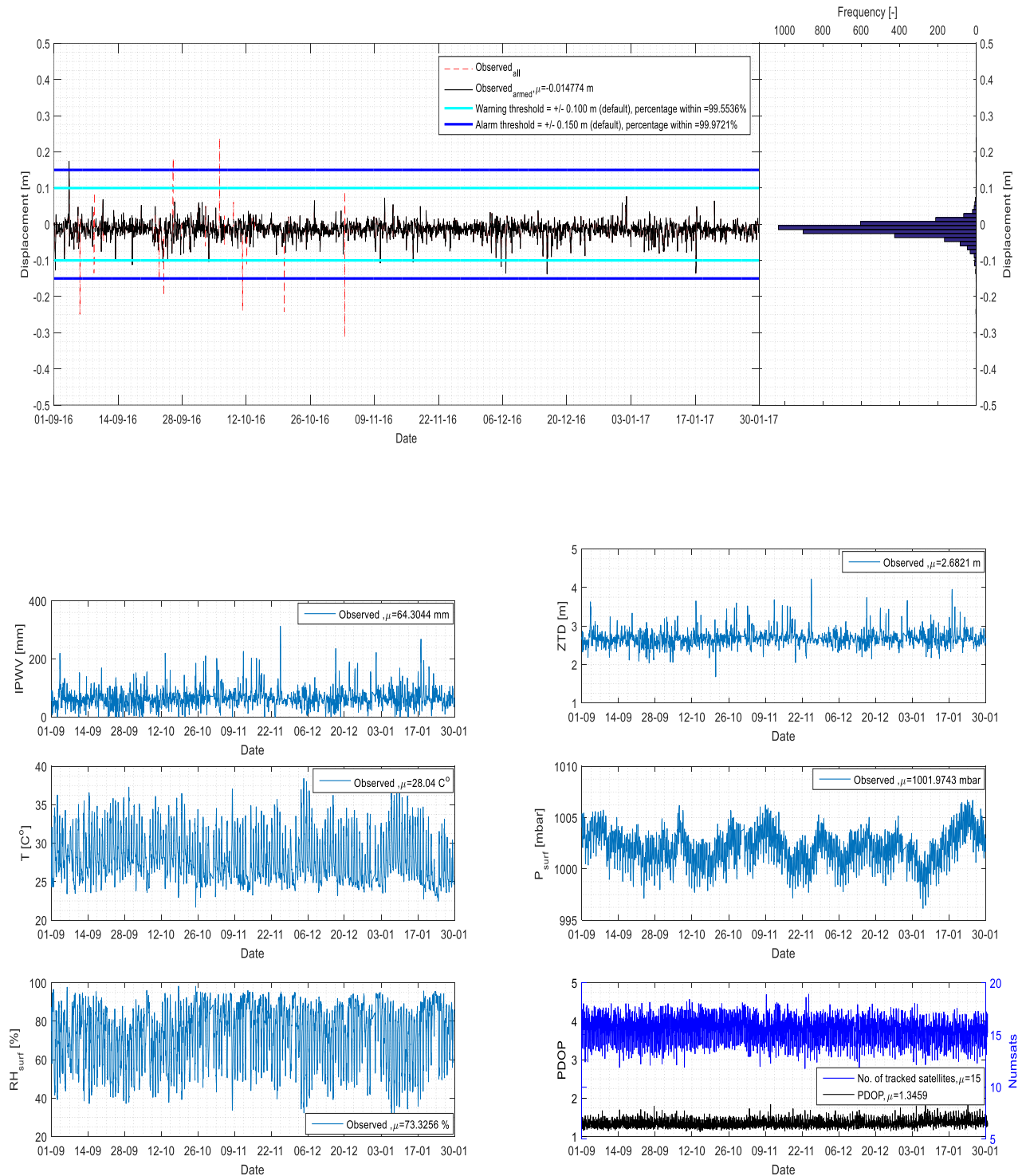
Figure A.5.10: Graphs visualizing the displacements in the height component (top), and the Tropospheric information, PDOP values and number of tracked satellites (bottom) as observed by the SNYU CORS (period: 01-09-'16 – 30-01-'17).

SNUS

SNUS, northing
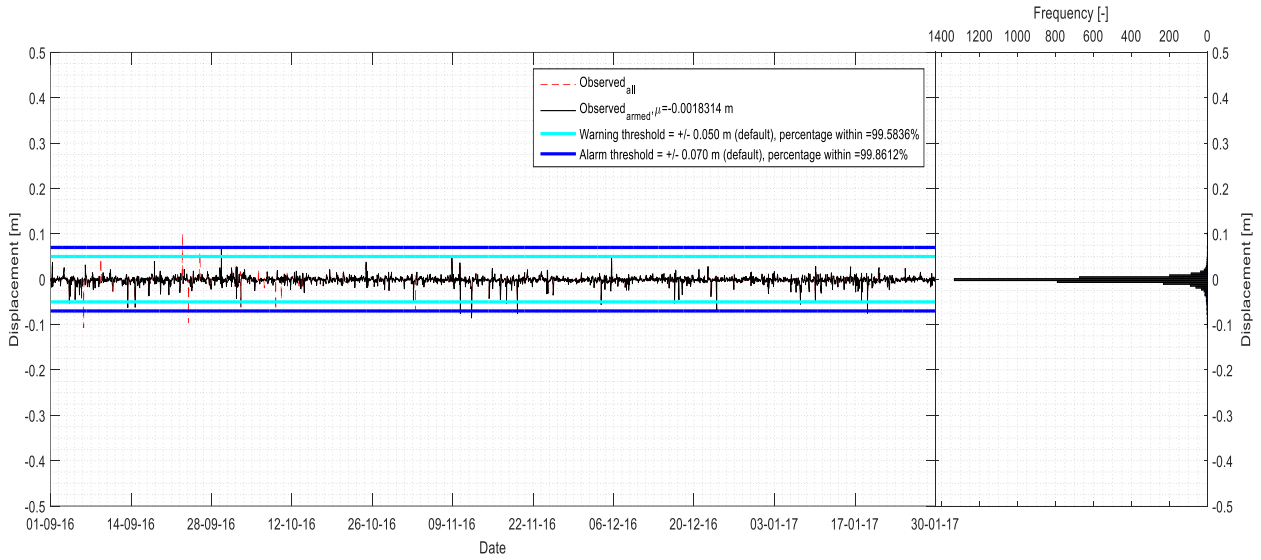
SNUS, easting
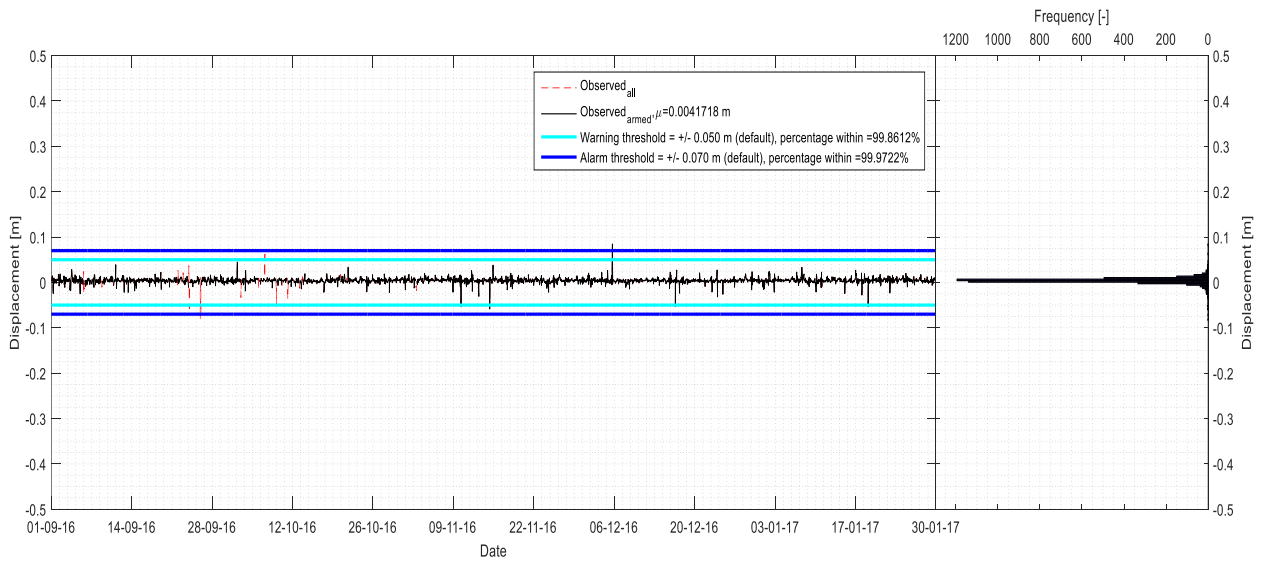
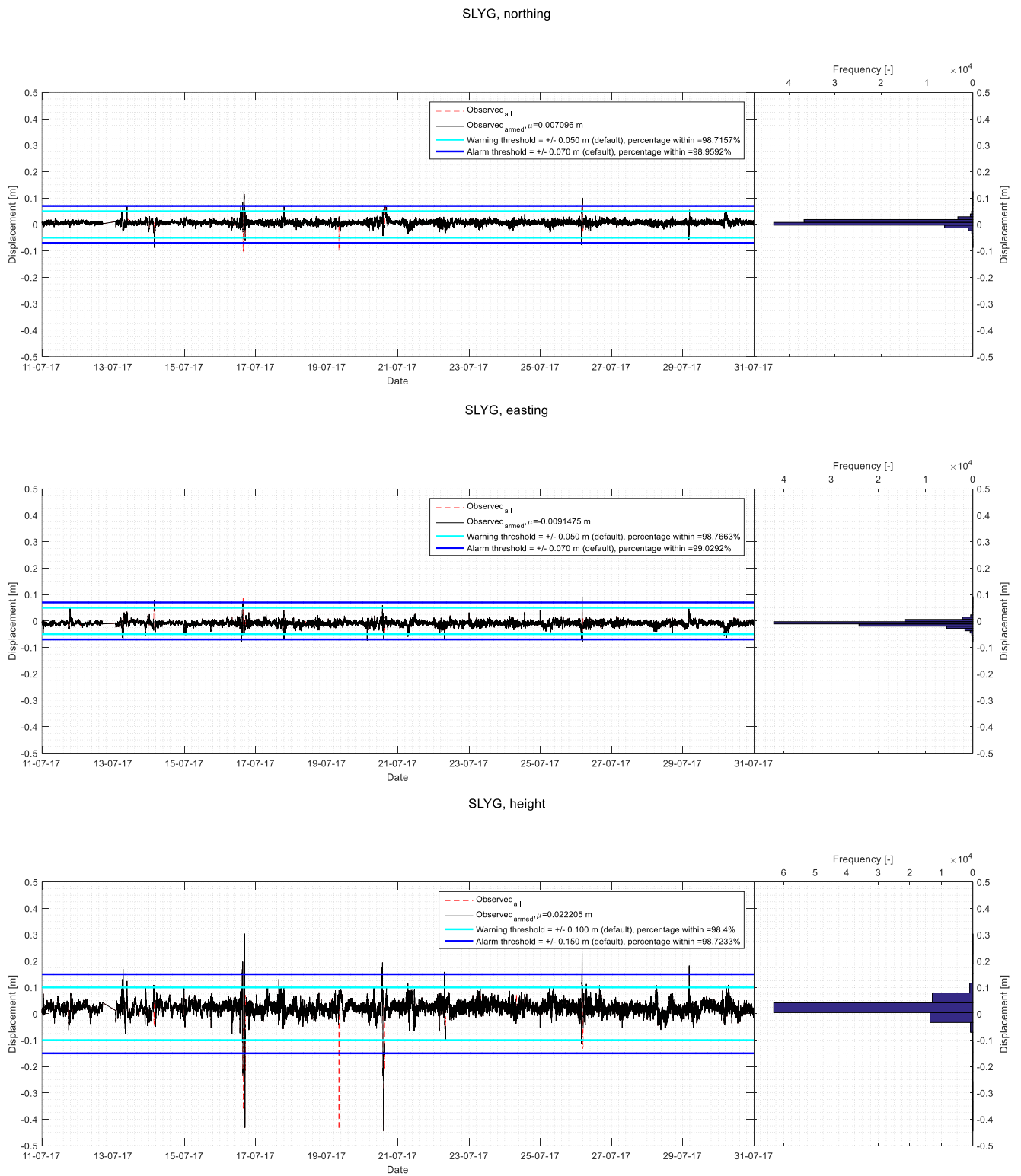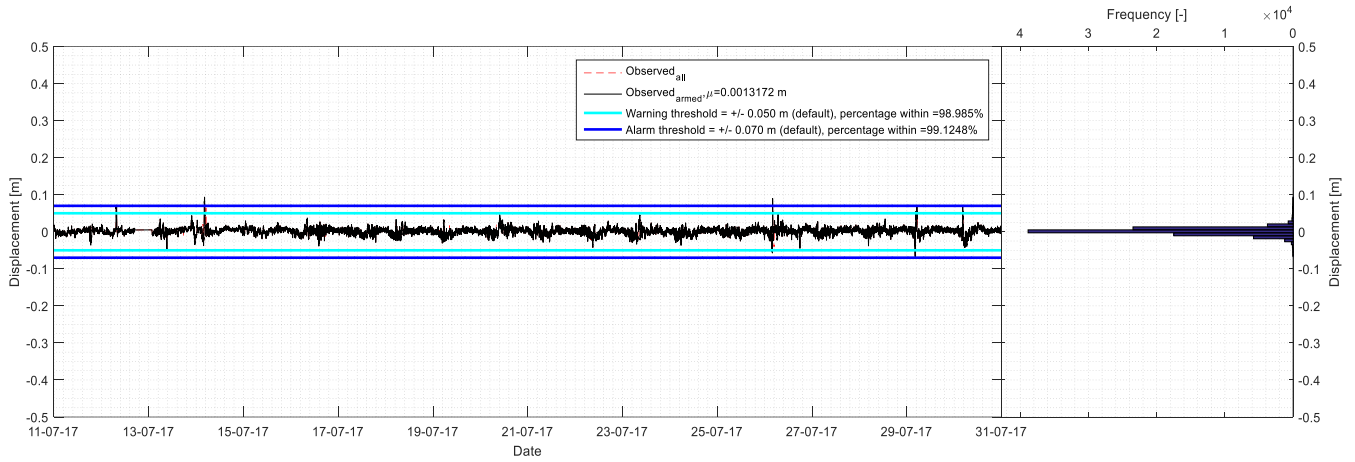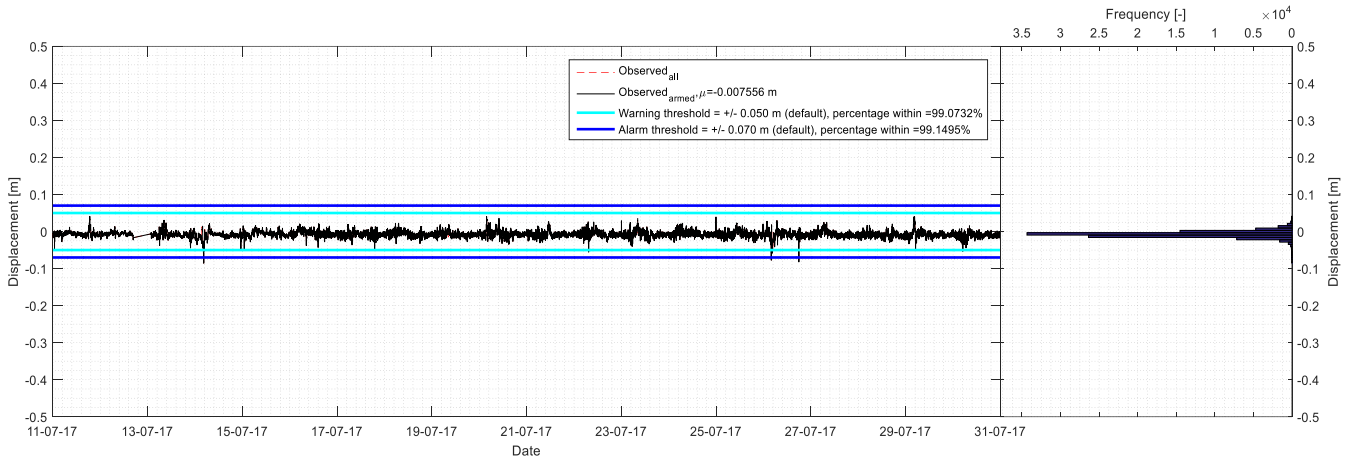*Figure A.5.11: Graphs visualizing the displacements in the northing component (top), and the easting component (bottom) as observed by the SNUS CORS (period: 01-09-'16 – 30-01-'17).*
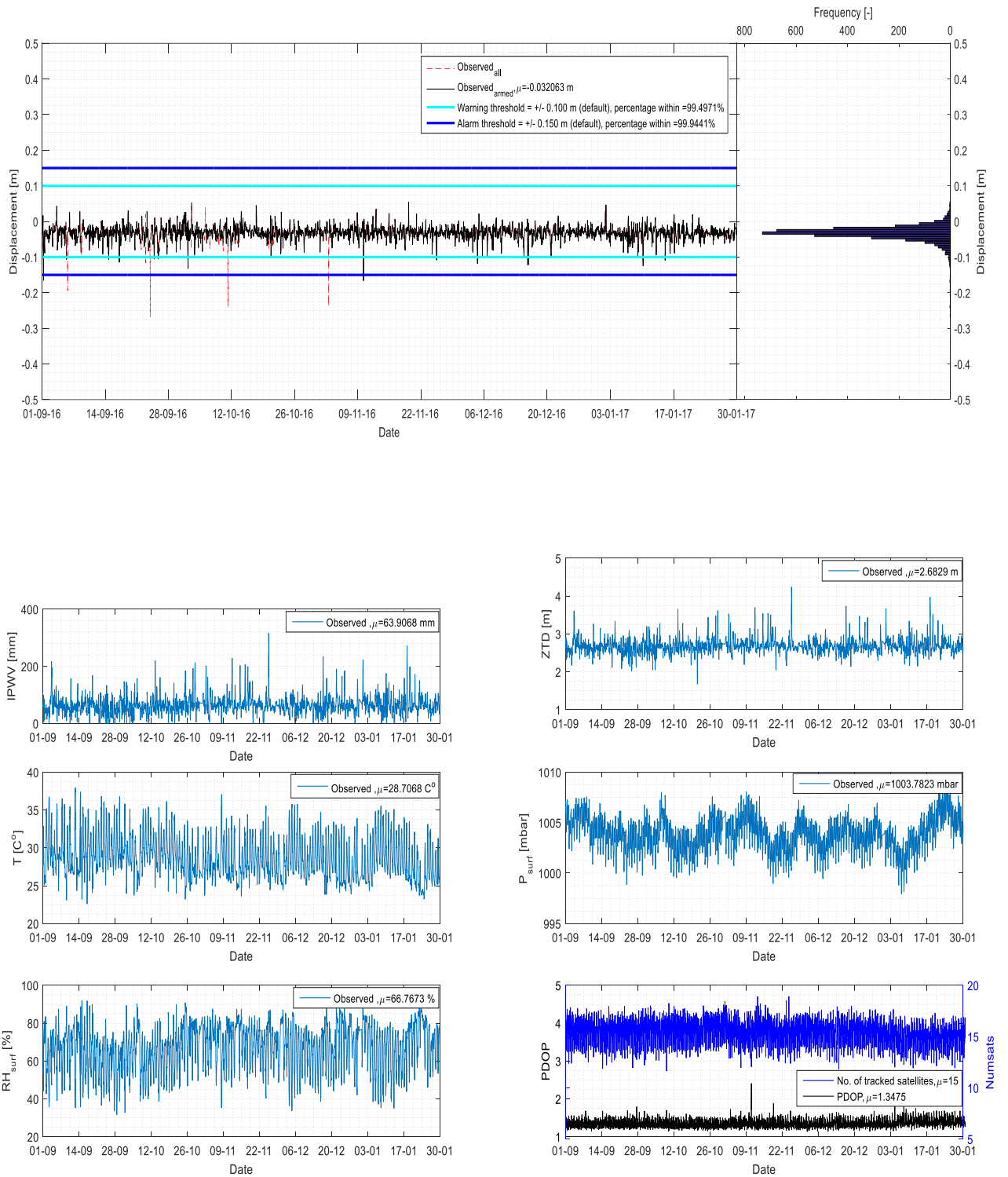
Figure A.5.12: Graphs visualizing the displacements in the height component (top), and the Tropospheric information, PDOP values and number of tracked satellites (bottom) as observed by the SNUS CORS (period: 01-09-'16 – 30-01-'17).
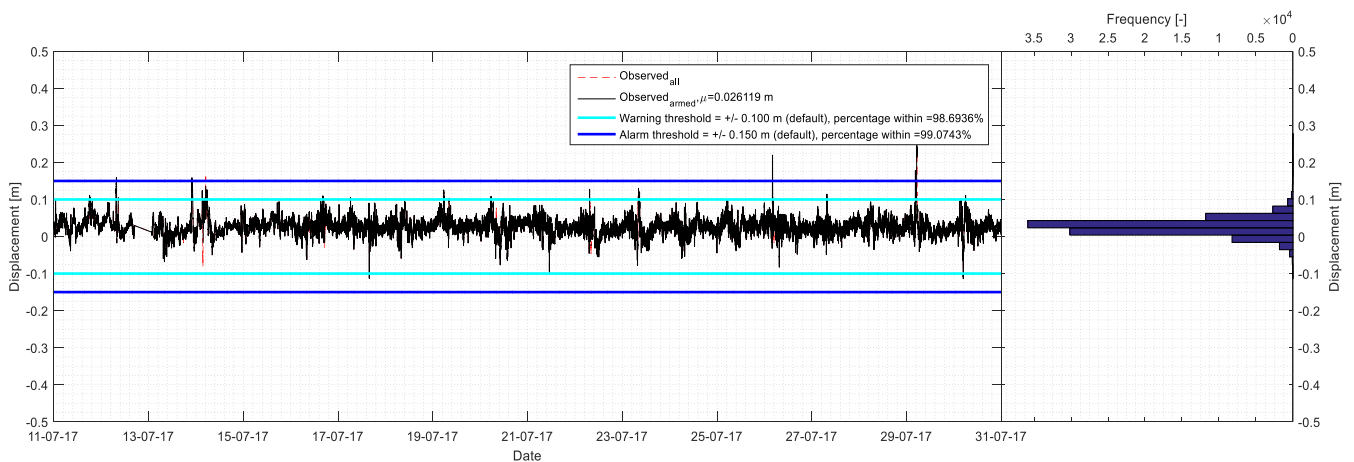
168
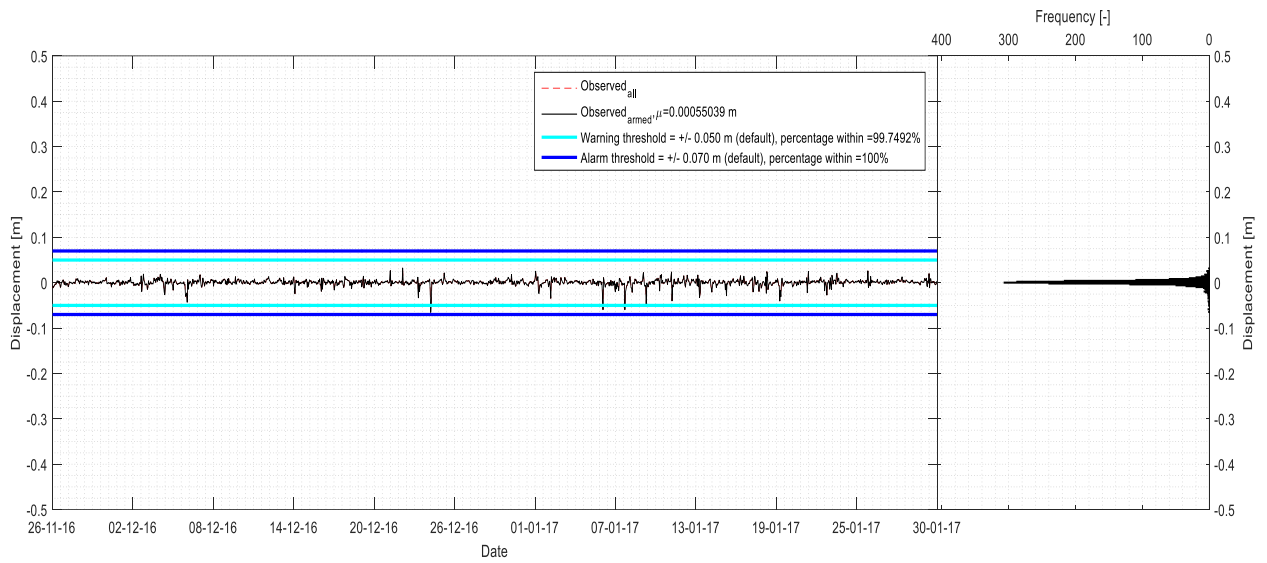
SNSC

SNSC, northing
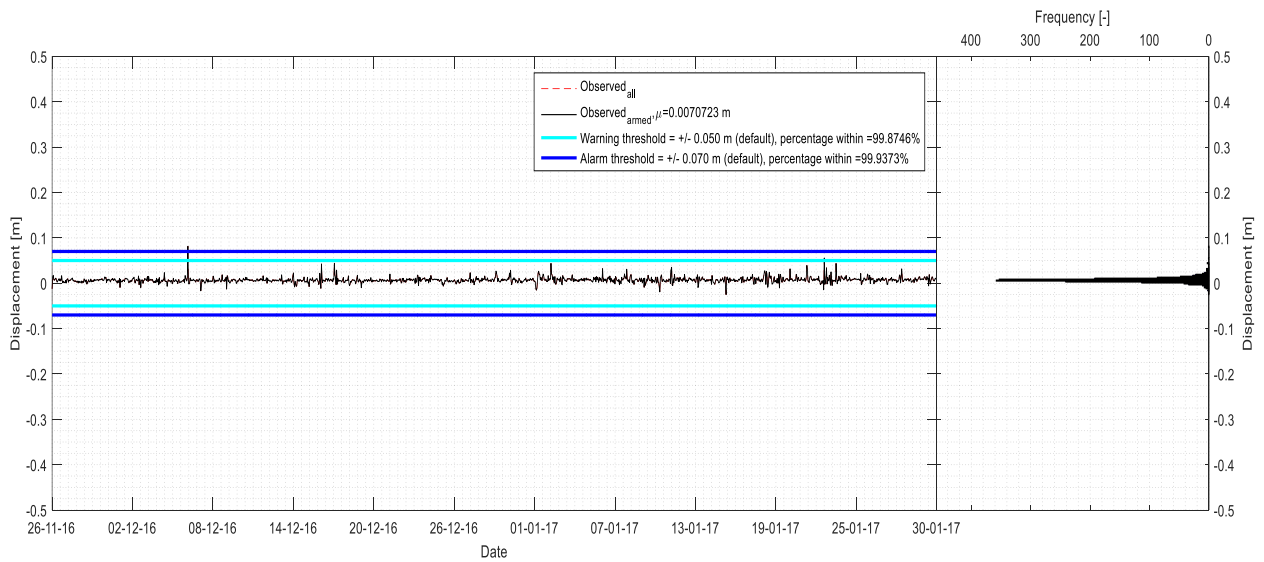
SNSC, easting

Figure A.5.13: Graphs visualizing the displacements in the northing component (top), and the easting component (bottom) as observed by the SNSC CORS (period: 26-11-'16 – 30-01-'17).
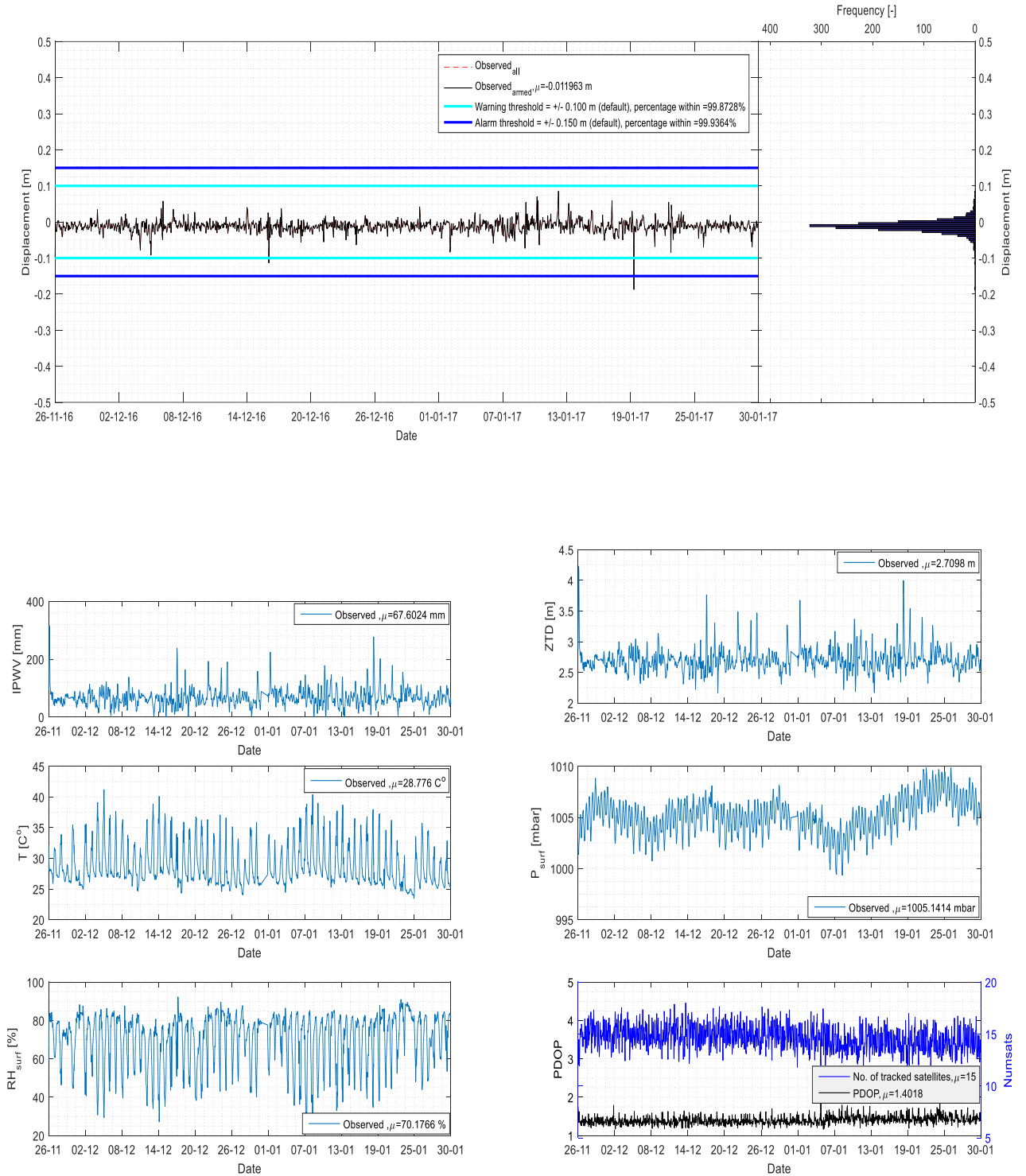
Figure A.5.14: Graphs visualizing the displacements in the height component (top), and the Tropospheric information, PDOP values and number of tracked satellites (bottom) as observed by the SNSC CORS (period: 26-11-'16 – 30-01-'17).
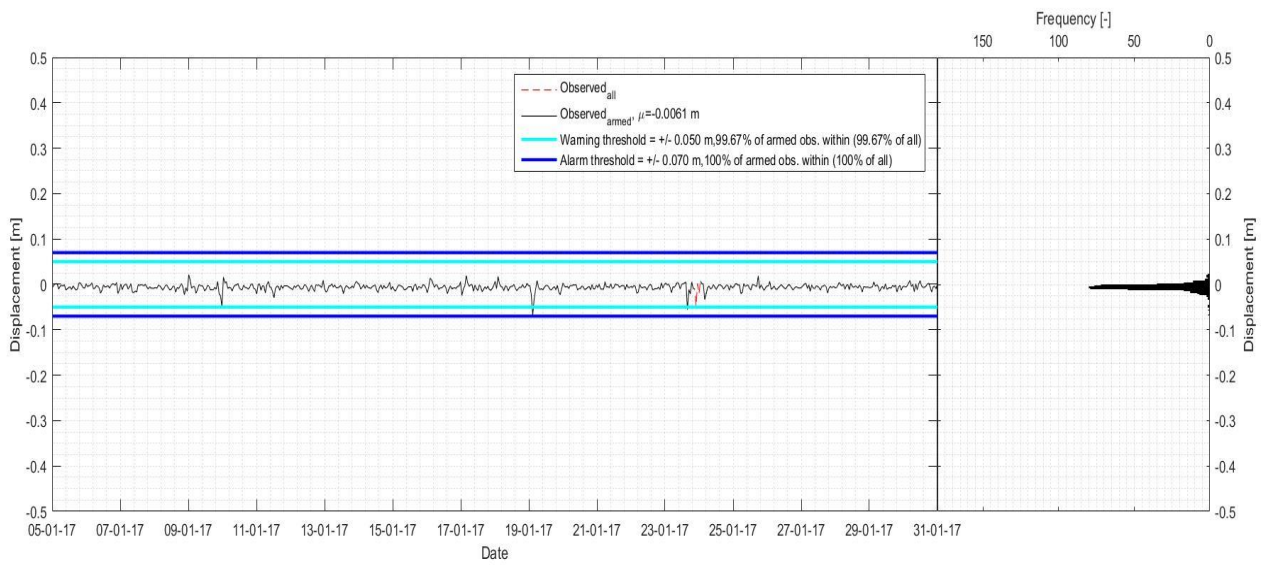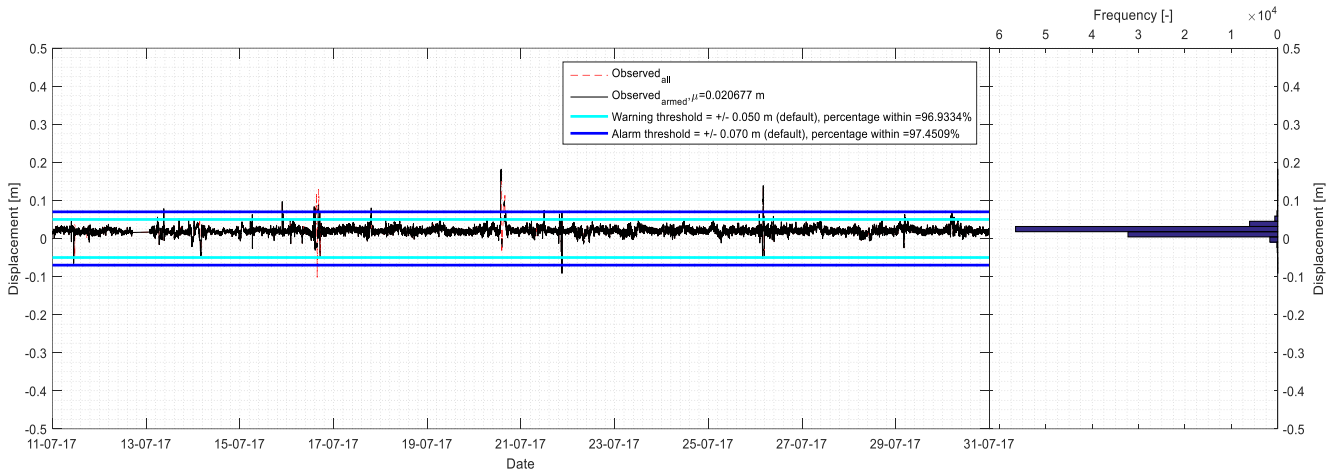
SING
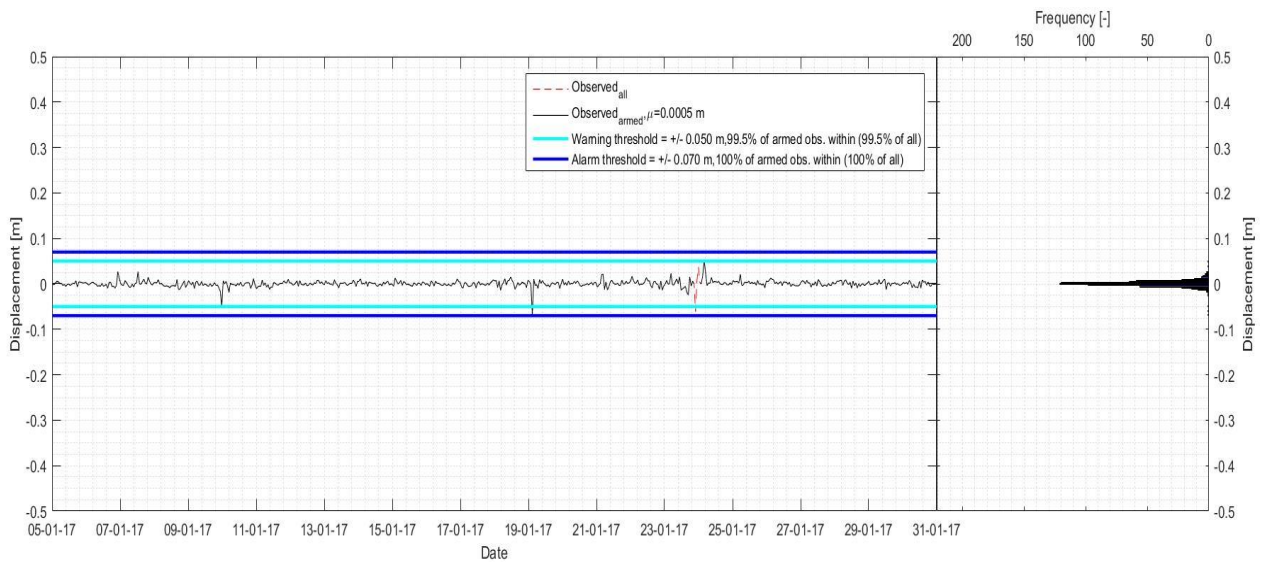
Figure A.5.15: Graphs visualizing the displacements in the northing component (top), and the easting component (bottom) as observed by the SING CORS (period: 05-01-'16 – 31-01-'17).
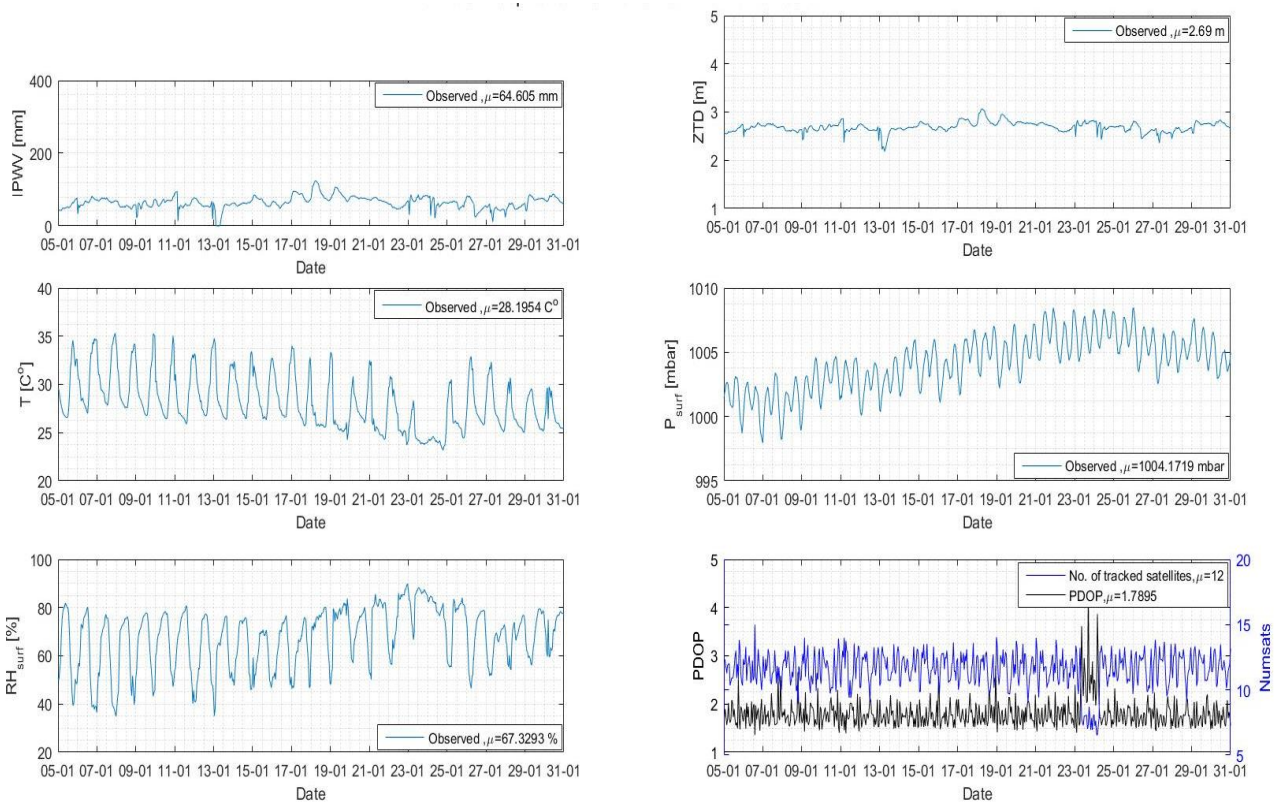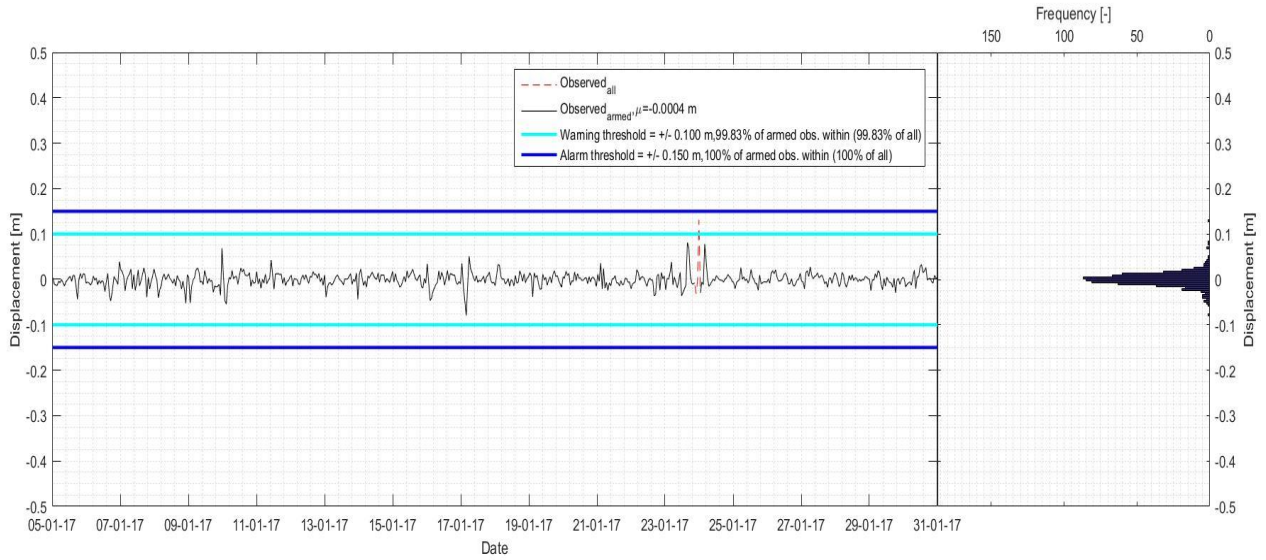
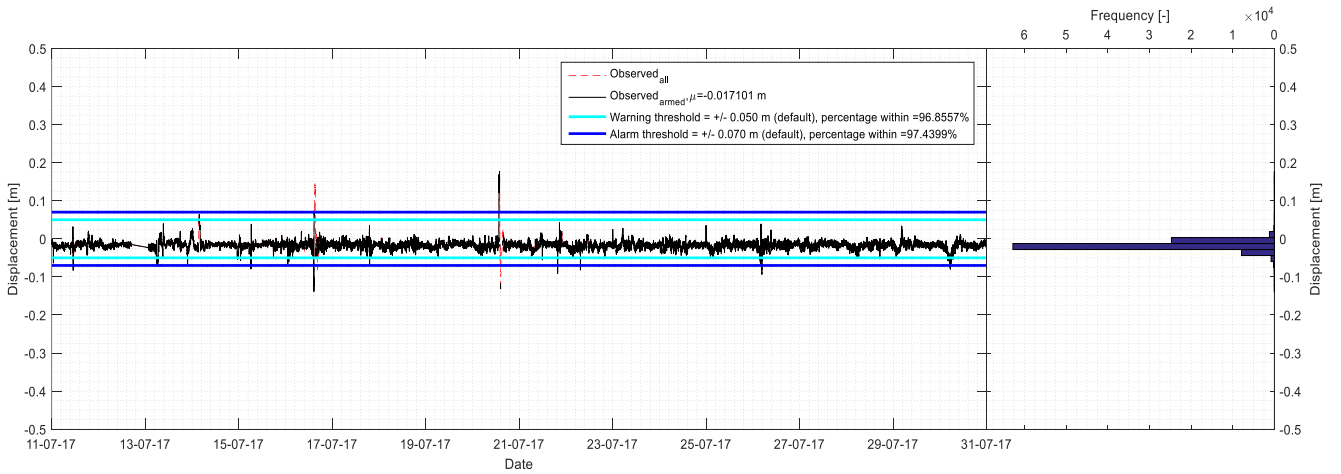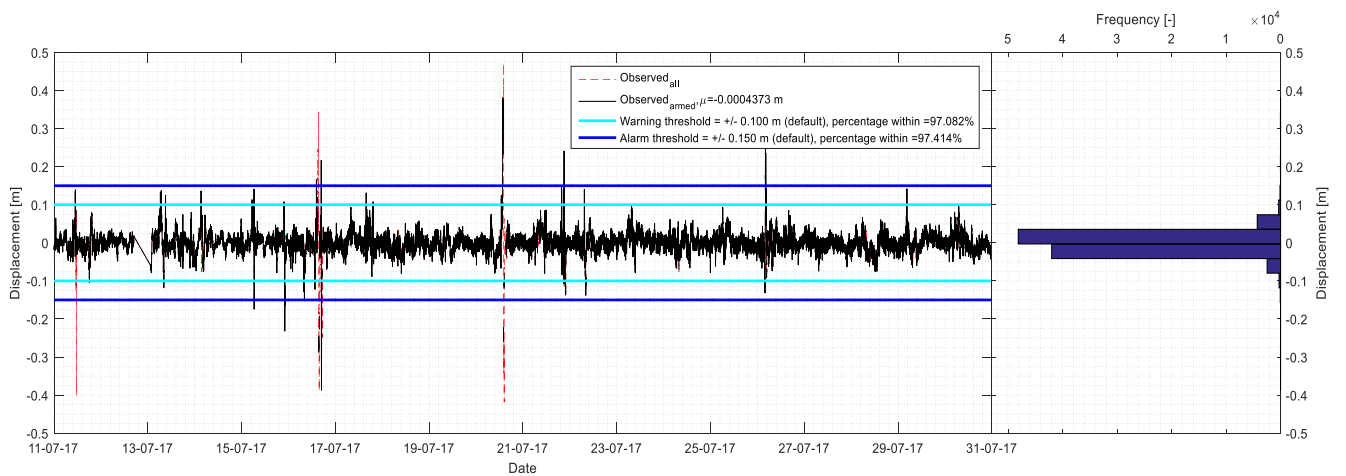*Figure A.5.16: Graphs visualizing the displacements in the height component (top), and the Tropospheric information, PDOP values and number of tracked satellites (bottom) as observed by the SING CORS (period: 05-01-'17 – 31-01-'17).*
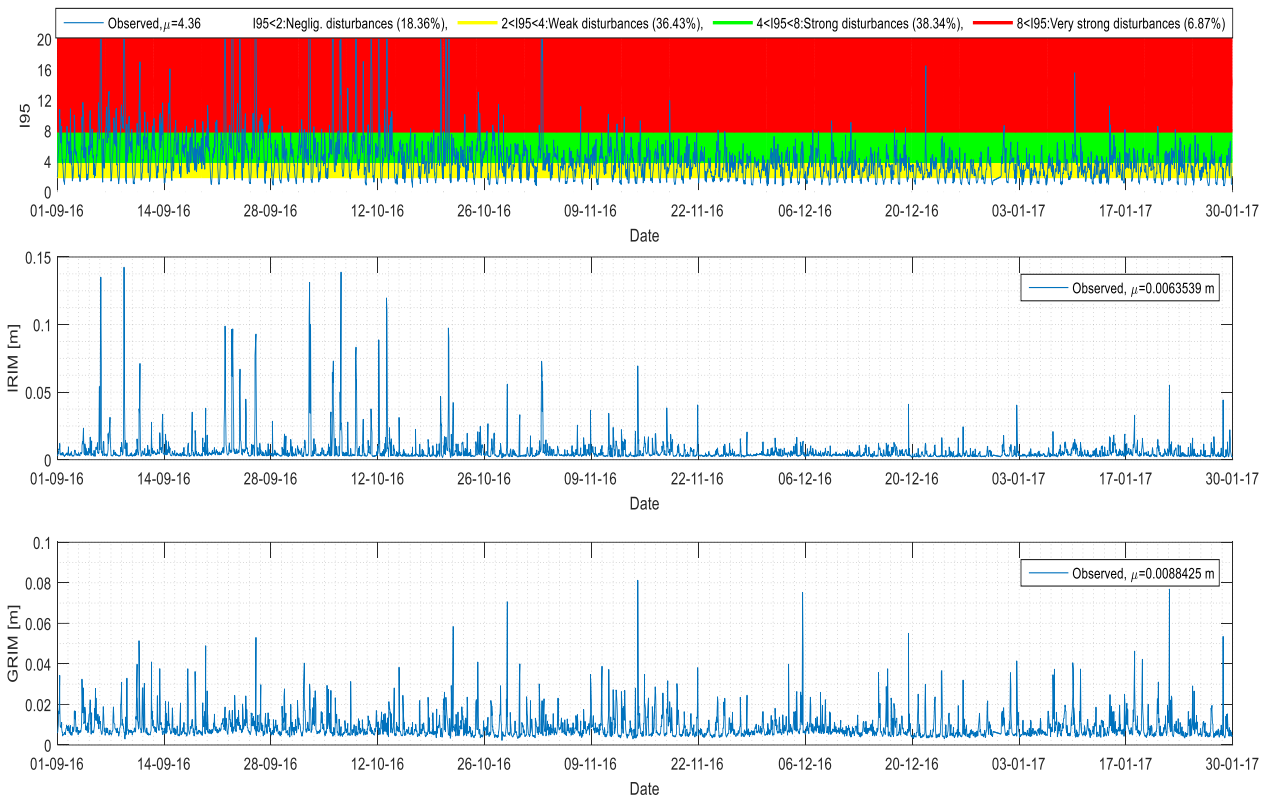
Figure A.5.17: Graphs visualizing the I95/GRIM/IRIM values as observed by SiReNT (period: 01-09-'16 – 30-01-'17).

Figure A.6.1: Graphs visualizing the I95/GRIM/IRIM values as observed by SiReNT during September 2016. For a more detailed explanation of the graphs, see 'Appendix 6 and Appendix 7 Figures explained'.

SLYG

Figure A.6.2: Graphs visualizing the IM displacements (top), and the Tropospheric information, PDOP values and number of tracked satellites (bottom) as observed by the SLYG CORS during September 2016. For a more detailed explanation of the graphs, see 'Appendix 6 and Appendix 7 Figures explained'.

175
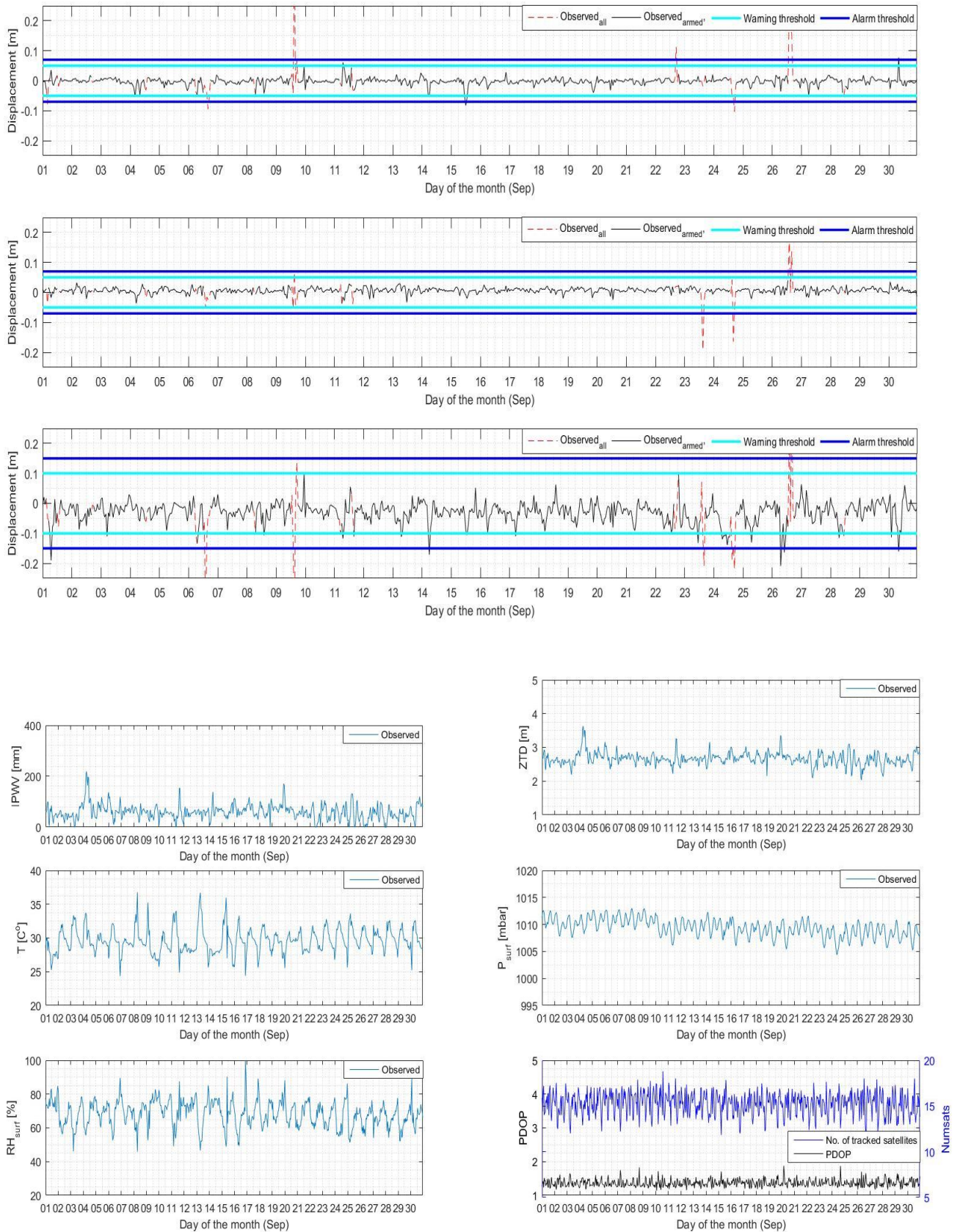
SSTS

Figure A.6.3: Graphs visualizing the IM displacements (top), and the Tropospheric information, PDOP values and number of tracked satellites (bottom) as observed by the SSTS CORS during September 2016.

SSMK
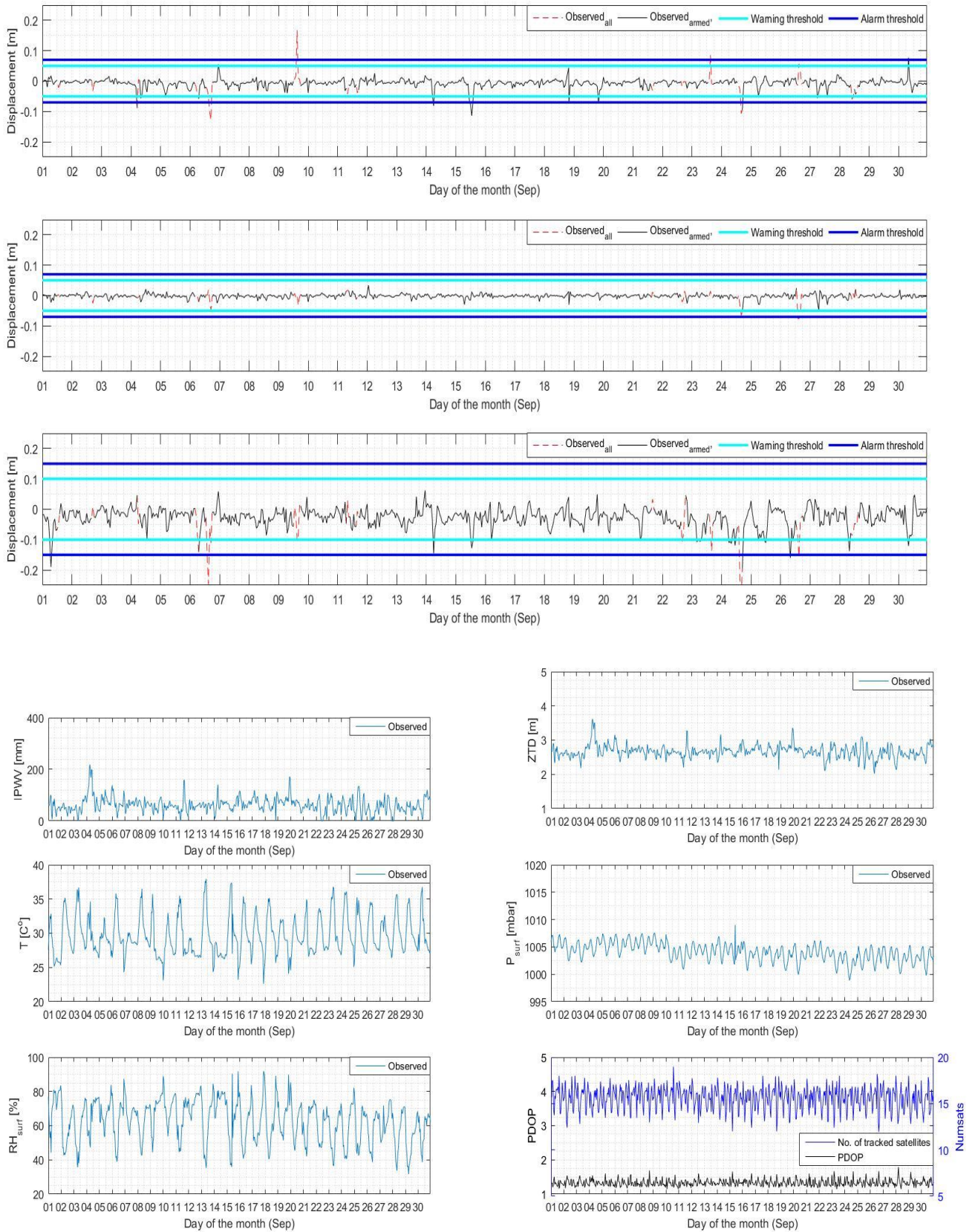
Figure A.6.4: Graphs visualizing the IM displacements (top), and the Tropospheric information, PDOP values and number of tracked satellites (bottom) as observed by the SSMK CORS during September 2016.

SRPT
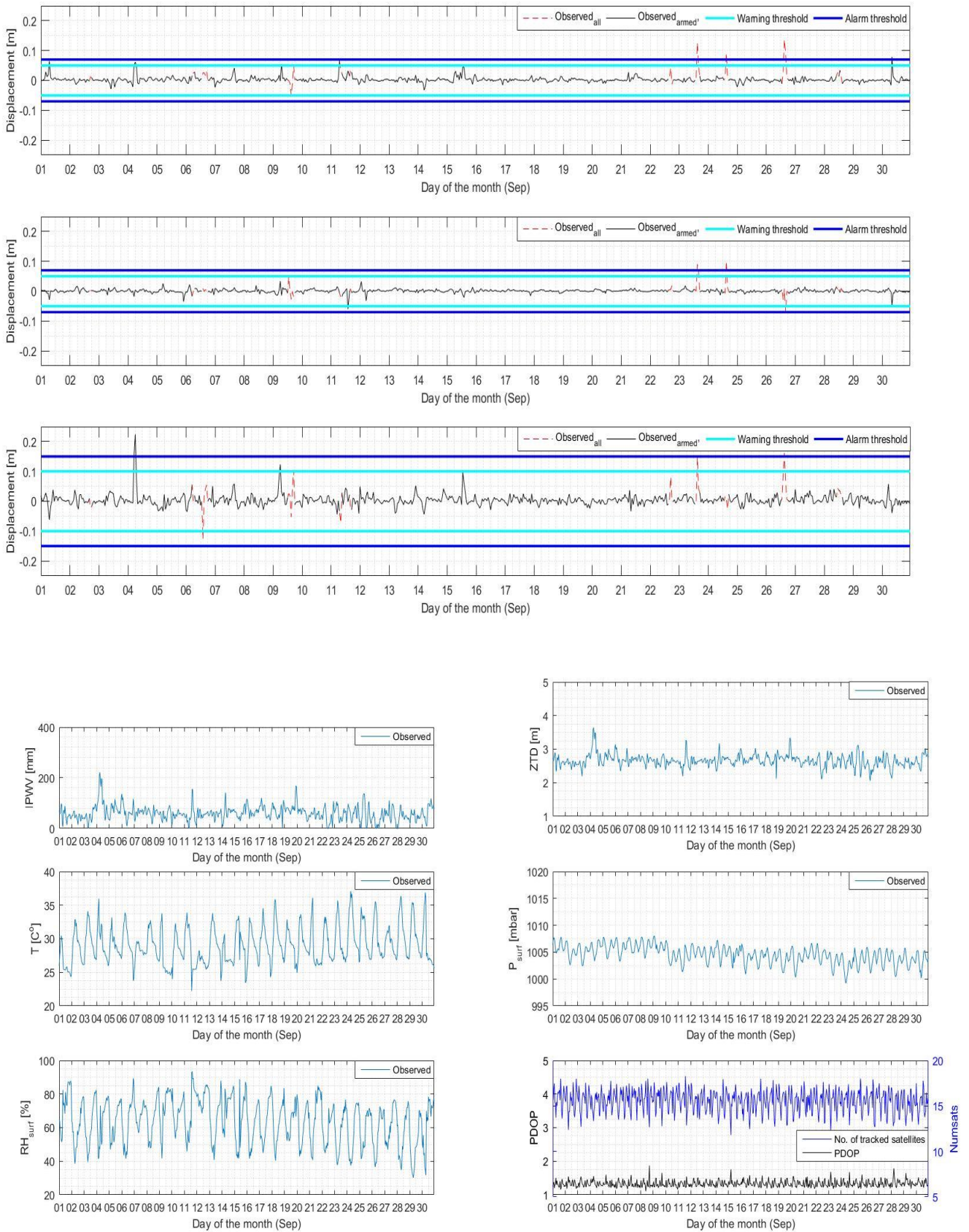
Figure A.6.5: Graphs visualizing the IM displacements (top), and the Tropospheric information, PDOP values and number of tracked satellites (bottom) as observed by the SRPT CORS during September 2016.

SNYU
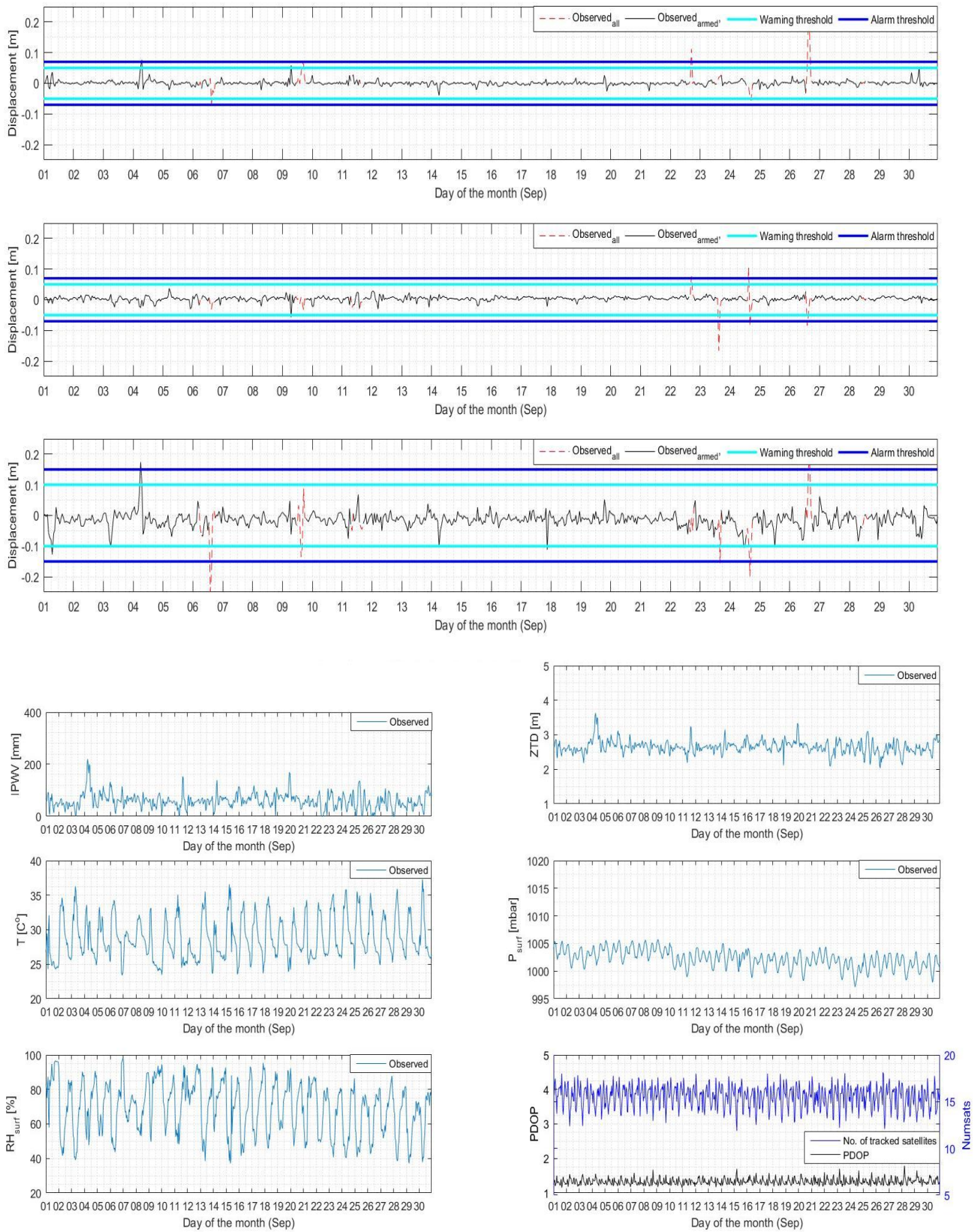
Figure A. 6.6: Graphs visualizing the IM displacements (top), and the Tropospheric information, PDOP values and number of tracked satellites (bottom) as observed by the SNYU CORS during September 2016.

SNUS
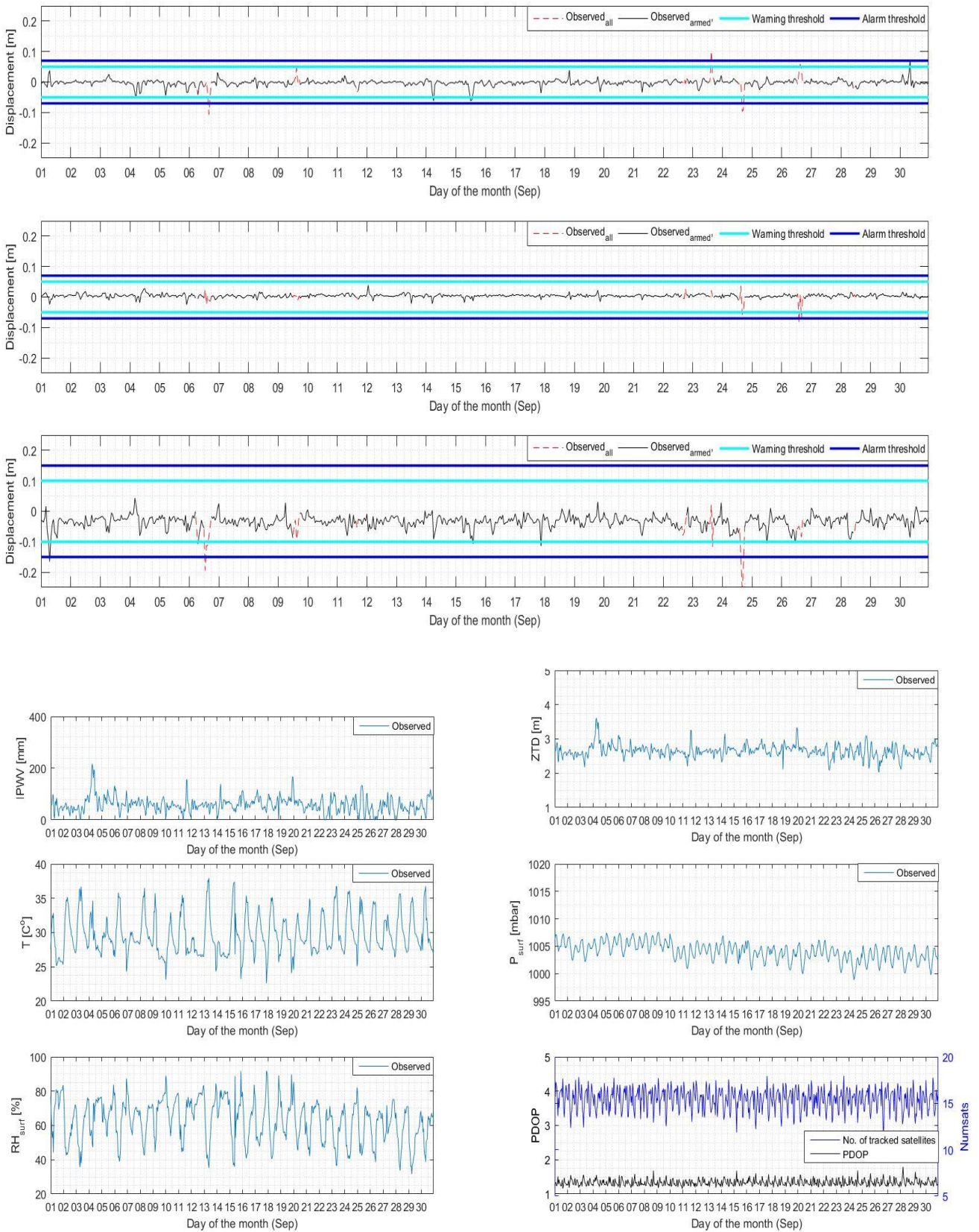
Figure A. 6.7: Graphs visualizing the IM displacements (top), and the Tropospheric information, PDOP values and number of tracked satellites (bottom) as observed by the SNUS CORS during September 2016.

Appendix 7: *IM displacement data and atmospheric information (RTK engine module in Baseline mode) from October 2016*
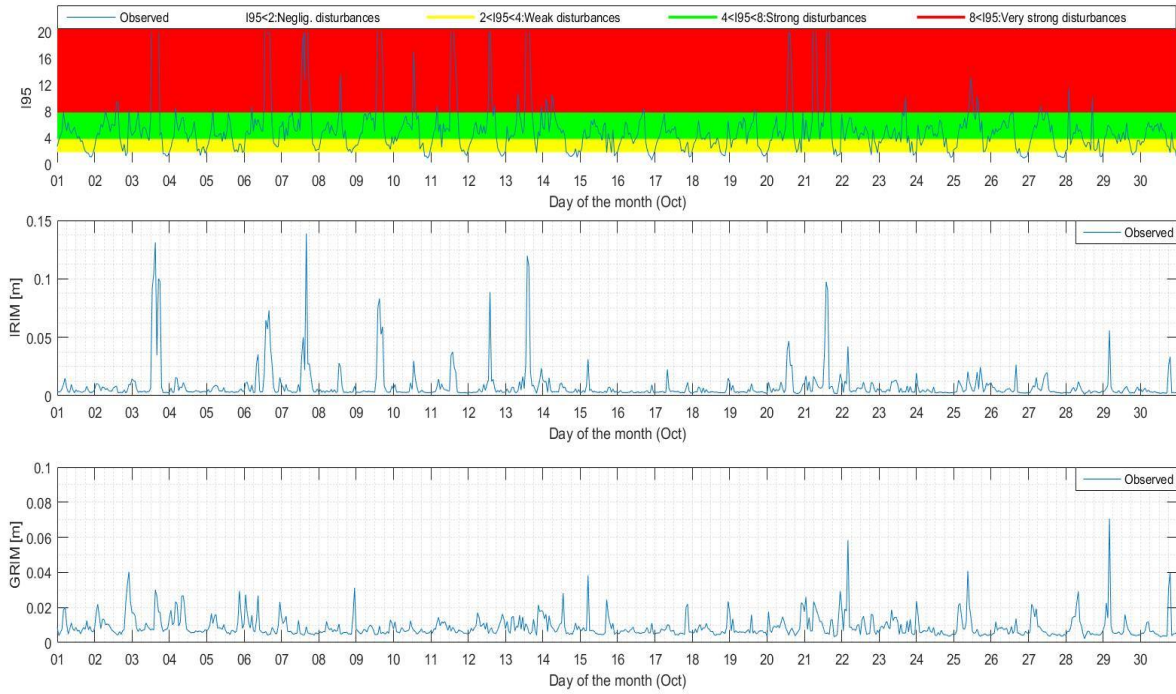
Figure A.7.1: Graphs visualizing the I95/GRIM/IRIM values as observed by SiReNT during October 2016. For a more detailed explanation of the graphs, see 'Appendix 6 and Appendix 7 Figures explained'.
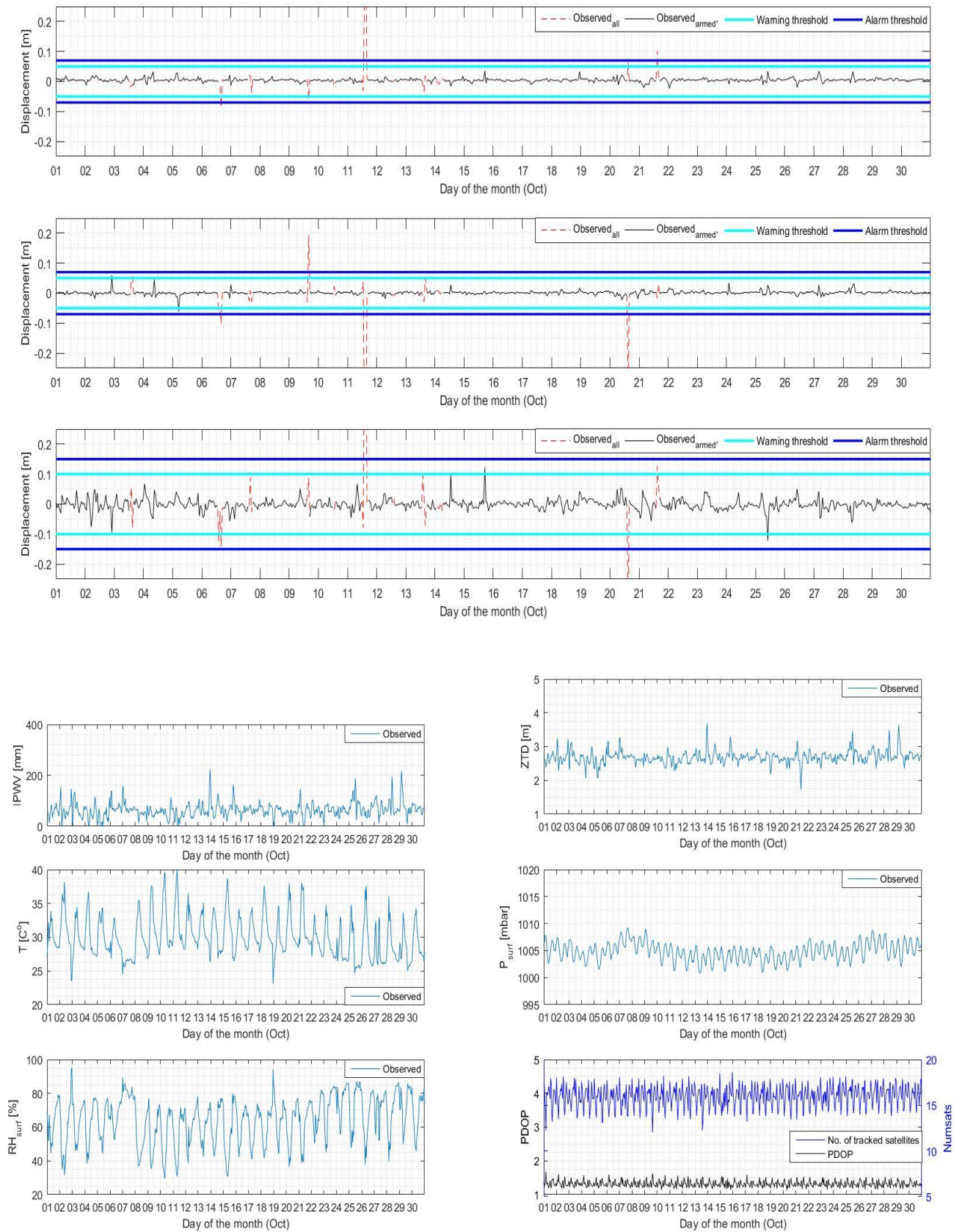
SLYG

Figure A.7.2: Graphs visualizing the IM displacements (top), and the Tropospheric information, PDOP values and number of tracked satellites (bottom) as observed by the SLYG CORS during October 2016. For a more detailed explanation of the graphs, see 'Appendix 6 and Appendix 7 Figures explained'.

SSTS
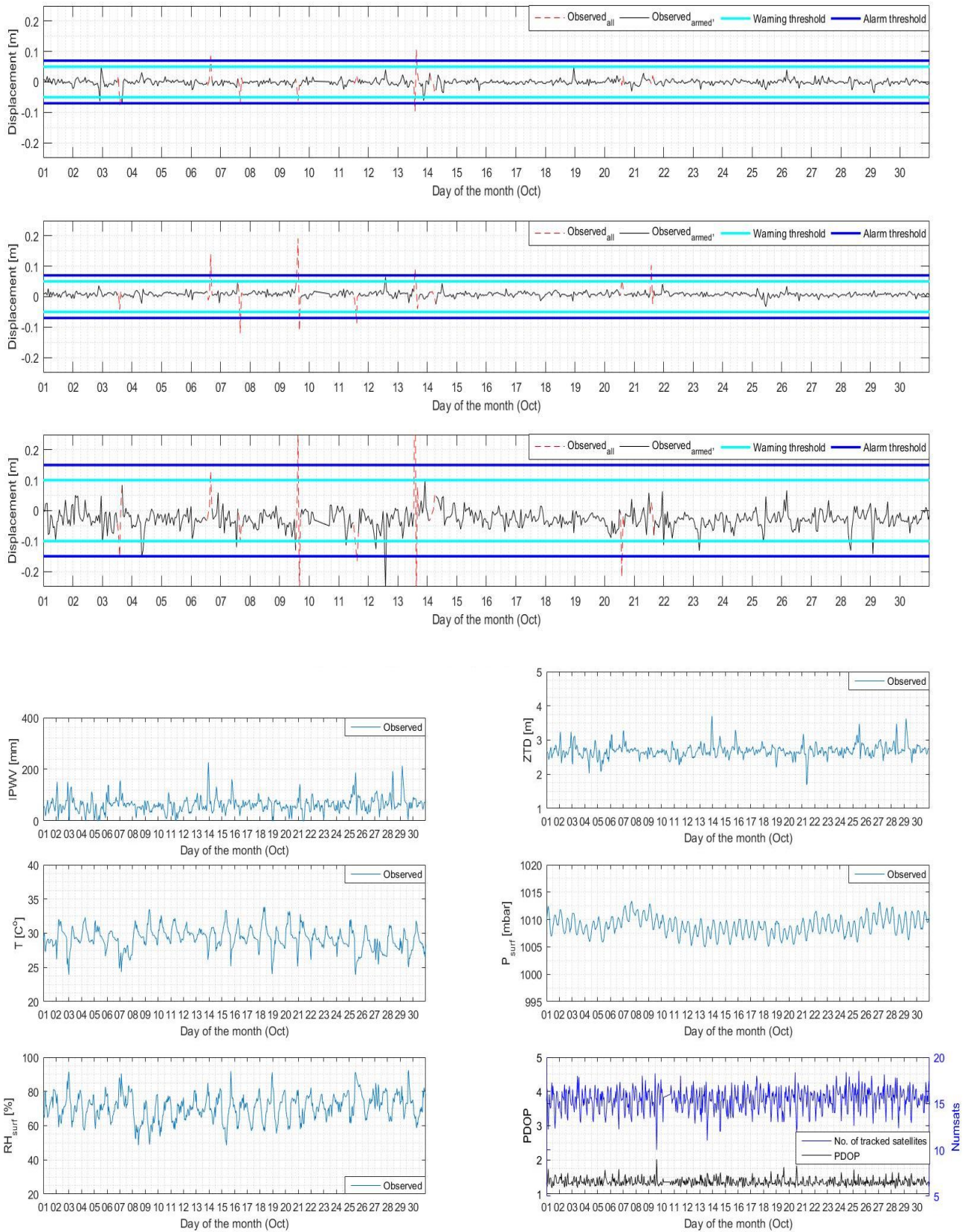
Figure A.7.3: Graphs visualizing the IM displacements (top), and the Tropospheric information, PDOP values and number of tracked satellites (bottom) as observed by the SSTS CORS during October 2016.

SSMK

Figure A.7.4: Graphs visualizing the IM displacements (top), and the Tropospheric information, PDOP values and number of tracked satellites (bottom) as observed by the SSMK CORS during October 2016.

SRPT
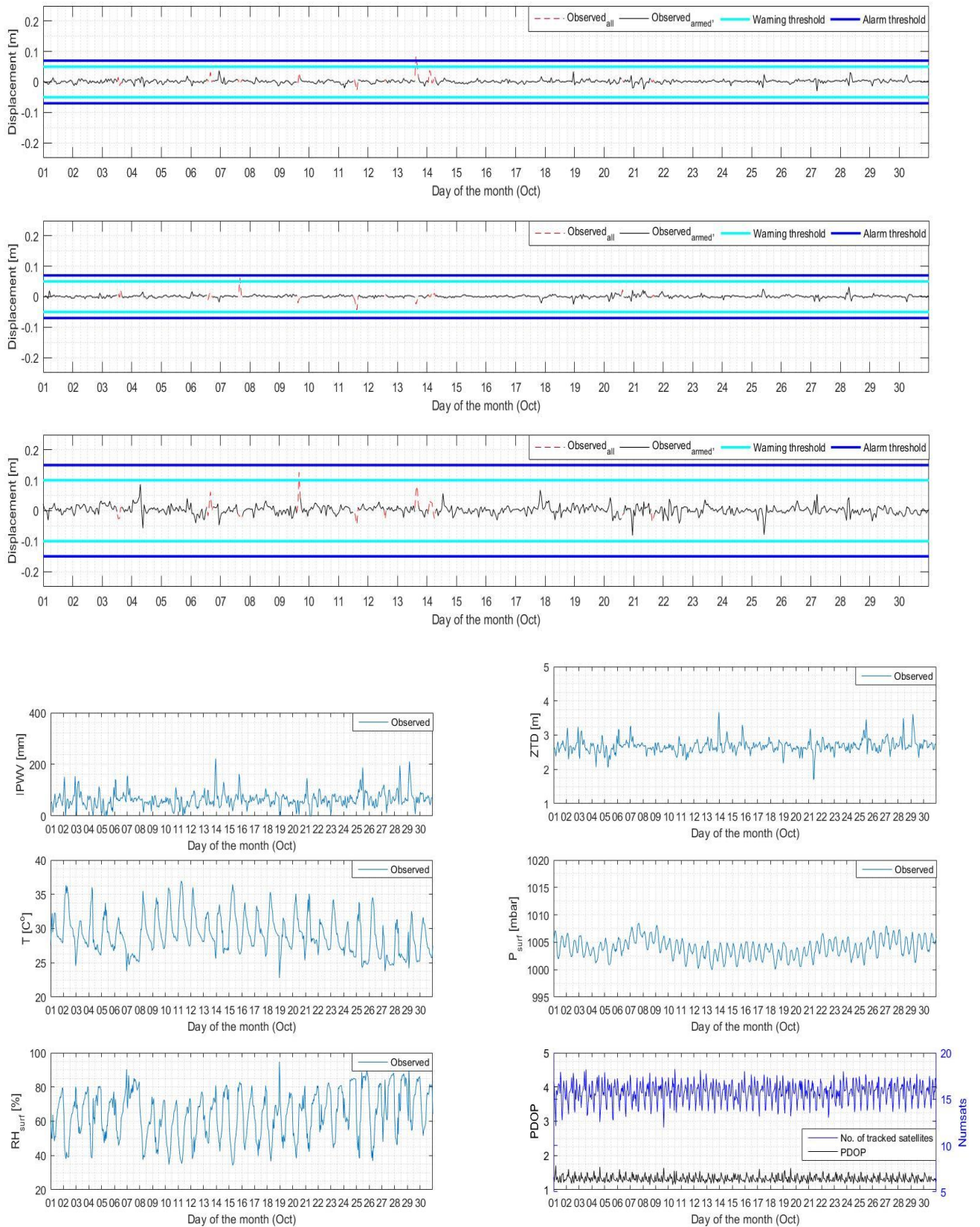
Figure A.7.5: Graphs visualizing the IM displacements (top), and the Tropospheric information, PDOP values and number of tracked satellites (bottom) as observed by the SRPT CORS during October 2016.

SNYU

Figure A. 7.6: Graphs visualizing the IM displacements (top), and the Tropospheric information, PDOP values and number of tracked satellites (bottom) as observed by the SNYU CORS during October 2016.

186

SNUS

Figure A. 7.7: Graphs visualizing the IM displacements (top), and the Tropospheric information, PDOP values and number of tracked satellites (bottom) as observed by the SNUS CORS during October 2016.

Appendix 8: *IM displacement data, from the RTK engine module in VRS mode*

SLYG

SLYG, northing

SLYG, easting

SLYG, height

Figure A.8.1: Graphs visualizing the displacements in the northing component (top), the easting component (middle), the height (bottom), as observed by the SLYG CORS (period: 11-07-'17 – 31-07-'17). For a more detailed explanation of the graphs, see '8.1 Figures/Table explained I'.

SRPT

SRPT, northing

SRPT, easting

SRPT, height

Figure A.8.2: Graphs visualizing the displacements in the northing component (top), the easting component (middle), the height (bottom), as observed by the SRPT CORS (period: 11-07-'17 – 31-07-'17).

SNSC

SNSC, northing

SNSC, easting

SNSC, height

Figure A.8.3: Graphs visualizing the displacements in the northing component (top), the easting component (middle), the height (bottom), as observed by the SNSC CORS (period: 11-07-'17 – 31-07-'17).
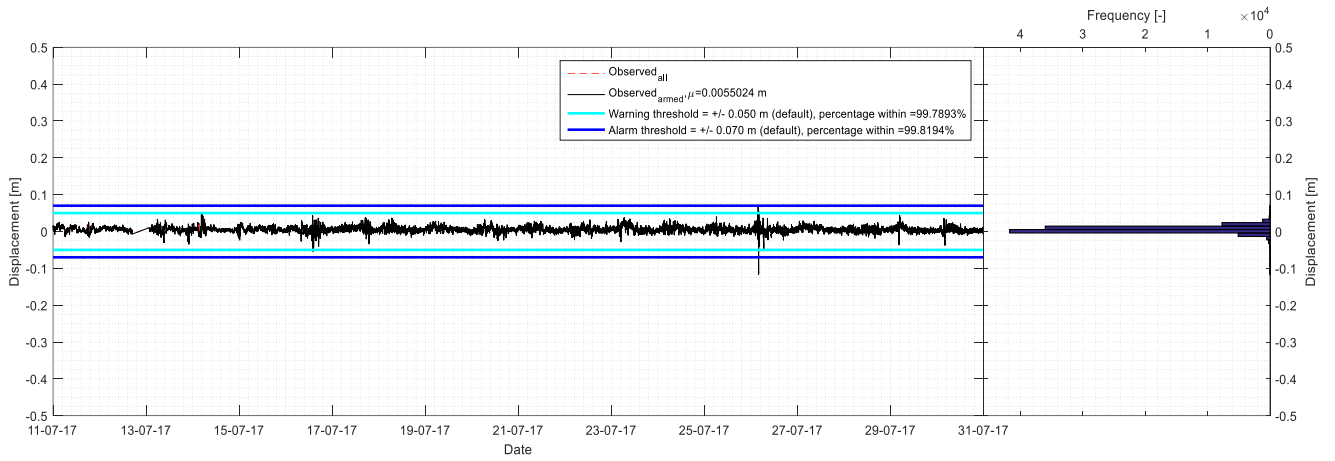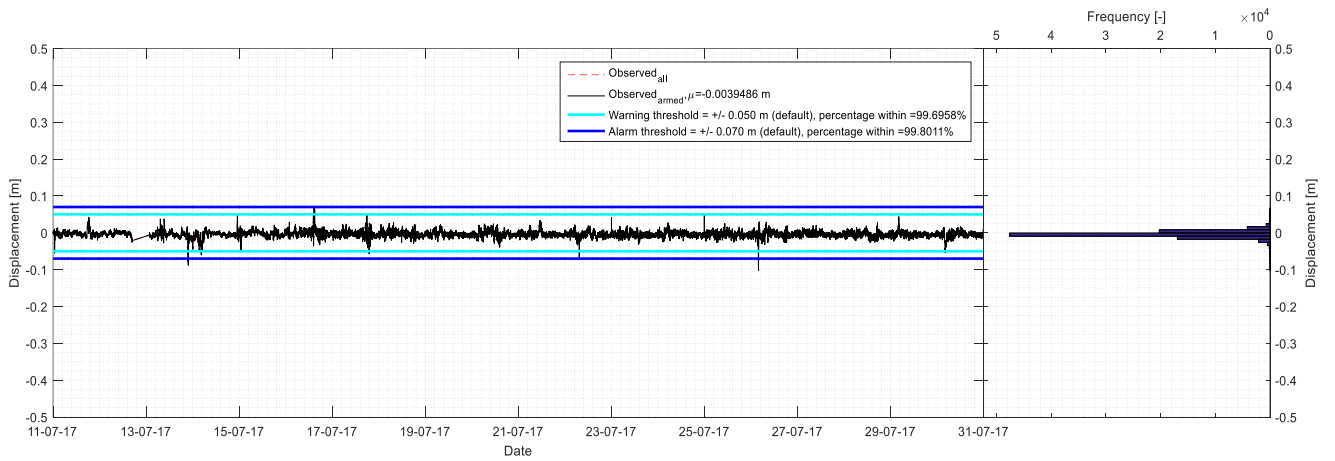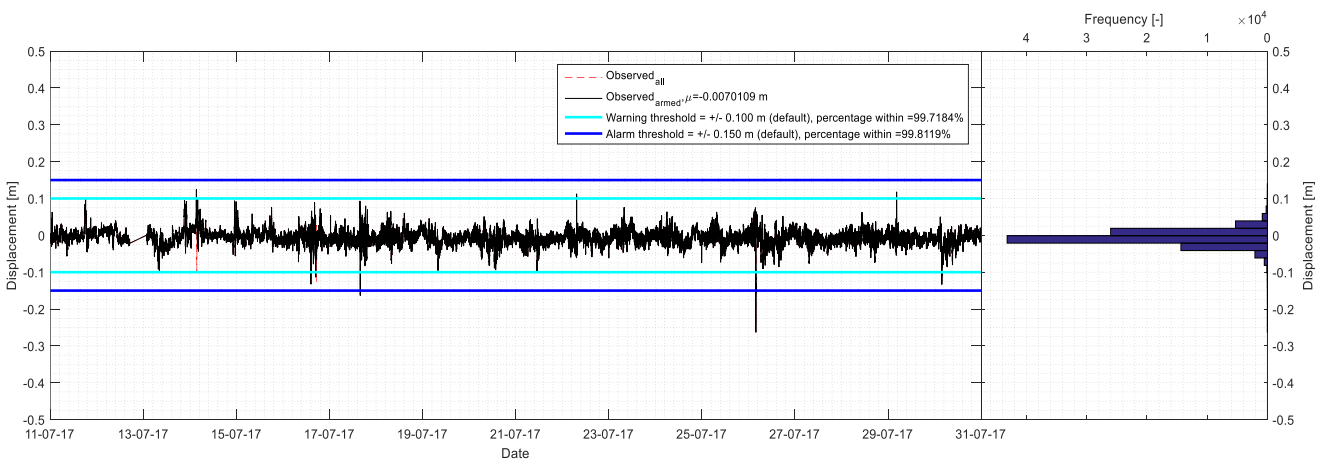
Figure A.8.4: Graphs visualizing the displacements in the northing component (top), the easting component (middle), the height (bottom), as observed by the SNUS CORS (period: 11-07-'17 – 31-07-'17).

191
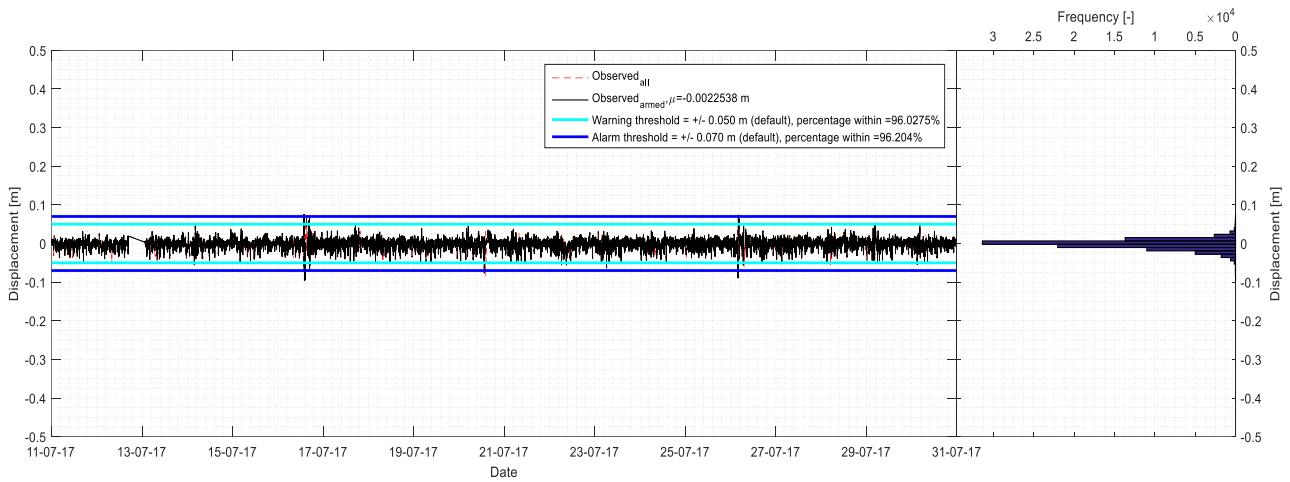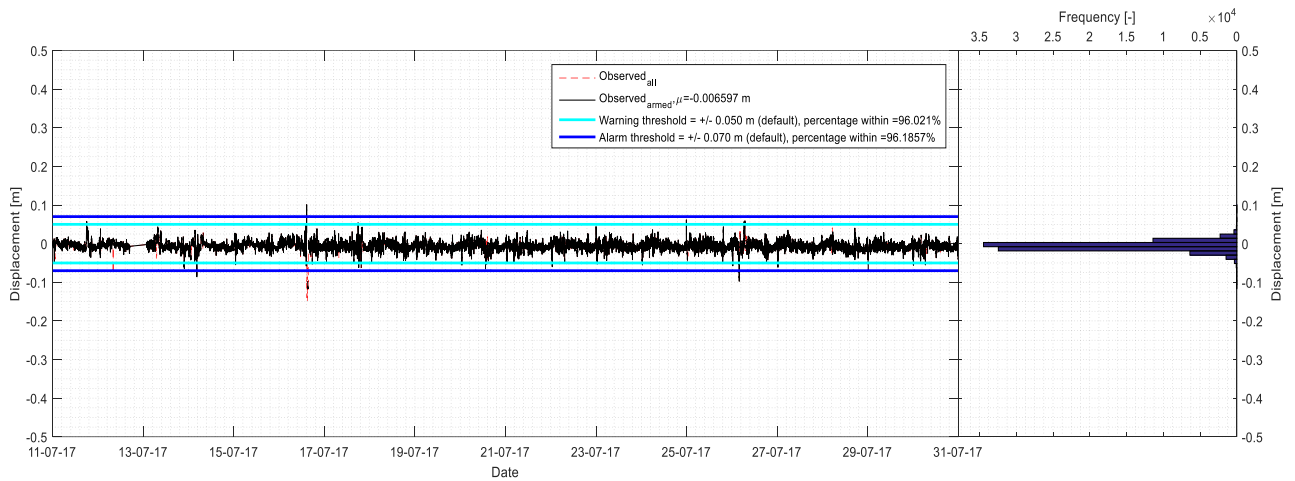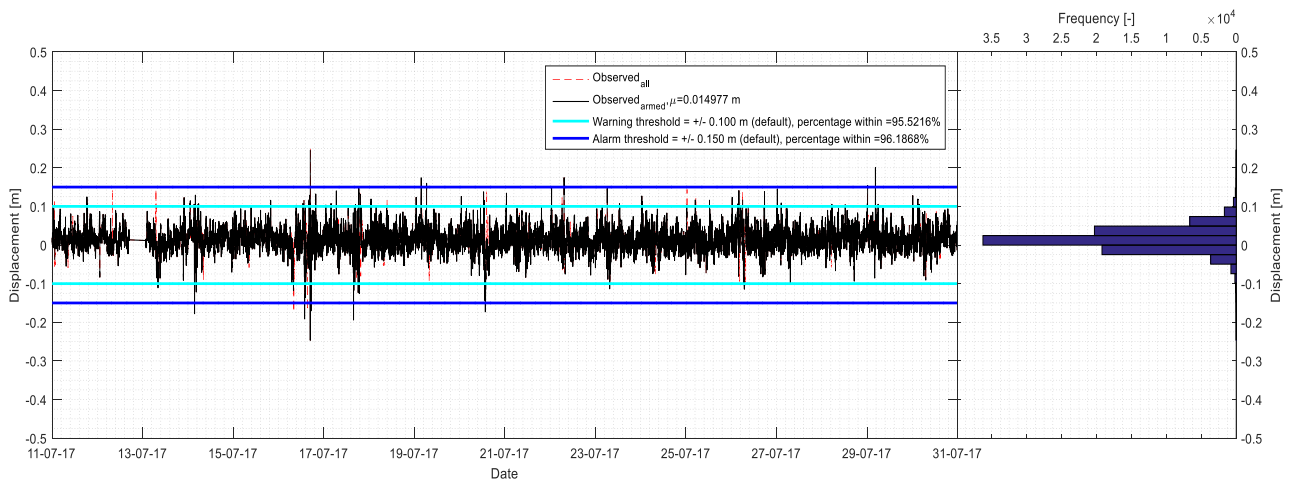
SING

Figure A.8.5: Graphs visualizing the displacements in the northing component (top), the easting component (middle), the height (bottom), as observed by the SING CORS (period: 11-07-'17 – 31-07-'17).

Appendix 9: *Rover (re-)initialization time, atmospheric information, PDOP value, the number of tracked satellites.*

SLYG
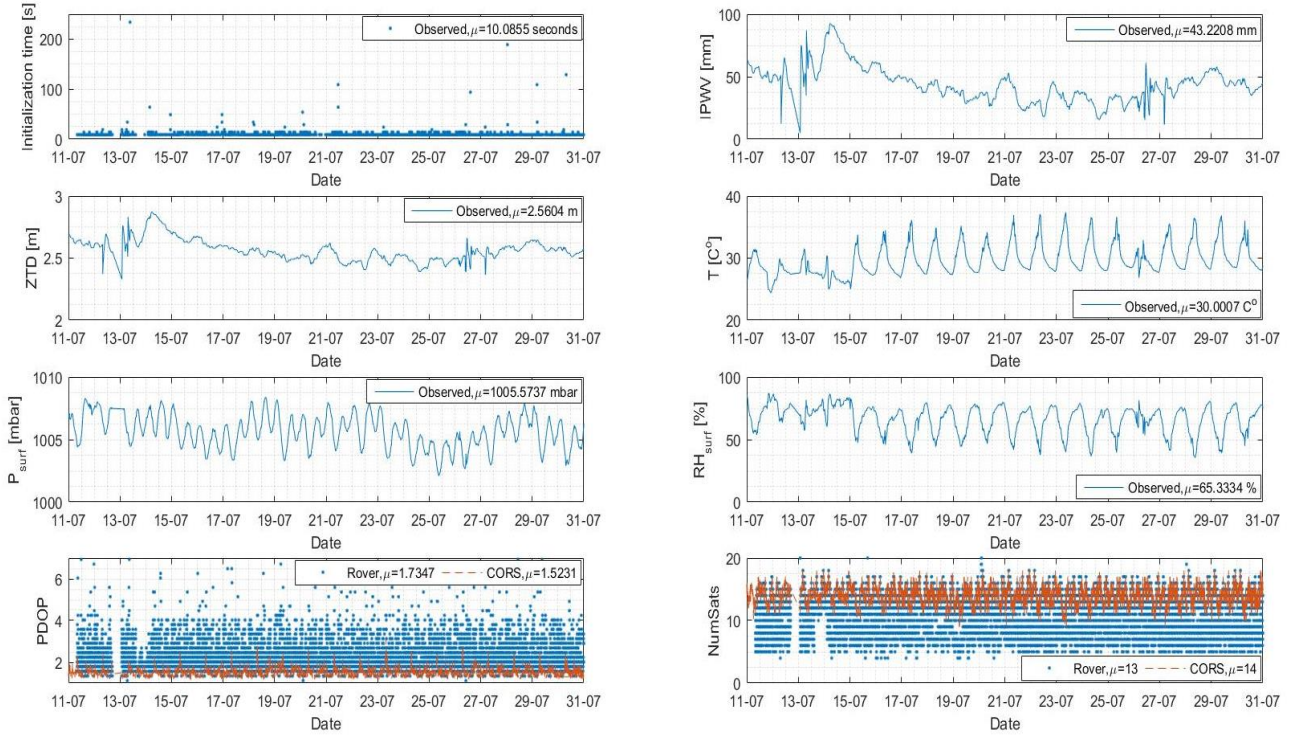
SRPT
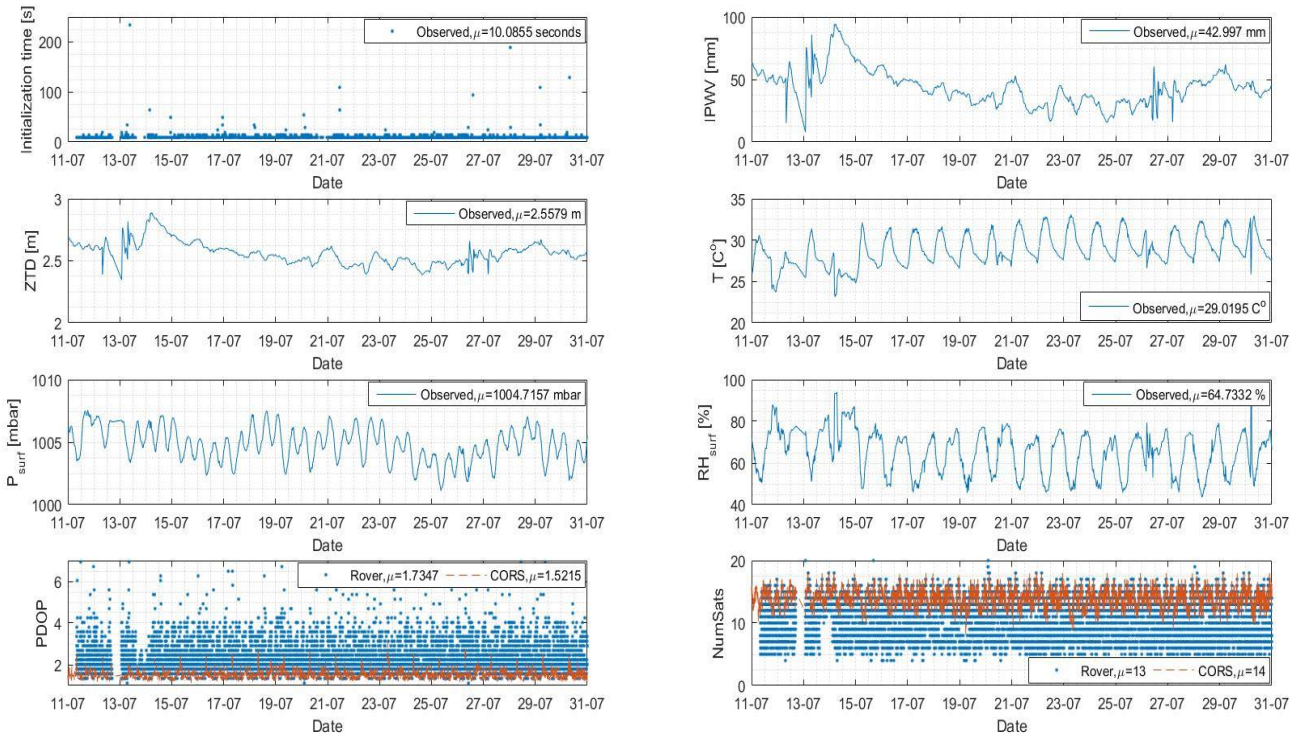
Figure A.9.1-2: Graphs visualizing the (re-)initialization time, Tropospheric information, PDOP value, and the number of tracked satellites as observed by the SLYG CORS (top), the SRPT CORS (bottom) (period: 11-07-'17 – 31-07-'17). For a more detailed explanation of the graphs, see '8.1 Figures explained II'.

SNSC
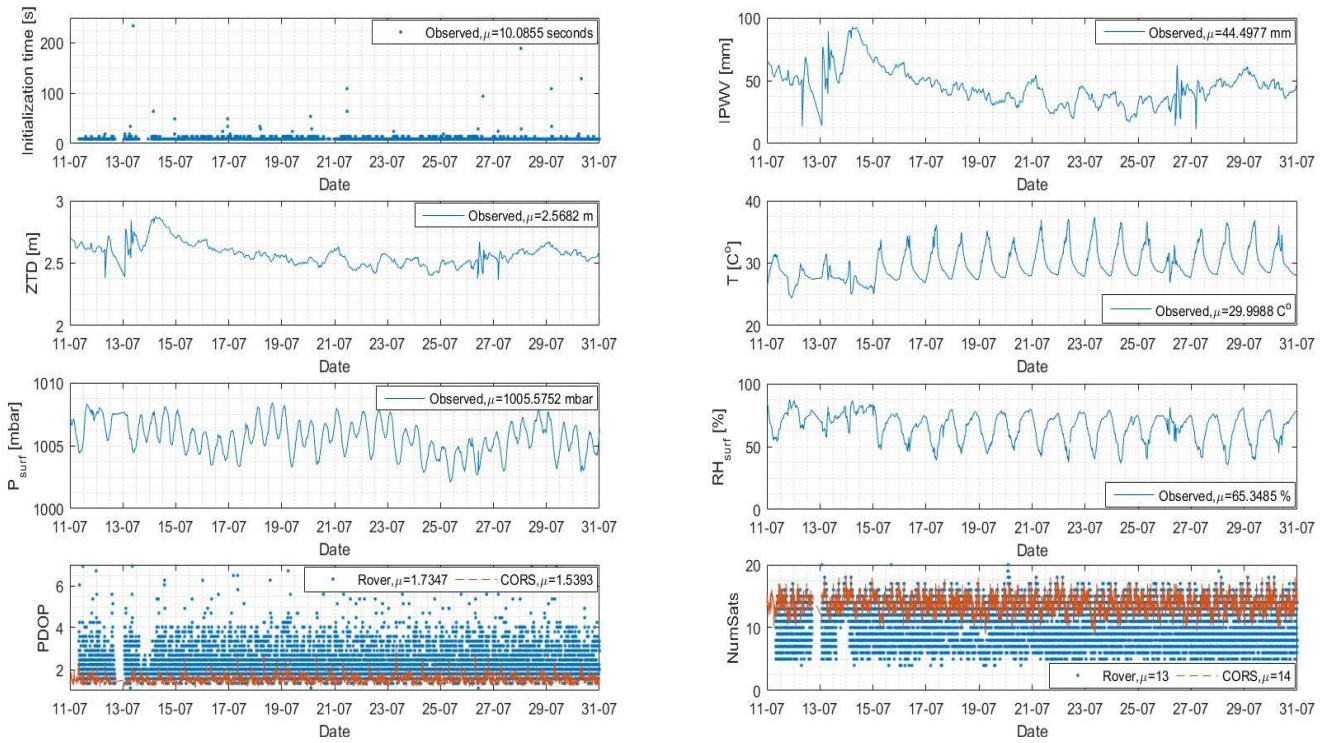
SNUS
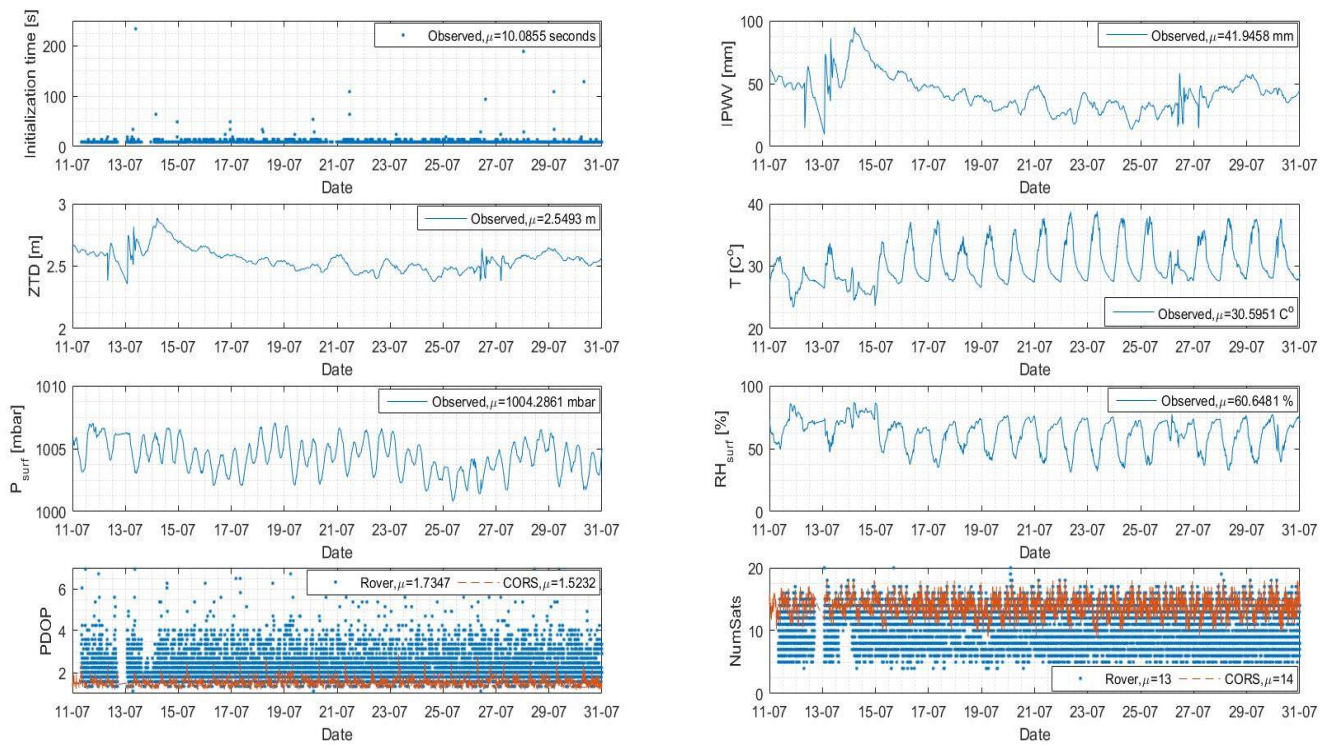
Figure A.9.3-4: Graphs visualizing the (re-)initialization time, Tropospheric information, PDOP value, and the number of tracked satellites as observed by the SNSC CORS (top), and the SNUS CORS (bottom) (period: 11-07-'17 – 31-07-'17).
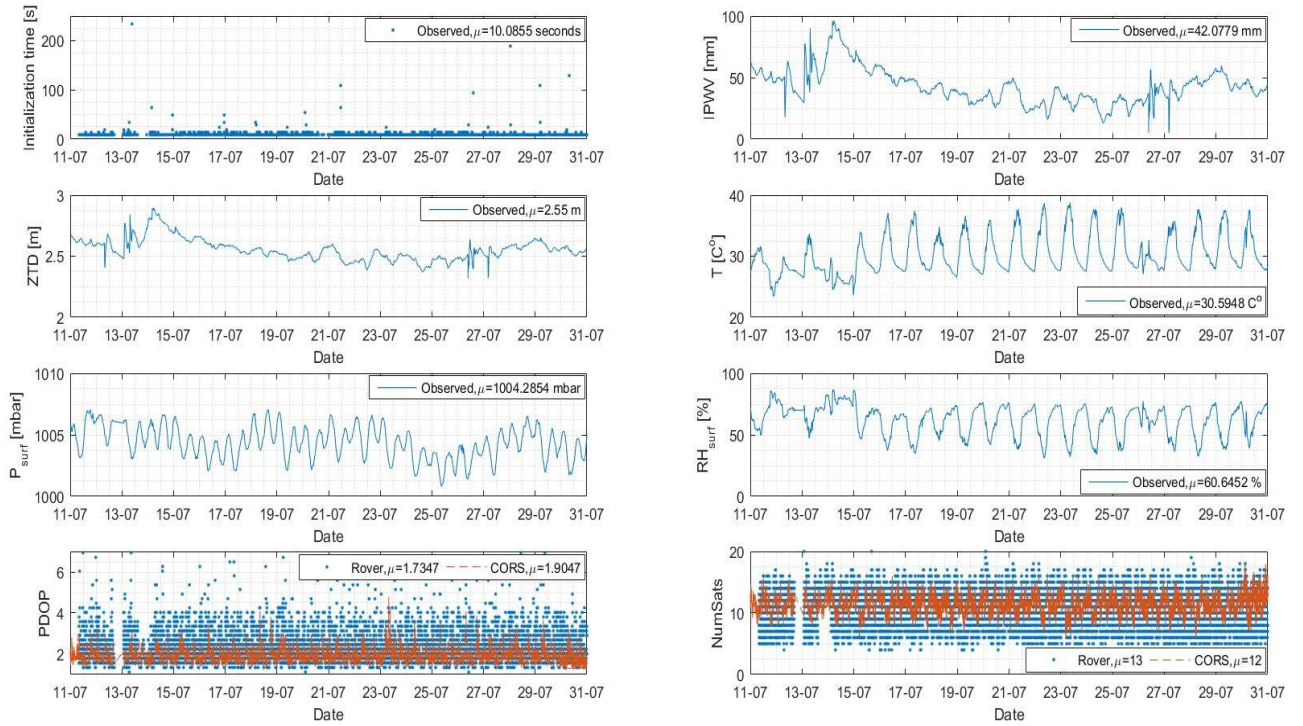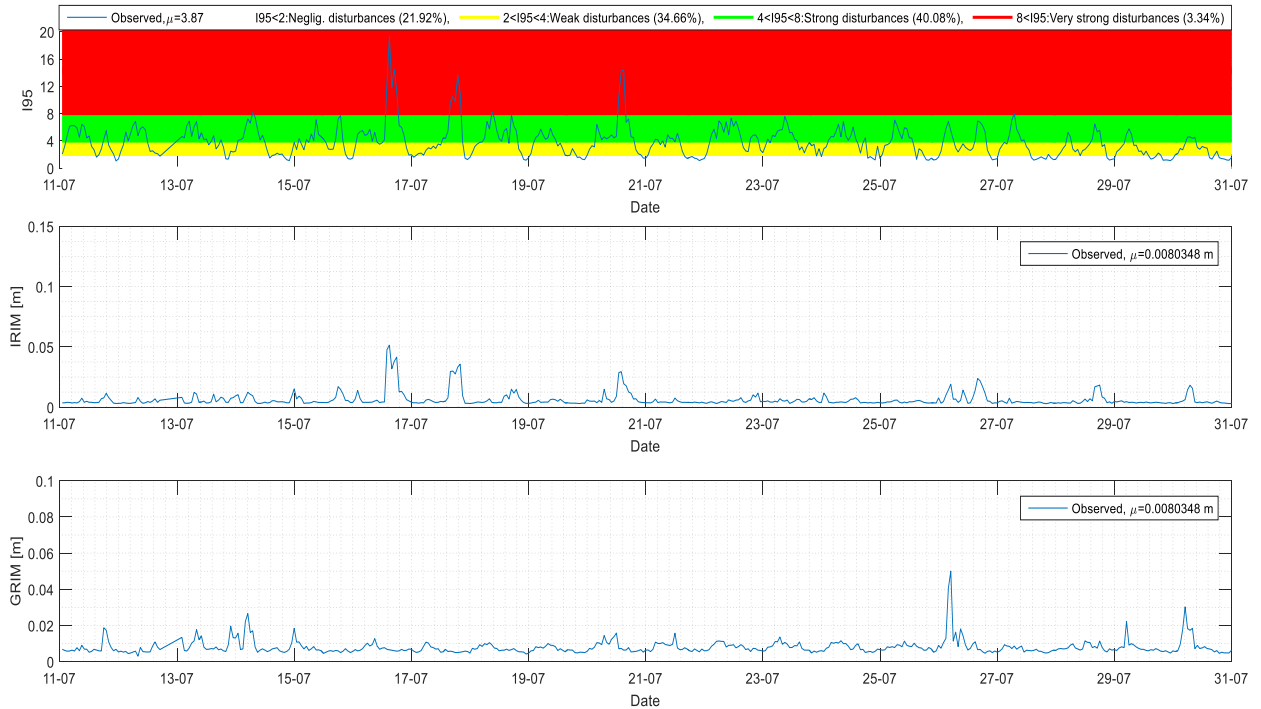
Figure A.9.5-6: Graphs visualizing the (re-)initialization time, Tropospheric information, PDOP value, and the number of tracked satellites as observed by the SING CORS (top), alongside with the I95/IRIM/GRIM graph (bottom) (period: 11-07-'17 – 31-07-'17). For a more detailed explanation of the graphs, see '8.1 Figures explained II'.

Appendix 10: *The correlation (Pearson) coefficient*

The correlation coefficient is a measure of the linear correlation (strength and direction) between two variables (x_1, x_2) [22][33][40] and is given by:

$$\rho_{x_1, x_2} = \frac{cov(x_1, x_2)}{\sigma_{x_1} \sigma_{x_2}}$$

The resulting value will be between -1 and +1 and have the following meaning:

- A value of -1 represents total negative linear correlation;
- A value of +1 represents total positive linear correlation;
- A value of 0 represents no linear correlation at all.

In case there is a total positive or negative correlation (+/- 1), variable x_2 is known when variable x_1 is known, and vice versa.
This can be visualized as well, by plotting one variable (x_1) versus the other (x_2) in a scatterplot (see Figure A.10.1).
The shape of the resulting point cloud is related to the amount of linear correlation between the two variables; from the shape of the cloud it can easily be determined whether the amount of correlation is high or low. Values close to the extremes (+/- 1), will have point clouds that are clearly showing a linear relation, the slope of which is dependent on the sign (+ versus -) (see Figure A.10.1, right). A correlation coefficient of 0 however will result in a random point cloud, which is not showing any linear correlation at all (see Figure A.10.1, middle).
Note that this correlation coefficient is scale free, and sensitive to outliers.
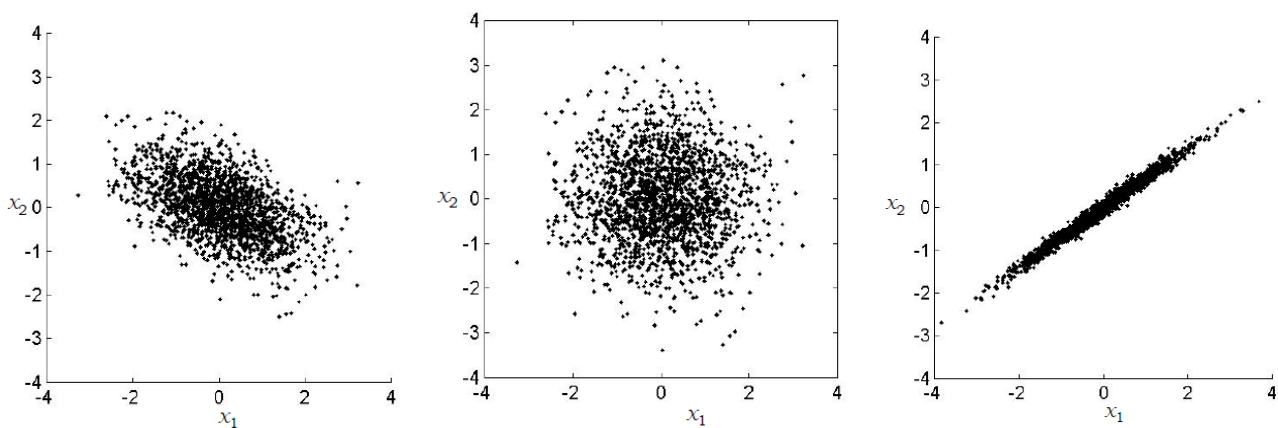
Figure A.10.1: Graphs visualizing examples of possible scatterplot shapes, left: a linear correlation coefficient of -0.5 (a negative linear correlation), middle: a linear correlation coefficient of 0 (no linear correlation), and right: a linear correlation coefficient of 0.99 (a very high positive linear correlation) [22].

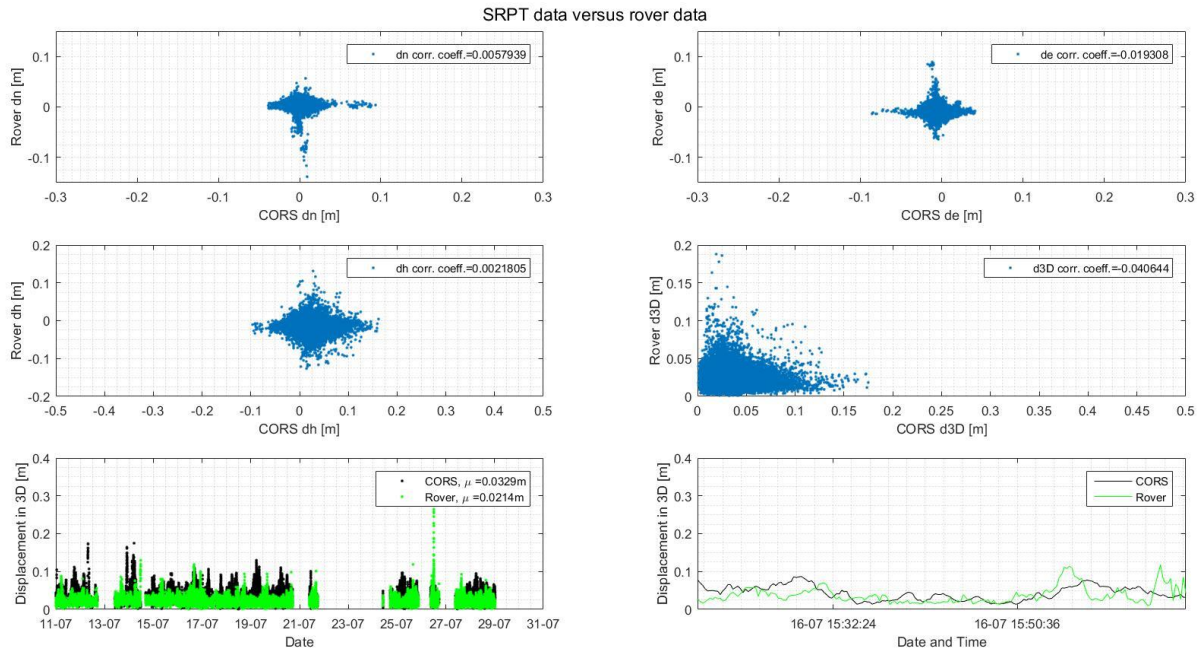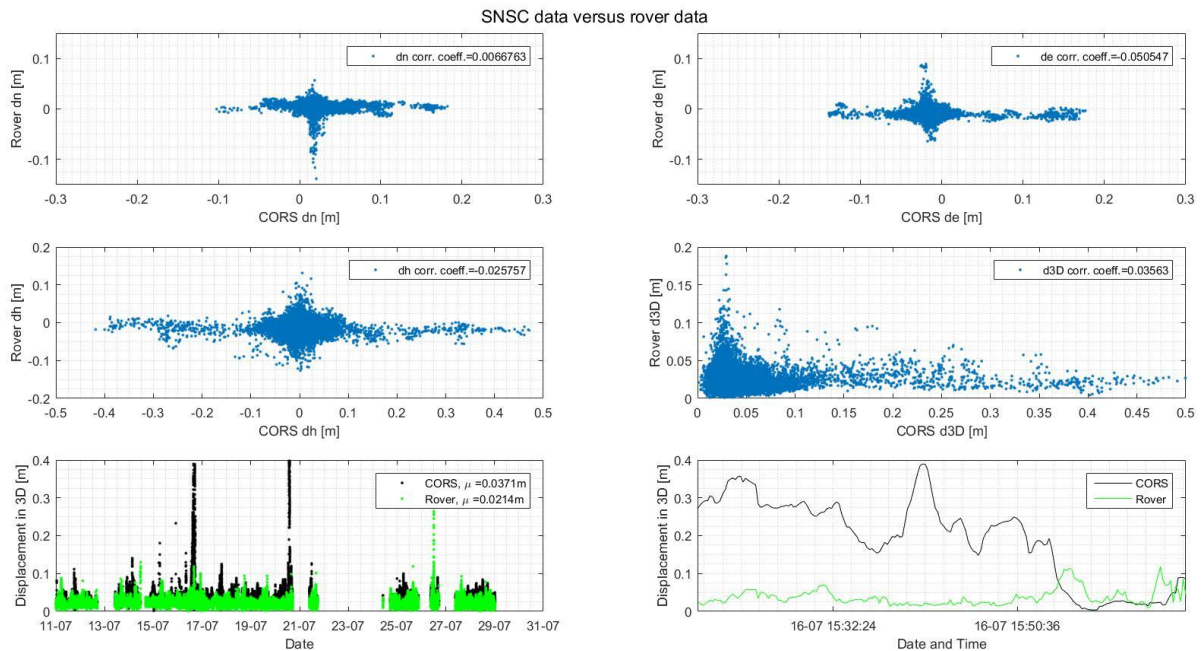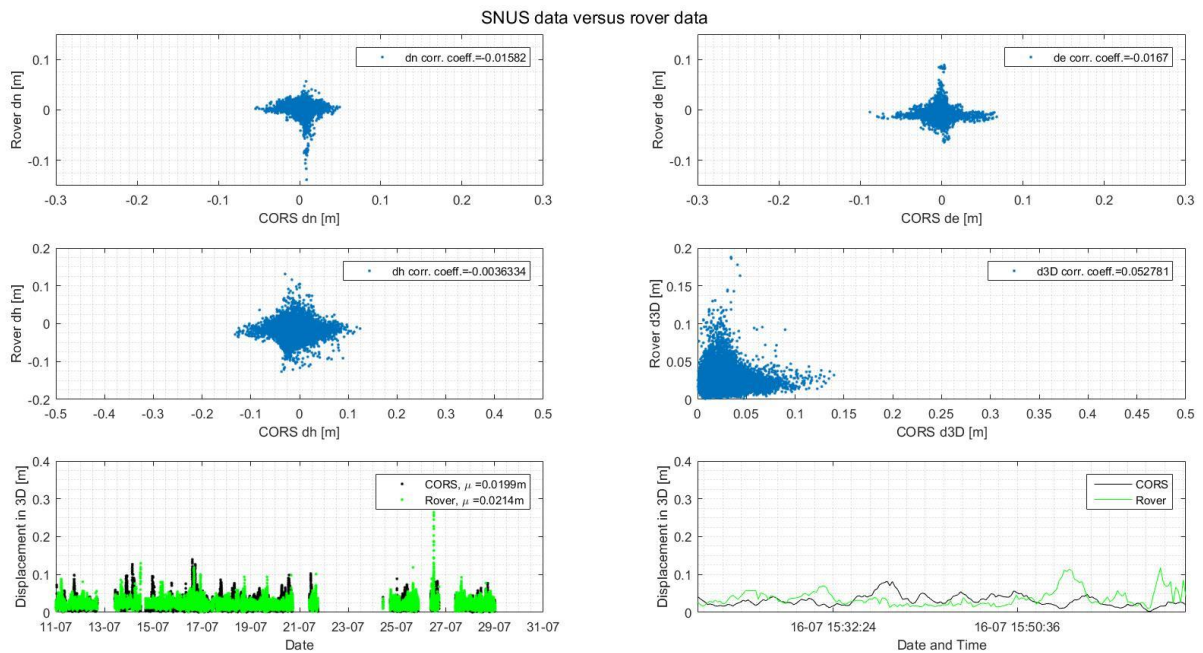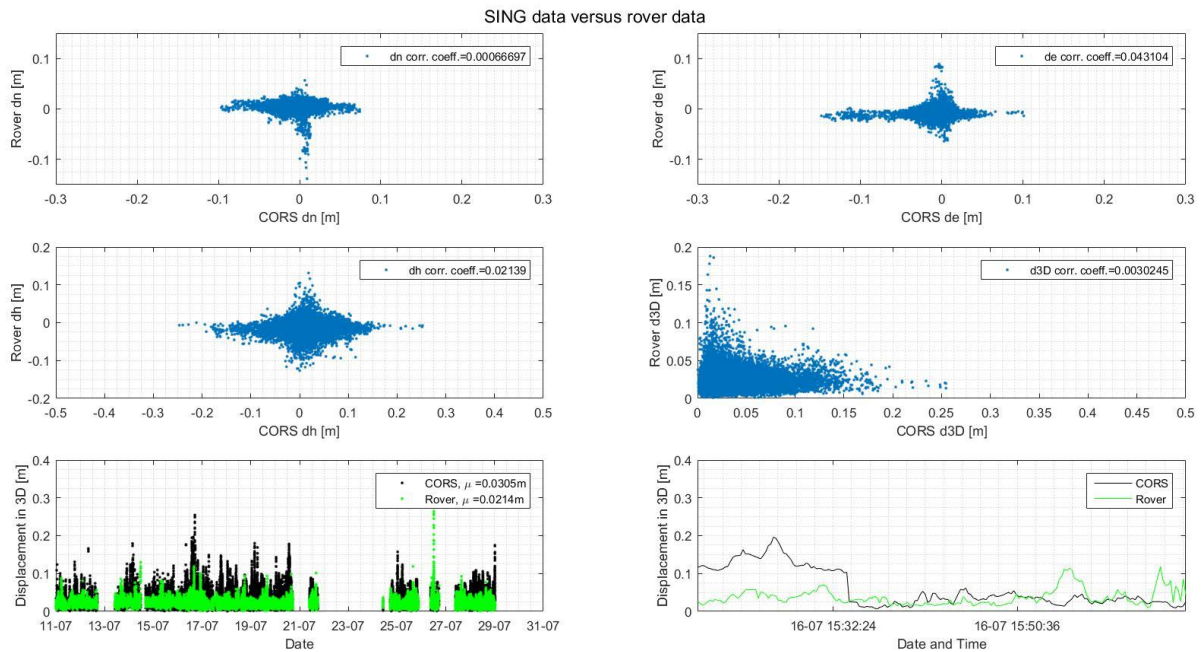**Appendix 11:** *The correlation graphs I*

SLYG
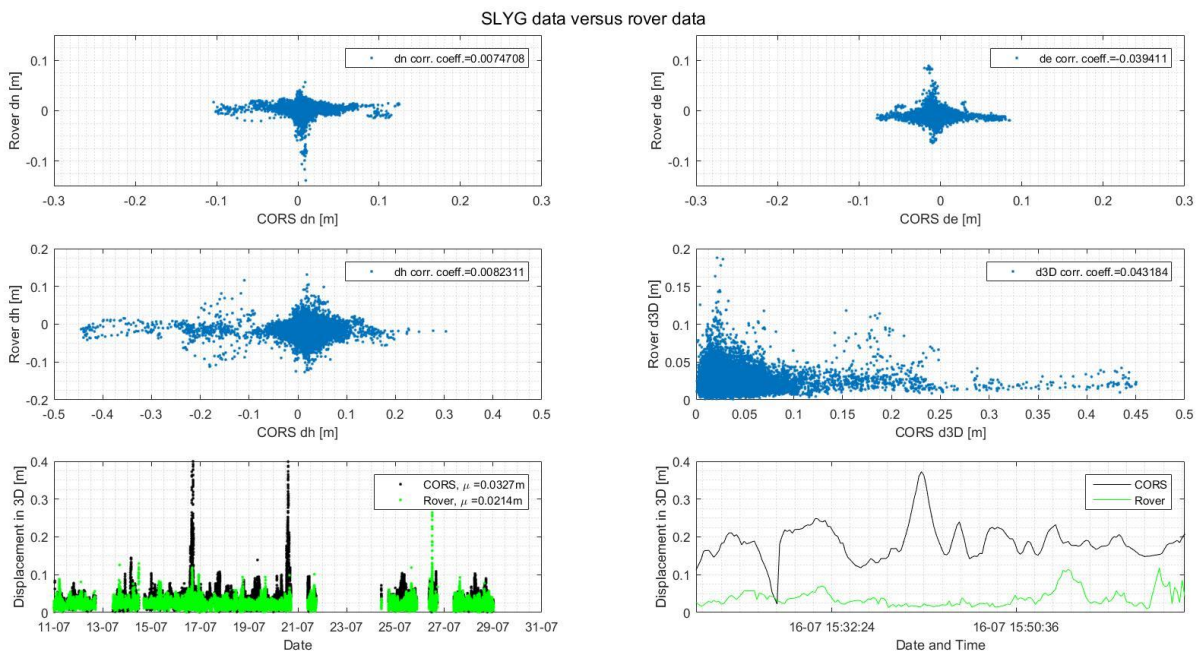
Figure A.11.1: Graphs visualizing the correlation between the SLYG IM displacement data and the Rover displacement data, and graphs visualizing the displacements in the 3D component, for both the Rover and the CORS (period: 11-07-'17 – 31-07-'17). The first are visualized in the upper and middle panels (; northing: upper left, easting: upper right, height: middle left, and 3D: middle right), and the latter is visualized in the bottom panels (; complete displacement data: bottom left, and zoomed in; bottom right). For a more detailed explanation of the graphs, see '8.1 Figures/Table explained IIII'.

SRPT

Figure A.11.2: Graphs visualizing the correlation between the SRPT IM displacement data and the Rover displacement data, and graphs visualizing the displacements in the 3D component, for both the Rover and the CORS (period: 11-07-'17 – 31-07-'17). The first are visualized in the upper and middle panels (; northing: upper left, easting: upper right, height: middle left, and 3D: middle right), and the latter is visualized in the bottom panels (; complete displacement data: bottom left, and zoomed in; bottom right).
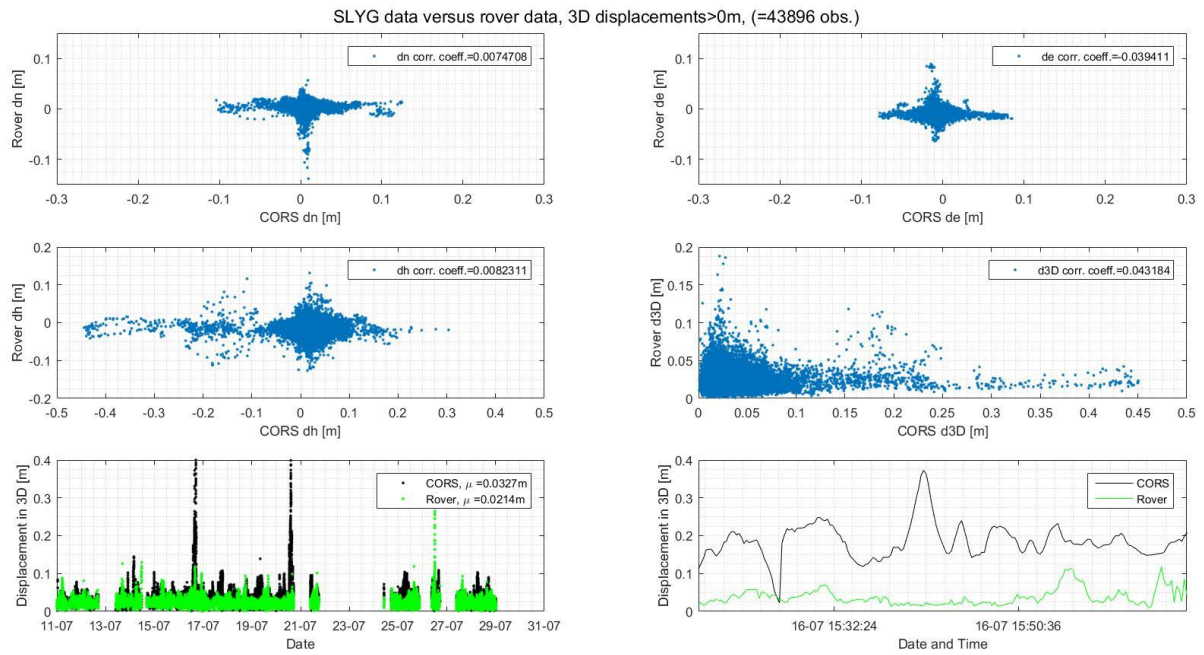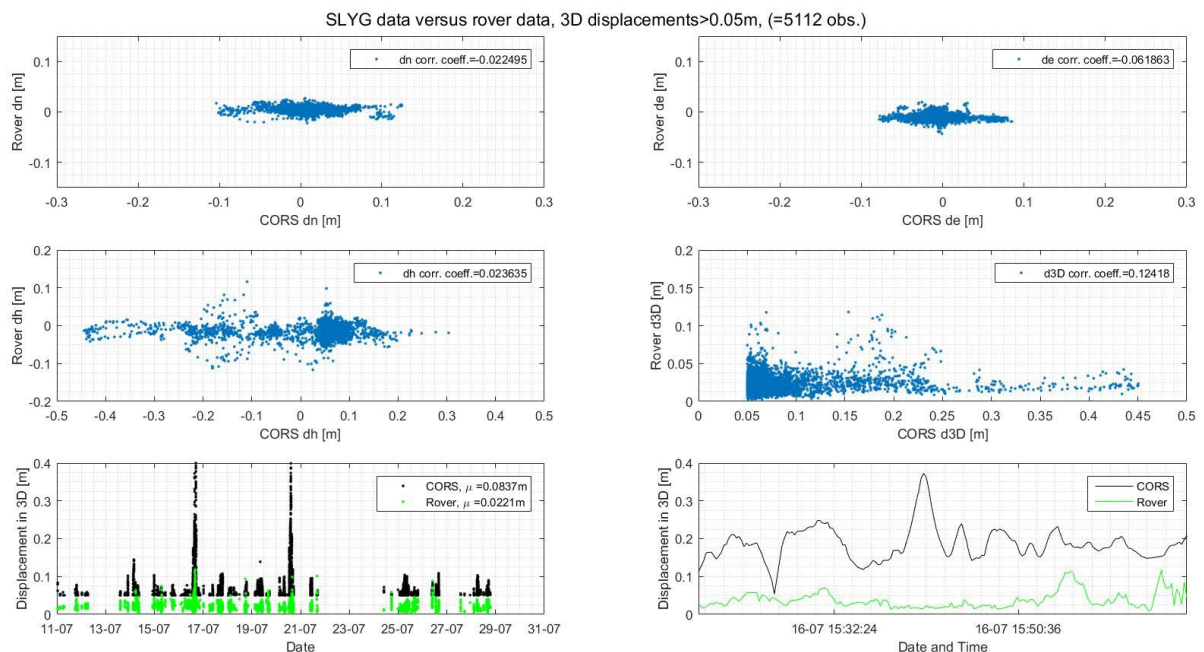
SNSC

Figure A.11.3: Graphs visualizing the correlation between the SNSC IM displacement data and the Rover displacement data, and graphs visualizing the displacements in the 3D component, for both the Rover and the CORS (period: 11-07-'17 – 31-07-'17). The first are visualized in the upper and middle panels (; northing: upper left, easting: upper right, height: middle left, and 3D: middle right), and the latter is visualized in the bottom panels (; complete displacement data: bottom left, and zoomed in; bottom right).

198

SNUS

Figure A.11.4: Graphs visualizing the correlation between the SNUS IM displacement data and the Rover displacement data, and graphs visualizing the displacements in the 3D component, for both the Rover and the CORS (period: 11-07-'17 – 31-07-'17). The first are visualized in the upper and middle panels (; northing: upper left, easting: upper right, height: middle left, and 3D: middle right), and the latter is visualized in the bottom panels (; complete displacement data: bottom left, and zoomed in; bottom right).
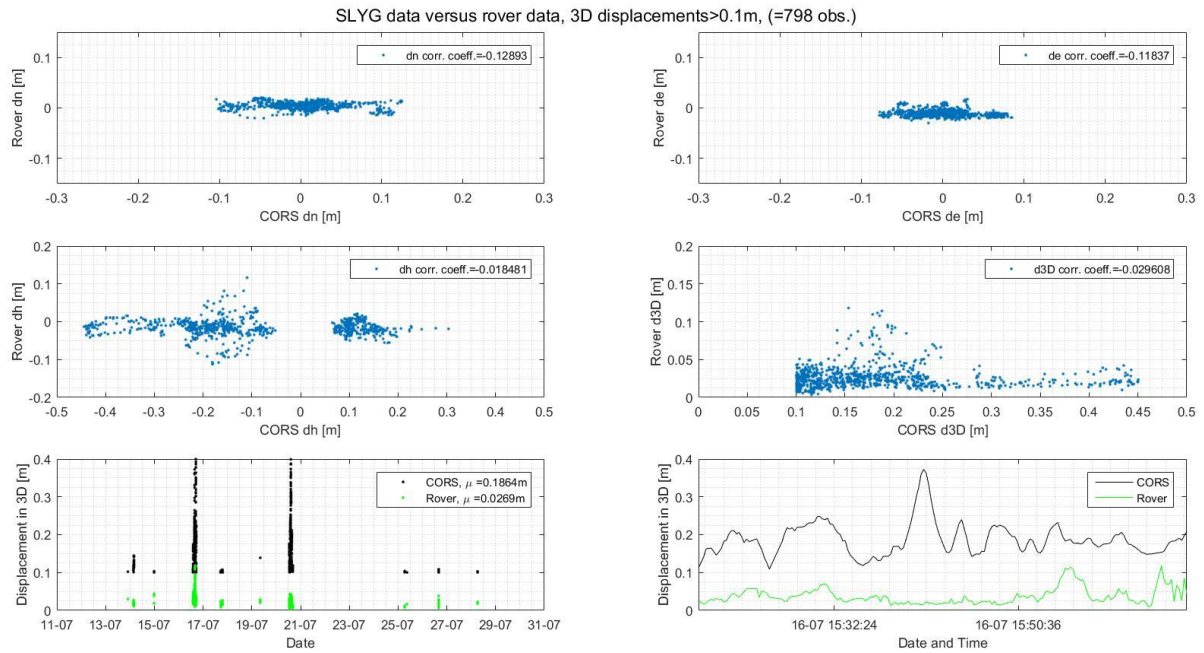
SING

Figure A.11.5: Graphs visualizing the correlation between the SING IM displacement data and the Rover displacement data, and graphs visualizing the displacements in the 3D component, for both the Rover and the CORS (period: 11-07-'17 – 31-07-'17). The first are visualized in the upper and middle panels (; northing: upper left, easting: upper right, height: middle left, and 3D: middle right), and the latter is visualized in the bottom panels (; complete displacement data: bottom left, and zoomed in; bottom right).
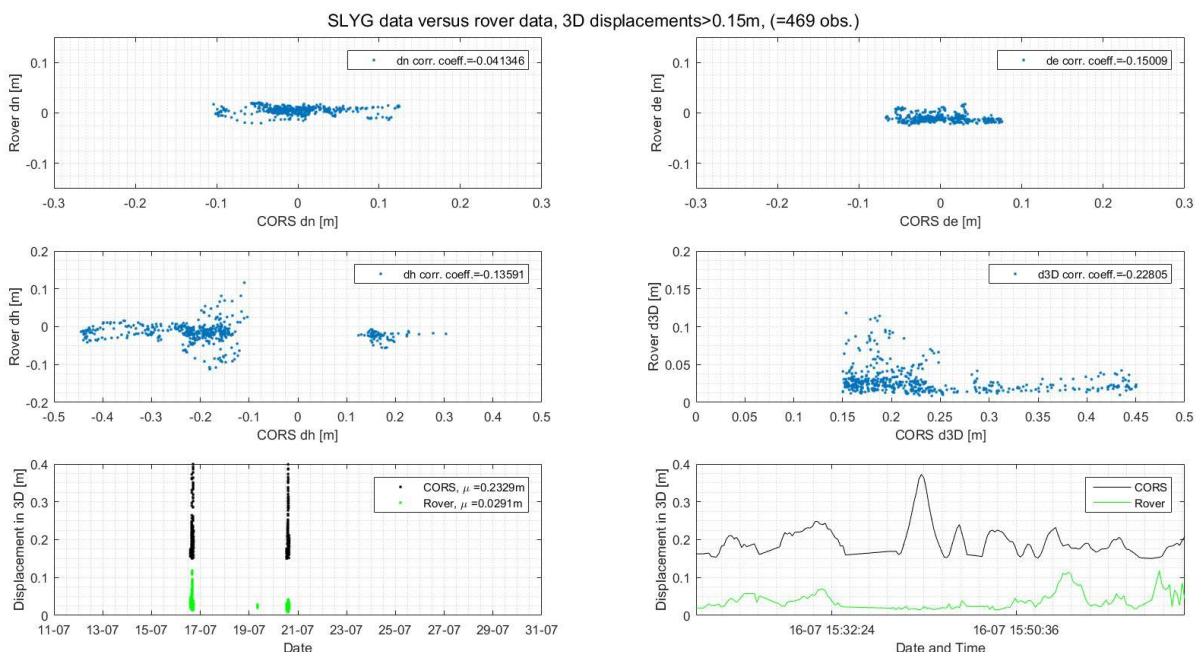
SLYG data versus rover data, 3D displacements>0m, (=43896 obs.)

Figure A.12.1: Graphs visualizing the correlation between the SLYG IM displacement data and the Rover displacement data, and graphs visualizing the displacements in the 3D component, for both the Rover and the CORS, everything of all 3D displacements. The first are visualized in the upper and middle panels (; northing: upper left, easting: upper right, height: middle left, and 3D: middle right), and the latter is visualized in the bottom panels (; complete displacement data: bottom left, and zoomed in; bottom right). For a more detailed explanation of the graphs, see '8.1 Figures/Table explained IIII'.

SLYG data versus rover data, 3D displacements>0.05m, (=5112 obs.)

Figure A.12.1: Graphs visualizing the correlation between the SLYG IM displacement data and the Rover displacement data, and graphs visualizing the displacements in the 3D component, for both the Rover and the CORS, everything of all 3D displacements exceeding 0.05 meters. The first are visualized in the upper and middle panels (; northing: upper left, easting: upper right, height: middle left, and 3D: middle right), and the latter is visualized in the bottom panels (; complete displacement data: bottom left, and zoomed in; bottom right).
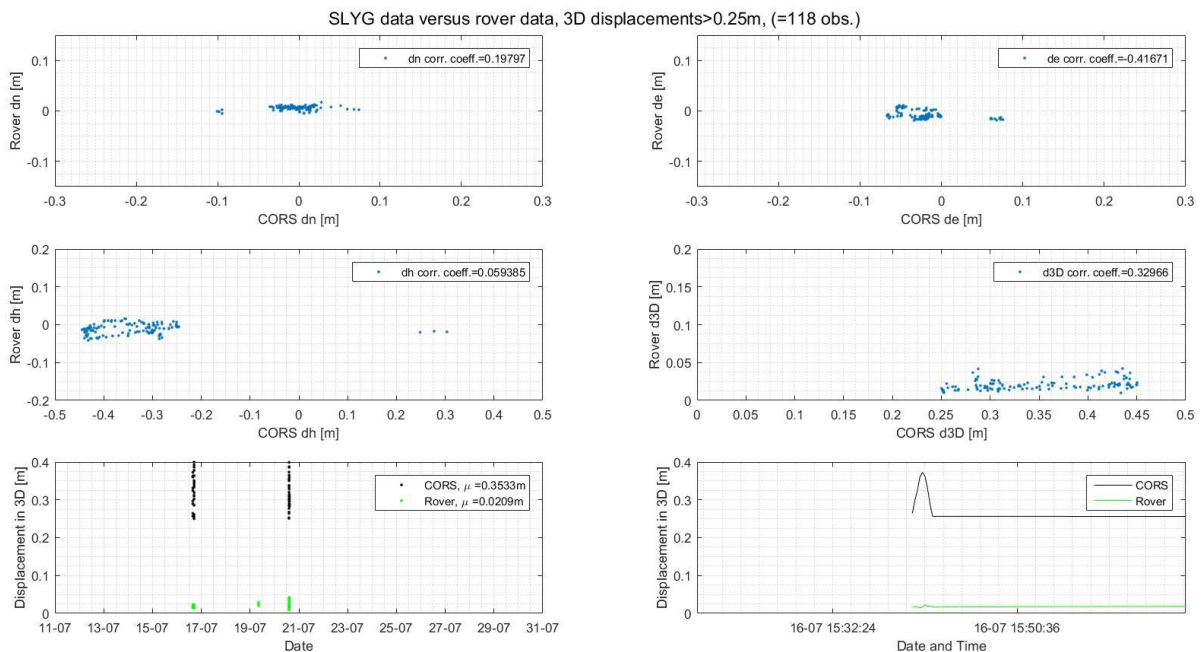
Figure A.12.3: Graphs visualizing the correlation between the SLYG IM displacement data and the Rover displacement data, and graphs visualizing the displacements in the 3D component, for both the Rover and the CORS, everything of all 3D displacements exceeding 0.1 meters. The first are visualized in the upper and middle panels (; northing: upper left, easting: upper right, height: middle left, and 3D: middle right), and the latter is visualized in the bottom panels (; complete displacement data: bottom left, and zoomed in; bottom right).

Figure A.12.4: Graphs visualizing the correlation between the SLYG IM displacement data and the Rover displacement data, and graphs visualizing the displacements in the 3D component, for both the Rover and the CORS, everything of all 3D displacements exceeding 0.15 meters. The first are visualized in the upper and middle panels (; northing: upper left, easting: upper right, height: middle left, and 3D: middle right), and the latter is visualized in the bottom panels (; complete displacement data: bottom left, and zoomed in; bottom right).
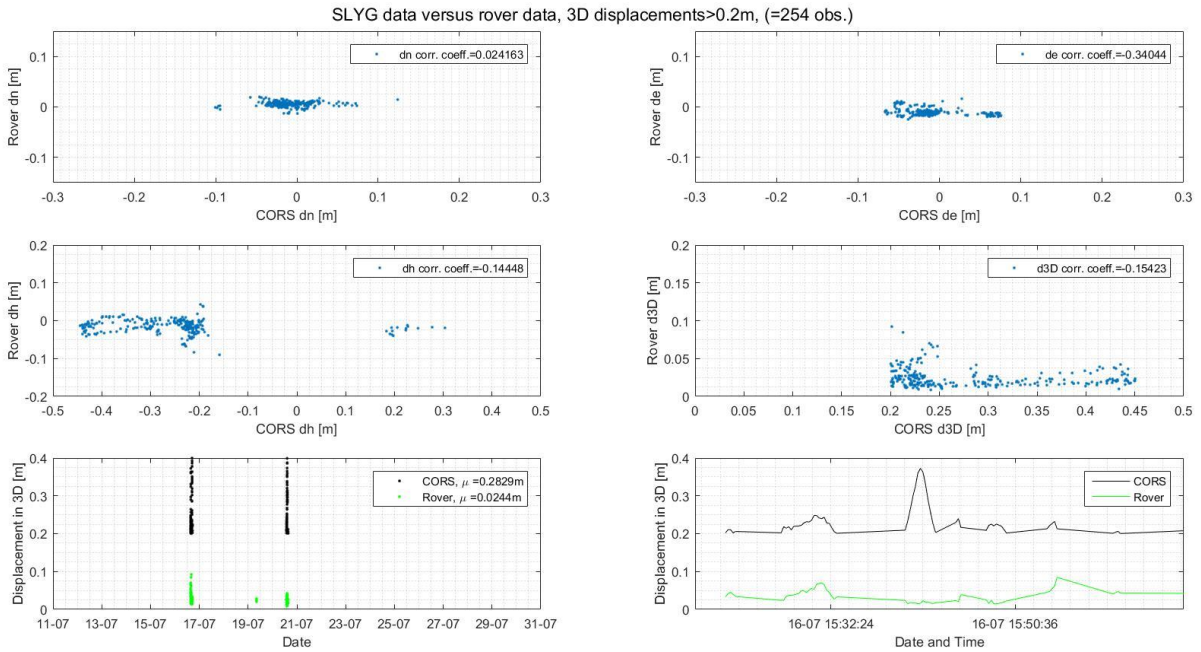
Figure A.12.5: Graphs visualizing the correlation between the SLYG IM displacement data and the Rover displacement data, and graphs visualizing the displacements in the 3D component, for both the Rover and the CORS, everything of all 3D displacements exceeding 0.20 meters. The first are visualized in the upper and middle panels (; northing: upper left, easting: upper right, height: middle left, and 3D: middle right), and the latter is visualized in the bottom panels (; complete displacement data: bottom left, and zoomed in; bottom right).

Figure A.12.6: Graphs visualizing the correlation between the SLYG IM displacement data and the Rover displacement data, and graphs visualizing the displacements in the 3D component, for both the Rover and the CORS, everything off all 3D displacements exceeding 0.25 meters. The first are visualized in the upper and middle panels (; northing: upper left, easting: upper right, height: middle left, and 3D: middle right), and the latter is visualized in the bottom panels (; complete displacement data: bottom left, and zoomed in; bottom right).
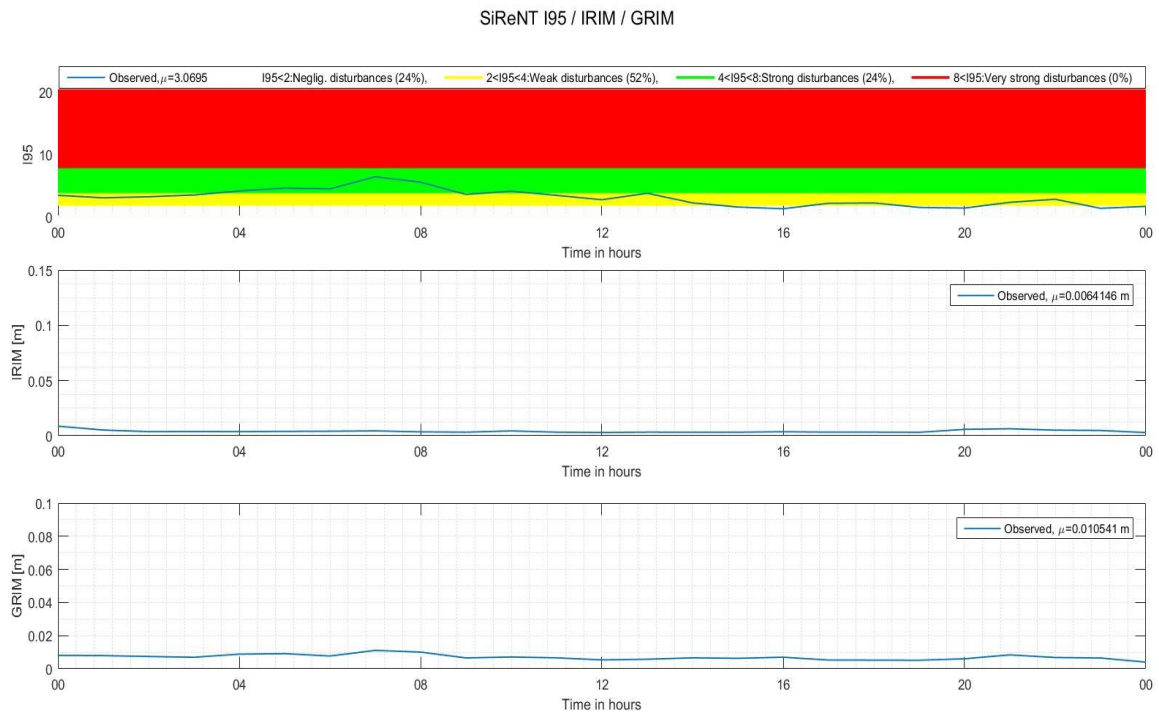
Figure A.13.1: Graphs visualizing the I95/IRIM/GRIM during this period. For a more detailed explanation of the graphs, see '9.1 Figures explained'.
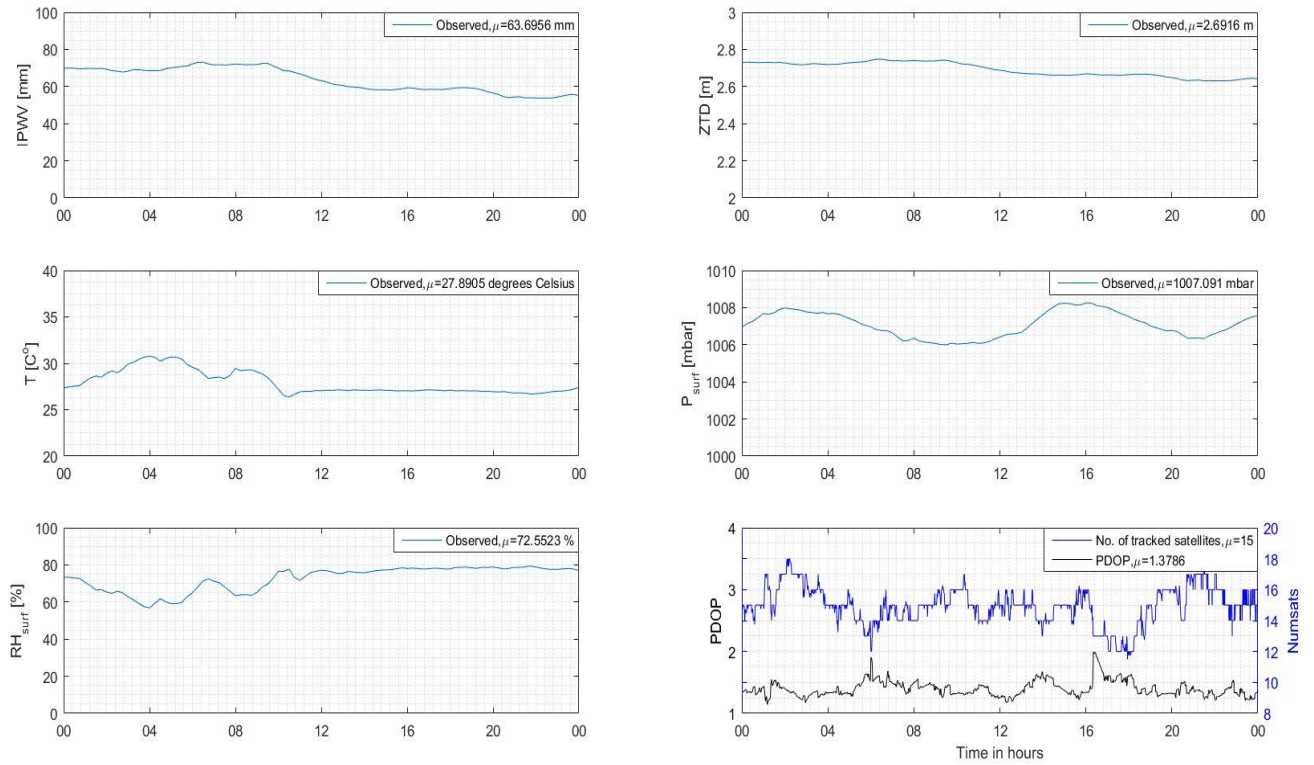
SLYG

Figure A.13.2: Graphs visualizing the Tropospheric information, PDOP value, and the number of tracked satellites, as observed by the SLYG CORS. For a more detailed explanation of the graphs, see '9.1 Figures explained'.
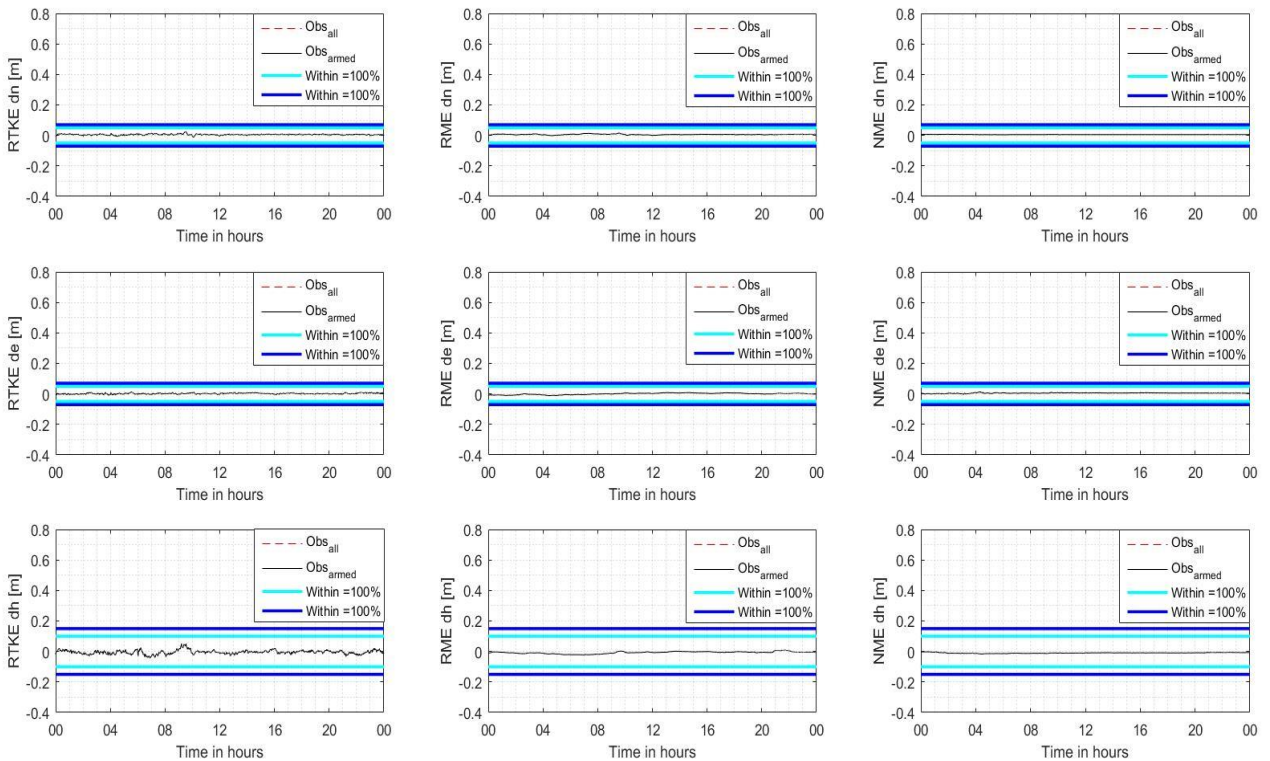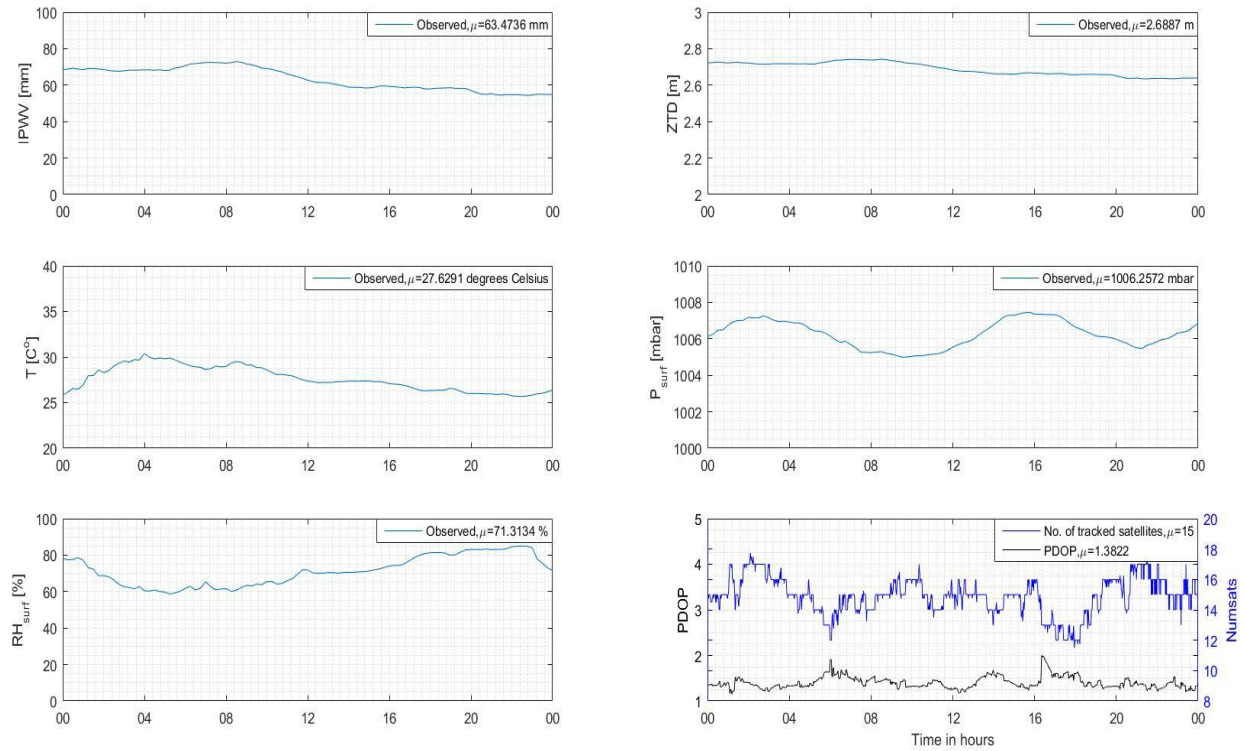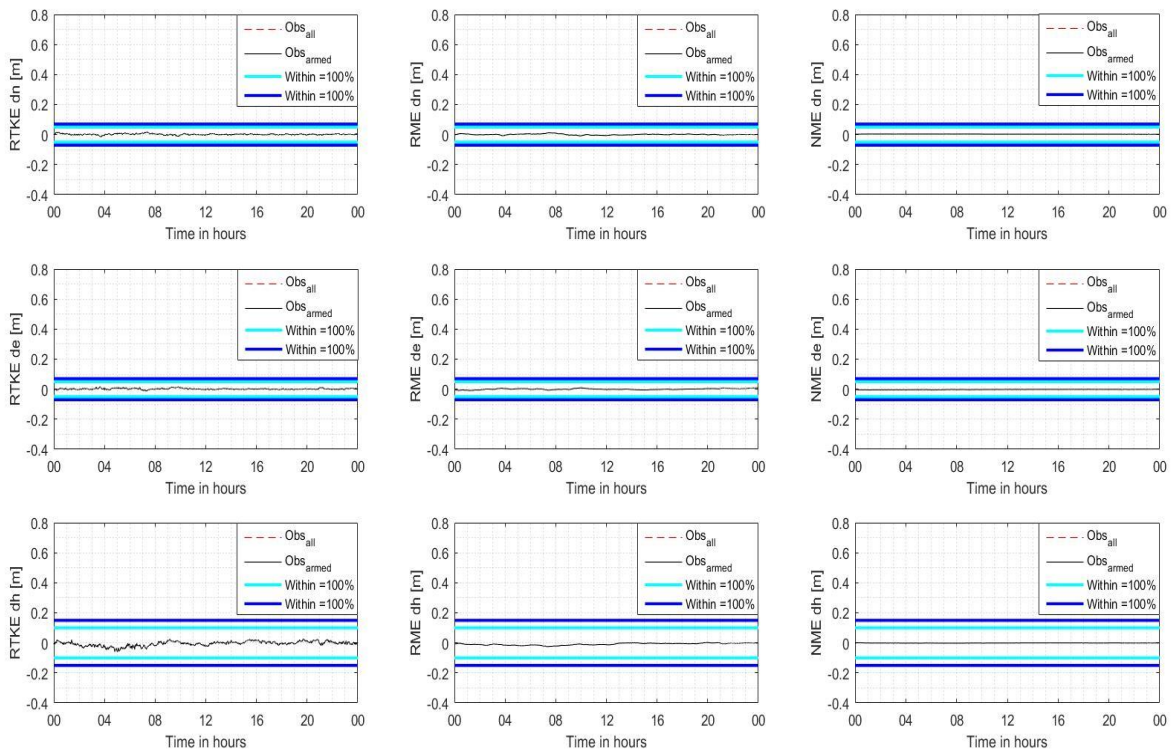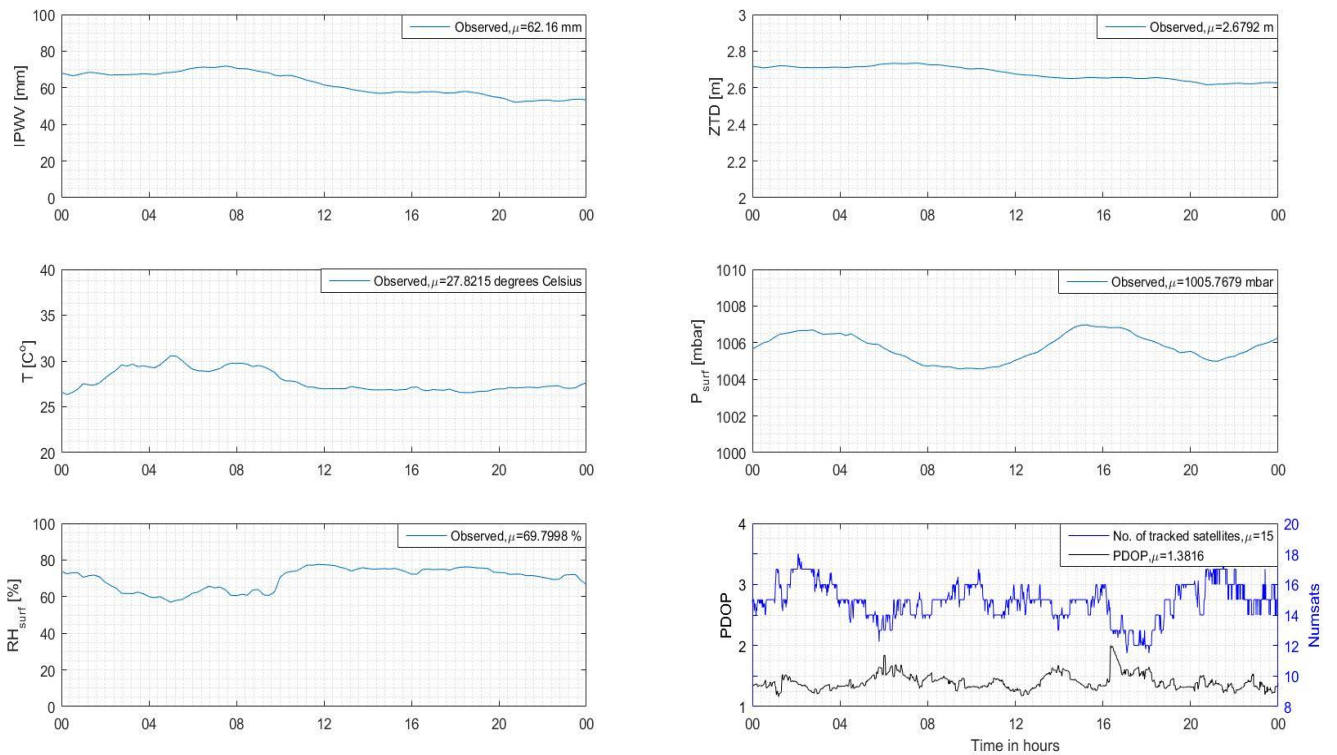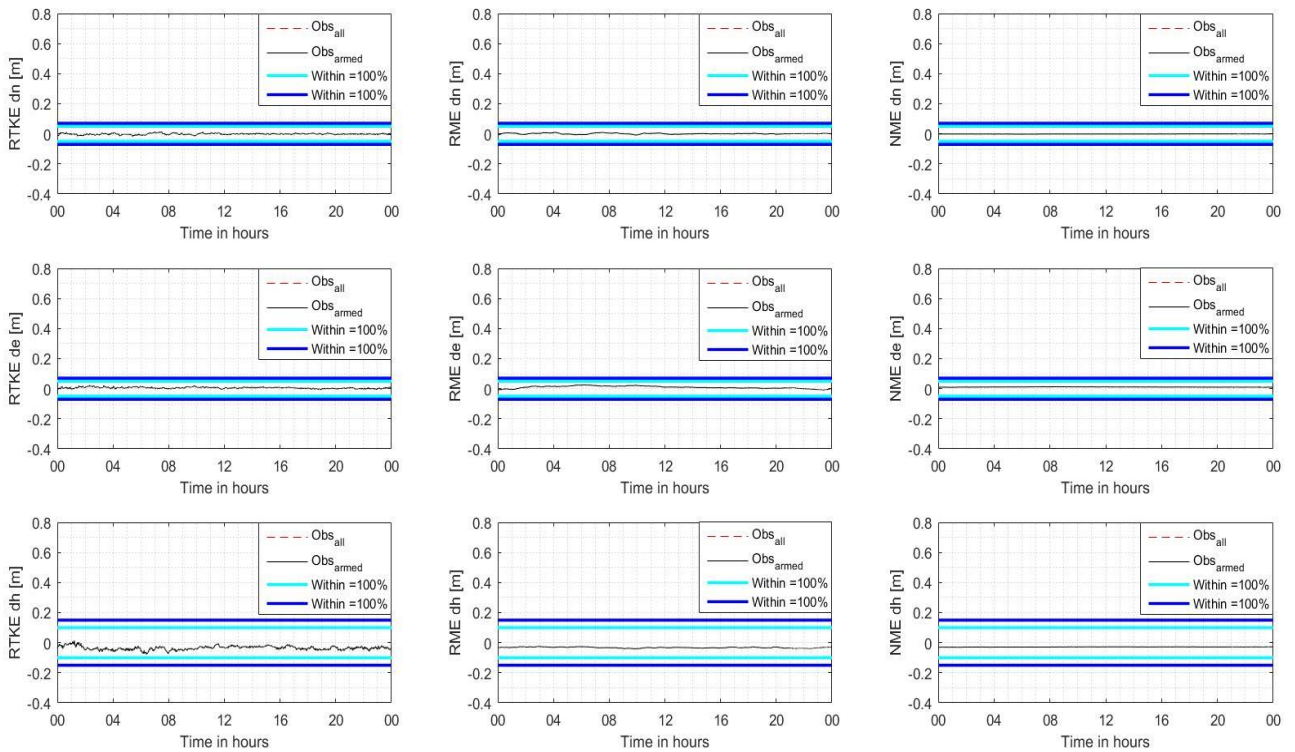

Figure A.13.3: Graphs visualizing the IM displacement data for several engine modules (RTK engine module: left, Rapid Motion engine module: middle, and the Network Motion engine module: right) as observed by the SLYG CORS. For a more detailed explanation of the graphs, see '9.1 Figures explained'.

SRPT

Figure A.13.4: Graphs visualizing the Tropospheric information, PDOP value, and the number of tracked satellites, as observed by the SRPT CORS.

Figure A.13.5: Graphs visualizing the IM displacement data for several engine modules (RTK engine module: left, Rapid Motion engine module: middle, and the Network Motion engine module: right) as observed by the SRPT CORS.
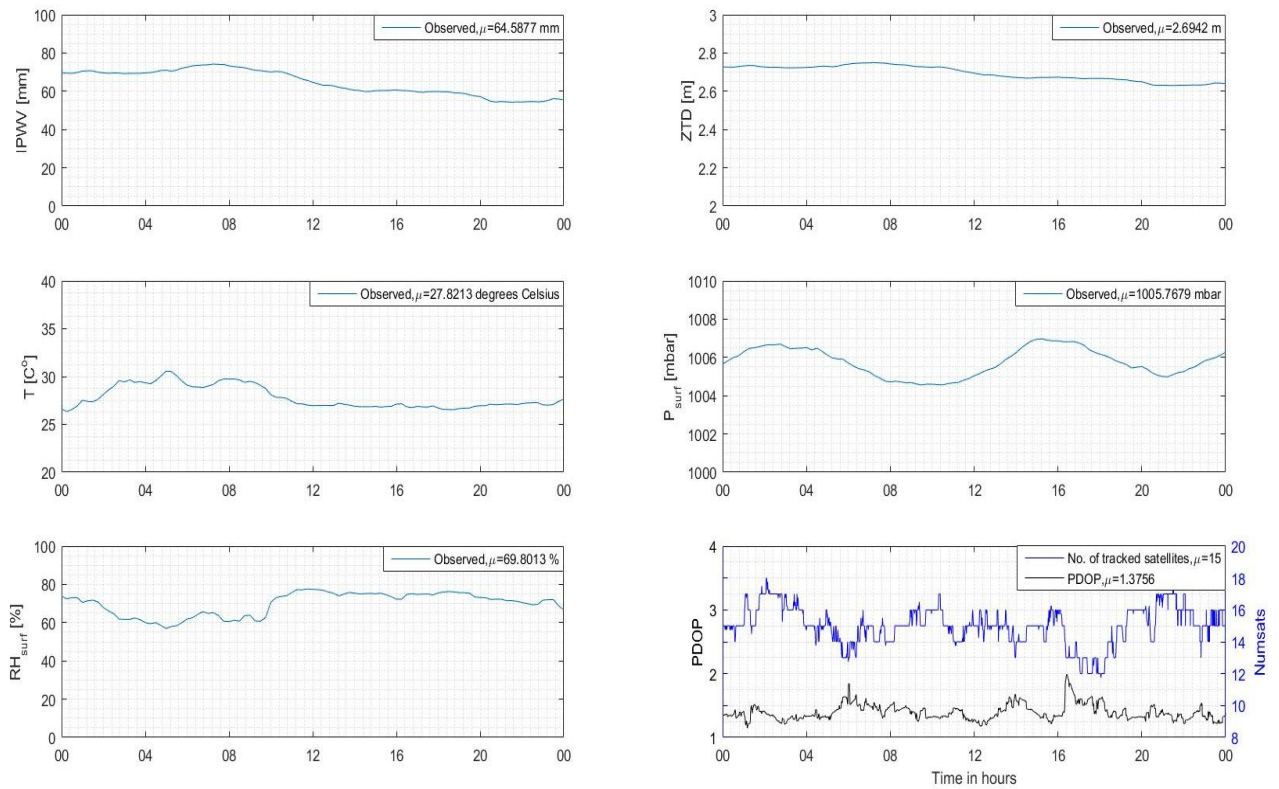
SNUS

Figure A.13.6: Graphs visualizing the Tropospheric information, PDOP value, and the number of tracked satellites, as observed by the SNUS CORS.
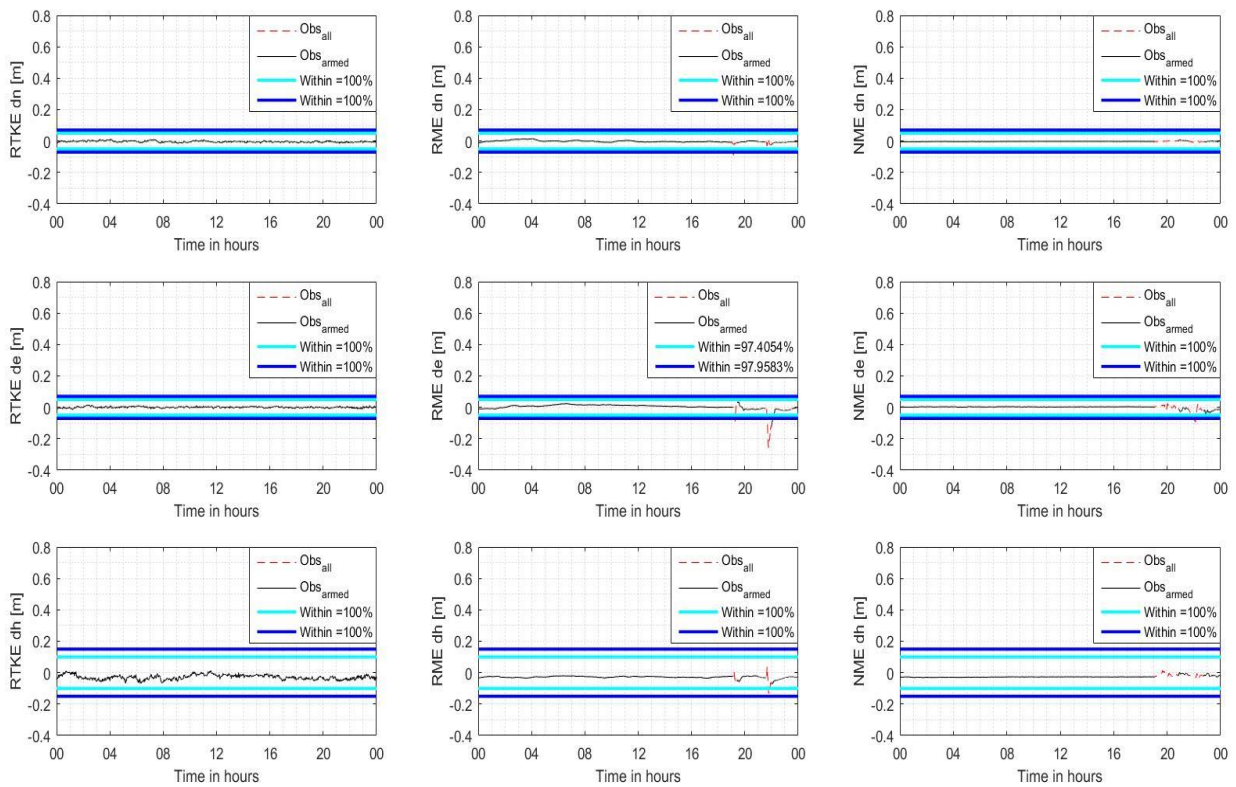

Figure A.13.7: Graphs visualizing the IM displacement data for several engine modules (RTK engine module: left, Rapid Motion engine module: middle, and the Network Motion engine module: right) as observed by the SNUS CORS.

206

SNYU

Figure A.13.8: Graphs visualizing the Tropospheric information, PDOP value, and the number of tracked satellites, as observed by the SNYU CORS.

Figure A.13.9: Graphs visualizing the IM displacement data for several engine modules (RTK engine module: left, Rapid Motion engine module: middle, and the Network Motion engine module: right) as observed by the SNYU CORS.
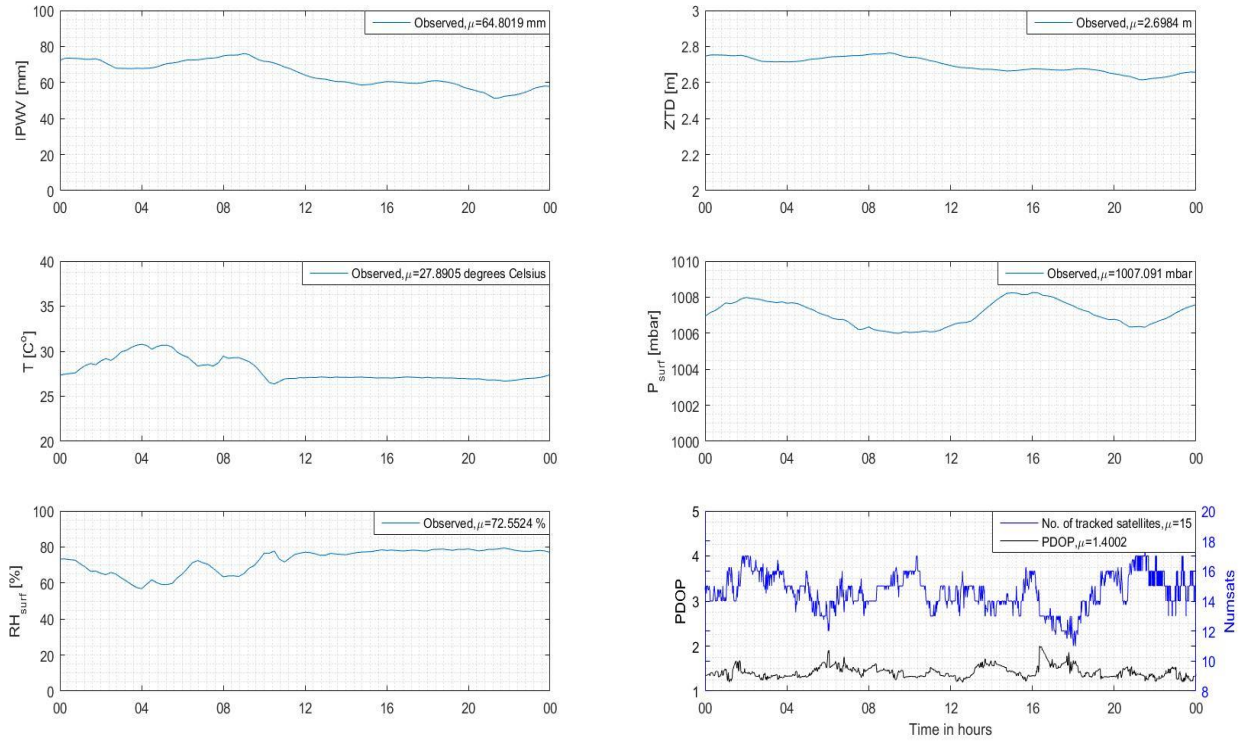
SNSC

Figure A.13.10: Graphs visualizing the Tropospheric information, PDOP value, and the number of tracked satellites, as observed by the SNSC CORS.
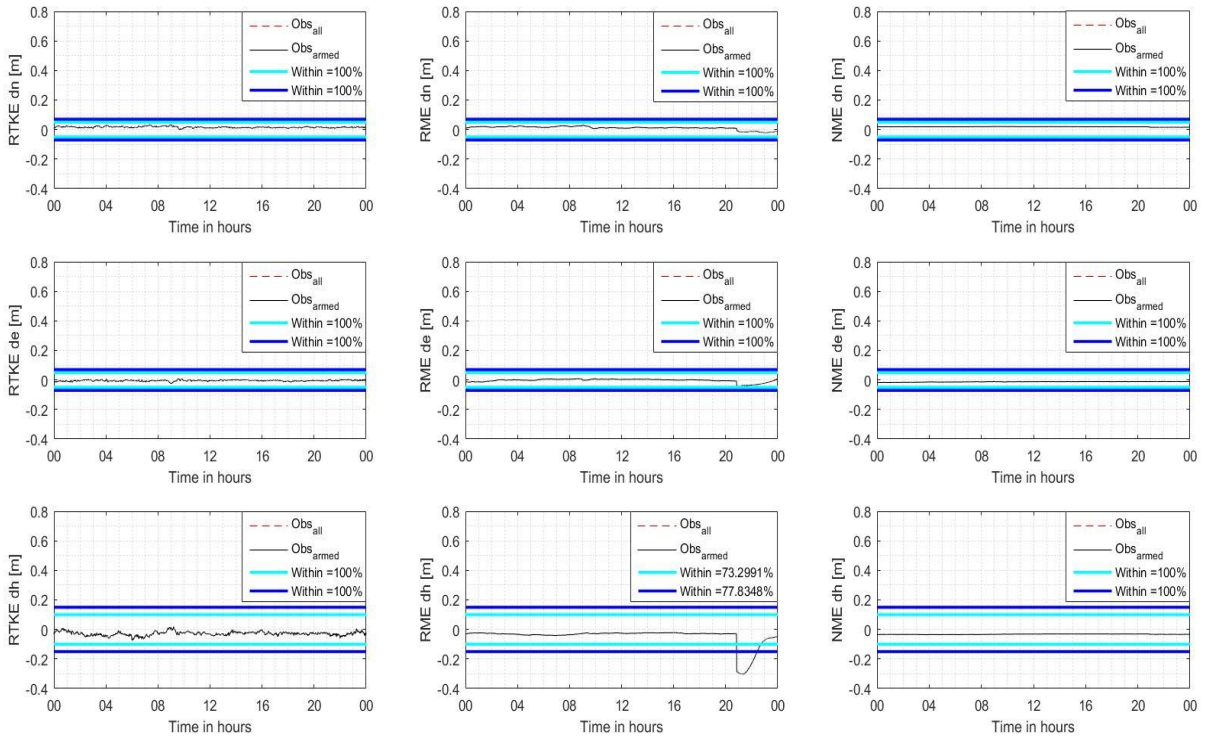

Figure A.13.11: Graphs visualizing the IM displacement data for several engine modules (RTK engine module: left, Rapid Motion engine module: middle, and the Network Motion engine module: right) as observed by the SNSC CORS.
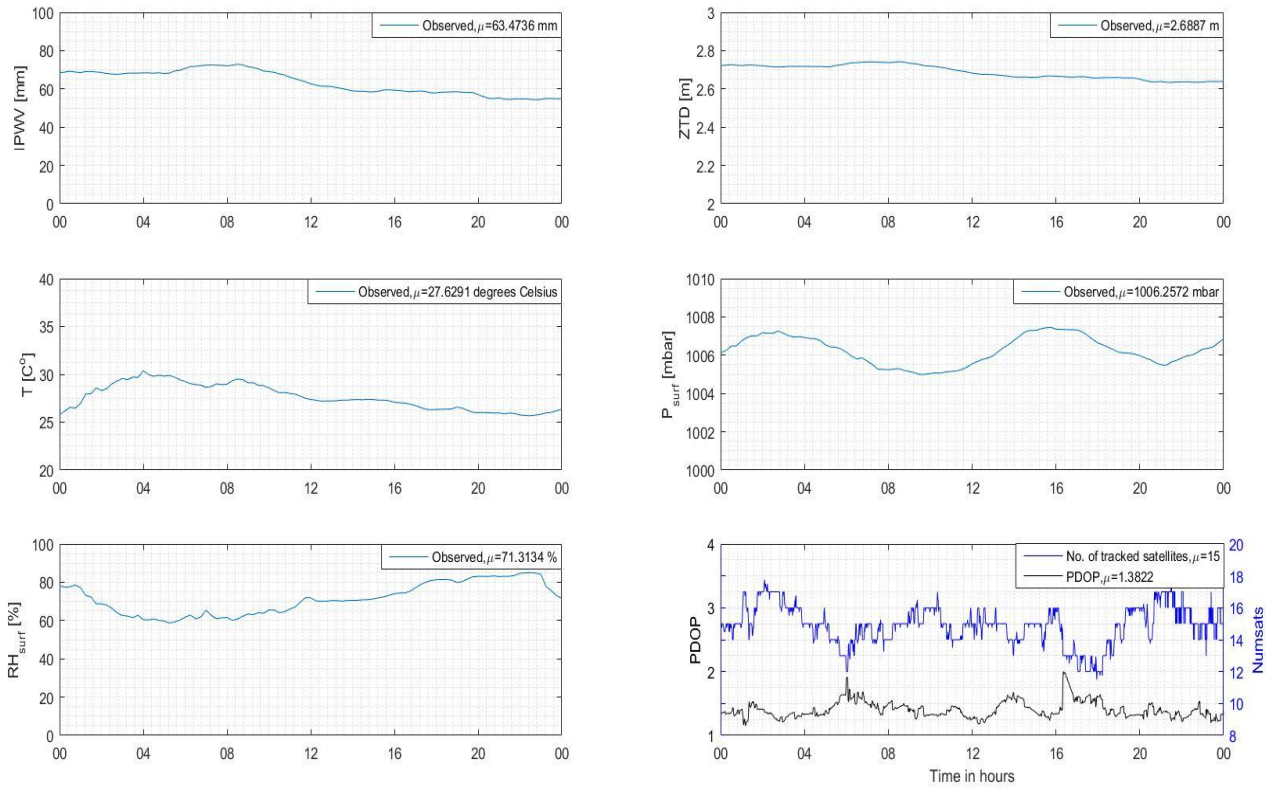
SSMK

Figure A.13.4: Graphs visualizing the Tropospheric information, PDOP value, and the number of tracked satellites, as observed by the SSMK CORS.
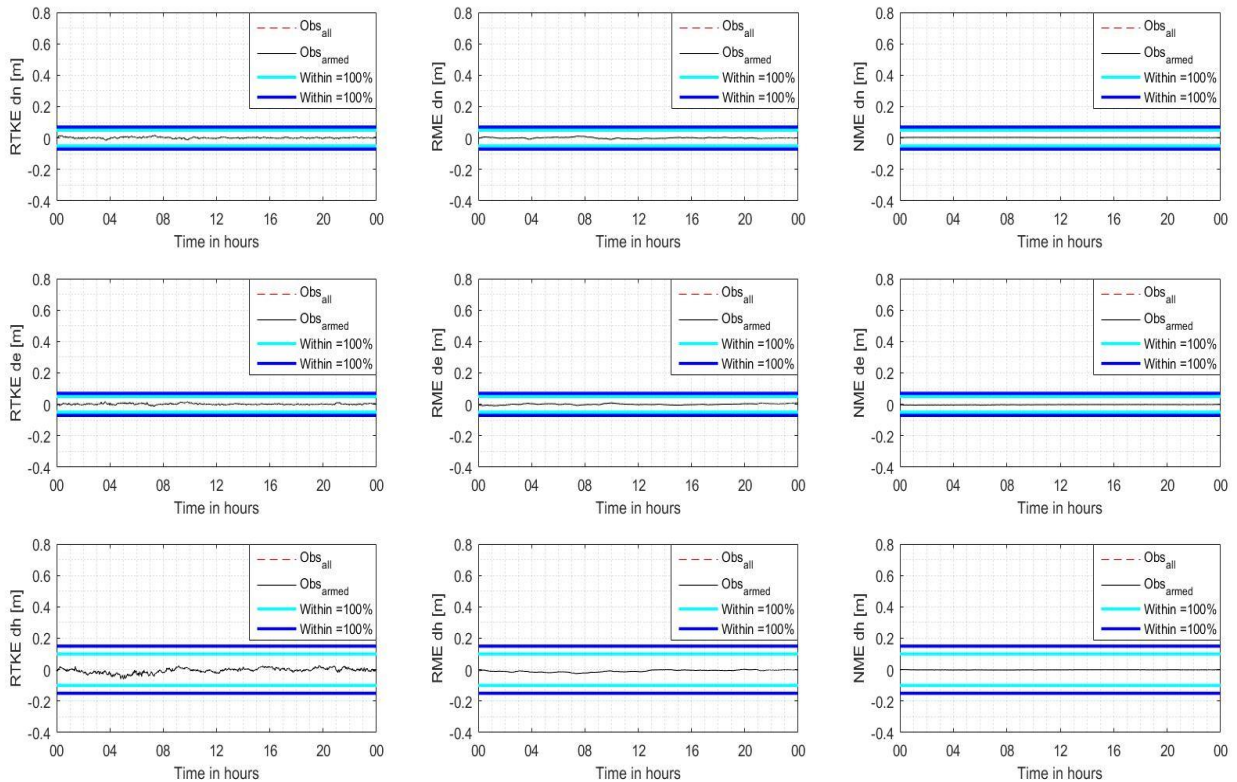

Figure A.13.5: Graphs visualizing the IM displacement data for several engine modules (RTK engine module: left, Rapid Motion engine module: middle, and the Network Motion engine module: right) as observed by the SSMK CORS.
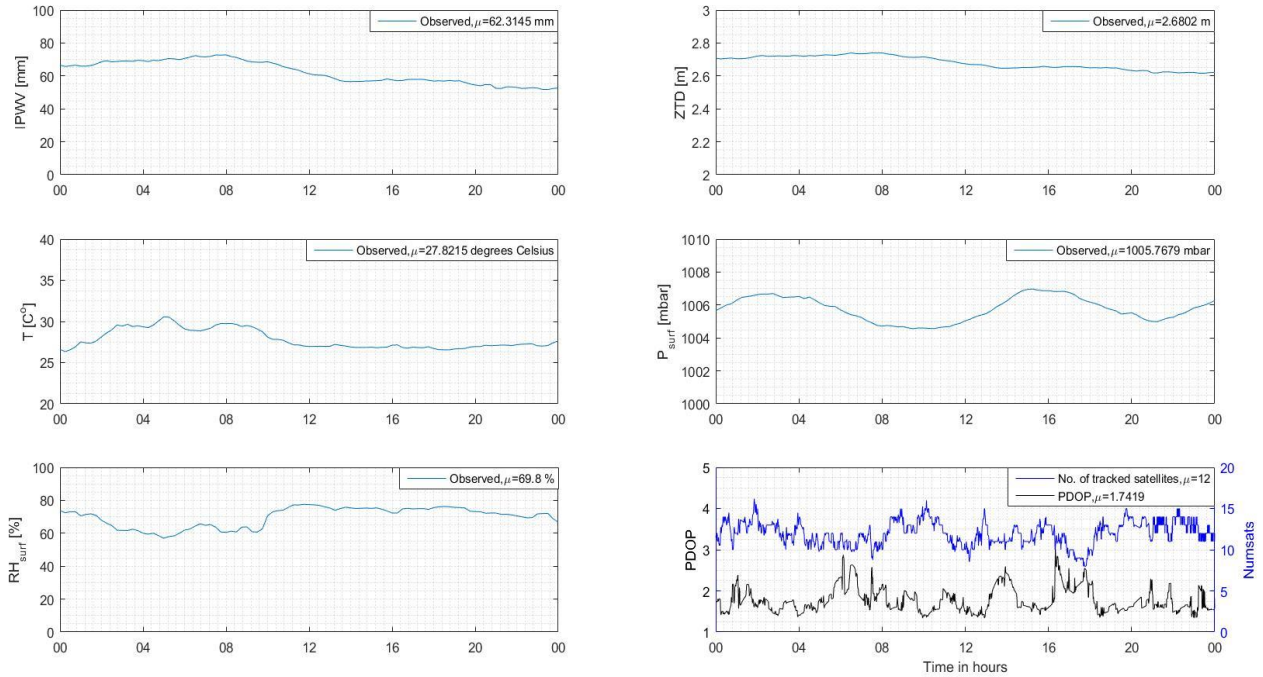
SING

Figure A.13.14: Graphs visualizing the Tropospheric information, PDOP value, and the number of tracked satellites, as observed by the SING CORS.
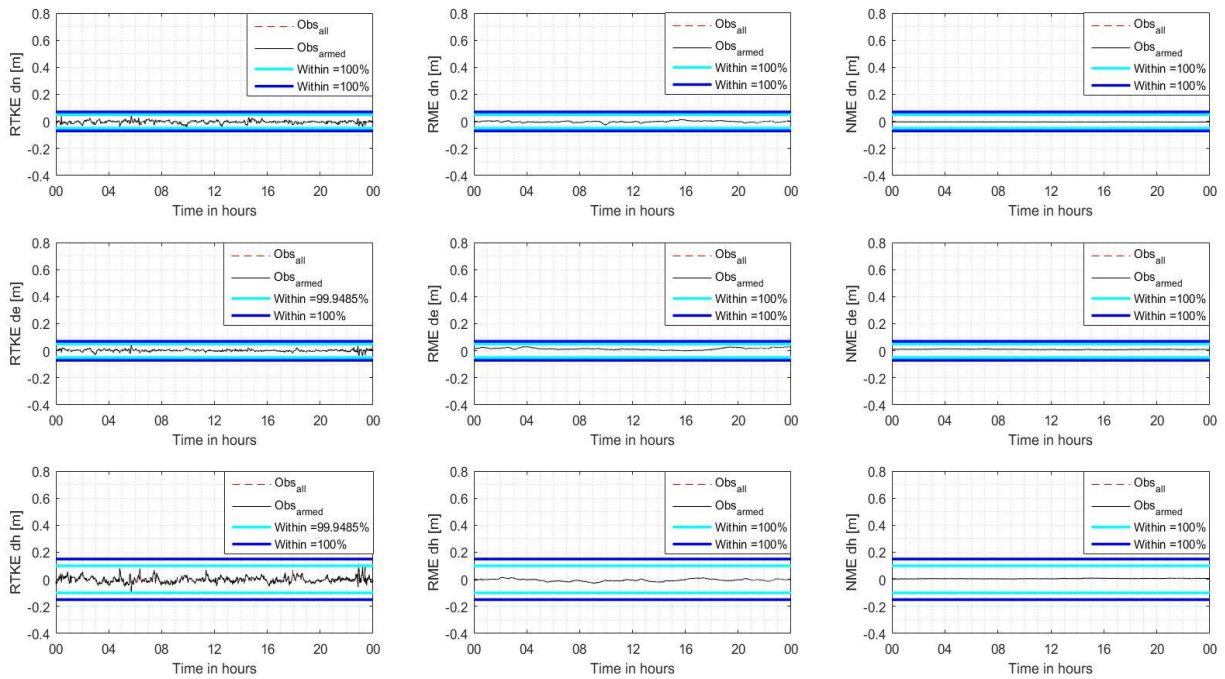

Figure A.13.15: Graphs visualizing the IM displacement data for several engine modules (RTK engine module: left, Rapid Motion engine module: middle, and the Network Motion engine module: right) as observed by the SING CORS.

Bibliography

[1]: Brown N, Kealy A, Millner J, Ramm P, Williamson I. Quality Control and Integrity Monitoring of the Victorian GPS Reference Station Network [internet]; 2017 [cited 2017 Jan.-Feb.]. Available from:
https://www.fig.net/resources/proceedings/fig_proceedings/fig_2002/Ts5-8/TS5_8_brown_etal.pdf

[2]: Chief Surveyor, CS Directive on Cadastral Survey Practices. 4rd ed. Singapore: Singapore Land Authority; 2015.

[3]: Dach R, Lutz S, Walser P, Fridez P. Bernese GNSS Software Version 5.2. User manual. Astronomical Institute, University of Bern, Bern Open Publishing, Bern. 2015

[4]: Defence Science and Technology Agency (DSTA). Geology of Singapore, 2nd edition. Singapore, Singapore

[5]: Department of Defense, Department of Homeland Security, and Department of Transportation. 2008 Federal Radionavigation Plan. Springfield, Virginia.

[6]: Department of Environment and Primary Industries (AU). Vicmap™ Catalogue 2013-14, Vicmap – Mapping for business intelligence [internet]; 2017 [cited 2017 Jan.-Feb.]. Available from: http://delwp.vic.gov.au/__data/assets/pdf_file/0004/261058/Vicmap-Catalogue-2013_14-WEB.pdf

[7]: Department of Geography College of Earth and mineral science, Pennsylvania State University [USA]. GEOG 862-GPS and GNSS for Geospatial Professionals [internet]. 2017 [cited 2017 Feb.-July.]. Available from: https://www.e-education.psu.edu/geog862/

[8]: Donahue B, Wentzel J, Berg R, Hains D, Sullivan P. Guidelines for RTK/RTN GNSS Surveying in Canada. Version 1.1. Canada; Surveyor General Branch, Earth Sciences Sector, Natural Resources Canada. 2013.

[9]: El-Rabbany A. Introduction to GPS, The Global Positioning System. Artech House, Boston | London; 2002.

[10]: GPSlands Geospatial Solutions. Singapore Satellite Positioning Reference Network (SiReNT) PIVOT Application training Manual (conducted for SLA).

[11]: Henning W. User Guidelines for Single Base Real Time GNSS Positioning. Version 2.1. United States of America: National Oceanic and Atmospheric Administration | National Geodetic Survey; 2011.

[12]: Henry JP. Network RTK 06-GPS [Lecture notes and internet]. Delft University of Technology; lecture notes provided at guest lecture May 2016. Available from: http://06-gps.nl/

[13]: Hewitson S, Wang J. GNSS receiver autonomous integrity monitoring (RAIM) performance analysis. GPS Solutions. 2005; 10(3): 155-170.

[14]: Hofmann-Wellenhof B, Legat K, Wieser M. Navigation Principles of Positioning and Guidance. 1st ed. Wien: Springer; 2003.

[15]: Hofmann-Wellenhof B, Lichtenegger H, Wasle E. GNSS -- Global Navigation Satellite Systems. 1st ed. Wien: Springer; 2008.

[16]: International GNSS service (International). IGS products [internet]; 2017 [cited 2017 Feb.-Apr.]. Available from: http://www.igs.org/products

[17]: Imparato D. GNSS-Based Receiver Autonomous Integrity Monitoring For Aircraft Navigation [Ph.D]. Delft University of Technology; 2016. Available from: http://repository.tudelft.nl/

[18]: Kleusberg A, Teunissen P. GPS for Geodesy. 1st ed. Berlin u.a: Springer; 1996.

[19]: KNMI (Koninklijk Nederlands Meteorologisch Instituut). Upper Air Humidity observations using GPS [internet]; 2016 [cited 2016 Nov.-Dec.]. Available from: https://www.knmi.nl/kennis-en-datacentrum/achtergrond/upper-air-humidity-observations-using-gps

[20]: Lui V. Improving real-time deformation monitoring quality by network RTK [Lecture notes]. Hong Kong: Leica Geosystems Limited. lecture notes available from: https://www.geodetic.gov.hk/smo/gsi/programs/common/satref_launch/5%20Improving%20real-time%20deformation%20monitoring%20quality%20by%20network%20RTK.pdf

[21]: Leick A, Tatarnikov D, Rapoport L. GPS satellite surveying. 1st ed. Hoboken: John Wiley & Sons; 2015.

[22]: Lindenbergh R. Geo-measurement processing [Lecture notes]. Delft University of Technology; lecture notes provided at lecture December 2016.

[23]: van der Marel H, Christian Tiberius C, Verhagen S. GPS for Civil Engineering and Geosciences [Lecture notes]. Delft University of Technology; lecture notes provided May-June 2016.

[24]: NETPOS Dashboard, providing insight in the availability and usability of NETPOS. Accessible at: https://services.netpos.nl/status/#/

[25]: Ochieng WY, Walsh KSD, Brodin G, Griffin S, Denney M. GPS Integrity and Potential Impact on Aviation Safety. UK: Civil Aviation Authority (CAA), Safety Regulation Group; 2004. Available from: https://publicapps.caa.co.uk/docs/33/CAPAP2003_09.PDF

[26]: Ochieng WY, Walsh KSD, Brodin G, Griffin S, Denney M. GPS Integrity and Potential Impact on Aviation Safety. The Journal of Navigation, the Royal Institute of Navigation. 2003; 56: 51–65. Available from: https://www.cambridge.org/core/journals/journal-of-navigation/article/gps-integrity-and-potential-impact-on-aviation-safety/D370C4383E8A03E485C4E09C4E42DF6C

[27]: Ooi WH, Shahrizal IM, Noordin A, Mustafa DS. Development of GNSS and DGPS integrity monitoring system in Malaysia. Banting: National Space Agency (ANGKASA) Space Application and Technology Development Unit. Received via email ANGKASA.

[28]: Ooi WH, Shahrizal IM, Noordin A, Mustafa DS, Musa TA, Othman R, Musliman IA. GNSS integrity monitoring system in Malaysia [Lecture notes]. The National Space Agency (ANKASA) Space Application and Technology Development Division & the Universiti Teknologi Malaysia GNSS and Geodynamics Research Group; lecture notes received via email ANGKASA.

[29]: Petovello M, Alves P. Real-Time Kinematic with Multiple Reference Stations [internet]; 2017 [cited 2017 Oct.]. Available from: http://www.insidegnss.com/node/717

[30]: Singapore Land Authority (SG). SVY21 About SiReNT [internet]; 2017 [cited 2017 Feb.-Apr.]. Available from: https://sirent.inlis.gov.sg/About.aspx

[31]: Survey and Mapping Office/Lands Department. the Government of the Hong Kong Special Administrative Region. Geodetic Survey Products & Services, Welcome to Hong Kong Satellite Positioning Reference Station Network (SatRef) [internet]; 2016 [cited 2016 Nov.-Dec.]. Available from: http://www.geodetic.gov.hk/smo/gsi/programs/en/gss/satref/

[32]: Teunissen PJG, Montenbruck O. Springer Handbook of Global Navigation Satellites Systems. Received via email Verhagen S.

[33]: Teunissen PJG, Tiberius CCJM, Simons DG. Probability and Observation Theory. Delft: Department of Geoscience and Remote Sensing, Faculty of Civil Engineering and Geosciences, Delft University of Technology; 2008.

[34]: Thombre S, Bhuiyan MZH, Söderholm S, Kirkko-Jaakkola M, Ruotssalainen L, Kuusniemi H. Tracking IRNSS Satellites for Multi-GNSS Positioning in Finland [Internet]; 2017 [cited 2017 Jun.-Aug.]. Available from: http://www.insidegnss.com/node/4279

[35]: Trimble Navigation Limited. Trimble Pivot Platform – Apps Overview [Lecture slides]; 2017 [cited 2017 Mar.-Jun.]. Available from: https://Trimbledimensions2014.smarteventscloud.com/connect/fileDownload/session/198E03 A5EDAD98DB1FE0456F1D0ECCCE/INFRA-8443_Li-INFRA-8443_Abendschein_Pagels.pdf

[36]: Trimble Navigation Limited. Trimble Pivot Platform Compiled HTML Help File. 2017 [cited 2017 Jan.-Jun.]. Provided by GPSlands Geospatial Solutions.

[37]: Trimble Navigation Limited. Trimble Pivot Platform GNSS Infrastructure Software Release Notes
Version 2.1 [Internet]; https://www.Trimble.com/infrastructure/pdf/Pivot_ReleaseNotes.pdf

[38]: Trimble Navigation Limited. Trimble Integrity Manager Datasheet [Internet]; 2017 [cited 2017 Feb.-Jun.]. Available from: http://www.optron.com/system-files/Trimble-integrity-ma-1301421007.pdf

[39]: Trimble Navigation Limited. Trimble Pivot solutions for the Ionosphere and Solar Maximum White Paper [Internet]; 2017 [cited 2017 Jan.-Feb.]. Available from: http://www.Trimble.com/Infrastructure/whitepapers.aspx

[40]: Verhagen S, Esfahany SS. Geo-measurement processing [Lecture notes]. Delft University of Technology; lecture notes provided at lectures September 2015.

[41]: Zaminpardaz S, Teunisen PJG, Nadarajah N. IRNSS/NavIC L5 Attitude Determination [Internet]; 2017 [cited 2017 Jun.-Aug.]. Available from: http://www.mdpi.com/1424-8220/17/2/274

Personal Communication

[42]: Asmussen H. GPSnet Support, Department of Environment, Land, Water and Planning, Victoria, Australia. April 2017.

[43]: Huisman L. Cadaster Netherlands and Delft Technical University, the Netherlands. March 2017.

[44]: Khoo V, Tan HSJ, Noor RM. Singapore Land Authority, Singapore. 2017-2018.

[45]: van der Marel H. Delft Technical University, the Netherlands. March 2017.

[46]: Pua R, Tho J, Kamath M. Trimble/GPSlands Support, Singapore. 2017-2018.

[47]: Wei S. Earth Observatory Singapore, Singapore. October 2017

[48]: Wong WY. Geodetic Survey Section, Lands Department, Hong Kong. April 2017.

Newspaper article

[49]: Tan A. Earthquake of magnitude 6.5 strikes west off Indonesia's Sumatra; tremors felt in Singapore. *The Straits Times, Singapore,* 13-09-2017. Available from: http://www.straitstimes.com/asia/se-asia/earthquake-of-magnitude-65-strikes-west-off-indonesias-sumatra